PLASTIC SHEAR BUCKLING OF SHIP HULL PLATING INDUCED BY GROUNDING

by

Stephen Rodgers Price (1)

B.S. Civil Eng. University of New Mexico (1977)

Submitted to the Department of Ocean Engineering
in partial fulfillment of the requirements for the degrees of

NAVAL ENGINEER

and

MASTER OF SCIENCE IN MECHANICAL ENGINEERING

at the
Massachusetts Institute of Technology
June, 1992

PLASTIC SHEAR BUCKLING OF SHIP HULL PLATING INDUCED BY GROUNDING

by

STEPHEN RODGERS PRICE

Submitted to the Department of Ocean Engineering on May 8, 1992
in partial fulfillment of the requirements for the degrees of
Naval Engineer and Master of Science in Mechanical Engineering

ABSTRACT

A study was conducted to develop an analytical model for predicting the horizontal resistance due to in-plane shear of ship's hull bottom plating that is undergoing deformation induced by grounding. First, four models were developed for predicting the load carrying capacity of a flat rectangular plate element when subjected to in-plane shear loads in both the elastic and plastic buckling ranges. Seven plate buckling experiments were then conducted which were used to validate the analytical model results. Finally, the plate element model was incorporated into a global model description for the bottom plating of a very large crude carrier (VLCC) which is undergoing a deformation process induced by grounding.

The results of the study demonstrated that a suitable plate element model could be developed for accurately predicting within 10 percent both the in-plane shear load capacity as well as the plastic buckling wavelength of a flat rectangular plate. The best prediction was obtained from the buckled element which is initially rectangular.

The grounding resistance due to in-plane shear was roughly an order of magnitude greater than that from other sources not including shear. Thus it seems that fracture or some other "weaker" failure modes will pre-empt the shear deformation mode.

Thesis Supervisor: Dr. Tomasz Wierzbicki
Title: Professor of Applied Mechanics, Department of Ocean Engineering

Table of Contents

1. Introduction and Background

The serious environmental damage caused by the spillage of oil or other hazardous cargo from tankers in recent years has forced ship designers to look for hull structural designs that are more robust against the likelihood of rupture of the hull plating in the event of a grounding. In some designs this may entail addition of a second inner hull. Another idea proposed by Wierzbicki[1] among others is to design a uniform strength hull structure that contains a larger number of more densely positioned but smaller structural elements. An example of a uniform strength hull is the unidirectionally stiffened double hull currently being studied by the U.S. Navy[2]. The principle is to make the hull plating support structure flexible enough to deform with the hull, thus preventing the hull plate from rupturing at the welded joints where it is connected to the otherwise rigid structural frame. To effect such a design an understanding needs to be developed of the various structural resisting force and energy absorption mechanisms as well as the structural failure modes for a ship hull. These analyses should then lead to an optimal approach for strengthening a ship hull to better resist hull penetration and thus reduce the likelihood of cargo spillage.

During a grounding, four mechanisms of work dissipation have been identified by Wierzbicki[3]:

(1) Global lifting of the ship hull against gravity

(2) Frictional forces between hull and shallow bottom

(3) Membrane rupture of ship's hull plate

(4) Plastic deformation of hull plating and bottom structural elements

One of the hull plate plastic deformation mechanisms in item (4) above is due to in-plane shear deformations that develop within the hull plate during a grounding. Previous

---

[1] T. Wierzbicki, E. Rady, D.B. Peer J.G. Shin, "Damage Estimates in High Energy Grounding of Ships", Massachusetts Institute of Technology, Department of Ocean Engineering, *Joint Industry Program on Tanker Safety*, Report No. 1, June 1990.

[2] J. Beach, "Advanced Surface Ship Hull Technology, Cluster B", *Naval Engineers Journal*, vol. 103, no. 6, November 1991, pp 27-37.

[3] T. Wierzbicki, D.B. Peer, E. Rady, "The Anatomy of Tanker Grounding", Massachusetts Institute of Technology, Department of Ocean Engineering, *Joint Industry-MIT Program on Tanker Safety*, Report No. 2, May 1991.

work conducted by Wierzbicki [1,3] and Peer [4] which formulated an analytical model for tanker grounding recognized the existence of plastic work done by in plane shear forces but deferred the estimation of this work to future studies.

This paper presents an analytical model for plastic work done by in plane shear forces on a flat rectangular plate element. An experimental study is conducted and the results are compared with these analytical results to validate the model. The new model of a localized plastic shear buckling element is then incorporated into a global model which describes the deformation of the hull plating during a grounding assuming a simplified geometry. Finally, a comparison is made between work absorbed by shear buckling and by other mechanisms during a grounding, previously formulated by Peer[4], in order to determine the importance of shear buckling mechanisms in dissipation of kinetic energy during a grounding.

Stated simply, the objectives of this study are threefold:

(1) Develop analytical models for elastic pre and post-buckling behavior, plastic in-plane shear post-buckling behavior, and plastic in-plane deformation without buckling, of a single prismatic element

(2) Validate this model with experimental results

(3) Incorporate this model into the global ship grounding model and determine the importance of shear buckling as an energy dissipation mechanism

Three limits on the applicability of the theory must be considered before studying the details of this model and how it can be applied to the ship grounding problem. First, hull membrane rupture is not permitted since hull rupture changes the geometry and boundary conditions of the problem and the point at which hull plate rupture occurs is difficult to quantify. Therefore, the present model is applicable only to grounding geometries which allow the hull structure to "dish" inward while the plating rides up and over the obstacle on the ocean bottom.

Second, the present model assumes symmetric deformation about the keel of the ship. This assumption is necessary to avoid the need to describe the hydrodynamic stability characteristics of the grounded vessel, which otherwise would greatly complicate the analysis.

---

[4] D.B. Peer, "Coupling Global Motion and Local Deformation in Tanker Grounding", Massachusetts Institute of Technology, Department of Ocean Engineering, *Joint Mit-Industry Program on Tanker Safety*, Report No. 4, May 1991.

Third, this local model is incorporated into a ship that is assumed to be longitudinally framed at certain intervals with transverse webs at a specified spacing l and longitudinal bulkheads spaced at an interval l_1. The transition zone of deformation forward of the rock η is assumed to be a multiple of the transverse web spacing while the transverse extent of damage is assumed to be limited to the distance between longitudinal bulkheads. This structural geometry is chosen to be representative of today's very large crude carrier, (VLCC). It should be noted, therefore, that while the results from the local buckling element model are applicable to any ship with unsupported areas of rectangular flat plate, the results from the global ship grounding model are only applicable to the particular structural geometry chosen and would have to be redone for ships with a different hull structure. The main reason for this is the differing degree of constraints placed on hull deformation by the transverse webs and the longitudinal bulkheads in different designs.

2. Summary of Elastic Shear Buckling Response

To gain an insight into the plastic shear buckling problem, it is necessary to look first at shear buckling of a flat plate in the elastic range. The exact solution to the elastic shear buckling problem for plates of infinite length has been derived by Southwell and Skan[5]. Since that time plates of finite length have been analyzed by other investigators. A brief discussion of this previous work follows so that a foundation can be laid on which to base the problem formulation for the plastic buckling model discussed herein.

A plate subjected to uniform in-plane shear has an out of plane displacement $w(x,y)$ that obeys the following differential equation in terms of the shear force per unit length along loaded edges N^{o}_{xy} and the flexural plate rigidity D.

$$\nabla^4 w - \left[\frac{2N^{o}_{xy}}{D}\right]\frac{\partial^2 w}{\partial x \partial y} = 0 \qquad D = \frac{Eh^3}{12(1-\nu^2)} \tag{1}$$

The general solution to the above differential equation (1) is assumed in terms of the plate width or stiffener spacing b to be:

$$w(x,y) = C\, e^{(i\lambda y)/b}\, e^{(ikx)/b} \tag{2}$$

The coordinates x and y in the above formula correspond to the respective length and width directions of the plate. The constant C is an arbitrary constant that varies with the flexural plate bending stiffness. The constants k and λ correspond to spatial buckling wave numbers in the x and y directions, respectively.

Substitution of the general solution (2) into the Differential Equation (1) yields the following fourth order polynomial in λ and k.

$$\lambda^4 + 2k^2\lambda^2 + \frac{2N^{o}_{xy}}{D}k\lambda + k^4 = 0 \tag{3}$$

---

[5]R. Southwell and S. Skan, "On the Stability under Shearing Forces of a flat Elastic Strip", National Physical Laboratory, Aerodynamics Department, *Proceedings of The Royal Society of London*, ser. A, vol. 105, 1924, pp. 582-607.

Equation (3) has four roots λ_1, λ_2, λ_3, and λ_4 which are described as four transverse buckling wave numbers. These roots can be obtained for a given critical shear force buckling load per unit length N^o_{xy} and the longitudinal buckling mode wave number k. Southwell and Skan[5] determined the exact solution for the out-of-plane displacement of a flat elastic strip under uniform shear applied along its edges of infinite length. Solutions were obtained for two types of boundary conditions, clamped and simply-supported.

The complex form of the general solution for out of plane displacement w(x,y) is:

$$w(x,y) = \left[C_1 e^{i\lambda_1 y/b} + C_2 e^{i\lambda_2 y/b} + C_3 e^{i\lambda_3 y/b} + C_4 e^{i\lambda_4 y/b}\right] e^{ikx/b} \qquad (4)$$

Substitution of the general solution (4) into four homogeneous boundary conditions leads to a determinantal equation from which the critical values of N^o_{xy} may be found. The four boundary condition equations below correspond to the conditions for clamped edges which most closely approximate the model for a longitudinally stiffened hull plate.

$$w(y=0) = 0 \qquad w(y=b) = 0 \qquad w'(y=0) = 0 \qquad w'(y=b) = 0$$

Southwell and Skan carried out such an analysis and determined a result for the critical buckling load in shear which is:

$$N^o_{xy} = K_s \frac{\pi^2 D}{b^2} \qquad (5)$$

where K_s is defined as the critical shear stress buckling coefficient. The critical shear buckling coefficients for an infinitely long flat plate are 5.35 for simply-supported edges and 8.98 for clamped edges. Since the bottom hull plating on a longitudinally framed ship extends for several hundred feet and is welded to the longitudinals, we can assume that the inter-longitudinal plating spans are clamped rectangular plates of approximate infinite length for which $K_s = 8.98$. The critical shear stress is obtained by substituting into Equation (5) the expression for the flexural plate rigidity and dividing by the thickness h.

$$\sigma_{cr} = \frac{N^o_{xy}}{h} = \frac{8.98\ \pi^2 E h^2}{12(1-\nu^2)b^2} \qquad (6)$$

Southwell and Skan also determined the real form of the general solution for the deformed shape $w(x,y)$.

$$w(x,y) = C\left[\cos\left\{\frac{kx}{b} + (\alpha+\beta)\frac{y}{b}\right\} + K\cos\left\{\frac{kx}{b} + \frac{(\alpha-\beta)y}{b}\right\} + L\sinh\left\{\frac{\delta y}{b}\right\}\sin\left\{\frac{Kx}{b} - \frac{\alpha y}{b}\right\} + M\cosh\left\{\frac{\delta y}{b}\right\}\cos\left\{\frac{kx}{b} - \frac{\alpha y}{b}\right\}\right] \quad (7)$$

Reference 5 gives the values for the constant coefficients K , L , and M as well as the buckling parameters k , β , and α , which depend upon the boundary conditions. For clamped edges these constants are:

$K = 0.6728$ $\quad L = -0.0131$ $\quad M = -0.0008925$ $\quad k = 2\pi/3.2$

$\alpha = -1.977$ $\quad \beta = 1.804$ $\quad \delta = 4.334$

A surface plot of the out-of-plane displacement $w(x,y)$, given by Equation (7) for clamped edges, is shown in Figure 1.

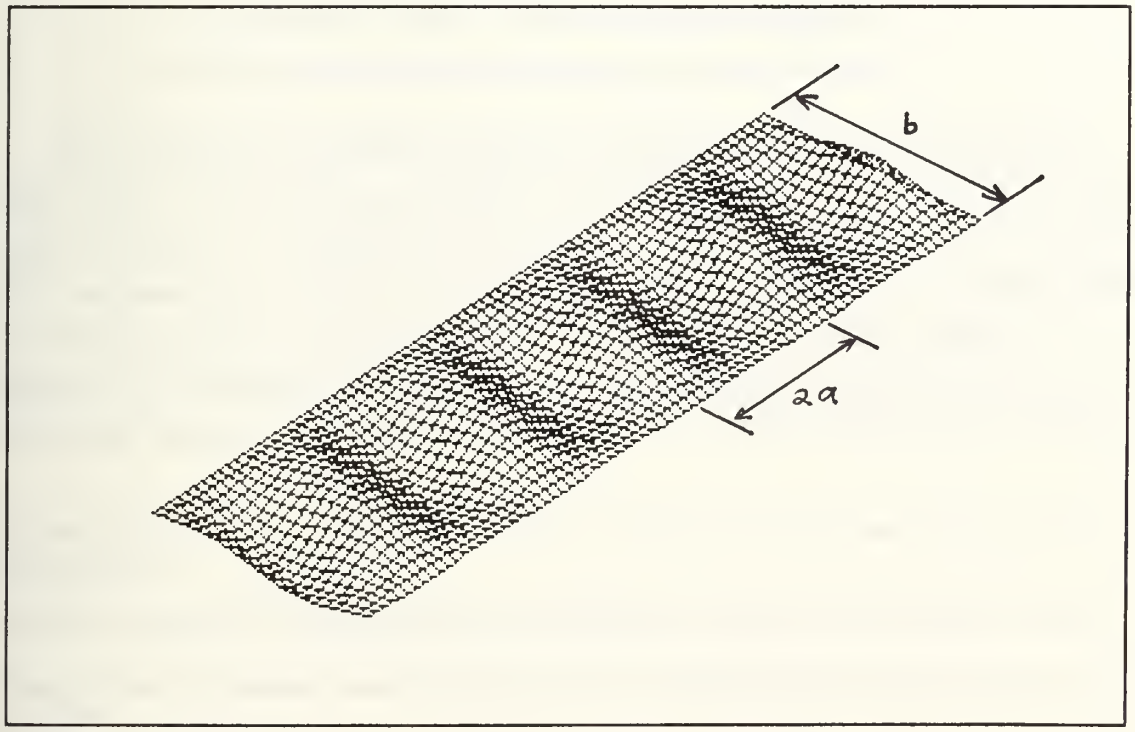

Figure 1: Plot of elastic shear buckling solution $w(x,y)$

The longitudinal buckling wavelength 2a shown in Figure 1 has also been determined by Southwell and Skan for both clamped and simply-supported boundary conditions. For a dimensionless wavelength defined by $\Lambda \equiv 2a/b$:

$\Lambda = 2.67$ --- for simply supported boundaries

$\Lambda = 1.60$ --- for clamped boundaries

After publication of the Southwell and Skan solution, additional analyses were conducted by structural engineers in the 1930s through the 1970s to determine the critical shear stress buckling coefficient K_s for plates of finite length with various degrees of restraint applied to their edges. In 1936 Timoshenko[6] solved for an approximate critical shear stress buckling coefficient for buckling of a finite length rectangular flat plate with simply-supported edges. Two years later Iguchi[7] presented an analysis of a flat rectangular plate with three different edge conditions.

(1) All edges rigidly clamped
(2) Long edges clamped, short edges simply-supported
(3) Long edges simply-supported, short edges clamped

Up to this point, the solutions obtained by Southwell and Skan, Timoshenko, and Iguchi referred to the buckling mode shape as symmetric due to the symmetry of the mode shape with respect to a diagonal across the plate at the node line slope. In 1947 Stein and Neff[8] examined both a symmetric and an asymmetric buckling mode for a rectangular plate with all edges simply-supported and in 1948 Budiansky and Connor[9] investigated symmetric and asymmetric buckling modes for a fully clamped rectangular plate. Gerard and Becker[10] presented a comprehensive review of this work in 1957 showing that the

---

[6] Timoshenko, S. P., *Theory of elastic stability*, McGraw Hill, New York and London, First edition, 1936, pp 357-363.

[7] Iguchi, S., "Buckling of rectangular plates under shear stresses", *Ingenier-Archiv*, Part IX, p 1, 1938.

[8] Stein, M., Neff, J., "Buckling stress of simply-supported rectangular flat plates in shear", *NACA TN 1222*, 1947.

[9] Budiansky, B., Connor, R.W., "Buckling stresses of clamped rectangular flat plates in shear", *NACA TN 1559*, 1948.

[10] Gerard, G., Becker, H., "Handbook of structural stability, Part 1-Buckling of flat plates", *NACA TN 3781*, 1957.

asymmetric buckling mode has a lower K_S than the symmetric mode for a small range of plate aspect ratios. Gerard and Becker also presented a series of plots and tables from which K_S could be calculated for an intermediate level of edge restraint between the simply-supported and clamped conditions.

In 1963 Cook and Rockey[11] presented a solution for the in-plane shear buckling of a rectangular plate which is clamped along one edge and simply-supported on the other three edges. They also refined the solution for the case of two opposite edges simply-supported and the other edges clamped for various plate aspect ratios. A variational approach was utilized with the following approximation for the plate out-of-plane displacement $w(x,y)$.

$$w(x,y) = \sum_{m=0}^{\infty} \sum_{n=1}^{\infty} a_{mn} \cos\left(\frac{m \pi x}{d}\right) \sin\left(\frac{n \pi y}{b}\right)$$

The constants d and b are the respective length and width dimensions of the rectangular plate. The accuracy of this Fourier series solution was enhanced by carrying out the calculations using up to 45 coefficients "a_{mn}".

Additional research conducted in the 1970s by Rockey[12,13,14] focused on the ultimate load plastic behavior of plate girders loaded in shear and developed a design method for predicting the collapse behavior of plate girders. Although the girder problem differs somewhat from the hull plate shear buckling problem in the application of the external load, the web response to the shear load near the ends of a simply-supported girder is similar to that of a flat rectangular plate to in-plane shear applied along its clamped edges. This is because the bending stresses induced within the web are small compared to the shear stresses close to the ends of the girder. Figure 2 illustrates, however, that the shear stress

---

[11] Cook, I.T., Rockey, K.C., "Shear buckling of rectangular plates with mixed boundary conditions", *The Aeronautical Quarterly*, vol.XIV, March 1963, pp 349-356.

[12] Rockey, K.C., Skaloud, M., "The ultimate load behavior of plate girders loaded in shear", *The Structural Engineer*, vol. 50, no. 1, Jan 1972, pp 29-48.

[13] Rockey, K.C., Evans, H.R., Porter, D.M., "The ultimate load behavior of longitudinally reinforced plate girders", structural analysis, non-linear behavior and techniques, *Transport and Road Research Lab* Report SR 164UC, Crowthorne 1975, pp 162-174.

[14] Rockey, K.C., Evans, H.R., Porter, D.M., "A design method for predicting the collapse behavior of plate girders", *Proc. Instn. Civ. Engrs.*, part 2, vol. 65, Mar 1978, pp 85-112.

through the depth of the web is not uniform as is the case in our problem. The flanges of the symmetric girder shown in Figure 2 act to restrain the web from buckling in a manner similar to the longitudinal stiffeners of a flat plate.

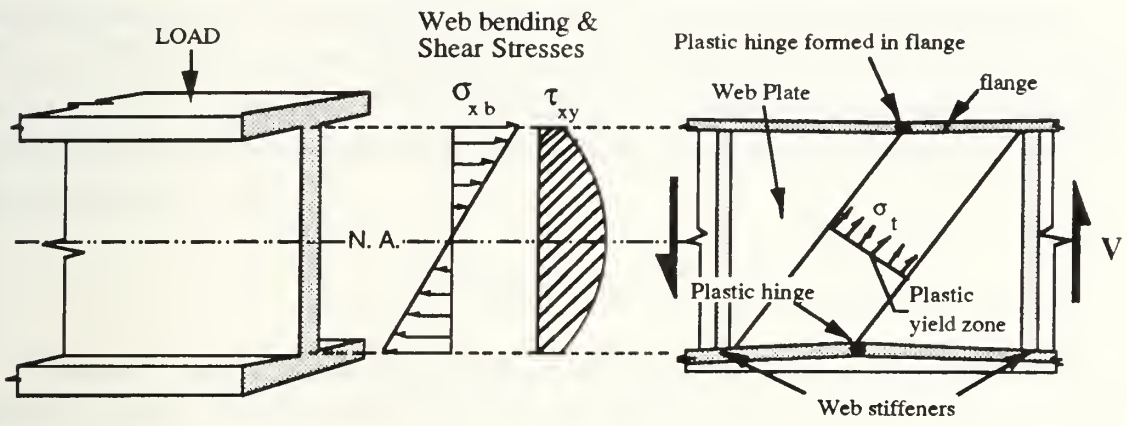

Figure 2: Failure Model for Symmetrical Girder Loaded in Shear

The plate girder experiments and analyses conducted by Rockey, Evans, Porter, and Skaloud give some insight into the pure shear problem by illustrating with numerous photographs and contour plots how buckling of the web is induced. The web buckling mode which develops when the flanges are strong enough to resist plastic hinge formation resembles the pure shear problem although the mode shape is strongly affected by the placement of web stiffeners unlike the hull plate of a longitudinally framed ship.

The research conducted after Southwell and Skan's initial solution of the infinite plate and discussed up to this point has focused on developing an accurate value for the critical shear stress buckling coefficient K_S for plates of finite length. As discussed earlier it is proposed that for a longitudinally framed ship hull the plate length may be assumed to be infinite. Therefore, the Southwell and Skan solution for a clamped plate of infinite length is sufficient to provide the insight necessary for this hull plate buckling analysis.

3. Formulation of Analytical Models

3.1 Plastic Buckling Model

The derivation of an analytical model for plastic shear buckling is based upon the principle that the rate of external work is equal to the rate of internal energy dissipation $\dot{E}_{internal} = \dot{E}_{external}$ for a stress field satisfying equilibrium and a strain field derived from a continuous displacement field. The rate of external work applied per unit length of the plate is equal to the shearing force per unit length multiplied by the translation velocity $\dot{s}$ of one plate edge relative to the other.

$$\dot{E}_{external} = F_s \dot{s}$$

The rate of internal plastic work absorbed within the plate can be expressed in terms the internal stress and strain fields integrated over the volume.

$$\dot{E}_{int} = \int_V \sigma_{\alpha\beta} \dot{\varepsilon}_{\alpha\beta} \, dV$$

$$\dot{E}_{int} = \int_S \left[\int_{-h/2}^{h/2} \sigma_{\alpha\beta} \dot{\varepsilon}_{\alpha\beta} \, dz \right] dS$$

The Love-Kirchhoff hypothesis can be applied to this problem, giving a linear strain distribution through the thickness of the plate that depends on the curvature.

$$\varepsilon_{\alpha\beta} = \overset{o}{\varepsilon}_{\alpha\beta} + z K_{\alpha\beta}$$

The strains $\overset{o}{\varepsilon}_{\alpha\beta}$ and curvatures $K_{\alpha\beta}$ correspond to mean values through the thickness of the material. The strain rate becomes:

$$\dot{\varepsilon}_{\alpha\beta} = \dot{\overset{o}{\varepsilon}}_{\alpha\beta} + z \dot{K}_{\alpha\beta}$$

Therefore, the rate of internal plastic work can be expressed as:

$$\dot{E}_{int} = \int_S \left[\int_{-h/2}^{h/2} \sigma_{\alpha\beta} \left(\dot{\varepsilon}^{o}_{\alpha\beta} + z \, \dot{K}_{\alpha\beta} \right) dz \right] dS$$

Since $\dot{\varepsilon}^{o}_{\alpha\beta}$ and $\dot{K}_{\alpha\beta}$ are constant through the thickness of the material they can be brought outside the integral.

$$\dot{E}_{int} = \int_S \left[\dot{\varepsilon}^{o}_{\alpha\beta} \int_{-h/2}^{h/2} \sigma_{\alpha\beta} \, dz + \dot{K}_{\alpha\beta} \int_{-h/2}^{h/2} \sigma_{\alpha\beta} \, z \, dz \right] dS$$

The internal plastic work can now be expressed in terms of the membrane forces and bending moments.

$$N_{\alpha\beta} \equiv \int_{-h/2}^{h/2} \sigma_{\alpha\beta} \, dz \qquad M_{\alpha\beta} \equiv \int_{-h/2}^{h/2} \sigma_{\alpha\beta} \, z \, dz$$

$$\dot{E}_{int} = \int_S \left[\dot{\varepsilon}^{o}_{\alpha\beta} N_{\alpha\beta} + \dot{K}_{\alpha\beta} M_{\alpha\beta} \right] dS$$

The rate of plastic work for the prismatic buckling element can be written in an expanded form in terms of in-plane mean strain rates ($\dot{\varepsilon}_{xx}$, $\dot{\varepsilon}_{xy}$, $\dot{\varepsilon}_{yy}$) and mean curvature rates ($\dot{K}_{xx}$, $\dot{K}_{xy}$, $\dot{K}_{yy}$). The corresponding generalized stresses are membrane forces (N_{xx}, N_{xy}, N_{yy}) and bending moments (M_{xx}, M_{xy}, M_{yy}). For an element with plastic hinges the rate of internal plastic work is:

$$\dot{E}_{internal} = \int_S \left(N_{xx}\dot{\varepsilon}_{xx} + 2N_{xy}\dot{\varepsilon}_{xy} + N_{yy}\dot{\varepsilon}_{yy} \right) dS +$$

$$\int_S M_{xx}\dot{K}_{xx} + 2M_{xy}\dot{K}_{xy} + M_{yy}\dot{K}_{yy} + \sum_i M_o^{(i)} \dot{\theta}^{(i)} L^{(i)} \qquad (8)$$

The last term in Equation (8) corresponds to the energy dissipation in the buckling element plastic hinges where $M_o = \frac{\sigma_o t^2}{4}$ is the fully plastic bending moment, σ_o is the constant flow strength, and $\dot{\theta}^{(i)}$ is the rate of rotation at the i^{th} hinge line of length $L^{(i)}$. The plastic hinge moment M_o is actually an approximation for the von Mises plastic hinge moment assuming plane strain.

$$M_o = \frac{2\,\sigma_o t^2}{\sqrt{3}\,4}$$

The large out-of-plane distortions associated with buckling in the plastic region make it difficult to determine an exact solution for the continuous, non-linear distribution of strains within the plate. Therefore, certain assumptions are made to simplify the geometry which make it possible to formulate an approximate solution for the plate resistance in shear during plastic buckling.

3.1.1 Geometry of Buckling Model

To formulate a geometry for plastic shear buckling of the plate, a simplified buckling shape is assumed based on intuition provided from the elastic buckling solution and from experiments. Prismatic buckling elements are chosen to replace the elastic elements corresponding to one half of the longitudinal buckling wavelength 2a as shown in Figure 3.

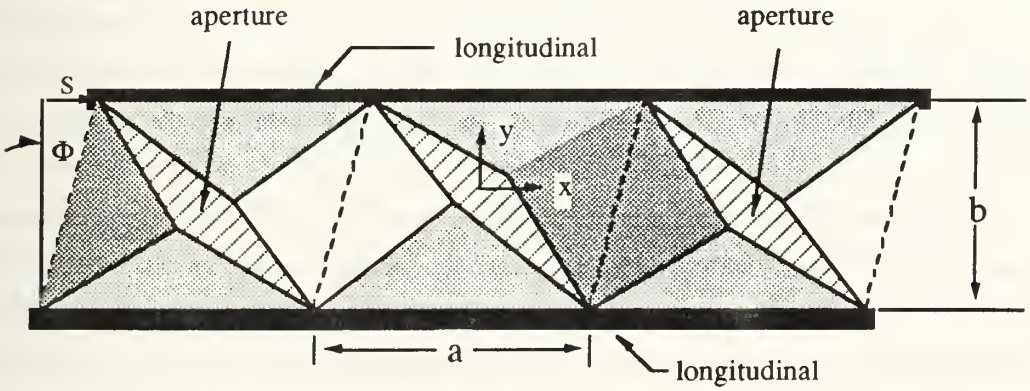

Figure 3: Prismatic buckling element model

The crossed hatched areas shown in Figure 3 indicate apertures, which do not really exist but are used to conceptually visualize the membrane stretching and shearing which must occur as the element buckles out-of-plane. The derivation of this analytical model is

based upon the geometry of a single buckling element of width b and length a and an initial angular orientation β relative to the transverse direction. The half wavelength "a" must be chosen later after analysis of both experimental and analytical buckling results. This buckling element, which is the foundation for the analytical model, is shown in Figures 4A and 4B.

The formulation for the plastic work due to element shear assumes that the out-of-plane deformations are small enough so that the relative displacements between the opposing edges of the aperture can be projected onto a horizontal plane and still accurately represent the actual relative displacements which induce shear in the element. In other words, the three dimensional nature of the aperture is not considered so that displacements which induce out-of-plane bending and torsion across the aperture can be neglected.

To obtain the deformed geometry in Figure 4B assume that the four triangular sub-elements which comprise a single buckling element retain their original shape which opens an aperture along the compressed diagonal. The entire element undergoes in-plane rotation by an angle Φ and the flat sub-elements undergo out-of-plane rotations θ_1 and θ_3 along their respective longitudinal and transverse edges. This hypothetical element with the aperture can absorb plastic work only within its plastic hinges. Then assume that to account for membrane and shear strains within the element the aperture does not exist resulting in membrane and shear strains being induced within the element which can be measured from the displacement discontinuities which exist across the aperture.

The geometric construction of this deformed geometry for the aperture rests on maintaining the bisector angles α_1 and α_2, shown in both Figures 4A and B, constant while translating the upper longitudinal edge a distance s relative to the lower longitudinal edge. The angles α_1 and α_2 are equal to $(\pi/2-\beta)$. The points P_1 and P_2 are the apex points of the aperture and also exhibit the maximum out-of-plane displacement in the deformed geometry. These points diverge from the centroid of the undeformed element during plastic shear deformation forming the aperture. Later on it will be shown that the trajectories of these "apex" points during progressive buckling must be calculated so that the total shear strain and membrane strain within the element can be determined. These trajectories are equal but opposite in sign and are shown as the vectors $+u_o$ and $-u_o$ in Figure 4.

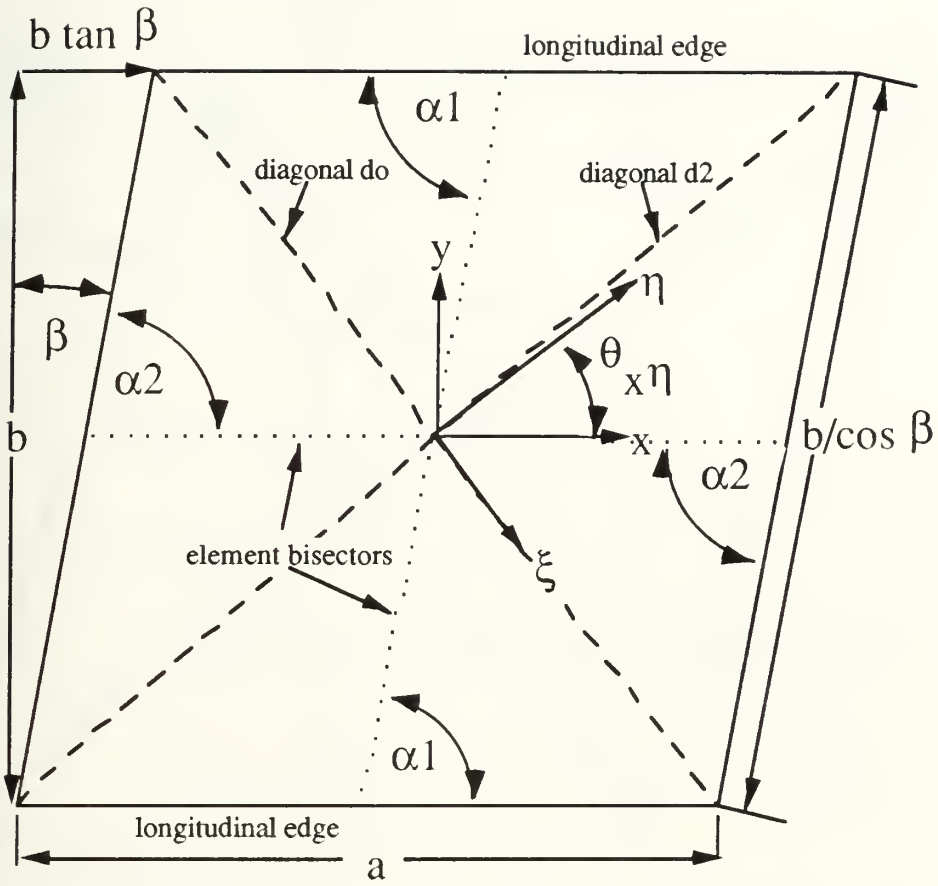

Figure 4A: Prismatic buckling element undeformed geometry

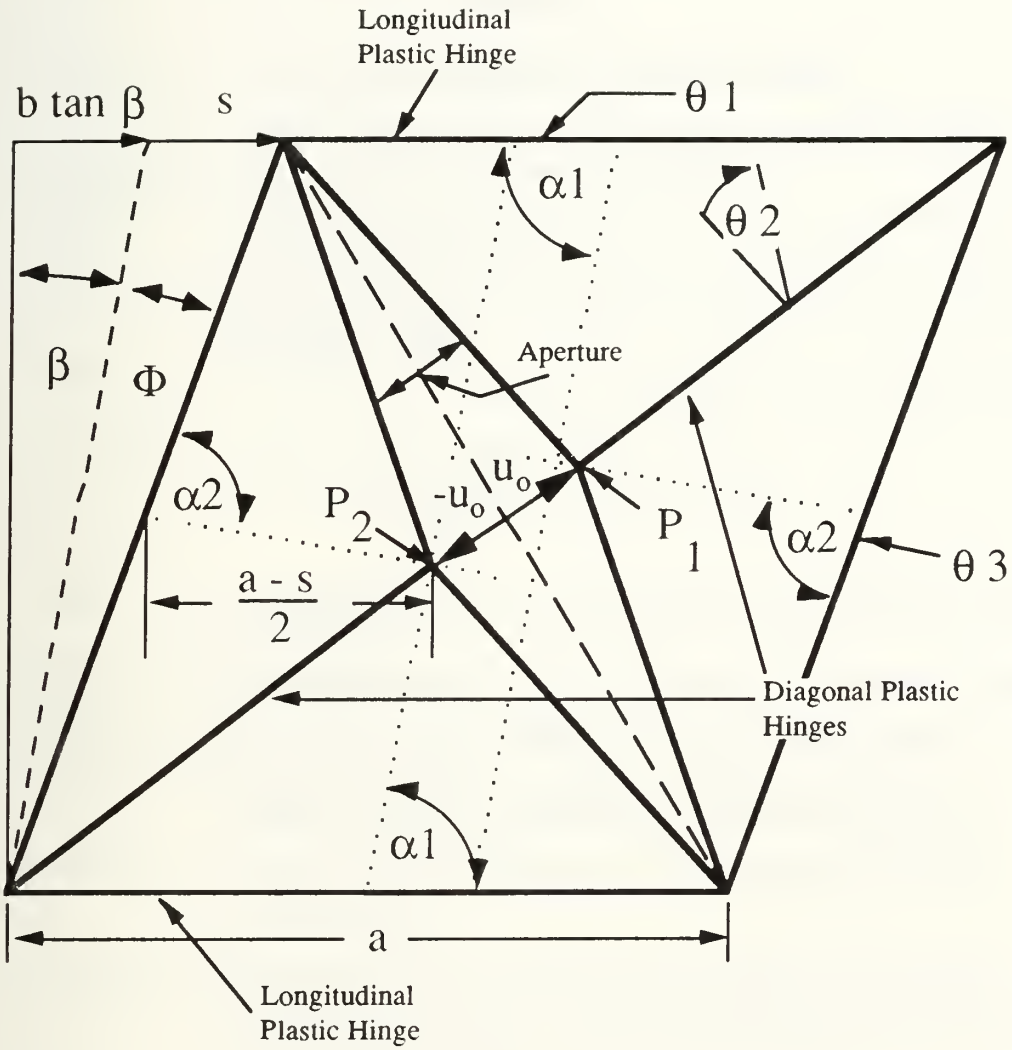

Figure 4B: Prismatic buckling element deformed geometry

Complete definitions for all parameters shown in Figures 4A and 4B are given below.

Definitions

a ---------- one half of the longitudinal buckling wavelength

b ---------- width of plate element corresponding to longitudinal spacing

(α_1, α_2) -- element bisector angles equal to ($\pi/2-\beta$)

β ---------- initial angular orientation in radians of buckling element with respect to transverse direction

s ---------- relative translation in the longitudinal direction between element longitudinal edges

Φ --------- element shear rotation angle, from Figure 3 it can be seen that:

$$\Phi = \tan^{-1}\left[\frac{s\cos(\beta)}{b/\cos(\beta)}\right] = \tan^{-1}\left[\frac{s}{b}\cos^2(\beta)\right]$$

$\pm\theta_1$ ----- out-of-plane rotation about longitudinal axis for longitudinal edge plastic hinges

$\pm\theta_2$ ----- out-of-plane angular rotation for element diagonal plastic hinges

$\pm\theta_3$ ----- out-of-plane angular rotation for element transverse edges

(x, y) ---- Cartesian coordinates with origin at element centroid and aligned with element longitudinal and transverse directions

(ξ,η) ----- local coordinates with origin at element centroid and aligned parallel and normal to aperture center axis projected onto the horizontal plane

(u_o, $-u_o$) --- displacement vectors which define the respective trajectories of apex points P1 and P2 in the horizontal plane, these vectors can be decomposed into two components in either the Cartesian or local coordinate systems, $u_o = (u_x, u_y)$ or (u_ξ, u_η)

$\theta_{x\eta}$ ------- angle measured between x and η coordinate axes, from Figure 3:

$$\theta_{x\eta} = \tan^{-1}\left(\frac{a - b\tan\beta - s}{b}\right)$$

Other variables that are not indicated in Figures 4A and B that will be used in our formulation include:

λ -------- longitudinal non-dimensional buckling half-wavelength ($\lambda = a/b$)

$\gamma_{\xi\eta}$ ------ shear strain relative to local coordinates

$\tau_{\xi\eta}$ ------ shear stress relative to local coordinates

t ------ plate thickness

S ----- surface area of element

A_o ---- maximum amplitude of aperture or distance between points P1 and P2, from Figures 4A and B:

$$A_o = | 2 u_o |$$

w_o ---- maximum out-of-plane displacement of plate at apex points P_1 and P_2

ε_η ----- strain along the η axis

M_o ---- plastic hinge moment based on von Mises criterion

$$M_o = \frac{2 \sigma_o t^2}{\sqrt{3}\ 4} \quad \text{approximated by} \quad M_o = \frac{\sigma_o t^2}{4}$$

NDSF -- non-dimensional or "normalized" shear force obtained by dividing the shear force on an element of specified length by M_o

3.1.2 Shear Strain Plastic Work

The shear strain in the buckled element has been approximated by measurement of a shear discontinuity across the aperture of the element. The relative motion in the ξ direction between the opposing edges of the aperture is utilized to measure a shear strain across the aperture which in turn can be used to approximate the shear work across the aperture that is actually distributed in a continuous fashion throughout the element.

In general, membrane deformations of thin plates involve both stretching and shear. The relative motion in the ξ direction between the opposing triangular sub-element edges which form the aperture boundaries is utilized to visualize and quantify the shear strains present within the buckled element for which there is no aperture. For the buckled element which has no aperture this motion can not occur thus inducing shear strains across the element aperture axis ξ. The first step in this formulation is to check whether or not there are any initial element orientations β such that the shear strain is zero after deformation occurs. This process will allow us to better understand the mechanism by which shear strains develop in the prismatic element.

For the shear strain to be zero, the aperture apex points P_1 and P_2 must move along a trajectory that is at all times normal to the local aperture center axis ξ. This means that

only membrane stretching must occur for the aperture edges to remain connected. For this to be true $\theta_{x\eta}$ must equal the arctangent of (u_y/u_x).

$$\theta_{x\eta} = \tan^{-1}\left(\frac{a - b\tan\beta - s}{b}\right) = \tan^{-1}\left(\frac{u_y}{u_x}\right) \qquad (9)$$

The displacements u_x and u_y can be obtained from Figure 4B:

$$u_x = \frac{s}{2}$$

$$u_y = \left(\frac{a - s}{2}\right)\tan\Phi = \left(\frac{a - s}{2}\right)\left(\frac{s}{b}\right)\cos^2\beta$$

The following relationship for zero shear can be obtained by substituting for u_x and u_y into Equation (9).

$$\frac{a - b\tan\beta - s}{b} = \frac{\left(\frac{a - s}{2}\right)\left(\frac{s}{b}\right)\cos^2\beta}{s/2} = \left(\frac{a - s}{b}\right)\cos^2\beta$$

Algebraic simplification of this no-shear condition yields:

$$(a - b\tan\beta - s) = (a - s)\cos^2\beta \qquad (10)$$

In this formulation, β can assume any value between 0 and $\pi/2$. Since the no shear condition, Equation (10), is only satisfied if $\beta = 0$, shear exists within the aperture for all $(0 < \beta < \pi/2)$.

An approximate shear strain $\gamma_{\xi\eta}$ can be defined as the angular difference between the opposing trajectories of points P_1 and P_2 shown in Figure 4B and the axis η which is normal to the aperture centerline.

$$\gamma_{\xi\eta} \equiv \left[\tan^{-1}\left(\frac{u_y}{u_x}\right) - \theta_{x\eta}\right]$$

Substituting for u_x and u_y gives:

$$\gamma_{\xi\eta} = \left[\tan^{-1}\left(\frac{(a - s)\cos^2\beta}{b}\right) - \tan^{-1}\left(\frac{a - b\tan\beta - s}{b}\right)\right]$$

In terms of the non-dimensional half-wavelength λ and element shear rotation Φ, the shear strain is:

$$\gamma_{\xi\eta} = \left[\tan^{-1}\left(\lambda\cos^2\beta - \tan\Phi\right) - \tan^{-1}\left(\lambda - \tan\beta - \frac{\tan\Phi}{\cos^2\beta}\right)\right] \qquad (11)$$

The expression for total shear strain plastic work E_s within the element is given by:

$$E_s = t\int_S \tau_{\xi\eta}\,\gamma_{\xi\eta}\,dS$$

If the additional assumption is made that the plate has isotropic material properties it can be stated that for plastic behavior:

$$\tau_{\xi\eta} = \frac{\sigma_o}{\sqrt{3}}$$

The absolute value of $\gamma_{\xi\eta}$ must be taken when making the above substitution for $\tau_{\xi\eta}$ to keep the contribution to the total work positive. The shear strain $\gamma_{\xi\eta}$ can be taken outside the integral since it is assumed to be constant across the element aperture.

$$E_s = \frac{\sigma_o\, t}{\sqrt{3}}\left|\gamma_{\xi\eta}\right|\int_S dS$$

To complete the derivation, the surface area integral must be calculated. This surface integral is the area of the aperture gap opening which is the length of diagonal d_o shown in Figure 4A multiplied by the average gap width $A_o/2$.

$$\int_S dS = \frac{A_o\sqrt{(a - b\tan\beta)^2 + b^2}}{2}$$

Therefore, the shear strain plastic work is:

$$E_s = \frac{\sigma_o t A_o}{2\sqrt{3}} |\gamma_{\xi\eta}| \sqrt{(a - b\tan\beta)^2 + b^2} \qquad (12)$$

In terms of λ and Φ, Equation (12) becomes:

$$E_s = \frac{\sigma_o t\, bA_o}{2\sqrt{3}} |\gamma_{\xi\eta}| \sqrt{(\lambda - \tan\beta)^2 + 1} \qquad (13)$$

The only unknown in Equation (13) is A_o which can easily be expressed in terms of u_x and u_y as:

$$A_o = 2\sqrt{(u_x)^2 + (u_y)^2}$$

$$A_o = 2\sqrt{\left(\frac{s}{2}\right)^2 + \left(\frac{a - s}{2}\right)^2 \left(\frac{s}{b}\cos^2\beta\right)^2}$$

$$A_o = 2\sqrt{\left(\frac{s}{2}\right)^2 + \left(\frac{(as - s^2)}{2b}\cos^2\beta\right)^2}$$

In terms of λ and Φ, A_o becomes:

$$A_o = b\sqrt{\left(\frac{\tan\Phi}{\cos^2\beta}\right)^2 + \left[\left(\lambda\frac{\tan\Phi}{\cos^2\beta} - \frac{\tan^2\Phi}{\cos^4\beta}\right)\cos^2\beta\right]^2}$$

$$A_o = \frac{b\tan\Phi}{\cos^2\beta}\sqrt{1 + (\lambda\cos^2\beta - \tan\Phi)^2} \qquad (14)$$

At this point the plastic work on a single element due to shear strains measured across a closed aperture has been calculated in terms of constant parameters and the non-dimensional variables λ and Φ. Returning to Equation (13) the rate of shear strain plastic work can be expressed as:

$$\dot{E}_s = \left(\frac{\sigma_o t\, b}{2\sqrt{3}}\sqrt{(\lambda - \tan\beta)^2 + 1}\right)\frac{d}{dt}\left[A_o\left|\gamma_{\xi\eta}\right|\right]$$

$$\dot{E}_s = \left(\frac{\sigma_o t\, b}{2\sqrt{3}}\sqrt{(\lambda - \tan\beta)^2 + 1}\right)\left[A_o\left|\dot{\gamma}_{\xi\eta}\right| + \dot{A}_o\left|\gamma_{\xi\eta}\right|\right]$$

The component of normalized shear force per unit length in the longitudinal direction due to aperture shear strain is obtained by dividing $\dot{E}_s$ by the shear velocity $\dot{s}$, the plastic hinge moment M_o, and the element length a, substituting the above and rearranging:

$$\frac{NDSF_s}{\text{unit length}} \equiv \frac{\dot{E}_s}{\dot{s}\, M_o\, a} = \frac{\dot{E}_s \cos^2\beta \cos^2\Phi}{\dot{\Phi} b\, M_o\, a}$$

$$\frac{NDSF_s}{\text{unit length}} = \left[\frac{\sigma_o t\, b\sqrt{(\lambda - \tan\beta)^2 + 1}\,\cos^2\beta\cos^2\Phi}{2\sqrt{3}\,\dot{\Phi}\, b\left(\frac{\sigma_o t^2}{4}\right)a}\right]\left[A_o\left|\dot{\gamma}_{\xi\eta}\right| + \left|\gamma_{\xi\eta}\right|\dot{A}_o\right]$$

$$\frac{NDSF_s}{\text{unit length}} = \left(\frac{2\cos^2\beta\cos^2\Phi}{\sqrt{3}\, bt\,\lambda\dot{\Phi}}\right)\sqrt{(\lambda - \tan\beta)^2 + 1}\,\left[A_o\left|\dot{\gamma}_{\xi\eta}\right| + \left|\gamma_{\xi\eta}\right|\dot{A}_o\right]$$

$$\frac{NDSF_s}{\text{unit length}} = \frac{2\cos^2\beta\cos^2\Phi}{\sqrt{3}\, t}\sqrt{\left(1 - \frac{\tan\beta}{\lambda}\right)^2 + \frac{1}{\lambda^2}}\,\left[\left(\frac{A_o}{b}\right)\frac{\left|\dot{\gamma}_{\xi\eta}\right|}{\dot{\Phi}} + \left|\gamma_{\xi\eta}\right|\left(\frac{\dot{A}_o}{\dot{\Phi}\, b}\right)\right] \qquad (15)$$

Equation (15) expresses the shear strain component of the non-dimensional shear force per unit length in a form suitable for calculations using a spreadsheet. In order to perform

these calculations, the three non-dimensional parameters inside the brackets of Equation (15) must be determined by separate calculations. These parameters are defined as:

(1) $\frac{A_o}{b}$ --- ratio of maximum aperture opening to plate width

(2) $\frac{|\dot{\gamma}_{\xi\eta}|}{\dot{\Phi}}$ --- ratio of shear strain rate to shear rotation rate

(3) $\frac{\dot{A}_o}{\dot{\Phi} b}$ --- ratio of aperture opening velocity to the shear translation velocity difference between plate longitudinal edges at $\beta = 0$ and small Φ

From Equation (14):

$$\frac{A_o}{b} = \frac{\tan\Phi}{\cos^2\beta}\sqrt{1 + \left(\lambda \cos^2\beta - \tan\Phi\right)^2} \qquad (16)$$

The time rate of change of the maximum aperture gap (14) is:

$$\dot{A}_o = \frac{d}{dt}(A_o) = \frac{b\,\dot{\Phi}}{\cos^2\beta\,\cos^2\Phi}\left[\frac{2\tan^2\Phi - 3\lambda\tan\Phi\cos^2\beta + \lambda^2\cos^4\beta + 1}{\sqrt{\tan^2\Phi - 2\lambda\tan\Phi\cos^2\beta + \lambda^2\cos^4\beta + 1}}\right]$$

Therefore:

$$\frac{\dot{A}_o}{\dot{\Phi}\, b} = \frac{1}{\cos^2\beta\,\cos^2\Phi}\left[\frac{2\tan^2\Phi - 3\lambda\tan\Phi\cos^2\beta + \lambda^2\cos^4\beta + 1}{\sqrt{\tan^2\Phi - 2\lambda\tan\Phi\cos^2\beta + \lambda^2\cos^4\beta + 1}}\right] \qquad (17)$$

Equation (11) gives:

$$\left|\dot{\gamma}_{\xi\eta}\right| = \left|\frac{d}{dt}\gamma_{\xi\eta}\right| = \dot{\Phi}\sec^2\Phi\left|\frac{1}{\cos^2\beta\left[1 + \left(\lambda - \tan\beta - \frac{\tan\Phi}{\cos^2\beta}\right)^2\right]} - \frac{1}{1 + \left(\lambda\cos^2\beta - \tan\Phi\right)^2}\right|$$

$$\frac{\left|\dot{\gamma}_{\xi\eta}\right|}{\dot{\Phi}} = \sec^2\Phi \left| \frac{1}{\cos^2\beta\left[1+\left(\lambda - \tan\beta - \frac{\tan\Phi}{\cos^2\beta}\right)^2\right]} - \frac{1}{1+\left(\lambda\cos^2\beta - \tan\Phi\right)^2} \right| \qquad (18)$$

Equations (15), (16), (17), and (18) are utilized to calculate the shear strain component of the normalized shear force on a spreadsheet. The results of these calculations are presented in Chapter 5 and the calculations themselves are included in Appendix B.

3.1.3 Membrane Strain Plastic Work

To determine the membrane strain contribution to the internal plastic work, a principal coordinate system (ξ, η) is chosen such that ε_η is aligned with the element's stretched diagonal d_2 shown in Figure 4A. The component $\varepsilon_\xi = 0$ so that the membrane plastic work becomes:

$$\dot{E}_m = \int_S N_o\, \dot{\varepsilon}_\eta \, dS$$

To determine ε_η, the cross section of the element along the stretched diagonal d_2 must be examined as shown in Figure 5.

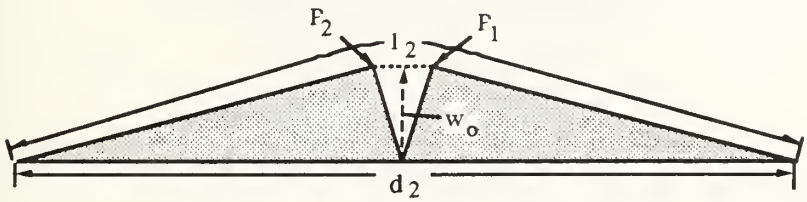

Figure 5 Element stretched diagonal cross section

The membrane strain ε_η can be determined in terms of the original stretched diagonal length d_o and the final arc length of the membrane l_2 along the stretched diagonal. Figure 4B gives the dimensions necessary to calculate d_o and d_2.

$$d_o^2 = (a + b\tan\beta)^2 + b^2$$

$$d_2^2 = (a + s + b\tan\beta)^2 + b^2$$

The arc length of the out-of-plane membrane l_2 can be determined from Figure 5.

$$\left(\frac{l_2}{2}\right)^2 = w_o^{\,2} + \left(\frac{d_2}{2}\right)^2$$

$$l_2^{\,2} = 4w_o^{\,2} + \left(a + s + b\tan\beta\right)^2 + b^2$$

The Green-Lagrange strain then becomes:

$$\varepsilon_\eta = \frac{1}{2}\left[\frac{l_2^{\,2} - d_o^{\,2}}{d_o^{\,2}}\right] = \frac{1}{2}\left[\frac{4w_o^{\,2} + \left(a + s + b\tan\beta\right)^2 - \left(a + b\tan\beta\right)^2}{\left(a + b\tan\beta\right)^2 + b^2}\right] \qquad (19)$$

The terms in the Equation (19) can be expanded and then simplified to obtain the following expression for the membrane strain.

$$\varepsilon_\eta = \frac{1}{2}\left[\frac{4w_o^{\,2} + 2as + s^2 + 2bs\tan\beta}{a^2 + 2ab\tan\beta + b^2\tan^2\beta + b^2}\right]$$

The time rate of change of the membrane strain becomes:

$$\dot{\varepsilon}_\eta = \frac{1}{2}\left[\frac{8w_o\dot{w}_o + 2a\dot{s} + 2s\dot{s} + 2b\tan\beta\,\dot{s}}{a^2 + 2ab\tan\beta + b^2\tan^2\beta + b^2}\right]$$

The rate of membrane strain plastic work can now be calculated. For a rigid-perfectly plastic material the normal force to the applied stress per unit length $N_o = \sigma_o t$. An additional observation can be made that at any cross section cut parallel to the stretched diagonal d_2 the triangular sections are all similar triangles. Due to this fact, the ratio of the plate surface arc length to the original flat diagonal length at every cross section is the same. Therefore, the membrane strain is spatially constant throughout the plate and only varies with time. The rate of incremental strain energy absorbed by a small incremental area dS

within the aperture due to membrane stresses is $d\dot{E}_m = \sigma_o \dot{\varepsilon}_\eta \, t \, dS$. The rate of membrane strain plastic work per unit length of plate is:

$$\dot{E}_m = \int_S N_o \dot{\varepsilon}_\eta \, dS = t \, \sigma_o \dot{\varepsilon}_\eta \int_S dS$$

For a per unit length strip of element: $\int_S dS = 1 * b$ and the rate of membrane plastic work is:

$$\dot{E}_m = t \, \sigma_o b \, \dot{\varepsilon}_\eta = \frac{t \, \sigma_o b}{2} \left[\frac{8 w_o \dot{w}_o + 2a\dot{s} + 2s\dot{s} + 2b \tan\beta \, \dot{s}}{a^2 + 2ab \tan\beta + b^2 \tan^2\beta + b^2} \right]$$

The per unit length normalized membrane resistance $NDSF_m$/unit length of the buckling element is obtained by dividing $\dot{E}_m$ by the shear translation velocity $\dot{s}$ and the plastic hinge moment M_o .

$$\frac{NDSF_m}{\text{unit length}} = \frac{\dot{E}_m}{\dot{s} \, M_o} = \frac{\dot{E}_m \cos^2\beta \cos^2\Phi}{\dot{\Phi} \, b \, M_o} = \frac{t \, \sigma_o b \, \dot{\varepsilon}_\eta \cos^2\beta \cos^2\Phi}{\dot{\Phi} b \left(\frac{\sigma_o t^2}{4} \right)}$$

Substituting for $\dot{\varepsilon}_\eta$ yields:

$$\frac{NDSF_m}{\text{unit length}} = \frac{2b \cos^2\beta \cos^2\Phi}{t} \left[\frac{8 w_o \left(\frac{\dot{w}_o}{\dot{\Phi} b} \right) + 2a \left(\frac{\dot{s}}{\dot{\Phi} b} \right) + 2s \left(\frac{\dot{s}}{\dot{\Phi} b} \right) + 2b \tan\beta \left(\frac{\dot{s}}{\dot{\Phi} b} \right)}{a^2 + 2ab \tan\beta + b^2 \tan^2\beta + b^2} \right]$$

Noting that $\dot{s} = \frac{\dot{\Phi} \, b}{\cos^2\beta \cos^2\Phi}$ and dividing the numerator by b , the denominator by b^2 and then the entire membrane non-dimensional shear expression by b yields an expression in terms of the non-dimensional wavelength λ .

$$\frac{NDSF_m}{\text{unit length}} = \frac{4}{t}\left[\frac{4\left(\frac{w_o}{b}\right)\left(\frac{\dot{w}_o}{\dot{\Phi}\, b}\right)\cos^2\beta\,\cos^2\Phi + \frac{a}{b} + \frac{s}{b} + \tan\beta}{\frac{a^2}{b^2} + 2\,\frac{a}{b}\tan\beta + \tan^2\beta + 1}\right]$$

$$\frac{NDSF_m}{\text{unit length}} = \frac{4}{t}\left[\frac{4\left(\frac{w_o}{b}\right)\left(\frac{\dot{w}_o}{\dot{\Phi}\, b}\right)\cos^2\beta\,\cos^2\Phi + \lambda + \frac{\tan\Phi}{\cos^2\beta} + \tan\beta}{\lambda^2 + 2\,\lambda\tan\beta + \tan^2\beta + 1}\right] \qquad (20)$$

To complete this derivation, two unknowns in Equation (20), w_o and $\dot{w}_o$, must first be determined. The buckled element geometry shown in Figure 6 gives the information necessary to solve for w_o.

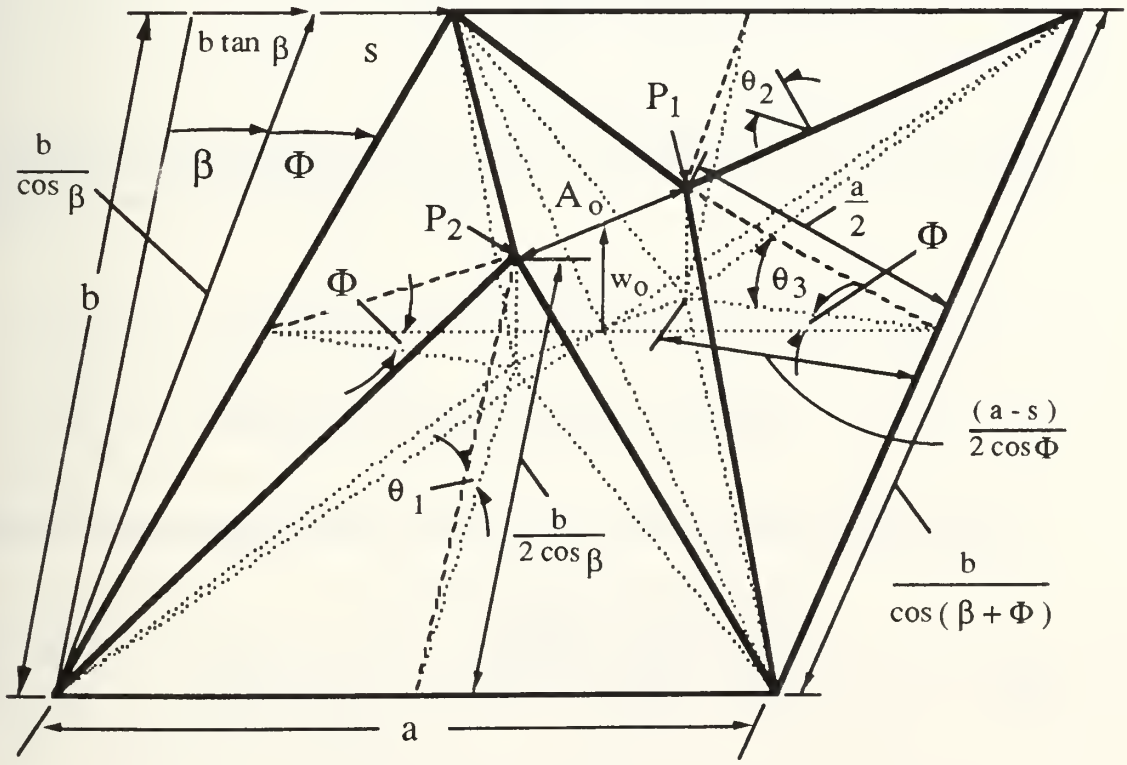

Figure 6: Upward buckled element geometry

From Figure 6:

$$w_o^{\,2} = \left(\frac{a}{2}\right)^2 - \left(\frac{a - s}{2\cos\Phi}\right)^2$$

$$w_o = \frac{1}{2}\sqrt{a^2 - \left(\frac{a - s}{\cos\Phi}\right)^2} = \frac{1}{2}\sqrt{a^2 - \left(\frac{a^2 - 2sa + s^2}{\cos^2\Phi}\right)}$$

Multiplying and dividing by b permits the following expressions for w_o and $\dot{w}_o$ to be obtained in terms of λ and Φ.

$$w_o = \frac{b}{2}\sqrt{\lambda^2 + \left(\frac{\frac{2\lambda\tan\Phi}{\cos^2\beta} - \frac{\tan^2\Phi}{\cos^4\beta} - \lambda^2}{\cos^2\Phi}\right)} \tag{21}$$

$$\dot{w}_o = \frac{b\dot{\Phi}}{4}\left[\frac{\left(\frac{2\lambda}{\cos^2\beta} - \frac{2\tan\Phi}{\cos^4\beta}\right) + \left(\frac{2\lambda\tan\Phi}{\cos^2\beta} - \frac{\tan^2\Phi}{\cos^4\beta} - \lambda^2\right)\sin(2\Phi)}{\sqrt{\lambda^2\cos^8\Phi + \left(\frac{2\lambda\tan\Phi}{\cos^2\beta} - \frac{\tan^2\Phi}{\cos^4\beta} - \lambda^2\right)\cos^6\Phi}}\right] \tag{22}$$

Equation (20) introduces two new non-dimensional parameters for the determination of the non-dimensional membrane resistance.

(1) $\frac{w_o}{b}$ --- ratio of maximum out-of-plane displacement to plate width

(2) $\frac{\dot{w}_o}{\dot{\Phi}b}$ --- normalized out-of-plane displacement velocity

These non-dimensional parameters are easily calculated from Equations (21) and (22).

$$\frac{w_o}{b} = \frac{1}{2}\sqrt{\lambda^2 + \left(\frac{\frac{2\lambda\tan\Phi}{\cos^2\beta} - \frac{\tan^2\Phi}{\cos^4\beta} - \lambda^2}{\cos^2\Phi}\right)} \tag{23}$$

$$\frac{\dot{w}_o}{\dot{\Phi} b} = \frac{1}{4}\left[\frac{\left(\frac{2\lambda}{\cos^2\beta} - \frac{2\tan\Phi}{\cos^4\beta}\right) + \left(\frac{2\lambda\tan\Phi}{\cos^2\beta} - \frac{\tan^2\Phi}{\cos^4\beta} - \lambda^2\right)\sin(2\Phi)}{\sqrt{\lambda^2\cos^8\Phi + \left(\frac{2\lambda\tan\Phi}{\cos^2\beta} - \frac{\tan^2\Phi}{\cos^4\beta} - \lambda^2\right)\cos^6\Phi}}\right] \qquad (24)$$

Equations (20), (23) and (24) are presented in a form that is particularly well suited for calculations utilizing a spreadsheet. The non-dimensional parameters, Equations (23) and (24) are calculated first for various λ and Φ. Once determined these parameters are input into Equation (20) to calculate the non-dimensional membrane resistance per unit length. The results of these calculations are presented in Chapter 5 and the calculations themselves are included in Appendix B.

3.1.4 Plastic Work due to Bending

The final component of plastic work absorbed by the prismatic buckling element is due to bending stresses and strains within the plastic hinges. It is assumed that plastic hinges are formed within an out-of-plane hinge above the stretching diagonal and along the longitudinal edges adjacent to the stiffeners. The stretching diagonal hinge is assumed to connect above the centroid of the aperture as the element deforms. However, this results in a rolling hinge due to the fact that the two halves of this hinge that are split by the aperture move in opposing directions. The plastic work associated with this rolling hinge is neglected. The concentrated twisting and bending that occurs across the aperture is also neglected.

No plastic hinges are formed at the transverse edges of the element because adjacent elements buckle out-of-plane in opposite directions, thus preventing hinge formation. This intuition is developed from observation of the elastic buckling solution presented earlier.

Note that this computational model consists of sub-elements with flat surfaces such that plate curvatures are zero.

$$\dot{K}_{xx} = \dot{K}_{xy} = \dot{K}_{yy} = 0$$

The contribution from the second term in Equation (8) to the continuous rate of plastic work dissipation vanishes. Therefore, the only contribution for the rate of plastic work due to bending is the third term of Equation (8).

$$\dot{E}_b = \sum_i M_o^{(i)} \dot{\theta}^{(i)} L^{(i)}$$

The rate of bending work for two longitudinal hinges and one diagonal hinge becomes:

$$\dot{E}_b = M_o\left[2\dot{\theta}_1 L_1 + \dot{\theta}_2 L_2\right]$$

where L_1 and L_2 are the plastic hinge lengths and θ_1 and θ_2 are the hinge rotations of the longitudinal and diagonal plastic hinges. Examination of the geometry in Figure 6 yields the following expressions for the longitudinal hinge rotation θ_1 and the transverse element boundary rotation θ_3.

$$\theta_1 = \sin^{-1}\left(\frac{w_o}{\frac{b}{2\cos\beta}}\right) = \sin^{-1}\left(\frac{2w_o\cos\beta}{b}\right)$$

$$\theta_3 = \sin^{-1}\left(\frac{w_o}{\frac{a}{2}}\right) = \sin^{-1}\left(\frac{2w_o}{a}\right)$$

The rotation of the diagonal hinge θ_2 can be solved for in terms of θ_1 and θ_3 for the geometry where $\beta = 0$ and small rotations are assumed so that the small angle approximation can be applied.

$$\theta_2 = \sqrt{\theta_1^2 + \theta_3^2} = \sqrt{\left[\sin^{-1}\left(\frac{2w_o\cos\beta}{b}\right)\right]^2 + \left[\sin^{-1}\left(\frac{2w_o}{a}\right)\right]^2}$$

The hinge rotation rates can now be expressed in terms of $\dot{w}_o$.

$$\dot{\theta}_1 = \frac{d}{dt}\left[\sin^{-1}\left(\frac{2w_o\cos\beta}{b}\right)\right] = \frac{2\left(\frac{\dot{w}_o}{b}\right)\cos\beta}{\sqrt{1 - 4\left(\frac{w_o}{b}\right)^2\cos^2\beta}} = \frac{2\dot{w}_o\cos\beta}{\sqrt{b^2 - 4w_o^2\cos^2\beta}}$$

$$\dot{\theta}_3 = \frac{d}{dt}\left[\sin^{-1}\left(\frac{2w_o}{a}\right)\right] = \frac{\frac{2\dot{w}_o}{a}}{\sqrt{1 - \left(\frac{2w_o}{a}\right)^2}} = \frac{2\dot{w}_o}{\sqrt{a^2 - 4w_o^2}}$$

$$\dot{\theta}_2 = \frac{d}{dt}\left[\sqrt{\left[\sin^{-1}\left(\frac{2w_o\cos\beta}{b}\right)\right]^2 + \left[\sin^{-1}\left(\frac{2w_o}{a}\right)\right]^2}\right]$$

Several algebraic steps are necessary to derive a simplified expression for $\dot{\theta}_2$.

$$\dot{\theta}_2 = \frac{\left(\frac{\dot{w}_o}{2}\right)\left[2\sin^{-1}\left(\frac{2w_o\cos\beta}{b}\right)\frac{\frac{2\cos\beta}{b}}{\sqrt{1-\left(\frac{2w_o\cos\beta}{b}\right)^2}}\right] + 2\sin^{-1}\left(\frac{2w_o}{a}\right)\frac{\frac{2}{a}}{\sqrt{1-\left(\frac{2w_o}{a}\right)^2}}}{\sqrt{\left[\sin^{-1}\left(\frac{2w_o\cos\beta}{b}\right)\right]^2+\left[\sin^{-1}\left(\frac{2w_o}{a}\right)\right]^2}}$$

$$\dot{\theta}_2 = 2\dot{w}_o\left[\frac{\frac{(\cos\beta/b)\sin^{-1}(2w_o\cos\beta/b)}{\sqrt{1-(2w_o\cos\beta/b)^2}} + \frac{(1/a)\sin^{-1}(2w_o/a)}{\sqrt{1-(2w_o/a)^2}}}{\sqrt{\left[\sin^{-1}\left(\frac{2w_o\cos\beta}{b}\right)\right]^2+\left[\sin^{-1}\left(\frac{2w_o}{a}\right)\right]^2}}\right]$$

$$\dot{\theta}_2 = 2\dot{w}_o\left[\frac{\frac{\cos\beta\sin^{-1}(2w_o\cos\beta/b)}{\sqrt{b^2-(2w_o\cos\beta)^2}} + \frac{\sin^{-1}(2w_o/a)}{\sqrt{a^2-(2w_o)^2}}}{\sqrt{\left[\sin^{-1}\left(\frac{2w_o\cos\beta}{b}\right)\right]^2+\left[\sin^{-1}\left(\frac{2w_o}{a}\right)\right]^2}}\right]$$

$$\dot{\theta}_2 = 2\left(\frac{\dot{w}_o}{b}\right)\left[\frac{\frac{\cos\beta\sin^{-1}\left[2\cos\beta\left(\frac{w_o}{b}\right)\right]}{\sqrt{1-4\left(\frac{w_o}{b}\right)^2\cos^2\beta}} + \frac{\sin^{-1}\left(\frac{2w_o}{\lambda b}\right)}{\sqrt{\lambda^2-4\left(\frac{w_o}{b}\right)^2}}}{\sqrt{\left\{\sin^{-1}\left[2\cos\beta\left(\frac{w_o}{b}\right)\right]\right\}^2+\left[\sin^{-1}\left(\frac{2w_o}{\lambda b}\right)\right]^2}}\right]$$

The rate of plastic work due to bending at the plastic hinges can be expressed in terms of the hinge rotation rates by Equation (25) since the longitudinal hinge length $L_1 = a$ and the diagonal hinge length L_2 can be expressed as:

$$L_2 = \sqrt{(a + b\tan\beta)^2 + b^2}$$

The total rate of bending work dissipation by the buckling element is:

$$\dot{E}_b = 2M_o a\left|\dot{\theta}_1\right| + M_o\left|\dot{\theta}_2\right|\sqrt{(a + b\tan\beta)^2 + b^2} \qquad (25)$$

The first term in Equation (25) is the rate of plastic work due to bending in the longitudinal hinges while the second term is the rate of plastic work in the diagonal hinge.

The per unit length normalized shear force component due to bending $NDSF_b$ can be obtained by dividing the rate of bending energy absorption by the shear translation velocity $\dot{s}$, the plastic hinge moment M_o, and the element length a.

$$\frac{NDSF_b}{\text{unit length}} = \frac{\dot{E}_b}{\dot{s}\, M_o\, a} = \frac{\dot{E}_b \cos^2\beta \cos^2\Phi}{\dot{\Phi}\, b\, M_o\, a}$$

$$\frac{NDSF_b}{\text{unit length}} = \cos^2\beta \cos^2\Phi \left[\frac{2\left|\dot{\theta}_1\right|}{\dot{\Phi} b} + \sqrt{\left(1 + \frac{\tan\beta}{\lambda}\right)^2 + \frac{1}{\lambda^2}}\left(\frac{\left|\dot{\theta}_2\right|}{\dot{\Phi} b}\right)\right]$$

Substituting for $\left|\dot{\theta}_1\right|$ and $\left|\dot{\theta}_2\right|$ into the expression for $NDSF_b$ yields the following result.

$$\frac{NDSF_b}{\text{unit length}} = \left(\frac{4}{b}\right)\left|\frac{\dot{w}_o}{\dot{\Phi} b}\right|\left[\frac{\cos^3\beta \cos^2\Phi}{\sqrt{1 - 4\left(\frac{w_o}{b}\right)^2 \cos^2\beta}}\right] + \ldots \qquad (26)$$

$$\left(\frac{2\cos^2\Phi \cos^2\beta}{b}\right)\sqrt{\left(1 + \frac{\tan\beta}{\lambda}\right)^2 + \frac{1}{\lambda^2}}\left|\frac{\dot{w}_o}{\dot{\Phi} b}\right|\left[\frac{\dfrac{\cos\beta \sin^{-1}\left(\frac{2w_o}{b}\cos\beta\right)}{\sqrt{1 - 4\left(\frac{w_o}{b}\right)^2\cos^2\beta}} + \dfrac{\sin^{-1}\left(\frac{2w_o}{\lambda b}\right)}{\sqrt{\lambda^2 - 4\left(\frac{w_o}{b}\right)^2}}}{\sqrt{\left[\sin^{-1}\left(\frac{2w_o}{b}\cos\beta\right)\right]^2 + \left[\sin^{-1}\left(\frac{2w_o}{\lambda b}\right)\right]^2}}\right]$$

It is interesting to note that Equation (26) contains the same non-dimensional parameters that were calculated earlier in Equations (23) and (24) for the membrane strain plastic work.

$$(1)\ \frac{w_o}{b} \qquad \text{and} \qquad (2)\ \frac{\dot{w}_o}{\dot{\Phi} b}$$

3.1.5 Total Internal Plastic Work

The shear strain, membrane strain, and bending components of the normalized shear force are added together to calculate the total non-dimensional shear force or NDSF per unit length in the longitudinal direction.

$$\frac{NDSF}{\text{unit length}} = \frac{NDSF_s}{\text{unit length}} + \frac{NDSF_m}{\text{unit length}} + \frac{NDSF_b}{\text{unit length}}$$

Equations (15), (20), and (26) form the three components of the normalized shear force per unit length of the plastic buckling model that will be extensively used in Chapter 5 for comparison with non-dimensionalized experimental results. The purpose of normalization of the shear force is to formulate a result which depends solely on the dimensional parameters of plate thickness and width as well as the non-dimensional parameters λ and Φ. Experimental results from materials of different yield strengths and plate lengths can be compared directly once the data have been normalized.

3.2 Elastic Buckling Models

The difficulty faced with determining the shear force associated with plastic buckling is that the non-dimensional plastic buckling half wavelength ($\lambda = a/b$) is unknown. Another problem which must be faced is that the plastic buckling model does not accurately predict the shear force at small Φ since the plate exhibits elastic rather than plastic behavior in this region. To overcome these difficulties it is necessary to examine the elastic behavior of the plate both before and after buckling occurs.

Plate elastic behavior at small Φ is examined in this section. The shear force required to bring about in-plane plastic flow in the plate without buckling is also formulated at the end of this chapter. Finally, in Chapter 5 a comparison is made between the results from

all analytic models and experimental results resulting in the ability to predict how λ and the normalized shear force vary over the entire range of shear rotation Φ.

The following derivations can be simplified by defining for $\beta = 0$ that $\Phi = \tan^{-1}\left(\frac{s}{b}\right)$ or for small Φ: $\Phi = \frac{s}{b}$. This is the same definition for Φ that was used earlier for an initial buckling orientation angle of zero ($\beta = 0$) and can be derived from the earlier definition by setting $\beta = 0$.

3.2.1 Elastic Pre-buckling Load

A variational approach is utilized to determine the elastic pre-buckling plate behavior. The goal of this analysis is to derive a simple relationship between the normalized shear force per unit length and the shear translation angle Φ.

It is known from elementary mechanics that $\tau_{xy} = G\gamma_{xy} = 2G\varepsilon_{xy}$ where the shear modulus, $G = \frac{E}{2(1+\nu)}$, and $\varepsilon_{xy} = \frac{1}{2}\gamma_{xy}$. The principle of virtual work relates the external work done on the plate to the internal elastic strain energy stored in the plate for a given displacement field. The external work done on plate element of area $S = ab$ by shear force F moving through a displacement δs is: $\delta W = F\,\delta s$. The internal strain energy stored within the plate element of surface area $S = ab$ is:

$$\delta U = t \int_S \tau_{xy}\,\delta\varepsilon_{xy}\,dS$$

In the elastic regime, the principle of virtual work states that the incremental work done by an external force F_e on the element is equal to the internal elastic strain energy stored within the element.

$$F_e\,\delta s = t \int_S \tau_{xy}\,\delta\varepsilon_{xy}\,dS = t \int_S 2G\varepsilon_{xy}\,\delta\varepsilon_{xy}\,dS \qquad (27)$$

Two dimensional shear strain is defined as:

$$\varepsilon_{xy} \equiv \frac{1}{2}\left[\frac{\partial u}{\partial y} + \frac{\partial v}{\partial x}\right]$$

For this analysis it is assumed that the transverse displacement $v = 0$ and that $\frac{\partial v}{\partial x} = 0$. Therefore, the shear strain is:

$$\varepsilon_{xy} = \frac{1}{2}\frac{\partial u}{\partial y}$$

The first variation of the shear strain is given by:

$$\delta\varepsilon_{xy} = \frac{1}{2}\,\delta\left(\frac{\partial u}{\partial y}\right) .$$

From the problem geometry already established, $\frac{\partial u}{\partial y} = \frac{s}{b} = \Phi$ for $\beta = 0$ and small $\frac{s}{b}$ and although Φ varies with time it is a constant within the spatial domain of the plate at any particular instant. Therefore, substituting for $\frac{\partial u}{\partial y}$ into the above expressions for ε_{xy} and $\delta\varepsilon_{xy}$ gives: $\varepsilon_{xy} = \frac{1}{2}\Phi$ and $\delta\varepsilon_{xy} = \frac{1}{2}\delta(\Phi)$. The shear strain and its first variation, ε_{xy} and $\delta\varepsilon_{xy}$, can then be substituted into Equation (27) yielding:

$$F_e\,\delta s = \frac{G\,t}{2}\int_S \Phi\,\delta\Phi\,dS = \frac{G\,t}{2}\,\Phi\,\delta\Phi\int_S dS$$

Although the plate has not yet buckled, consider a plate element of the same length a and width b as the plastic buckling element defined in the previous chapter. Therefore, the above integral for the element becomes:

$$F_e\,\delta s = \frac{G\,t\,a\,b}{2}\,\Phi\,\delta\Phi$$

The elemental shear force F_e can be expressed in terms of λ and Φ by noting that $\lambda = \frac{a}{b}$ and $\delta\Phi = \frac{\delta s}{b}$.

$$F_e\,\delta s = \left(\frac{G\,t\,\lambda\,b\,\Phi}{2}\right)\delta s \qquad\qquad F_e = \left(\frac{G\,t\,\lambda\,b}{2}\right)\Phi \qquad (28)$$

where $K_\Phi = \left(\frac{G\,t\,\lambda\,b}{2}\right)$ is the elastic pre-buckling stiffness coefficient

Equation (28) relates the shear force within the elastic range on an element of width b, length a, and thickness t to the in-plane shear rotation Φ. The term in parentheses is the element's elastic stiffness coefficient K_Φ for the pre-buckling mode of shear.

The normalized shear force per unit length can be obtained by dividing the element force F_e by the plastic hinge moment M_o and the element length a. The result is a normalized shear force $NDSF_{elastic}$ per unit length in the longitudinal direction for the elastic pre-buckled condition.

$$\frac{NDSF_{elastic}}{\text{unit length}} = \frac{F_e}{M_o\, a} = \left[\frac{G\, t\, \lambda\, b}{2\, M_o\, a}\right]\Phi = \left[\frac{G\, t}{2\, M_o}\right]\Phi \qquad (29)$$

The plastic hinge moment $M_o = \frac{\sigma_o\, t^2}{4}$ was stated earlier to be an approximation of the hinge moment for von Mises $M_o = \frac{2\,\sigma_o t^2}{\sqrt{3}\,4}$. The shear modulus $G = \frac{E}{2(1+\nu)}$. Substituting for these constants into (29) yields:

$$\frac{NDSF_{elastic}}{\text{unit length}} = \left[\frac{E}{\sigma_o\, t\,(1+\nu)}\right]\Phi \qquad (30)$$

The above expression (30) gives the final result which will be used for comparison with experimental results in Chapter 7. The stiffness coefficient for non-dimensional elastic shear per unit length becomes:

$$K_{\Phi_{ND}} = \frac{E}{\sigma_o t\,(1+\nu)}$$

3.2.2 Elastic Post-buckling Load

From this point on, to simplify notation, the element shear force and shear rotation angle at which buckling occurs are designated F_{cr} and Φ_{cr} respectively. Also, designate F_{e_B} as the elastic elemental shear force after buckling. To derive the shear force for the elastic post buckling regime, the assumption is made that the relationship between this force and the shear rotation Φ remains linear. This is reasonable to assume given the fact that the plate remains in the elastic range and the shear rotation Φ is small. The next assumption is that the elastic stiffness coefficient after buckling (for $\Phi > \Phi_{cr}$) is reduced to

half of its original value. This assumption is based on the fact that a clamped plate will lose approximately half of its elastic stiffness when it distorts out-of-plane under uniform compression. Hence it is assumed that the loss of stiffness due to buckling is the same in compression buckling and shear buckling. The above two assumptions lead to the following formulas for the buckling element shear force in the elastic range.

$$F_e = \left[\frac{G\,t\,b\,\lambda}{2}\right]\Phi \qquad \text{(element shear force prior to buckling)} \qquad (31)$$

$$F_{e_B} = F_{cr} + \left[\frac{G\,t\,b\,\lambda}{4}\right]\left(\Phi - \Phi_{cr}\right) \quad \text{(element shear force after buckling)} \qquad (32)$$

The shear rotation angle Φ_{cr} and critical buckling load F_{cr} must be substituted into (32) to solve for F_{e_B}. The critical shear force per unit length from Equation (5) is:

$$N_{xy_o} = 8.98\left[\frac{\pi^2 D}{b^2}\right]$$

The critical normalized shear force per unit length is:

$$NDSF_{cr}\text{ /unit length } = N_{xy_o}/M_o = \frac{8.98\,\pi^2\,E\,t}{3(1-\nu^2)\,\sigma_o\,b^2}$$

In order to determine the force on a single buckled element F_{cr}, the shear force per unit length N_{xy_o} must be multiplied by the element length a. Therefore, $F_{cr} = N_{xy_o} * a$.

$$F_{cr} = \frac{8.98\,\pi^2\,E\,t^3\,\lambda}{12(1-\nu^2)\,b} \qquad \text{(critical buckling force on a single buckled element)}$$

The critical shear rotation for buckling Φ_{cr} can be solved for by setting the elastic pre-buckling shear force equal to the critical buckling load.

$$F_e = \left[\frac{G\,t\,b\,\lambda}{2}\right]\Phi = \left[\frac{E\,t\,b\,\lambda}{4(1+\nu)}\right]\Phi_{cr} = \frac{8.98\,\pi^2\,E\,t^3\,\lambda}{12(1-\nu^2)\,b}$$

Therefore:

$$\Phi_{cr} = \frac{8.98\,\pi^2(1+\nu)\,t^2}{3\,(1-\nu^2)\,b^2}$$

Now that F_{cr} and Φ_{cr} have been determined these expressions can be substituted back into Equation (32) to determine the shear force F_{eB} over the entire elastic post-buckling range.

$$F_{eB} = \frac{8.98\,\pi^2 E t^3 \lambda}{12(1-\nu^2) b} + \left[\frac{E t b \lambda}{8(1+\nu)}\right]\left[\Phi - \left(\frac{8.98\,\pi^2(1+\nu) t^2}{3(1-\nu^2) b^2}\right)\right]$$

The post buckled normalized shear force, $NDSF_{el_B}$, per unit length in the elastic regime can be determined from the post-buckled shear force by dividing by M_o and the element length a.

$$\frac{NDSF_{el_B}}{\text{unit length}} = \frac{F_{e_B}}{M_o\, a}$$

$$\frac{NDSF_{el_B}}{\text{unit length}} = \frac{8.98\,\pi^2 E t}{3(1-\nu^2)\sigma_o b^2} + \left[\frac{E}{2 t \sigma_o (1+\nu)}\right]\left[\Phi - \frac{8.98\,\pi^2(1+\nu) t^2}{3(1-\nu^2) b^2}\right] \qquad (33)$$

Equation (33) is the approximate solution for the elastic post-buckling load over the entire range of $\Phi > \Phi_{cr}$. The above equation is only good as long as the plate behaves elastically. It does not predict the onset of plastic behavior. Therefore, development of a complete analytical model rests on combining the results of both the elastic and plastic models and then comparing them with experimental results to determine the range of Φ over which each model is valid. This will be addressed further in Chapter 5.

3.3 Analytical Model for Plastic Flow without Buckling

To complete this analysis the in-plane plastic flow or "no buckling plastic flow" (NBPF) mode must be addressed. This behavior is expected to occur in plates with a relatively small width to thickness (b/t) ratio for which the critical angle Φ_{cr} for elastic buckling approaches infinity as shown in Figure 7. A plot of Φ_{cr} versus b/t ratio is shown in Figure 7.

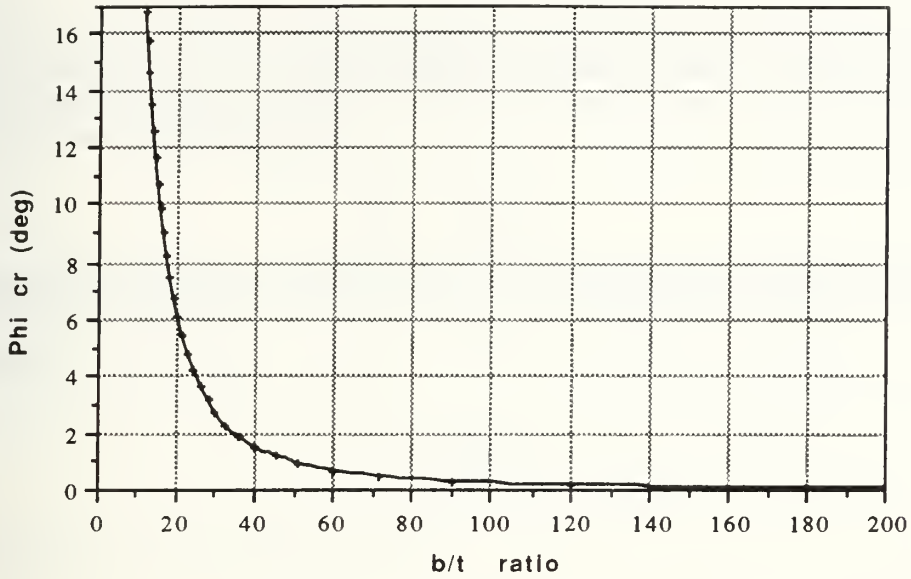

Figure 7: Critical shear rotation for elastic buckling versus b/t ratio

From Figure 7 it can be seen that Φ_{cr} increases rapidly as the b/t ratio drops. This makes sense intuitively since it is expected that thick stocky plates will have a much higher resistance to out-of-plane distortion due to their higher bending rigidity. A greater force is required to achieve the larger critical shear translation angles for buckling at low b/t ratios. Therefore, it is expected that plastic failure will occur prior to the onset of buckling for plates with relatively low b/t ratios.

The purpose of this formulation is to determine the shear force required to cause plastic failure without buckling. There are four assumptions which must be made in order to determine this stress.

(1) The boundary conditions on the plate are such that it is being loaded in uniform shear and tension along its longitudinal edges and no out-of-plane displacement or rotation occurs along the clamped edges.

* ***Note to reader:*** For pure in-plane shear of an isotropic plate with edges maintained a constant distance apart the strain ε_y in the transverse direction is zero. This follows from showing that for a displacement u in the x direction that satisfies strain-displacement, stress-strain, and equilibrium relations and is dependent only on y, with $v = w = 0$, $\varepsilon_y = 0$ is the only solution. This condition was not noticed until a more general derivation was completed and is introduced later in this formulation on page 45.

(2) This derivation assumes that for small shear strains γ_{xy} the incremental change in shear strain equals the incremental change in the shear rotation Φ. This is in contrast to the classical definition of shear strain which relates the shear strain increment to the tangent of the shear rotation Φ :

$$\Delta\gamma_{xy} = \Delta(\tan \Phi)$$

Therefore the shear strain within the plate is a constant equal to the shear translation s divided by the plate width b and the shear rotation angle Φ is small so that $\dot{\Phi} \cong \dot{s} / b$.

$$\varepsilon_{xy} = \frac{1}{2}\frac{\partial u}{\partial y} = \frac{s}{2b}$$

(3) The strain in the x direction is zero.

(4) The plate material is assumed to obey the von Mises yield condition in a plane stress (bi-axial) stress field.

$$F = \sigma_x^2 + \sigma_y^2 - \sigma_x\sigma_y + 3\tau_{xy}^2 - \sigma_o^2 = 0 \tag{34}$$

The strain rates are determined from the associated flow rule.

$$\dot{\varepsilon}_{\alpha\beta} = \dot{\kappa}\frac{\partial F}{\partial \sigma_{\alpha\beta}}$$

$$\dot{\varepsilon}_x = \dot{\kappa}\frac{\partial F}{\partial \sigma_x} = \dot{\kappa}(2\sigma_x - \sigma_y) \tag{35}$$

$$\dot{\varepsilon}_y = \dot{\kappa}\frac{\partial F}{\partial \sigma_y} = \dot{\kappa}(2\sigma_y - \sigma_x) \tag{36}$$

$$\dot{\varepsilon}_{xy} = \dot{\varepsilon}_{yx} = \frac{1}{2}\dot{\kappa}\frac{\partial F}{\partial \tau_{xy}} = 3\dot{\kappa}\tau_{xy} \tag{37}$$

The stresses σ_x , σ_y , and τ_{xy} can be solved for from the three flow rule equations. First manipulate (35) to solve for σ_y and then substitute for σ_y into (36) to solve for σ_x solely in terms of the strain rates.

$$\sigma_y = 2\sigma_x - \frac{\dot{\varepsilon}_x}{\dot{\kappa}}$$

$$\dot{\varepsilon}_y = \dot{\kappa}\left[2\left(2\sigma_x - \frac{\dot{\varepsilon}_x}{\dot{\kappa}}\right) - \sigma_x\right]$$

$$\dot{\varepsilon}_y = \dot{\kappa}\left[3\sigma_x - \frac{2\,\dot{\varepsilon}_x}{\dot{\kappa}}\right] = 3\dot{\kappa}\sigma_x - 2\,\dot{\varepsilon}_x$$

$$\sigma_x = \frac{1}{3\,\dot{\kappa}}\left(\dot{\varepsilon}_y + 2\,\dot{\varepsilon}_x\right) \tag{38}$$

The next step is to solve for σ_y in terms of the strain rates by substituting (38) into (35).

$$\dot{\varepsilon}_x = \dot{\kappa}\left[2\left(\frac{1}{3\,\dot{\kappa}}\left(\dot{\varepsilon}_y + 2\,\dot{\varepsilon}_x\right)\right) - \sigma_y\right]$$

$$\frac{\dot{\varepsilon}_x}{\dot{\kappa}} = \frac{2}{3\,\dot{\kappa}}\left(\dot{\varepsilon}_y + 2\,\dot{\varepsilon}_x\right) - \sigma_y$$

$$\sigma_y = \frac{1}{3\,\dot{\kappa}}\left(2\dot{\varepsilon}_y + \dot{\varepsilon}_x\right) \tag{39}$$

From (37) τ_{xy} can be expressed in terms of the shear strain rate.

$$\tau_{xy} = \frac{\dot{\varepsilon}_{xy}}{3\,\dot{\kappa}} \tag{40}$$

The constant $\dot{\kappa}$ can now be determined by substituting for σ_x, σ_y, and τ_{xy} into the von Mises yield condition.

$$F = \left[\frac{1}{3\,\dot{\kappa}}\left(\dot{\varepsilon}_y + 2\,\dot{\varepsilon}_x\right)\right]^2 + \left[\frac{1}{3\,\dot{\kappa}}\left(2\,\dot{\varepsilon}_y + \dot{\varepsilon}_x\right)\right]^2 - \left[\frac{1}{3\,\dot{\kappa}}\right]^2\left[\left(\dot{\varepsilon}_y + 2\dot{\varepsilon}_x\right)\left(2\dot{\varepsilon}_y + \dot{\varepsilon}_x\right)\right] + 3\left(\frac{\dot{\varepsilon}_{xy}}{3\,\dot{\kappa}}\right)^2 - \sigma_o{}^2 = 0$$

$$\left(\frac{1}{3\,\dot{\kappa}}\right)^2\left[\left(\dot{\varepsilon}_y + 2\dot{\varepsilon}_x\right)^2 + \left(2\dot{\varepsilon}_y + \dot{\varepsilon}_x\right)^2 - \left(\dot{\varepsilon}_y + 2\dot{\varepsilon}_x\right)\left(2\dot{\varepsilon}_y + \dot{\varepsilon}_x\right) + 3\left(\dot{\varepsilon}_{xy}\right)^2\right] = \sigma_o{}^2$$

Expanding and then combining terms yields:

$$\left(3\sigma_o\dot{\kappa}\right)^2 = 3\dot{\varepsilon}_y{}^2 + 3\dot{\varepsilon}_x{}^2 + 3\dot{\varepsilon}_x\dot{\varepsilon}_y + 3\dot{\varepsilon}_{xy}{}^2$$

and gives the following expression for $\dot{\kappa}$.

$$\dot{\kappa} = \frac{1}{\sqrt{3}\,\sigma_o}\sqrt{\left(\dot{\varepsilon}_y^{\,2} + \dot{\varepsilon}_x^{\,2} + \dot{\varepsilon}_x\dot{\varepsilon}_y + \dot{\varepsilon}_{xy}^{\,2}\right)} \tag{41}$$

In order to solve for the shear force applied to the plate the rate of external work applied must be equated to the rate of total internal plastic work absorbed within the plate. If F_S is defined as the shear force applied per unit length of plating then:

$$F_s\dot{s} = t\int_S \bar{\dot{e}}\, dS \qquad (S = 1 * b) \tag{42}$$

$$\bar{\dot{e}} \equiv \sigma_{\alpha\beta}\,\dot{\varepsilon}_{\alpha\beta} \quad = \text{(rate of plastic work dissipation per unit volume of material)}$$

This integral will be taken over a plate surface area of unit length so that $S = 1 * b$. For a plane stress field the rate of work dissipation can be expanded into the following form.

$$\bar{\dot{e}} = \sigma_x\dot{\varepsilon}_x + 2\tau_{xy}\dot{\varepsilon}_{xy} + \sigma_y\dot{\varepsilon}_y$$

The rate of plastic work dissipation $\bar{\dot{e}}$ can be solved for in terms of the strain rates by substituting for σ_x , σ_y , and τ_{xy} from Equations (38), (39), and (40).

$$\bar{\dot{e}} = \frac{1}{3\dot{\kappa}}\left(\dot{\varepsilon}_y + 2\dot{\varepsilon}_x\right)\dot{\varepsilon}_x + 2\left(\frac{\dot{\varepsilon}_{xy}}{3\dot{\kappa}}\right)\dot{\varepsilon}_{xy} + \frac{1}{3\dot{\kappa}}\left(2\dot{\varepsilon}_y + \dot{\varepsilon}_x\right)\dot{\varepsilon}_y$$

$$\bar{\dot{e}} = \frac{1}{3\dot{\kappa}}\left(\dot{\varepsilon}_x\dot{\varepsilon}_y + 2\dot{\varepsilon}_x^{\,2} + 2\dot{\varepsilon}_{xy}^{\,2} + 2\dot{\varepsilon}_y^{\,2} + \dot{\varepsilon}_x\dot{\varepsilon}_y\right)$$

$$\bar{\dot{e}} = \frac{2}{3\dot{\kappa}}\left(\dot{\varepsilon}_x^{\,2} + \dot{\varepsilon}_x\dot{\varepsilon}_y + \dot{\varepsilon}_y^{\,2} + \dot{\varepsilon}_{xy}^{\,2}\right)$$

Substituting for $\dot{\kappa}$ from Equation (41) into the expression for plastic work dissipation rate yields following expression.

$$\bar{\dot{e}} = \frac{2\,\sigma_o}{\sqrt{3}}\sqrt{\dot{\varepsilon}_x^{\,2} + \dot{\varepsilon}_x\dot{\varepsilon}_y + \dot{\varepsilon}_y^{\,2} + \dot{\varepsilon}_{xy}^{\,2}} \tag{43}$$

Further simplification of the expression for rate of work dissipation is achieved by applying the initial assumption that $\dot{\varepsilon}_x = 0$.

$$\bar{\dot{e}} = \frac{2\,\sigma_o}{\sqrt{3}} \sqrt{\dot{\varepsilon}_y^{\,2} + \dot{\varepsilon}_{xy}^{\,2}} \tag{44}$$

The rate of work dissipation per unit volume can now be substituted into the integral (42) for calculating the total rate of plastic work absorbed per unit length of plate.

$$F_s\dot{s} = t \int_S \bar{\dot{e}}\, dS = t \int_S \frac{2\,\sigma_o}{\sqrt{3}} \sqrt{\dot{\varepsilon}_y^{\,2} + \dot{\varepsilon}_{xy}^{\,2}}\, dS$$

The strain rates are constant over the entire region of the plate for any instant in time and can be taken outside the surface integral.

$$F_s\dot{s} = \frac{2\,t\,\sigma_o}{\sqrt{3}} \sqrt{\dot{\varepsilon}_y^{\,2} + \dot{\varepsilon}_{xy}^{\,2}} \int_S dS$$

$$F_s\dot{s} = \frac{2\,t\,\sigma_o}{\sqrt{3}} \sqrt{\dot{\varepsilon}_y^{\,2} + \dot{\varepsilon}_{xy}^{\,2}} \int_0^b \int_0^1 dx\, dy$$

The surface area integral is equal to $(1 * b)$ so that the rate of internal plastic work absorbed per unit length becomes:

$$F_s\,\dot{s} = \frac{2\,t\,b\,\sigma_o}{\sqrt{3}} \sqrt{\dot{\varepsilon}_y^{\,2} + \dot{\varepsilon}_{xy}^{\,2}}$$

* ***Note to reader:*** As noted earlier the strain rate in the y-direction turns out to be zero when the plate stiffeners are constrained to have a constant separation distance between them. Since this condition is imposed during the buckling experiments, the total internal plastic work for the in-plane plastic flow deformation mode is:

$$F_s\,\dot{s} = \frac{2\,t\,b\,\sigma_o}{\sqrt{3}}\, \dot{\varepsilon}_{xy} \tag{45}$$

To proceed further with this formulation requires establishment of an approximate geometric relationship between the strain rate $\dot{\varepsilon}_{xy}$ and the non-dimensional geometric parameter Φ. One of the initial assumptions of this formulation was that the shear strain γ_{xy} was equal to s/b. $\varepsilon_{xy} = \frac{1}{2}\frac{\partial u}{\partial y} = \frac{s}{2b}$ The shear strain rate becomes:

$$\dot{\varepsilon}_{xy} = \frac{1}{2}\frac{\partial \dot{u}}{\partial y} = \frac{\dot{s}}{2b} \equiv \frac{\dot{\Phi}}{2}$$

The rate of external plastic work applied per unit length can now be obtained by substituting for $\dot{\varepsilon}_{xy}$ into (45).

$$F_s \dot{s} = \frac{t\, b\, \sigma_o}{\sqrt{3}} \dot{\Phi} \tag{46}$$

Dividing both sides by $\dot{s}$ and noting that $\dot{s} = \dot{\Phi} b$ yields an expression for shear force per unit length.

$$F_s = \frac{t\, \sigma_o}{\sqrt{3}} \tag{47}$$

The normalized shear force per unit length for plastic deformation without buckling becomes:

$$\frac{NDSF_{NBPF}}{\text{per unit length}} = \frac{4}{\sqrt{3}\, t} \tag{48}$$

The subscript notation "NBPF" stands for "no buckling plastic flow". The above expression can now be plotted with the non-dimensional shear force for both elastic and plastic buckling and completes the series of analytical models that are used to predict actual plate behavior. A comparison with experimental results will be presented in Chapter 5.

* ***Note to reader:*** It was noted earlier that $\varepsilon_y = 0$, however, the NBPF curves representing in-plane plastic flow in Figures 8, 9, and 27 as well all Figures in Appendix B were calculated assuming that the strain rate in the y-direction ε_y was not zero. Therefore, the curve exhibits strengthening due to additional plastic work in tension while Equation (48) predicts a constant force which originates at the same level for $\Phi = 0$.

3.4 The Complete Analytical Model

In Sections 3.1 through 3.3 various analytical models have been formulated to describe the behavior of the plate as it is subjected to an in-plane shear force uniformly distributed along its clamped edges. To complete this analysis, these models must be combined in such a way that they approximate the actual plate behavior over the complete range of Φ. To accomplish this, the previously derived solutions for non-dimensional shear force (NDSF) have been entered into a computer program and plotted against the shear rotation Φ through a range of Φ from 0 - 30 degrees and for initial buckling orientation angles β from 0 to 0.6 radians. The material parameters and geometry assumed for this plate are actual parameters from the experimental setup described in chapter 4. This facilitates comparison of this analysis with experimental results.

A plot of NDSF versus Φ from 0 - 3 degrees is shown in Figure 8. The selected range for Φ is small so that the elastic pre-buckling and post-buckling behavior can be shown. Another plot over an expanded range of Φ from 0 - 30 degrees is shown in Figure 9. The following plate parameters were entered for this analysis and are the only inputs necessary for these calculations.

(1) Young's Modulus ----- E = 29,000 ksi
(2) Plate Width ---------- b = 4 inches
(3) Plate Thickness -------- t = .0284 inches
(4) Plastic Flow Stress (mean over interval from Φ = 0 - 17 degrees) -- σ_0 = 43.4 ksi
(5) Poisson's Ratio ------- ν = 0.3

From Figure 8 it can be seen that the plate first behaves elastically without buckling up to an NDSF of 40 and Φ = 0.1 degrees. The sudden change in slope of the linear elastic curve at Φ = 0.1 degrees occurs when the critical load for elastic buckling is reached. This ideal buckling analysis assumes that the plate is perfectly flat and has no initial imperfections, therefore, the actual critical buckling load is going to be lower that this ideal value. In-plane plastic flow, shown as the "NBPF" curve, occurs at an NDSF slightly above 80. Elastic buckling occurs earlier due to its lower critical buckling load. Figure 8 illustrates that the plate will proceed into plastic buckling at wavelengths that are shorter than the initial elastic buckling wavelength solved for by Southwell and Skan which corresponds to a non-dimensional half-wavelength $\lambda = (1/2*\Lambda) = 0.8$. It also appears that

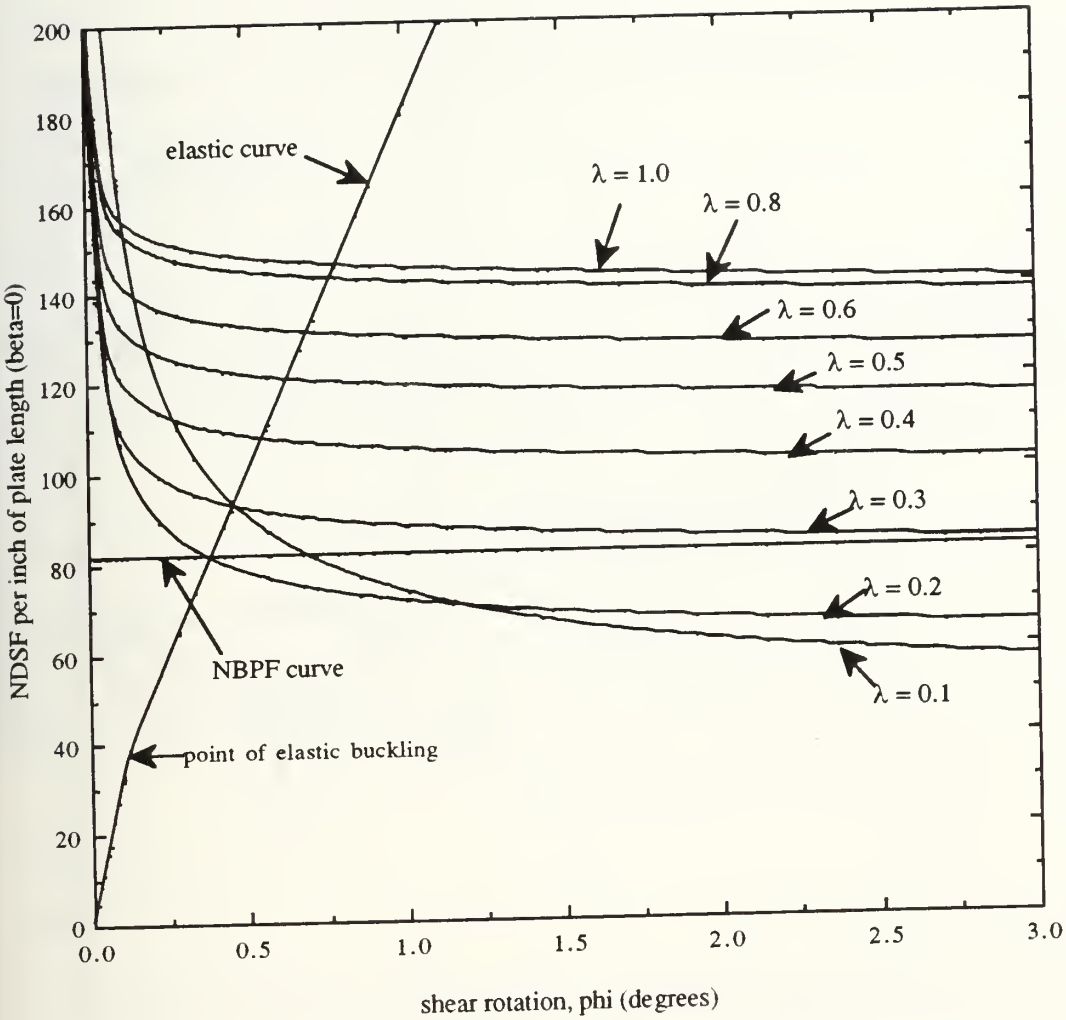

Figure 8: Non-dimensional shear force versus shear rotation angle (0-3 deg)

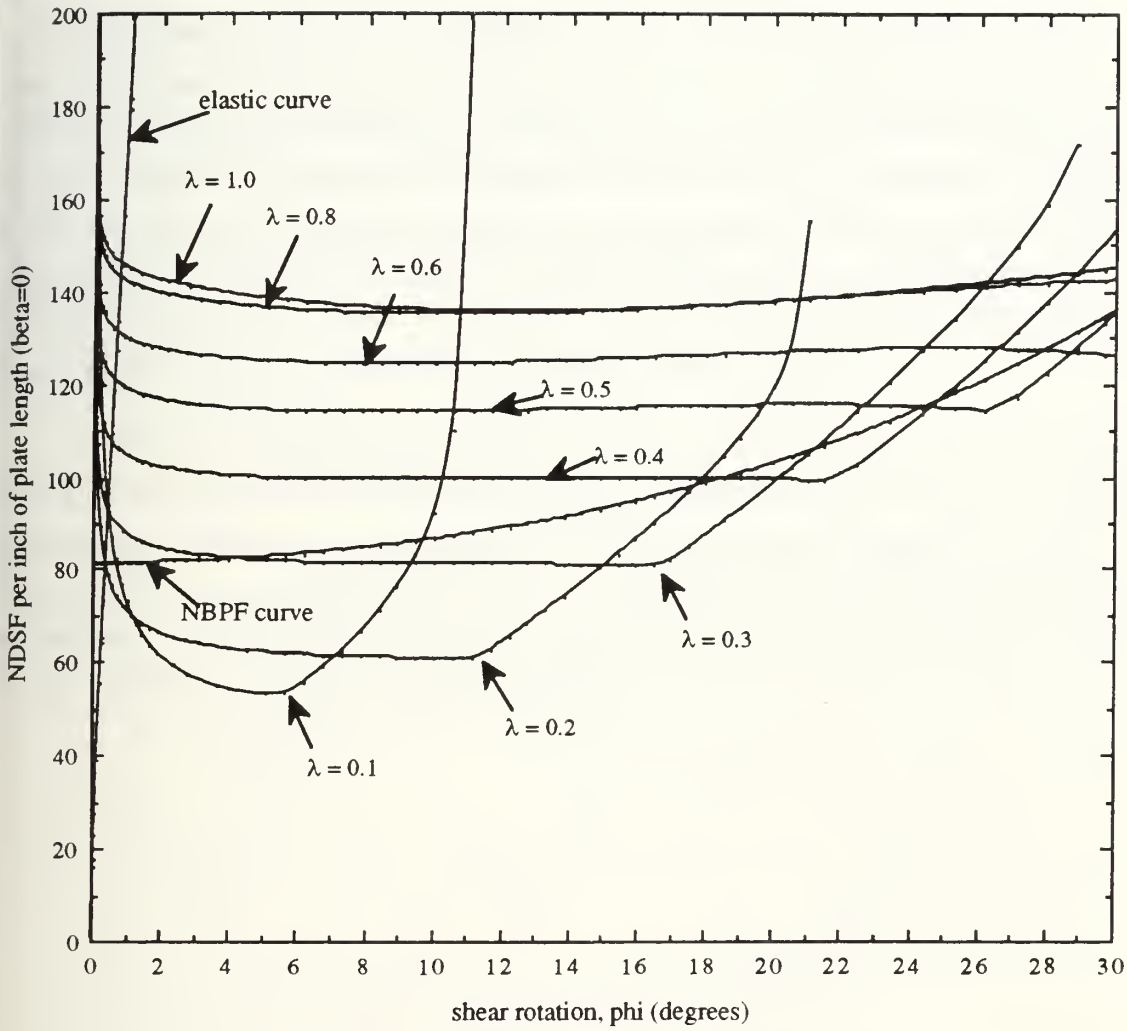

Figure 9: Non-dimensional shear force versus shear rotation angle (0-30 deg)

the initial plastic buckling half-wavelength λ for minimum resistance should be approximately 0.1, however, the plate must undergo a transition from the larger elastic buckling mode to a shorter wavelength plastic buckling mode.

Figure 9 shows the behavior of the plate over an expanded range of Φ. As Φ increases the non-dimensional shear force for the shorter wavelengths increases more rapidly than the longer wavelengths. Specifically, the wavelength corresponding to the minimum resistance buckling mode increases as the shear angle Φ increases. The in-plane plastic flow curve that assumes a buildup in tensile membrane stresses runs adjacent to but slightly above the successive minima of the plastic buckling curves corresponding to increasing values of λ. This is interesting to note since the formulation of the in-plane failure result is entirely independent of the plastic buckling formulation.

In summary, the loading trajectory initially follows the elastic pre- and post-buckling curves. It then intersects and closely follows the in-plane plastic flow curve at a normalized load slightly above 80 and then bifurcates into the specific plastic buckling curve which intersects and drops below the NBPF curve. To determine the exact behavior during these transitions, buckling experiments must be conducted that allow measurement of the actual λ observed during progressive shear buckling.

4. Discussion of Plate Shear Buckling Apparatus and Experiments

4.1 Experimental Apparatus and Setup

A reusable buckling apparatus was designed and built for the purpose of conducting in-plane shear load tests. Sheet steel specimens are bolted into a mild steel frame and yoke assembly shown in Figures 10A , 10B, and 11. The entire assembled apparatus is then attached through two 1/2 inch pin connections to an INSTRON 8501 mechanical testing machine. In-plane shear is applied to the plate by holding the yoke assembly bolted to the outer steel bar stiffeners with the upper head and pulling on the center bar stiffener with the lower head actuator.

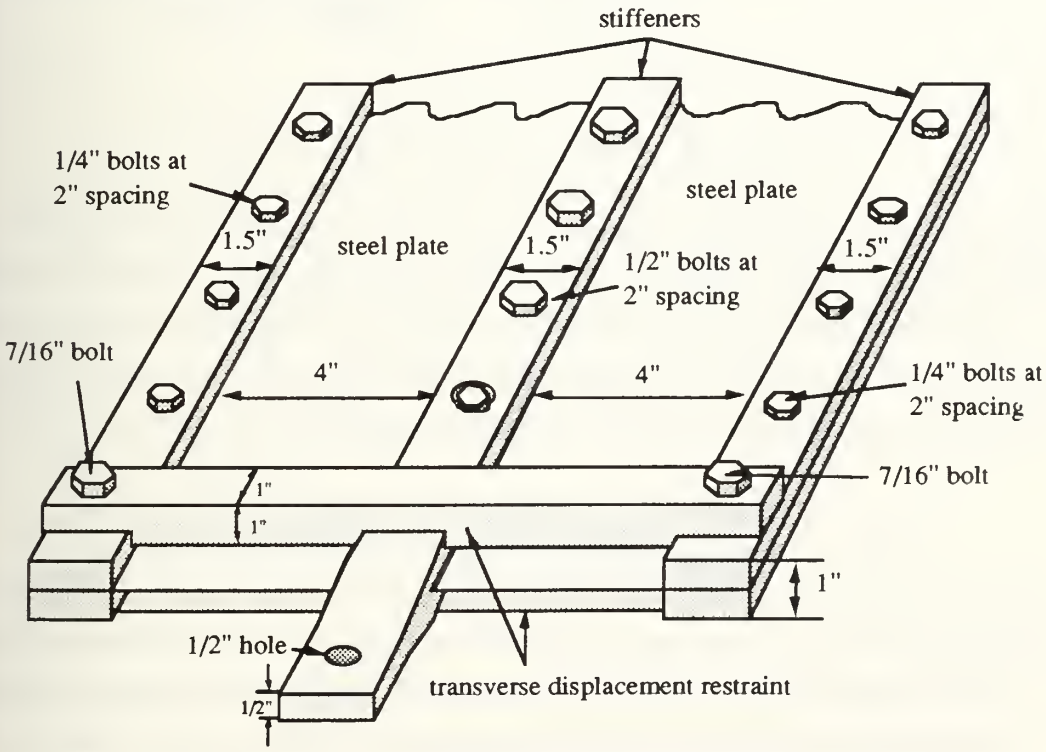

Figure 10A: Buckling apparatus (end angle view)

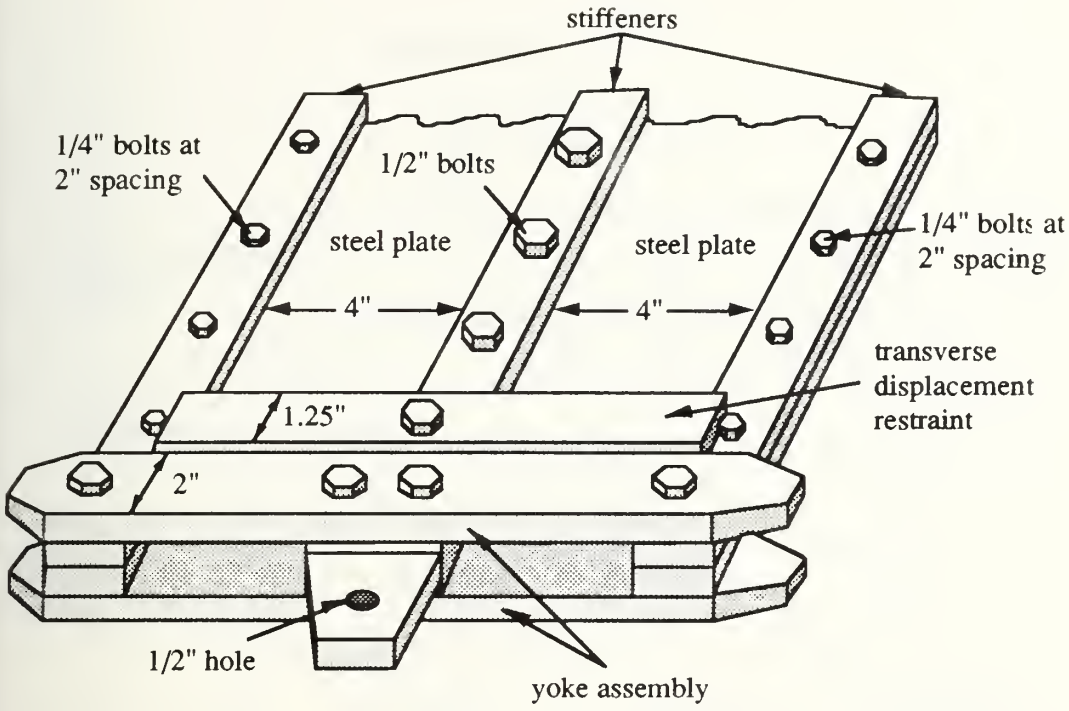

Figure 10B: Buckling apparatus (end angle view)

The outer steel stiffeners are prevented from moving closer together by cross bars bolted to the inner or outer stiffeners at each end of the apparatus. These cross members allow transverse tensile stresses to build up in the plate during buckling, while also permiting relative motion parallel to the machine loading axis between the center and outer bar stiffeners. These cross members are labeled as "transverse displacement restraints" in Figures 10A, 10B, and 11.

This steel frame is specifically designed to model the behavior of a ship's longitudinally stiffened hull plate structure subjected to in-plane shearing due to unequal longitudinal displacement of the stiffeners along each edge of the plate. This difference in longitudinal displacement between the two adjacent stiffeners causes in-plane shear to develop within the plate which can be induced by global indentation of the ship's hull structure. This hull indentation is modeled to be the result of a ship running into an underwater obstacle, such as a rocky bottom, and will be discussed further in Chapter 6.

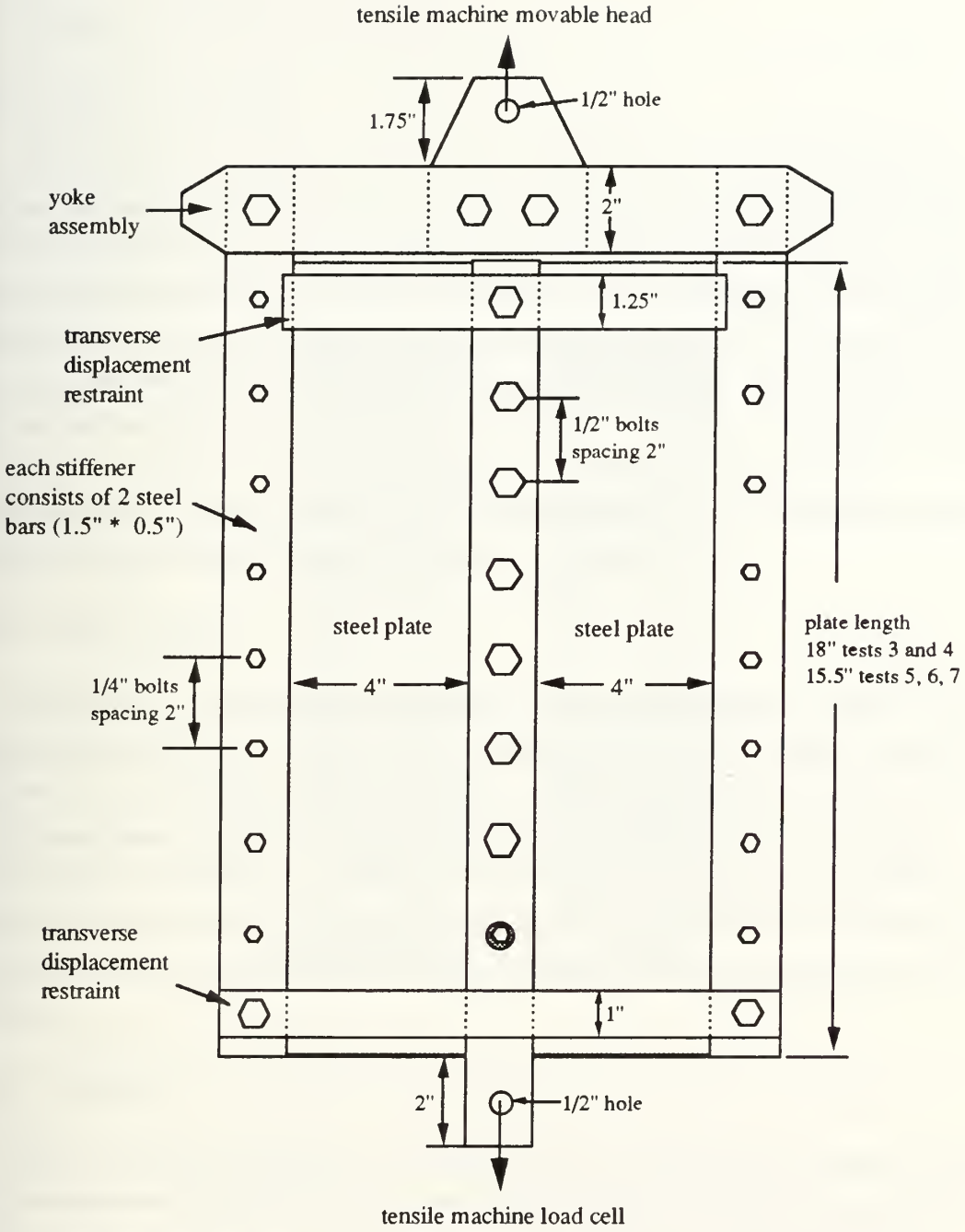

Figure 11: Buckling apparatus (plane view)

4.2 Design of Buckling Apparatus

4.2.1 Metal Test Frame

The priority for the design of the buckling test frame is that it be reusable so that various tests can be conducted on thin steel sheet metal. Another important factor is the load testing machine into which the test frame is to be fixed. The size and load carrying capacity of the tensile testing machine has dictated that the overall length of the apparatus should be no more than 24 inches for the plate thickness utilized. A final constraint is that the deflections within the test frame not be excessive at full load. This is necessary to approximate the rigid boundary conditions of the analytical model. A non-rigid frame can introduce errors in the load versus displacement test results which increase the displacements by a small amount and make the plate appear to have increased flexibility in shear buckling by allowing the plate to buckle more easily.

4.2.2 Steel Plating

The thickness of the steel plating was driven more by the thinnest the supplier had in inventory than by design concerns. Rough calculations assured that the plate would fail long before the metal frame and bolts. Another consideration is that if the plate were too thick, plastic failure would occur without buckling. This is undesirable because the purpose of the experiment is to validate the analytical model which assumes buckling. The thickness of plate chosen for the initial series of tests was 0.284 inches, which results in a theoretical critical buckling load that is well below the load for no-buckling plastic flow (NBPF).

4.2.3 Fasteners

The bolts used in this design were hardened, high strength, grade 8 fasteners. Failure of any fastener was considered unacceptable in this design due to the fact the it would interrupt the buckling test and might cause damage to the metal test frame. The high strength bolts can also take the torque necessary to apply significant pressure and increase friction between the plate surfaces and the stiffener bars. Friction between the 1/2 inch stiffener bars and the plate sandwiched in between them is considered important. Otherwise, localized failure can occur where the bolts penetrate the plate, since not enough of the shear load is distributed to the plate through friction.

4.2.4 Ball Bearing Slippage Restraint

After the first two buckling tests revealed that localized failure at the bolt holes was occurring in the center stiffener, a modification was made to the center stiffener to distribute the shear load more uniformly. This was achieved through the use of a dozen 1/4 inch ball bearings placed in 1/4 inch holes drilled into one stiffener bar to a depth of 1/8 inch while slightly larger (5/16") holes of the same depth are drilled in the other bar. The assembly of the bars with the ball bearings and steel plate sandwiched in between results in local plastic deformation of the steel plate, forcing it to conform to the surface of the ball bearings, thereby locking the steel plate in position and preventing slippage. The locations of the 1/4 inch holes drilled to a depth of 1/8 inch for the ball bearings are shown below in Figure 12.

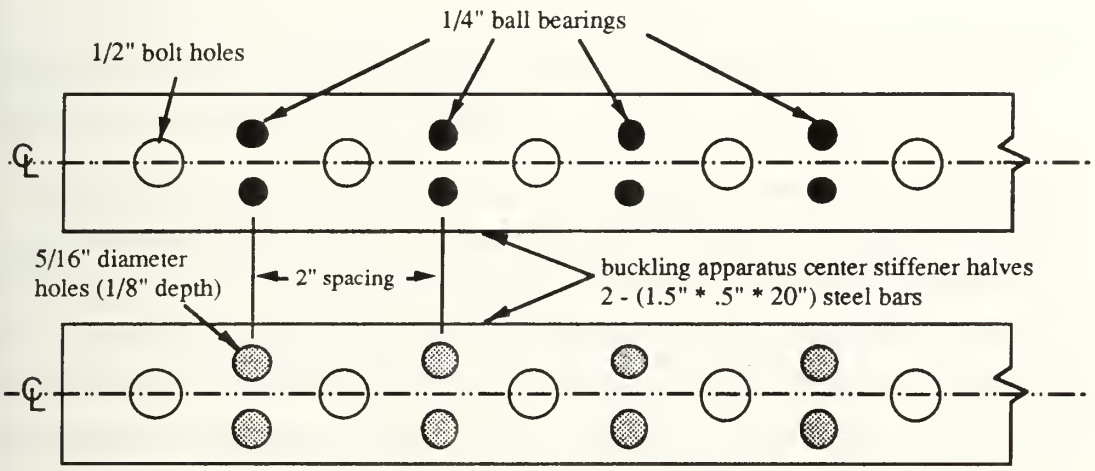

Figure 12: Ball bearing slippage restraint

Two important factors must be considered in the design of this slippage restraint. First, the twelve ball bearings should carry at least half of the load. The reasoning behind this is that the plating sandwiched between the outer stiffeners did not fail locally in the vicinity of the bolts during the first two tests. This plating is subjected to half of the load of the plating bolted to the center stiffener. Therefore, reducing the localized loading around the center stiffener bolts by one half should prevent localized failure of the plating. Second, the seven 1/2 inch bolts must be able to be torqued down with a sufficient force to plastically deform the plate over the ball bearings and cause both of the stiffener bars to come in contact with the plate.

Some preliminary calculations have been done to estimate the effectiveness of the ball bearing slippage restraints. The allowable shear of 10 kips to be held by the 12 ball

bearings gives a load of 0.833 kips/bearing. This force is transmitted from the bars through the ball bearings to the steel plating in the local vicinity surrounding the ball bearing. The diameter of the hemispherically deformed plating surrounding the ball bearing is assumed to be 5/16 inch, the diameter of the center stiffener holes into which the plate is to be pressed.

Therefore, the local stress on the plating surrounding the bolt is the shear force on the bearing divided by the circumference of the hemispherical region of plating and the plate thickness.

$$\text{Local Plate Normal Stress} \cong \frac{0.833 \text{ kips}}{\pi\left(\frac{5}{16} \text{ in}\right)(0.0284 \text{ in})} = 29.9 \text{ ksi}$$

Since this local plate normal stress is less than the plate yield stress it is assumed that no yielding will occur around the ball bearings.

The next step is to determine the mean force necessary to press the 12 ball bearings into the steel plate until both center stiffener bars are in contact with the plate. This has been accomplished by equating the external work of this mean force moving through a distance necessary to make the bars come into contact with the flat portion of plate (1/8 inch) to the plastic work necessary to obtain the local plating deformation. In order to see the mechanisms by which plastic work is done on the plate it is necessary to examine the deformed geometry of the plating surrounding the ball bearing as shown in Figure 13.

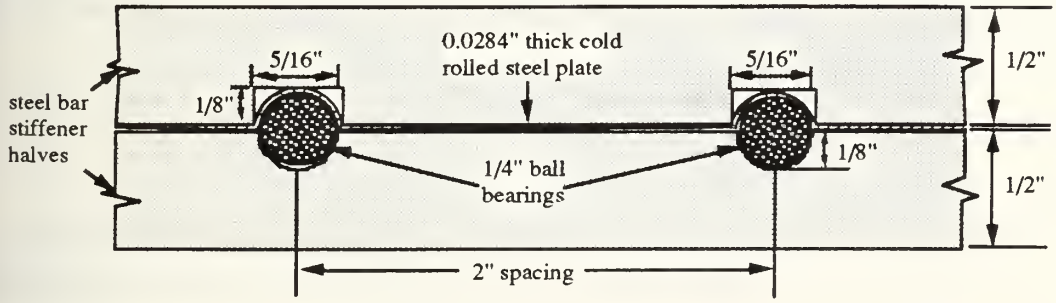

Figure 13: Cross section of ball bearing plate restraining mechanism

The plastic work done on the plating consists of two components, membrane work and bending work. The membrane work can be calculated by considering the fact that the original surface area of the plating is equal to the ball bearing maximum cross-sectional area and the final surface area is roughly equivalent to the surface area of a hemisphere of 5/16 inch diameter. If a plane stress condition is assumed everywhere in the plate, except in a 5/16 inch diameter circular plastic hinge where the plate initially deforms out-of-plane, both the bending and membrane energy contributions can be calculated.

The membrane work for plating of thickness t measured in inches becomes:

$$E_m = \sigma_o \, t \, [\text{increase in plate surface area}]$$

$$E_m = \sigma_o \, t \left[\frac{1}{2} \pi \left(\frac{1}{4} \text{ in} \right)^2 - \pi \left(\frac{1}{8} \text{ in} \right)^2 \right]$$

$$E_m = \sigma_o \, t \left[\frac{\pi}{64} \text{ in}^2 \right]$$

Assuming a plastic hinge rotation of approximately 75 degrees, the bending work becomes:

$$E_b = M_o \, \theta \, \pi \left(\frac{5}{16} \text{ in} \right) \qquad \text{where } \theta = \text{plastic hinge rotation angle} = 75^o$$

$$E_b = \left(\frac{\sigma_o t^2}{4} \right) \left(\frac{75\pi}{180} \right) \left(\pi \frac{5}{16} \text{ in} \right) = \sigma_o t^2 \left(\frac{25\pi^2}{768} \text{ in} \right)$$

The total strain energy absorbed for the plating deformed by twelve ball bearings becomes:

$$E_{int} = E_m + E_b = 12 \, \sigma_o \, t \left[\frac{\pi}{64} \text{ in}^2 + \left(\frac{25\pi^2}{768} \text{ in} \right) t \right]$$

The mean force F_m required to press the center steel stiffeners together can be obtained by equating the external work to the total strain energy .

$$F_m \, s = E_{int} = 12 \, \sigma_o \, t \left[\frac{\pi}{64} \text{ in}^2 + \left(\frac{25\pi^2}{768} \text{ in} \right) t \right]$$

$$F_m = \frac{12\,\sigma_o\,t}{s}\left[\frac{\pi}{64}\,in^2 + \left(\frac{25\pi^2}{768}\,in\right)t\right]$$

F_m can be solved for by substituting σ_o = 43.4 ksi, t = 0.0284 inch, and s = 1/8 inch.

$$F_m = 6888 \text{ lbf}$$

The force per bolt F_b for seven 1/2 inch bolts becomes:

$$F_b = \frac{F_m}{7} = 984 \text{ lbf}$$

The bolt tensile stress necessary to press the center bars together and deform the plate is obtained by dividing the force per bolt F_b by the bolt cross-sectional area.

$$\text{Bolt Stress} = \frac{984 \text{ lbf/bolt}}{\frac{\pi\,(.38")^2}{4}} = 8676 \text{ psi}$$

The above stress is much less than the maximum stress allowed for the high strength bolts, however the bolt torque necessary to achieve this stress must also be calculated to see if the bars can be pressed together solely by torquing down on them with a torque wrench.

The geometry of the 1/2 inch diameter bolt threads must be examined to calculate bolt torque. The lead of the bolt threads is the distance that the bolt moves for each turn of the threads. These bolts have 13 threads per inch so the lead is (1in/13 threads) or 0.07692 in/turn. The lead angle is defined as:

$$\theta = \text{lead angle} = \arctan\left[\frac{\text{lead}}{\pi\,(\text{thread diameter})}\right]$$

$$\theta = \arctan\left[\frac{.07692 \text{ in/thread}}{\pi\,(0.45 \text{ in})}\right] = 3.1 \text{ degrees}$$

The coefficient of friction between the bolt and nut surfaces can be assumed conservatively as $\mu_s = 0.6$. The friction angle is therefore defined as:

$$\phi_s = \arctan[\mu_s] = \arctan[0.6] = 31.0 \text{ degrees}$$

The forces acting on the bolt threads are oriented approximately 30 degrees off the bolt rotational axis for triangular shaped threads. Therefore, the axial force on the threads is equal to:

$$\text{Axial Force on Bolt Threads} = \frac{F_b}{\cos(30^\circ)}$$

A free body diagram of the forces acting on the bolt threads is shown below in Figure 14.

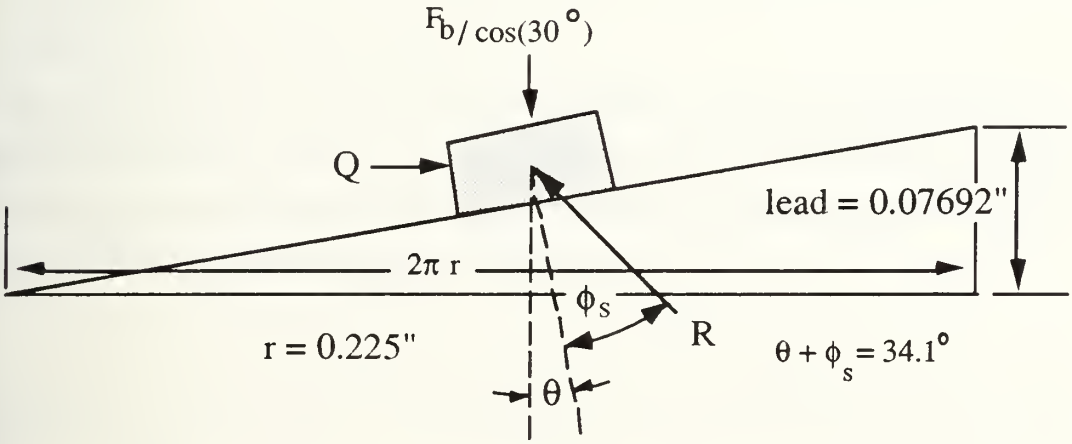

Figure 14: Bolt free body diagram

Figure 14 shows that the resultant force R and the radial force Q can be solved for by setting the summation of forces in the axial and radial directions equal to zero. The resultant force R can first be determined by setting the sum of the forces in the axial direction equal to zero.

$$R\cos(\theta + \phi_s) = \frac{F_b}{\cos(30^\circ)} \quad \rightarrow \quad R = \frac{984 \text{ lbf}}{\cos(34.08^\circ)\cos(30^\circ)} = 1372 \text{ lbf}$$

The radial force Q can now calculated for by setting the sum of forces in the radial direction equal to zero.

$$Q = R\sin(\theta + \phi_s) = (1372 \text{ lbf})\sin(34.08^\circ) = 769 \text{ lbf}$$

Now that the radial force Q has been calculated, the bolt torque can be solved for using the following formula.

$$\tau = Q\,(\text{Thread effective radius}) = 769\ \text{lbf}\,(0.225\ \text{in}) = 173\ \text{in-lbf} = 14.4\ \text{ft-lbf}$$

The bolt torque of 14.5 ft-lbf is relatively easy to achieve with a medium sized torque wrench. Therefore, it can be concluded that the center stiffener bars can be pressed together by torquing of the bolts alone.

4.3 Tensile Specimen Test Results

The stress-strain curves of both 0.0284" and 0.0262" sheet steel plates used in the buckling tests have been measured by conducting two series of tensile tests on seventeen 1/2 inch wide sheet type tensile test specimens fabricated in accordance with the ASTM, section A370 specifications and shown in Figure 15.

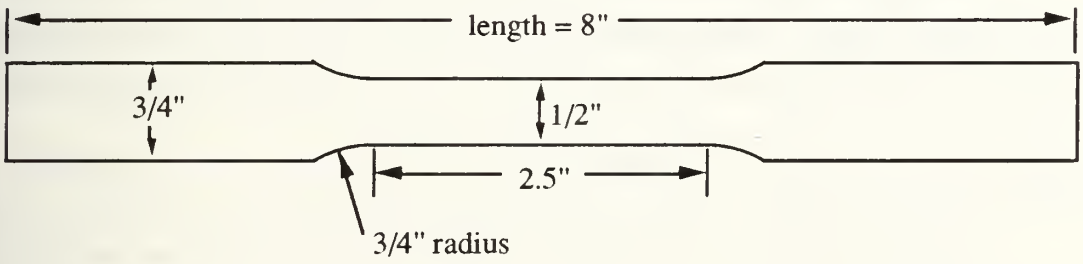

Figure 15: Tensile test specimen

Since the plate used for these experiments is cold rolled steel, a check for anisotropic mechanical behavior must be conducted. This has been accomplished on the first series of buckling tests by cutting the half the specimens parallel to and the other half perpendicular to the cold-rolled axis. For the second series of buckling tests specimens were cut parallel, perpendicular, and 45 degrees to the cold rolled axis to provide for complete data on in-plane orthotropy.

The IBM software program SYMPHONY was utilized for machine control and data recording and analysis during all phases of testing. A sampling interval of 0.1 sec was selected for the tensile tests and 1 sec for the buckling test. These sampling intervals were selected due to the fact that higher accuracy is needed during the tensile tests to accurately

letermine the yield point and because the buckling tests lasted too long (approx. 1 hour) to nake the higher sampling rate feasible due to insufficient computer memory. The buckling oad tests were conducted by using displacement rate control with a displacement ramp of).01 mm/sec. This equates to a total displacement of 36 mm in one hour which results in a arge enough shear translation to observe the full shear load capacity of the steel plate. The ensile tests were also conducted with displacement rate control but with an increased ɔositive displacement ramp of 0.05 mm/sec.

The load cell was balanced for zero load prior to each buckling test. Balancing of both he load cell and extensometer strain gage was done before each tensile test. These :alibrations have ensured that the load and strain signals are as close to zero as possible in he unloaded condition.

The output from the SYMPHONY data collection is two columns of load versus ɔercent strain data for the tensile tests. A correction factor of 0.4 had to be applied to the :aw strain data to take into account the extensometer gauge length for each of the tensile ests to give the actual percent strain. The load vs strain data was then verified by letermining Young's Modulus E for the first specimen tested. Young's Modulus E for he first specimen was measured to be 30,500 ksi providing an initial check of the data.

Two quantities are desired from each of the tensile tests. These are the 0.2% yield strength, and the average plastic flow stress measured over a strain range corresponding to he particular buckling test series. The plastic flow stress, σ_0, is that stress that is ɔostulated to be the most representative of the stresses in the plate during buckling and is herefore used to normalize the experimental buckling load data. A strain range of (0 - 6 %) was assumed for the first four buckling tests which approximately corresponds to the membrane strain along the stretched diagonal ε_η of the element due to a maximum shear rotation $\Phi_{max} \cong 20^\circ$.

$$\varepsilon_\eta = \frac{b(1/\cos\Phi - 1)}{b} = 1/\cos\Phi - 1$$

This calculation assumes that compressive normal stresses which build up in the element compressed diagonal to offset the tensile stresses are negligible due to the out-of-plane

buckling of the element along this diagonal. The maximum shear strain value $\tau_{xy} = \tan(\Phi) = \frac{s}{b}$ corresponding to the shear rotation Φ was not used due to the fact that this strain only exists throughout the plate surface if the plate remains in-plane and is not representative of the strain induced in a buckled element.

A strain range of (0 - 3 %) is assumed for the last three buckling tests corresponding to a maximum shear rotation $\Phi_{max} \cong 14^{\circ}$. The assumed maximum strains of 6 percent and 3 percent are close to the maximum stretched diagonal strains from the buckling tests shown in Table 1.

Table 1: Buckling tests maximum strain

Buckling Test	Φ Maximum (deg)	Stretched Diagonal Strain %
1	17.6	4.91
2	20.5	6.76
3	21	7.11
4	22.6	8.32
5	13.9	3.02
6	14.4	3.24
7	10.9	1.84

Average (tests 1-4): 6.78

Average (tests 5-7): 2.70

The average load over the assumed strain range is determined first for each specimen by calculating the area under the load versus strain curve for the assumed range of strain and then dividing this area by the strain range. The flow stress is then determined for each specimen by dividing this average load by the specimen cross-sectional area.

The flow stress and yield strength for both series of tensile tests are presented in Tables 2.1 and 2.2. The average yield strength and plastic flow stress are shown at the bottom of each table.

The standard deviation of the flow stress from the mean for the first series of tests is 0.83 ksi and the average flow stresses at zero degrees and 90 degrees to the cold rolled

axis are 44.15 ksi and 42.60 ksi respectively indicating some anisotropy. This level of anisotropy is considered small enough so that the mean flow stress from this series of tests can be used for normalization of the buckling test data.

Table 2.1: Tensile test results (0.0284" steel sheet)

Specimen	Knoop Hardness HK	Orientation to cold roll direction	Yield Stress (ksi)	Plastic Flow Stress (ksi)
2	129	0	38.70	44.43
4	124	0	38.13	43.68
6	123	0	38.52	44.40
8	123	0	38.47	44.10
1	122	90	37.17	42.39
3	120	90	37.92	43.03
5	119	90	37.01	42.30
7	116	90	37.70	42.68

Table 2.2: Tensile test results (0.0262" steel sheet)

Specimen	Knoop Hardness HK	Orientation to cold roll axis	Yield Stress (ksi)	Plastic Flow Stress (ksi)
1	89.7	0	32.86	34.85
2	94.3	0	33.09	35.05
3	94.3	0	33.04	34.96
4	92.7	90	31.41	34.60
5	110.7	90	51.96	49.02
6	112	90	49.43	46.60
7	95	45	34.03	35.97
8	95	45	34.00	36.10
9	94.7	45	33.74	36.23

Specimens 5 and 6 from the second test series show a yield strength and plastic flow stress that are significantly higher than all other specimens. The Rockwell Superficial Hardness of these specimens was also correspondingly greater by roughly 5 hardness units. These specimens were taken from the left over material from fabrication of the plates used in buckling tests 5 and 6 while all the other specimens were taken from a single plate that was reported by the supplier as being from the same lot of material. The measured strengths of the specimens taken from this plate were different enough to preclude use of these results for normalization of the buckling data. Therefore, only specimens 5 and 6, of the nine tensile tests using 0.0262" plate, can be utilized for normalization of the buckling test data that uses plating of this thickness. The mean values for yield strength and flow stress from Table 2.2 are unacceptable for use in the buckling tests because they include all the tests. The mean flow stress from specimens 5 and 6 to be used in buckling tests 5, 6, and 7 calculations is 47.81 ksi.

4.4 Buckling Load Test Results

Four shear buckling load tests on 0.0284" thick cold rolled sheet steel specimens and three shear buckling load tests on 0.0262" steel sheet have been conducted for comparison with the predicted load from the analysis performed in chapter 3. The output from the SYMPHONY data collection is in the form of two columns of load versus displacement data for the load tests. The displacement data from the buckling tests must be corrected due to the fact that some initial slippage always occurs within the buckling apparatus at the onset of loading. This data is corrected by determining the displacement at which the linear load curve intercepts the horizontal displacement axis and then subtracting this displacement from the raw displacement data to obtain a displacement corrected for slippage.

The first two buckling tests were conducted without a ball bearing plate slippage restraint installed in the center stiffener bars. Local plate tearing failure surrounding the center stiffener bolts during these first two tests demonstrated that torquing down on the center stiffener bolts to increase friction between the stiffener bars and the plate was not sufficient to prevent plate slippage. Some other mechanical means were needed to prevent this localized failure due to the fact that slippage, which allowed local tearing of the plate in the vicinity of the bolts, reduced the plate load carrying capacity. Therefore, although the first two buckling tests are useful in providing an indication that some kind of slippage restraint is necessary, the data itself is not useful in validating the analytical model results.

Tests 3 and 4 are conducted with the ball bearing slippage restraint in the center tiffener and the results show an increase in the overall shear resistance of the plate. Reinforcement of the center stiffener with the ball bearing slippage restraint results in educed local tearing in the center of the plate. However, the plate corners that are andwiched between the two outer edge stiffeners have started to undergo some plastic leformation and tearing that was not observed in the first two tests.

A comparison between the results from buckling tests 3 and 4 and the analytical model s made after dividing the measured force by the plastic hinge moment M_0 and then lividing again by the plate length of 18 inches to obtain a normalized shear force per unit ength in inches^{-1}. The non-dimensional results from tests 3 and 4 are plotted along with he results of the analytical models for comparison in Chapter 5.

Tests 5, 6, and 7 are conducted with a reduced plate length of 15.5" and a slightly educed plate thickness of 0.0262" in an attempt to both reduce the load on the testing nachine and revalidate the analytical model with a somewhat different plate geometry. Additionally, ball bearing slippage restraints are added to the side stiffeners in an attempt to prevent plastic deformation at the plate corners.

Tests 5, 6, and 7 demonstrated that the side stiffener slippage restraints indeed reduced he local plastic deformation at the plate corners, but increased tearing in the corners. These racks form in the vicinity of the bolt holes or ball bearing holes and propagate ongitudinally, in a direction perpendicular to the tensile stresses that build up in the ransverse direction. Therefore, the additional ball bearing slippage restraints within the dge stiffener are ineffective in accomplishing their intended purpose due to a reduction of ne local failure mode but increase of another.

The normalized loads per inch of plate length parallel to the machine loading axis from buckling tests 3 through 7 are shown in Figure 16. The shorter plates used in tests 5, 6, nd 7 lost their load resisting capacity at a lower Φ due to local cracking in the corners caused by the increased rigidity from adding ball bearing slippage restraints to the side tiffeners. The subsequent propagation of cracks from these corners further reduced the oad capacity of these plates.

Two other observations made during the buckling tests are the wavelength 2a and the nitial angle β relative to the transverse direction. The final orientation β of the buckling vaves was measured on the plates after removal from the testing machine and is between

0 and 50 degrees for all tests. The initial angle β is the difference between this final neasured angular orientation and the final angle of shear rotation Φ. For the first two tests he maximum shear rotation achieved is approximately 20 degrees which means that the nitial buckling orientation $\beta = 25$ degrees or 0.4 radians. The final plastic buckling vavelength 2a observed is approximately 2.1 inches. This equates to a $\lambda = a/b$ of 0.26.

Shortening of the plastic buckling wavelength was observed during all of the tests as ne shear deformation progressed. In an attempt to better understand the wavelength hortening phenomenon, the buckling wavelength has been measured during tests 5, 6, 7 at arious shear translation values s and plotted in non-dimensional form in Figure 17.

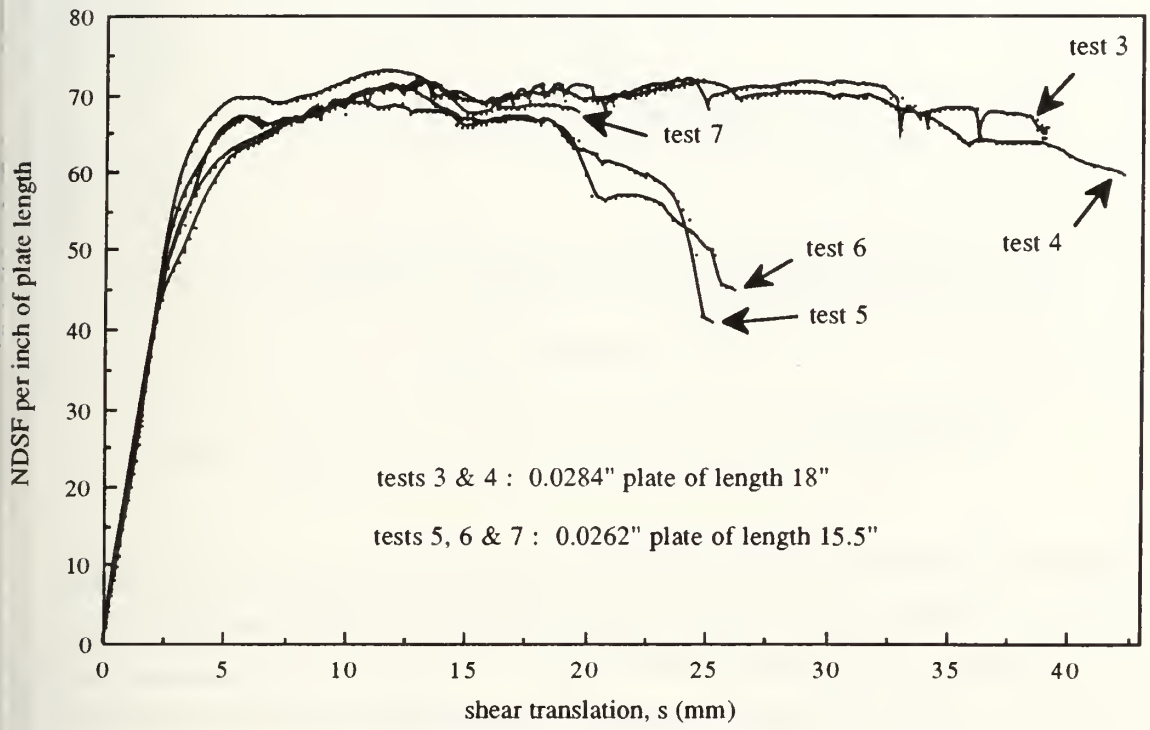

Figure 16: Normalized shear force buckling test results

For all tests the initial wavelength is between 6.5 inches and 7.0 inches. This equates) a full non-dimensional wavelength $\Lambda = 2a/b$ of 1.69 which is just slightly greater than ie elastic buckling wavelength $\Lambda = 1.6$ predicted by Southwell and Skan[5] for an finitely long flat plate with clamped edges. The fact that the initial wavelength is slightly eater than the Southwell and Skan solution can be justified by the fact that the clamped

edges of the plate are not perfectly rigid. The Southwell and Skan solution predicts a longer elastic wavelength $\Lambda = 2.67$ for simply-supported edges. Since the longitudinal supports for the plate are not perfectly rigid, the wavelength Λ should assume a value greater than the clamped but less than the simply-supported plate.

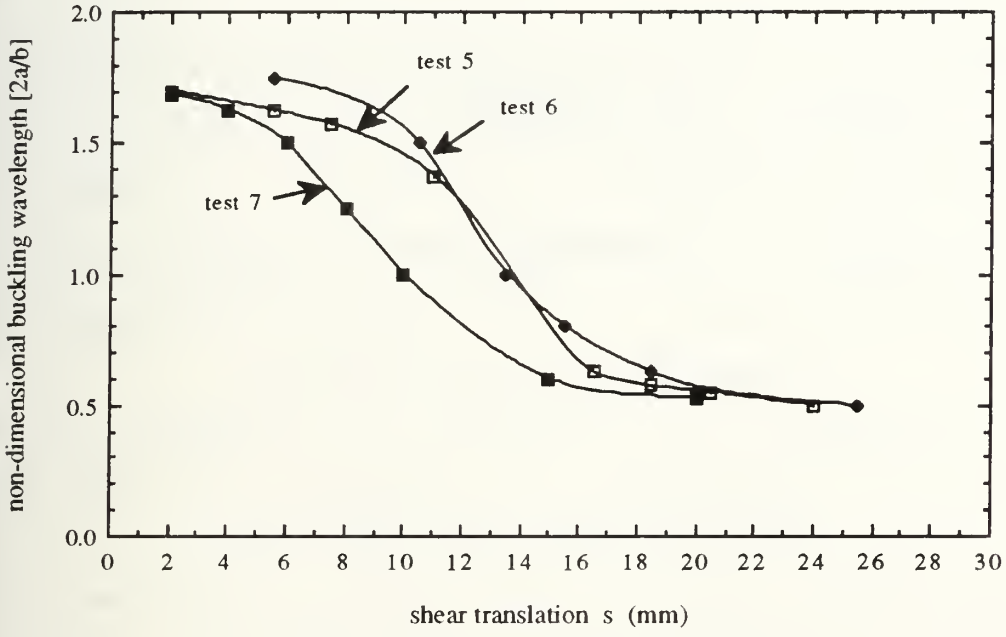

Figure 17: Observed non-dimensional buckling wavelength [2a/b]

Figure 17 shows the observed change in the non-dimensional buckling wavelength $\Lambda = 2a/b$ during tests 5, 6, and 7. Figure 17 also illustrates that a transition to a shorter buckling wavelength occurs between s values between 6 mm and 16 mm which correspond to Φ between 3.4 degrees and 9.0 degrees. The plastic buckling wavelength is initially nearly equal to the predicted elastic wavelength but slowly develops into a shorter wavelength buckling mode as s increases. This process starts when the peaks of the initial buckling waveform start to flatten out. As the shear translation continues, two new waves form on the flattened out maxima and minima of the original mode. These newly generated waves then move away from each other until a uniformly spaced buckling mode is formed with a wavelength that is one third of the original wavelength. The phases of this process are shown in Figure 18.

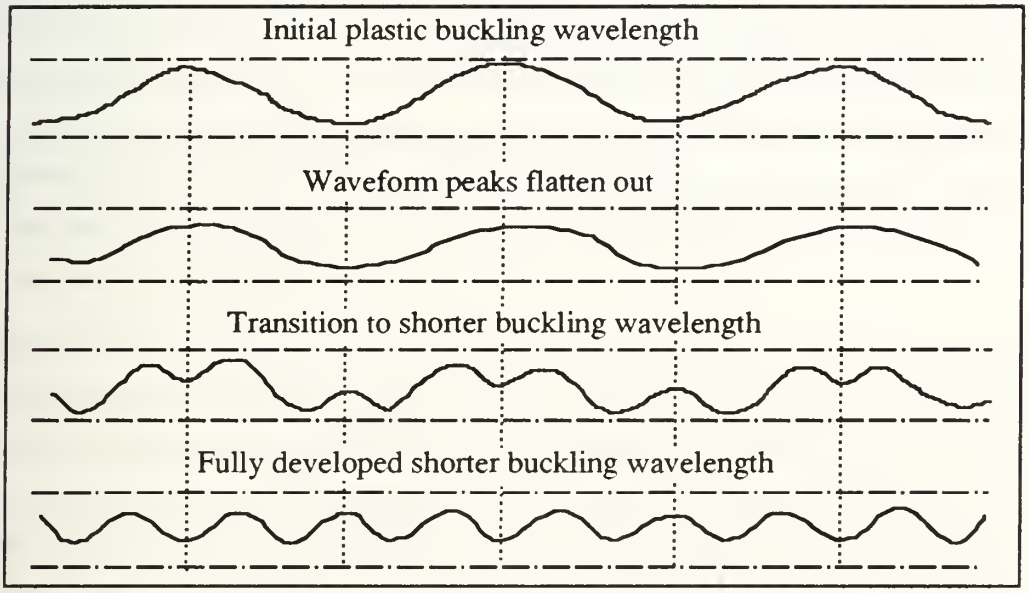

Figure 18: Buckling wavelength transition process

5. Comparison of Experimental and Analytical Results

The normalized shear force (F_S/M_O) per inch of plate length from buckling tests 3 and 4 has been plotted against the analytical models and is shown in Figures 20 and 21. The results from tests 5, 6, and 7 have already been compared with tests 3 and 4 in the previous chapter and are not plotted here but are presented in Appendix B. Figure 20 includes the plastic buckling model for ($0.1 < \lambda < 1.0$) and $\beta = 0$ radians. Figure 21 includes the plastic buckling model for $\beta = 0.4$ radians. The model for $\beta = 0.4$ is included here because the measured orientation of the buckling waves at the end of the tests is approximately 45° and subtracting the maximum shear rotation $\Phi = 20°$, obtained during tests 3 and 4, yields an initial angle β of 25° or 0.4 radians. The plastic model results calculated for β from 0.1 to 0.6 are included in Appendix B.

Figure 20 shows that the plastic buckling model for $\beta = 0$ is a good approximation for the non-dimensional shear force actually observed during the experiments. This model also predicts the transition of the plastic buckling wavelength to a shorter mode and comes very close to predicting the actual wavelength itself. Figure 20 illustrates that the NDSF curves for tests 3, and 4 fall between the NDSF curves corresponding to a half wavelength λ between 0.2 and 0.3. As stated before, the measured half-wavelength λ from these tests was approximately 0.26.

The plastic buckling curves for $\beta = 0.4$ in Figure 21 are significantly greater than the experimental results for tests 3 and 4. These results, however, have not taken into account the fact that the combination of membrane and shear stresses working together actually reduces the shear and membrane yield stresses. Up to this point the analysis has assumed that yield always occurred when membrane stresses equal σ_o and shear stresses $\tau_{xy} = \frac{\sigma_o}{\sqrt{3}}$. This is not an entirely accurate approximation because the actual yield condition is:

$$\sigma_x^2 + \sigma_y^2 - \sigma_x\sigma_y + 3\tau_{xy}^2 = \sigma_o^2$$

Since $\dot{\varepsilon}_x = \dot{\kappa}(2\sigma_x - \sigma_y)$ we can say that for $\dot{\varepsilon}_x = 0$ $\sigma_x = \frac{\sigma_y}{2}$. Therefore, the yield condition becomes:

$$\frac{3}{4}\sigma_y^2 + 3\tau_{xy}^2 = \sigma_o^2$$

Figure 19 graphically shows the relationship between membrane and shear stresses at yield. When $\tau_{xy} = 0$, $\sigma_y = \sqrt{\frac{4}{3}}\,\sigma_o$ and when $\sigma_y = 0$ $\tau_{xy} = \frac{\sigma_o}{\sqrt{3}}$.

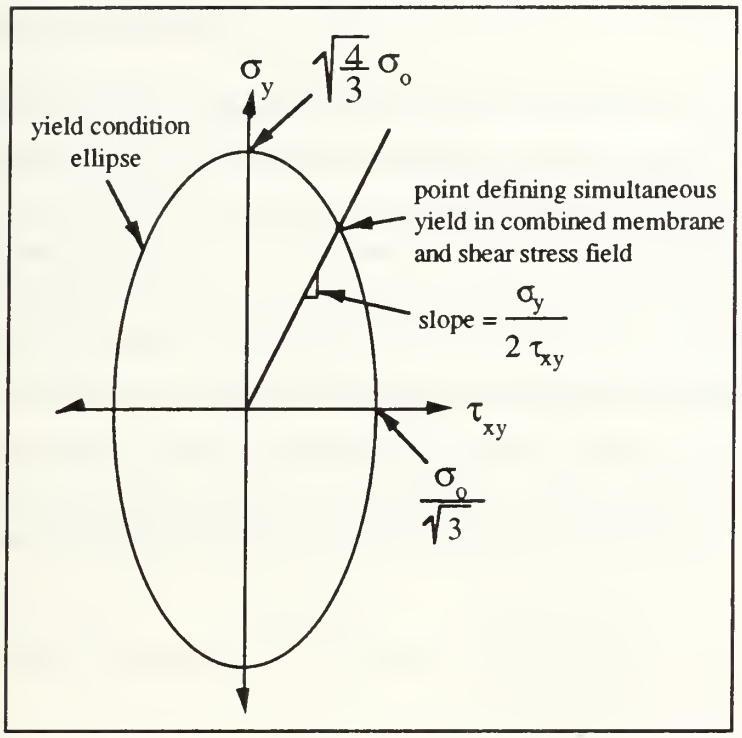

Figure 19: von Mises yield condition

The slope of the line which defines simultaneous yield in membrane and shear is:

$$\sigma_y = 2\,\tau_{xy}$$

The intersection of this line and the yield curve is representative of the stresses during buckling and can be obtained by substituting for $\sigma_y = 2\,\tau_{xy}$ into the yield condition.

$$\frac{3}{4}(2\,\tau_{xy})^2 + 3\tau_{xy}^2 = \sigma_o^2 \qquad \tau_{xy} = \frac{1}{\sqrt{6}}\,\sigma_o \qquad \sigma_y = \frac{2}{\sqrt{6}}\,\sigma_o$$

The actual values for τ_{xy} and σ_y are less than the assumed values used in the NDSF calculations by the following amounts.

$$\frac{\tau_{xy}(\text{actual})}{\tau_{xy}(\text{assumed})} = \frac{1}{\sqrt{2}} = 0.71 \qquad \frac{\sigma_y(\text{actual})}{\sigma_y(\text{assumed})} = \frac{2}{\sqrt{6}} = 0.82$$

A rough approximation for the amount of reduction in the NDSF curves for $\beta = 0.4$ of Figure 21 is approximately 25%. Even with this reduction in the NDSF buckling curves, they are still higher than the experimental data by approximately 40 NDSF units. Therefore, the $\beta = 0$ curves more accurately predict the non-dimensional shear force and associated buckling wavelength λ.

The predicted slopes of the linear elastic pre and post-buckling curves are much steeper than the actual test data due to the fact that the analytical model assumes a perfectly rigid steel frame. In fact, the buckling apparatus does have a finite amount of flexibility. This causes the actual shear translation s to increase above the values predicted by analysis. The elastic load curves for each of the tests display a break in slope between an NDSF of 40 and 50 at a shear translation of approximately 2.3 mm. This is probably the point where plastic deformation starts to occur and not the critical point of elastic buckling due to the fact that the observed onset of elastic buckling should not occur after the theoretically predicted buckling load. The predicted critical buckling normalized shear forces for elastic buckling formulated in Chapter 3 are given below for both series of tests.

$$\text{NDSF}_{cr}\text{/unit length} = N_{xy_o}/M_o = \frac{8.98\,\pi^2\,E\,t}{3(1-\nu^2)\,\sigma_o\,b^2}$$

NDSF/inch tests 3 and 4 : $38.8\ \text{in}^{-1}$

NDSF/inch tests 5, 6, and 7 : $37.1\ \text{in}^{-1}$

The no buckling plastic failure (NBPF) curve forms an upper envelope for all experimental test data since the normalized critical shear force required for plastic buckling is less than for in-plane deformation for the b/t ratio of the plating tested.

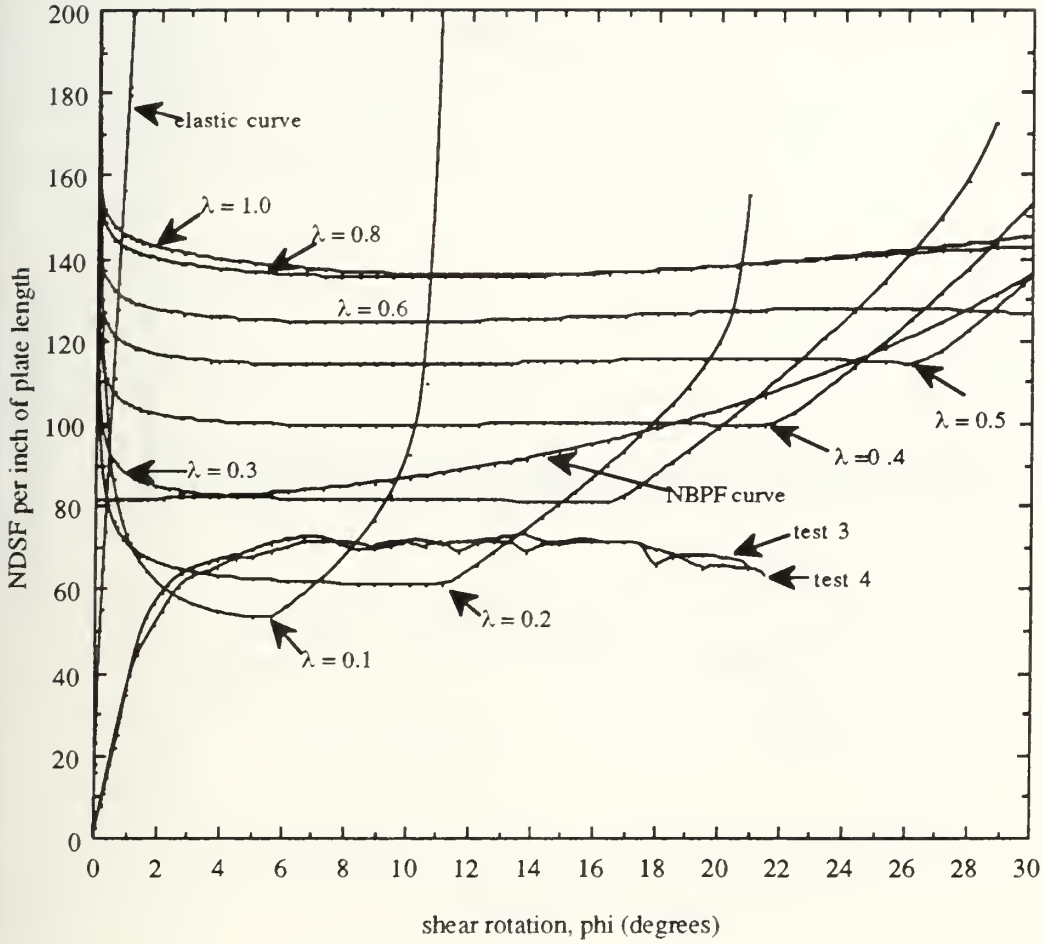

Figure 20: Comparison of analytical and experimental results (beta = 0)

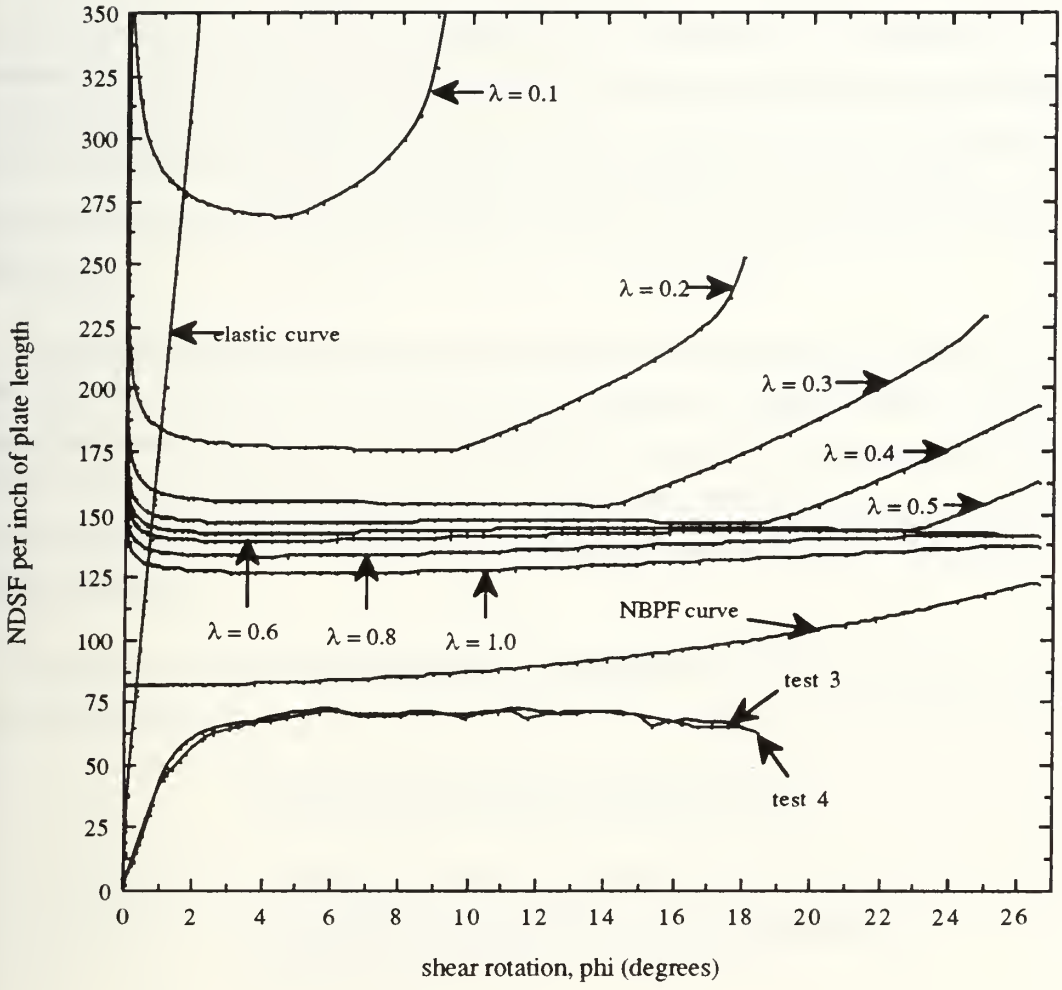

Figure 21: Comparison of analytical and experimental results (beta = 0.4)

6. Formulation of total grounding resistance due to shear

6.1 The Grounding Model

The previous five chapters have focused on the development and experimental validation of a plastic shear buckling model for a plate element between two longitudinals. This chapter seeks to incorporate this local model into a global model for deformation of a VLCC hull bottom induced by grounding. The final goal of this new formulation is to determine the total resistance to ship motion over a rock due to in-plane shear buckling mechanisms.

To solve for the total grounding resistance due to shear a global hull deformation geometry must be assumed that will allow use of the plastic buckling element model. The energy dissipation mechanisms other than shear have already been analyzed by Peer[4] and will be presented for comparison with the shear grounding results in chapter 7 to determine the relative importance of in-plane plastic shearing as an energy dissipation mechanism during grounding.

Before proceeding further, the parameters of the global hull deformation problem are defined as follows.

Parameters characterizing hull deformation

(x, y, z)	---	longitudinal, transverse, and vertical coordinates
(u, v, w)	---	longitudinal, transverse, and vertical displacements
L	---	overall length of ship
B	---	beam of ship
b	---	longitudinal stiffener spacing
l	---	transverse web frame spacing
l_l	---	transverse extent of damage and longitudinal bulkhead spacing
L_d	---	longitudinal extent of fully developed damage cross section
η	---	longitudinal extent of partially developed damage transition zone
n	---	transition zone parameter, number of transverse web frames included in damage transition zone
Δ_r	---	height of rock above ship keel prior to grounding
Δ_L	---	vertical lift of ship as it rides over rock during grounding
Δ_0	---	maximum amplitude of rock penetration into hull at the keel
Δ_i	---	maximum amplitude of rock penetration into hull at stiffener i

S_i --- total longitudinal displacement of hull plating in the vicinity of i-th stiffener occuring after stiffener has passed through damage transition region (assumes rigid stiffener and flexible shell plating)

$s_i(x)$ --- longitudinal displacement along deformed stiffener i measured at a distance x from the damage transition zone leading edge

ψ_i --- total arc length along deformed stiffener i within the transition region

$\psi_i(x)$ --- arc length along deformed stiffener i measured at a distance x from the damage transition zone leading edge

m --- total number of inter-longitudinal plate spans between the ship's centerline and the first longitudinal bulkhead

It is worth reminding the reader at this point that this formulation does not apply to grounding situations resulting in hull membrane rupture in the shear deformation region due to the fact that shear forces can only build up in the hull plating if it remains a continuous surface. Otherwise, the hull plating boundary conditions and geometry will not remain as previously assumed and the shear buckling problem will become extremely difficult to analyze.

There are several other assumptions that specifically apply to this global hull deformation model. First, the hull damage is assumed to be symmetric about the ship's keel or centerline. This allows external moments about the ship's yaw axis to be excluded which would otherwise lead to transverse components of grounding resistance causing damage to progress in both the transverse and longitudinal directions. This problem is extremely complex due to the progressive non-symmetry of the damage as well as the increased effect of complicated hull hydrodynamics on the problem.

The second assumption in this model involves the shape of the hull deformation. Figure 22 shows an assumed cross-sectional view and a longitudinal profile of the damage. The length of the damage progresses a distance $(L_d + \eta)$ where L_d is the longitudinal extent of the fully developed damage zone and η is the length of a damage transition zone. The length of this transition zone is assumed to be a multiple, n, of the transverse frame spacing, l, and the shape is assumed to be cosinusoidal with amplitude $\Delta_o/2$ at the keel.

$$\eta = n\,l$$

$$w_o(x) = \Delta_o/2\,[\,1 + \cos(\,\pi + \pi x/\eta\,)\,]$$

The transverse cross section of the damage is assumed to be wedge shaped and is limited by the spacing between longitudinal bulkheads l_1. The vertical penetration of the damage Δ_o is assumed to be twice the penetration of the rock above the ship's baseline in order to be consistent with the geometry analyzed by Peer. The rock height Δ_r is the sum of the rock's vertical penetration into the ship's keel $\Delta_o/2$ and the lift Δ_l of the ship's hull as it rides over the rock.

$$\Delta_r = \Delta_o/2 + \Delta_l$$

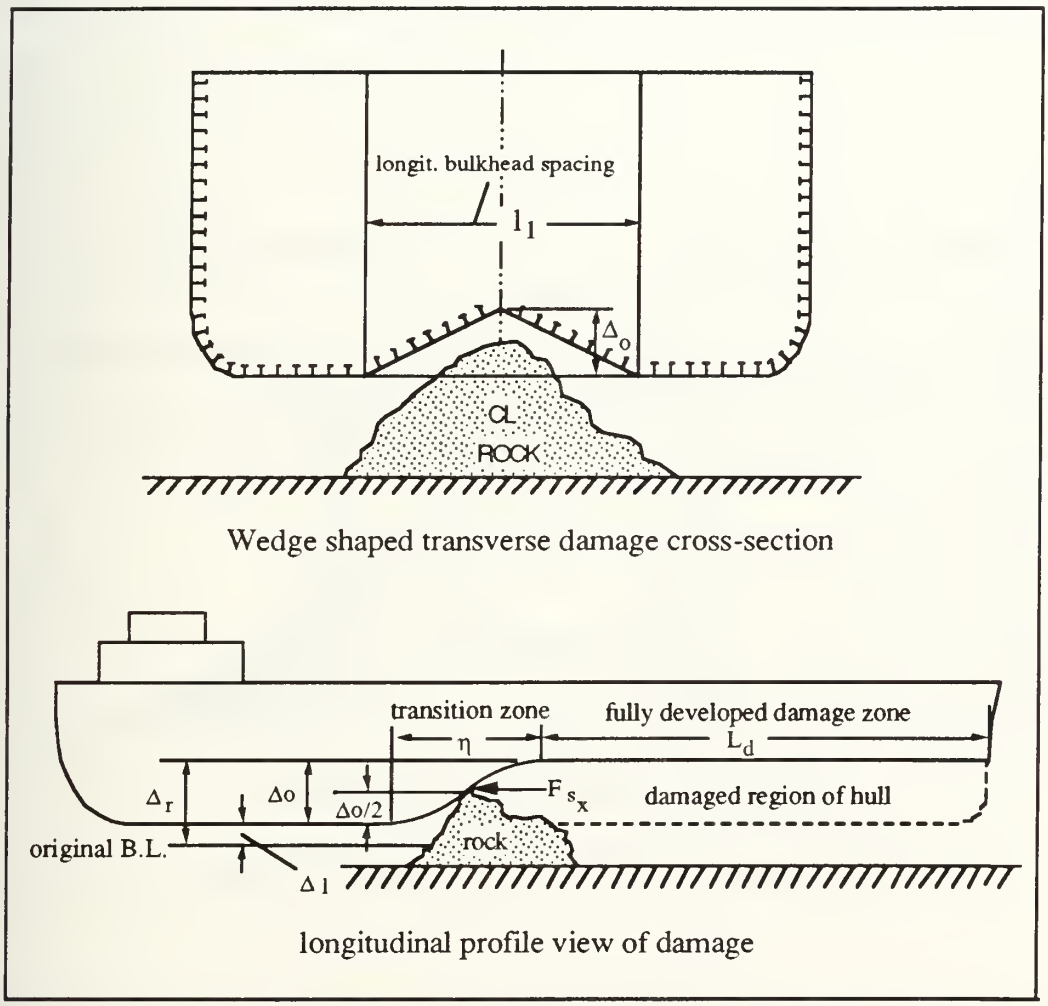

Figure 22: Grounding hull damage geometry

Figure 22 shows the overall extent of the transverse and longitudinal damage but fails to show the details of the damage transition zone. A more detailed profile view of the transition zone is given in Figure 23. The assumed longitudinal shape of the damage transition zone is chosen to be cosinusoidal to make the formulation easier while

maintaining some similarity to the shape assumed by Peer[4] to facilitate comparison with his results later on. The cosinusoidal damage profile can be extended to the longitudinal stiffeners by substituting Δ_i for Δ_o and realizing that, for the assumed wedge shaped cross section, Δ_i can be expressed as a linear function of Δ_o.

$$w_i(x) = \Delta_i/2 \, [\, 1 + \cos(\, \pi + \pi x/\eta \,) \,] \qquad (49)$$

$$\Delta_i = \left(\frac{m - i}{m}\right) \Delta_o$$

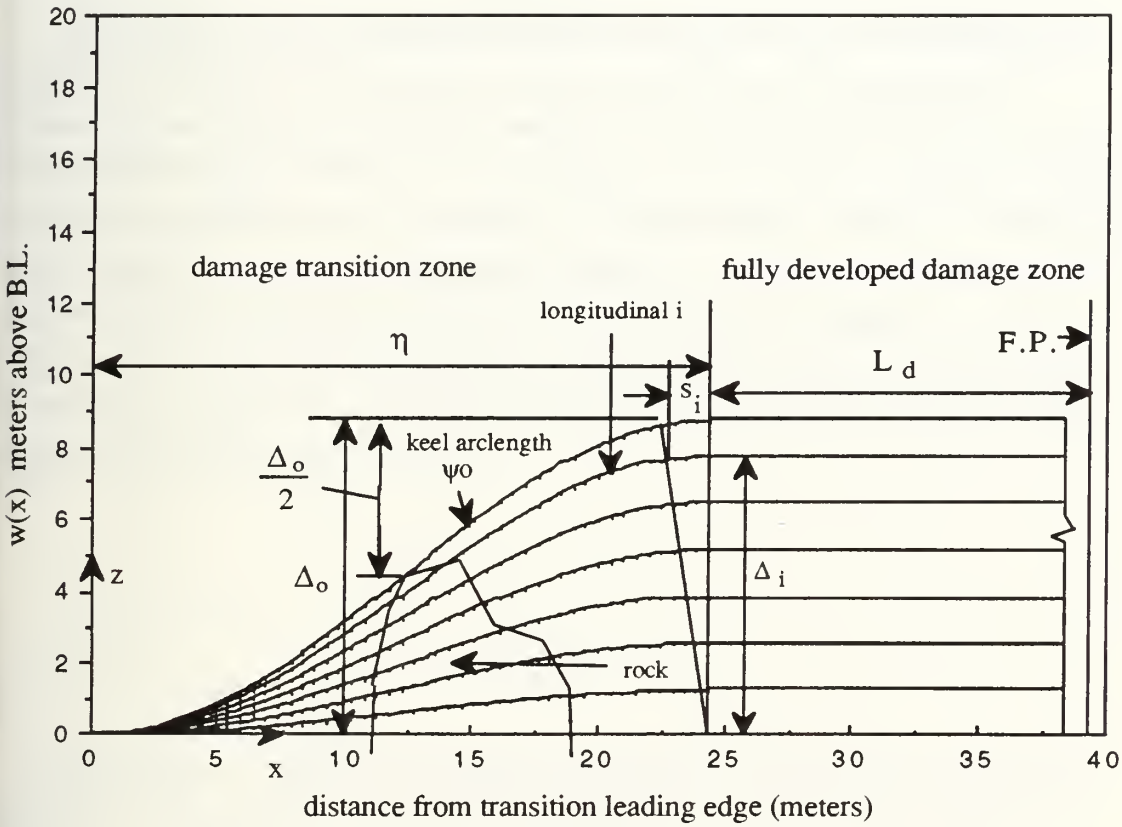

Figure 23: Damage transition zone for 5 m rock height

The constant m, which is the total number of inter-longitudinal plate spans between the keel and the first longitudinal bulkhead, can be determined from:

$$m = \frac{l_1}{2\,b}$$

The subscript "i" is an integer designating the longitudinal stiffener that also gives the number of inter-longitudinal plate spans between that stiffener and the keel. In summary,

The shape of the damage transition zone profile is defined by the keel profile and deformed longitudinal profiles with identical shape but of linearly decreasing amplitude as the stiffener transverse distance from the keel increases.

The next step in the development of the grounding model is to relate the global deformation in the damage transition zone to in-plane shearing of the inter-longitudinal plating. This is accomplished by observing that in-plane shear in the hull plating is induced by differences in the damage profile arc lengths of adjacent longitudinals.

The arc length of each of the longitudinals has been solved for numerically using a spreadsheet. Only half of the damage transition region needs to be analyzed due to symmetry about the keel. The damage transition zone has been partitioned into a series of plate elements of length $\eta/50$ and width b. For the purpose of this analysis partitioning the length of the transition zone into 50 elements provides sufficient accuracy in measuring the the arc length of the deformed longitudinals. The out-of-plane deformations of the keel $w_0(x)$ and all of the stiffeners $w_i(x)$ are determined first. The arc length, ψ_i, of each stiffener through the transition zone is then calculated numerically by summing up the incremental arc lengths for each partition along the x axis, $\Delta x = \eta/50$. The relationships used in this formulation are given below.

$$\Delta\psi_i = \sqrt{\Delta x_i^2 + \Delta y_i^2}$$

$$\psi_i = \sum_{j=1}^{n} \Delta\psi_i(\Delta x_j)$$

The subscript "i" designates the particular longitudinal along which the arc length is measured. The subscript "j" provides the designation of the Δx increment where the arc length measurement is taking place where $j = 1$ is defined as the increment closest to the transition zone leading edge. As an example $\Delta\psi_1(\Delta x_1)$ corresponds to the arc length from $x = 0$ to $x = \eta/50$ of the first longitudinal outboard of the keel.

The arc length ψ_i is the total arc length of longitudinal i measured through the transition zone length to the coordinate $x = \eta$. This change in arc length corresponds to a stretching of the hull plating surrounding the i-th longitudinal through the transition zone.

From Figure 23 the parameter S_i measures the total longitudinal displacement of a point along the deformed arclength of stiffener i from its original undeformed position to its

inal position after passing through the transition zone assuming an inextensional stiffener. Figure 24 shows a more detailed view of how a single stiffener deforms and causes stretching of the hull plating as it passes through the damage transition zone.

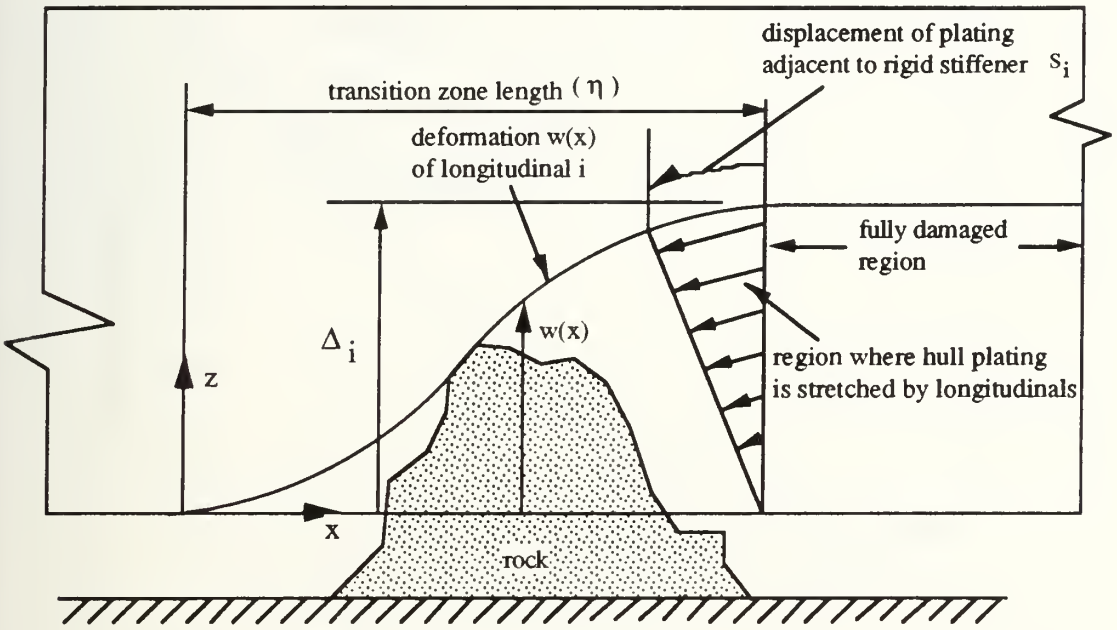

Figure 24: In-plane displacement of hull plating for rigid stiffeners

The total change in arc length for each longitudinal varies from a maximum value at the keel to zero at the first longitudinal bulkhead. The difference in the arc length profiles of adjacent longitudinals sets up differential longitudinal displacements, ΔSi, between the edges of the inter-longitudinal hull plating which results in in-plane shear deformation of the plating. Figure 25 shows how the longitudinal displacement of the hull plating surrounding each longitudinal varies as we progress off the ship's centerline axis.

It has been shown that in-plane shear forces are induced in the plating by a relative translation between adjacent stiffeners. This relative translation, $\Delta s_i(x)$, is just the difference in the plating displacement between adjacent stiffeners at a distance x from the transition zone leading edge. The maximum value for the relative translation, ΔS_i, occurs after the damage transition has passed and is shown in Figure 25 for longitudinals 1 and 2. The relative translation, $\Delta s_i(x)$, is a general form of the shear translation, s, used in the chapter 3 formulation. The chapter 3 buckling model assumed that one edge was stationary while the other edge translated a distance s. The current model assumes that both edges translate and that the relative translation, $\Delta s_i(x)$, induces the shear forces. In the current

nodel the shear translation varies in both space and time and must be numerically mapped over the transition zone surface; otherwise, the formulation is equivalent to the earlier formulation in chapter 3. Figure 26 illustrates the geometric similarity of the two models.

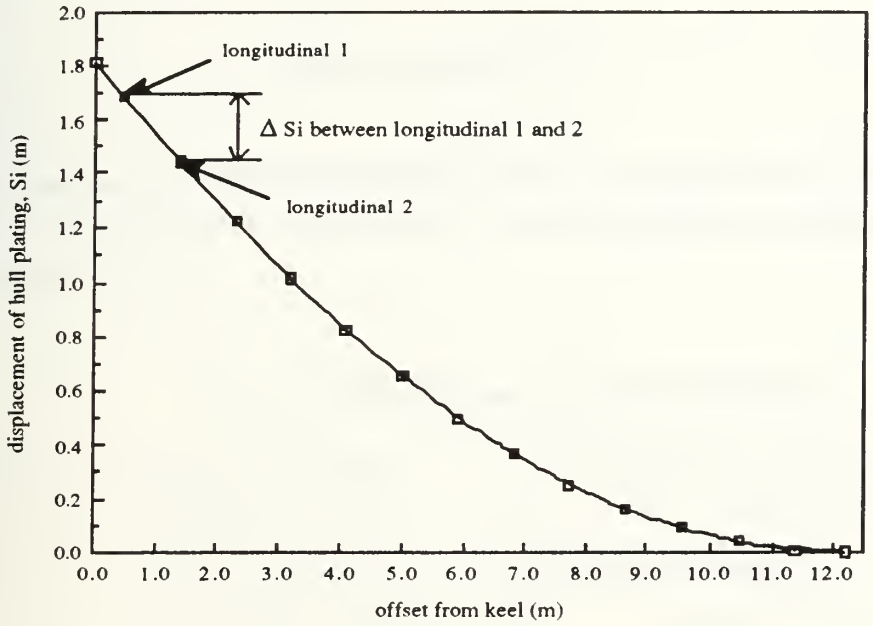

Figure 25: Maximum longitudinal displacement vs offset from keel

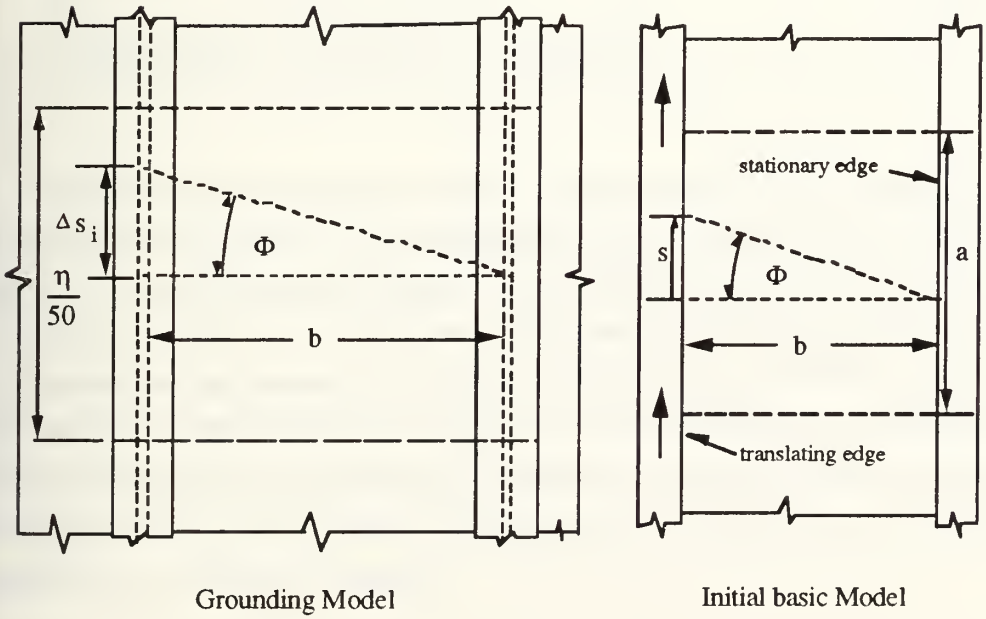

Figure 26: Plate element shear rotation geometry

Once the relative translation $\Delta s_i(x)$ is determined for each of the plate elements over ne surface of the transition zone the in-plane rotation Φ can be calculated for each of these lements by the following relationship.

$$\Phi_i(x) = \arctan\left(\frac{\Delta s_i(x)}{b}\right)$$

The non-dimensional shear force per unit length can now be mapped over the surface by using a plot of NDSF vs Φ for the representative VLCC dimensions and characteristic data shown in Table 3.

Table 3: VLCC dimensions and characteristic data

L = 313 m (1030 ft)	hull thickness = 19.1mm (3/4 in)
B = 56.6 m (185 ft)	b = 0.91 m (3 ft)
T_0 = 18.9 m (62 ft)	longitudinal T-stiffeners:
σ_0 = 393 MPa (57 ksi)	flange: (203 * 25.4 mm)
rupture strain = 0.12	(8" * 1")
l = 4.88 m (16 ft)	web: (711 * 12.7 mm)
l_1 = 24.4 m (80 ft)	(28" * 1/2")
Young's Modulus = 200,000 MPa (29,000 ksi)	

The NDSF model developed in chapter 3 was revised with new values from Table 3 for σ_0, hull plate thickness t , and longitudinal spacing b, and the results are plotted in Figure 27. The NDSF curves for plastic shear buckling in Figure 27 show an approximate lower bound of 3 for $0 < \Phi < 17$ degrees. The non-dimensional shear force per unit length can therefore be approximated by the elastic NDSF curve up to NDSF = 3 and by a constant value of three up to $\Phi = 17$ degrees as shown in Figure 28. Calculations of in-plane shear deformation are provided in Appendix A which show that the maximum value for Φ that occurs for a rock heights less than 5 meters and transition zone parameters greater than 5 is less than 17 degrees.

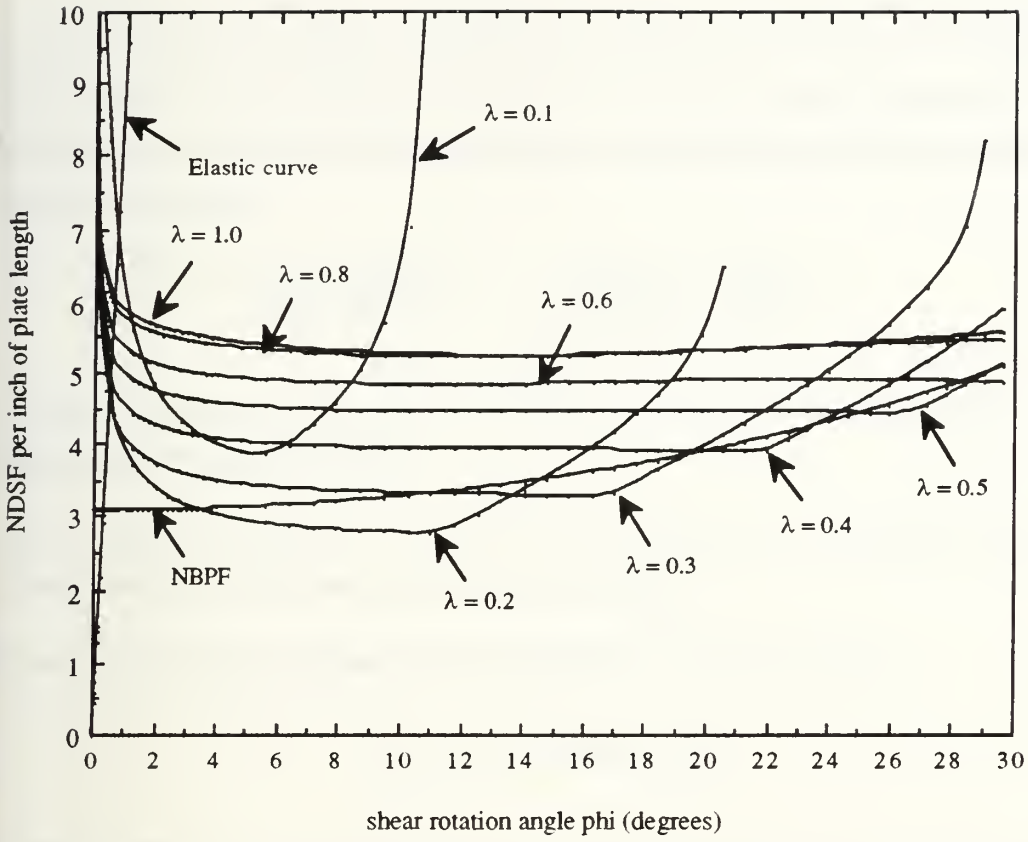

Figure 27: VLCC non-dimensional shear per unit length

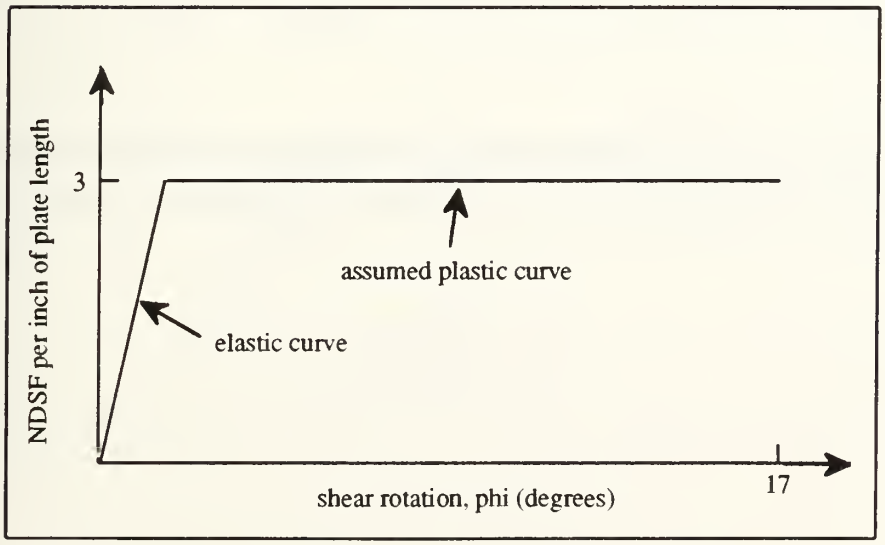

Figure 28: Approximation for VLCC NDSF(Φ) per inch of plate length

Use of Figure 28 provides a quick means to determine the non-dimensional shear force per unit length since Φ for each plate element on the damage transition surface has already been determined. The in-plane shear resistance for each plate element can now be calculated by multiplying the NDSF/unit length by the plate incremental length and the plastic hinge moment.

$$\frac{\text{shear resistance}}{\text{plate element}} = f_s = \left(\frac{\text{NDSF}}{\text{unit length}}\right) \times \left(\frac{\eta}{50}\right) \times M_o$$

Since the transition zone surface is not horizontal, the induced in-plane shear has both horizontal and vertical components.

Note to reader: An alternative approach in which the force is not projected in the horizontal direction is discussed at the end of this chapter.

The component of shear resistance in the x-direction is therefore given by:

$$f_{s_x} = f_s \cos\left[\arctan\left(w'(x)\right)\right]$$

The slope of the plate element surface in the x direction is given by w'(x) and is just the mean value of its longitudinal edge slopes which have already been computed.

$$w'(x)_{1\text{-}2} = \frac{w'_1(x) + w'_2(x)}{2} \equiv \frac{\partial z}{\partial x} \text{ of plate element between longitudinals 1 and 2}$$

We can finally compute the total horizontal grounding resistance, F_{S_x} in shear by numerically summing all of the plate element horizontal shear resistances over the transition zone surface.

$$F_{s_x} = 2\sum_{i=1}^{m}\sum_{j=1}^{50} f_{s_x}(i,j)$$

5.2 Results of Grounding Model Calculations

The total horizontal grounding resistance Fs_X has been computed on a spreadsheet for penetration depths from 1 to 10 meters and for transition zone parameters n from 1 to 15. The results are tabulated in Appendix A and plotted in Figures 29 and 30, from which several observations should be noted.

Figure 29 illustrates that, although the horizontal resistance increases as the damage penetration increases, it does so at a steadily decreasing rate. This is due to the fact that the surface slope of the deformed plating increases as out-of-plane deformations increase, thus reducing the horizontal component of the otherwise increasing in-plane shear force.

Figure 30 illustrates that large penetration depths produce a horizontal resistance that varies almost linearly with the transition zone parameter "n" while small penetration depths result in a horizontal resistance that approaches a constant value with n. The curve associated with a damage depth of one meter shows that the resistance is roughly constant for values of n greater than two meters.

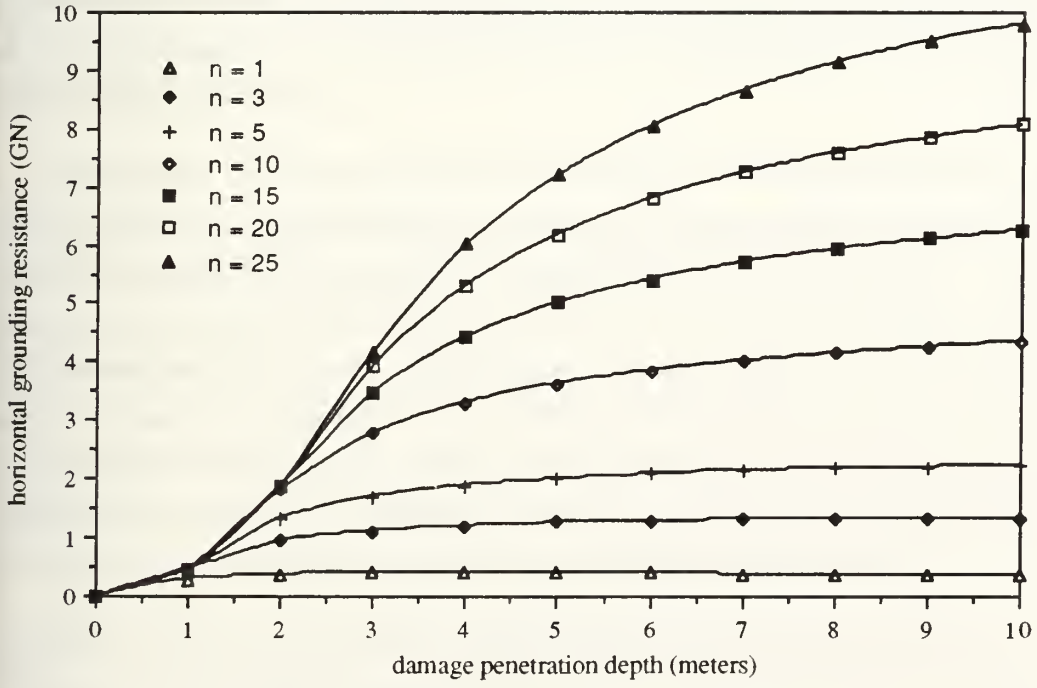

Figure 29: Horizontal resistance vs penetration depth vs transition parameter "n"

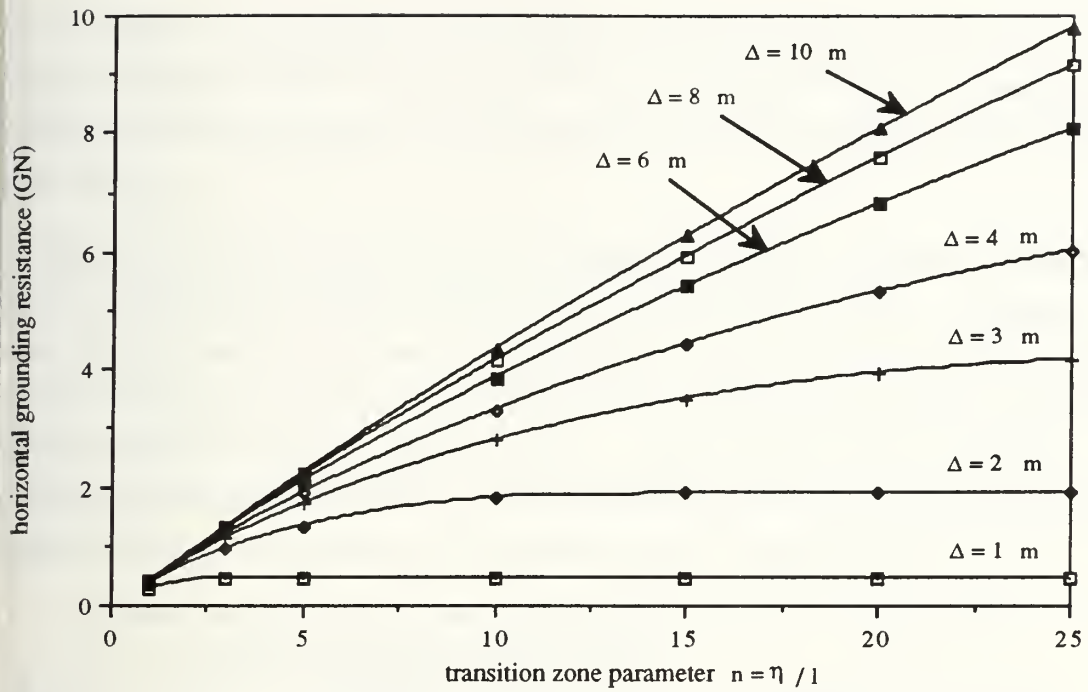

Figure 30: Horizontal resistance vs transition parameter "n" and penetration depth

Since the transition zone length is undetermined it is difficult to predict the horizontal esistance for large penetration depths using this model. However, since the resistance is ndependent of transition zone length for small penetration depths, the horizontal force for ninor hull deformations can be calculated from this analytical model without knowing the ransition zone parameter n.

Another point worth noting is that this model does not take into account the fact that 'or large penetration depths and short transition zone lengths (small n), the rupture strain 'or the hull material may be exceeded in certain locations on the plate surface. An initial ıssumption associated with this formulation was the no hull tearing or rupture would occur ;ince plate rupture would result in a significant and unpredictable loss of load carrying :apacity within the hull plating. In order to partially address this issue the model was used o calculate the uniaxial membrane strain in the longitudinal direction through the damage ransition region at the keel. The damage penetration which induced a longitudinal strain in he keel of 0.1 was calculated for transition zone lengths corresponding to n = 1 to n = 9.

It should be emphasized that this is a rough method of determining the parameters which will result in hull membrane rupture and does not take into account the complicated two dimensional nature of the strain field. However, this method does provide a means to

quickly estimate the combinations of grounding parameters, Δ_0 and n, which may risk inducing membrane rupture. Figure 31 shows how the penetration depth for inducing longitudinal membrane rupture of the keel hull plating varies depending on the transition zone length.

The most obvious conclusion that can be taken from Figure 31 is that the penetration depth required to induce keel membrane rupture increases linearly with n. The results show that for a transition zone parameter greater than five, the damage penetration must exceed 10 meters to induce rupture and that for damage penetration less than two meters, the rupture strain will not be exceeded for $n \geq 1$. The preceding results show that although hull membrane rupture is a concern it will not occur for small damage penetration depths where we can calculate the hull resistance since it is independent of n.

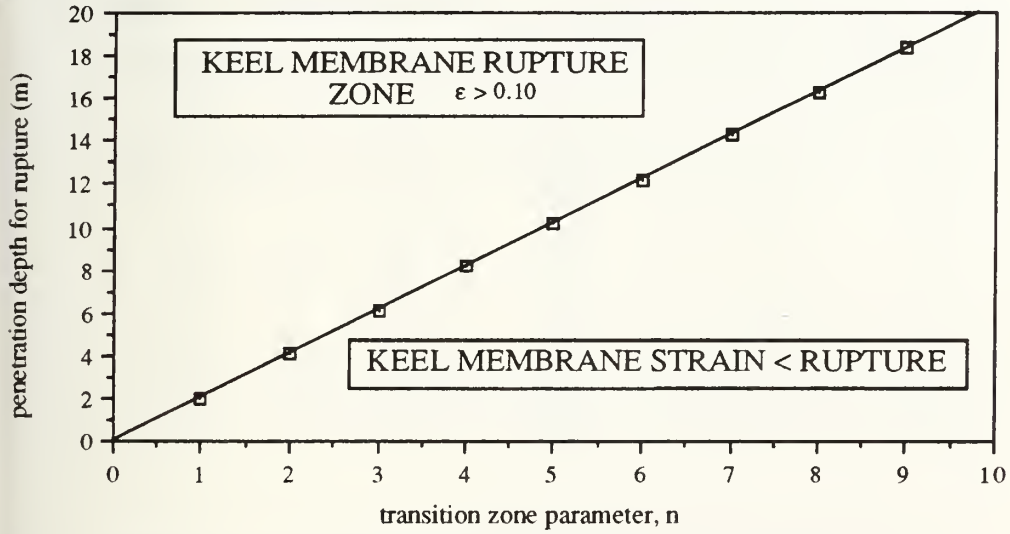

Figure 31: Limiting penetration depth vs "n" for prevention of keel membrane rupture assumed to be at a membrane strain of 0.1

5.3 Comparison with other Hull Failure Modes

Although the results show that for minor hull deformations the horizontal grounding force can be calculated independently of the transition zone length, no mention has yet been made of the fact that the structure may not fail in a shear buckling mode. The results discussed earlier are not valid unless the hull plating fails by the assumed geometry. It has already been stated that tearing or rupture of the hull plating will invalidate this model, however, no attempt has been made to compare the horizontal grounding resistance calculated from these other failure modes to that of the shear buckling model.

An attempt has been undertaken to compare the shear buckling failure mode with other modes of hull plate failure by comparing the results of the present model with those of Peer[4]. Peer considered internal work contributions from friction, crushing of transverse webs or bulkheads, and bending of longitudinal stiffeners and associated hull plating and performed an outer dynamic analysis on the ship hull to calculate the lift and penetration of the hull for a given rock height at various points along the ship length.

To perform this comparison the results of Peer's outer dynamic analysis are used for assumed rock heights of 3.5 meters and 5.0 meters which give damage penetration depths along the length of the VLCC for transition zone parameters of 5, 10 ,15, and 20. The penetration depths used are shown in Tables 4-1 and 4-2.

Table 4-1: Penetration depths used in comparison (rock height = 3.5 m)

Distance aft FP x (meters)	Δo (meters) n=5	Δo (meters) n=10	Δo (meters) n=15	Δo (meters) n=20
0	0.00	0.00	0.00	0.00
50	3.76	1.24	0.30	0.05
100	5.15	3.00	1.58	1.00
150	5.60	3.90	2.50	1.65
200	5.20	3.20	1.80	1.17
250	3.95	1.50	0.55	0.15
313	0.00	0.00	0.00	0.00

Table 4-2: Penetration depths used in comparison (rock height = 5 m)

Distance aft FP x (meters)	Δo (meters) n=5	Δo (meters) n=10	Δo (meters) n=15	Δo (meters) n=20
0	0.00	0.00	0.00	0.00
50	7.00	3.30	1.32	0.60
100	8.35	5.65	3.35	1.95
150	8.70	6.50	4.55	3.10
200	8.35	5.90	3.65	2.30
250	7.20	3.75	1.70	1.00
313	0.00	0.00	0.00	0.00

The horizontal grounding resistance has been calculated for each penetration depth and ransition zone parameter shown in Tables 4-1 and 4-2 using the grounding model and the esults are plotted in Figures 32 and 33.

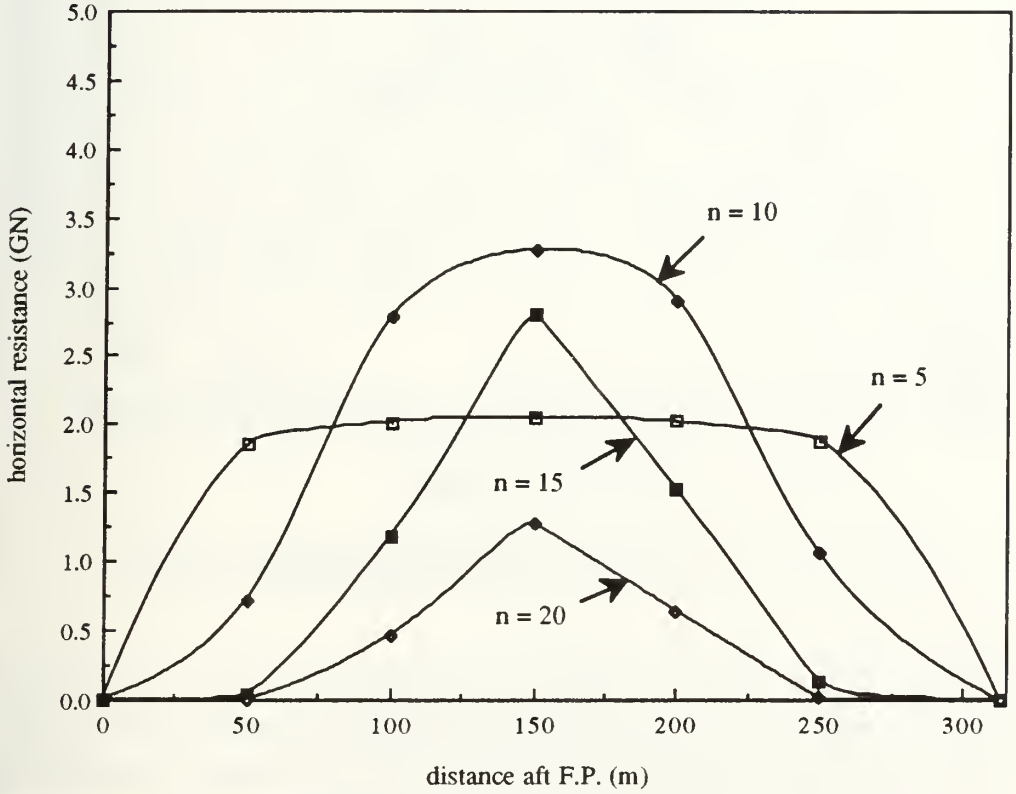

Figure 32: Horizontal grounding resistance for 3.5 m rock height

Several observations can be made from Figures 32 and 33. First of all, small transition zone parameters result in a horizontal grounding resistance that is more nearly constant over the length of the ship. The lifting of the ship at its bow and stern as it rides the obstacle results in a reduction in the damage penetration in these locations which in turn reduces the horizontal grounding resistance. It was shown by Peer[4] that short transition zone lengths generate less lift on the ship at its ends. This reduction in the lifting of the ship at its ends results in a more uniform grounding resistance along its length.

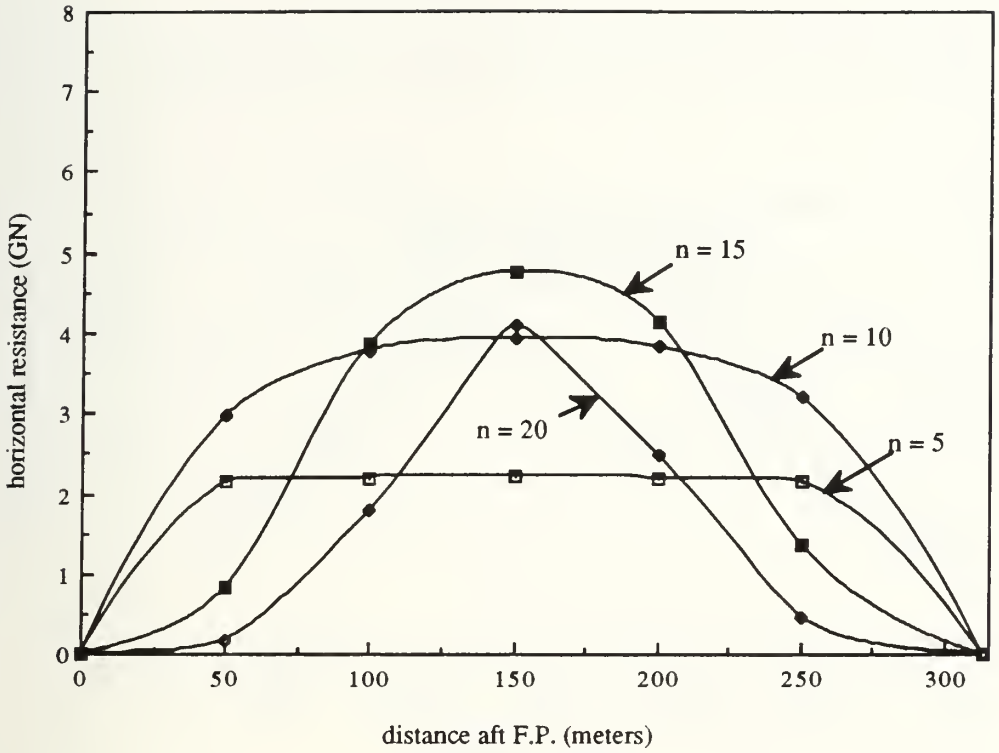

Figure 33: Horizontal grounding resistance for 5 m rock height

The larger rock height of 5 meters shown in Figure 33 results in a more uniform grounding resistance for all transition zone parameters less than 15. This is due to the fact that the ship does not ride over large obstacles as easily as smaller ones and a larger fraction of the total energy is dissipated within the hull structure. Since the fraction of energy dissipation associated with lifting of the ship is reduced, its effect on the total grounding resistance is also reduced.

Another interesting point is that the horizontal resistance for a short transition parameter (n = 5) does not change as the penetration depth increases. This can also be seen in Figure 29 which illustrates that for small transition lengths the resistance does not change as the penetration depth increases.

Finally, the point is reached where these results can be compared to Peer's grounding model. The resistances shown in Figures 32 and 33 are roughly an order of magnitude greater than those calculated by Peer[4]. To illustrate this, the grounding resistances, from Peer's model which neglects shear, are plotted for a rock height of 5 meters in Figure 34.

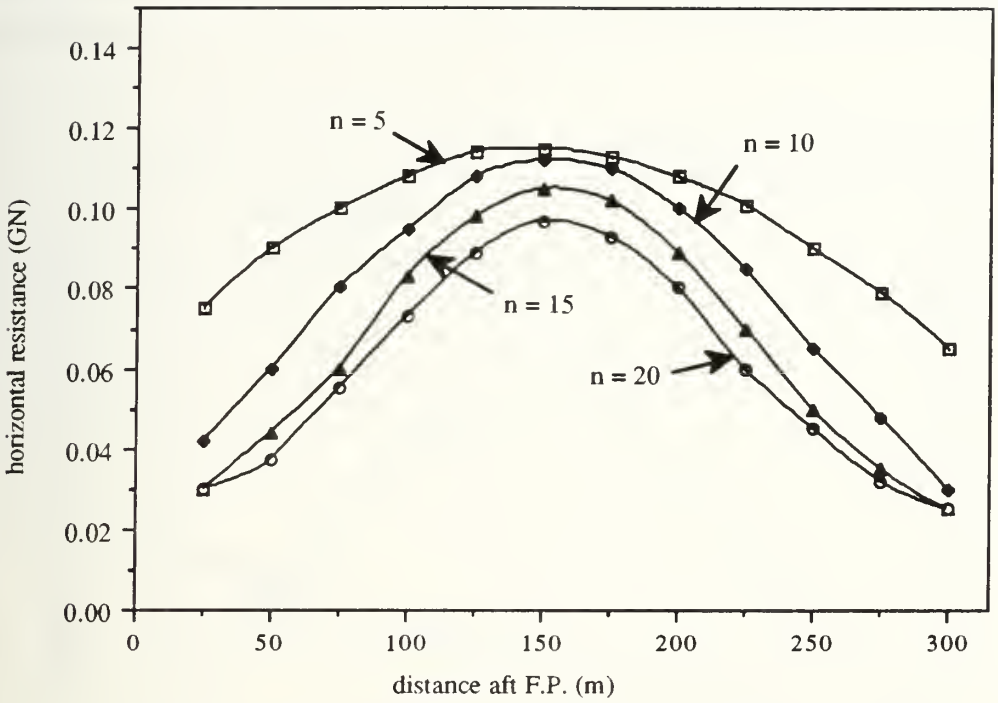

Figure 34: Horizontal resistance form Peer's grounding model for a 5 m rock height

The fact that Peer's results are much lower than those of the shear buckling model supports the conclusion that fracture may occur in the hull deformation process to pre-empt development of the high resistance associated with in-plane shear. The resistance of the hull structure to other structural failure modes is, under most circumstances, much less than that of shear buckling. Under these circumstances, the hull structure will fail by mechanisms other than shear. Further investigation of this phenomenon is beyond the scope of this paper.

Figures 29 and 30 show that if either the transition zone parameter or the penetration depth are small then the horizontal resistance force will also be small which may lead to a circumstance where the horizontal resistance force due to shear buckling is of the same order of magnitude as Peer's results. Another area that must be addressed is how increasing the transition zone parameter reduces the penetration depth for a given rock height. The effect on the horizontal grounding resistance has been observed by entering

the midships penetration depths for a 5 meter rock height from Peer's results into the shear buckling resistance model and plotting the calculated horizontal resistance. The result is shown in Figure 35.

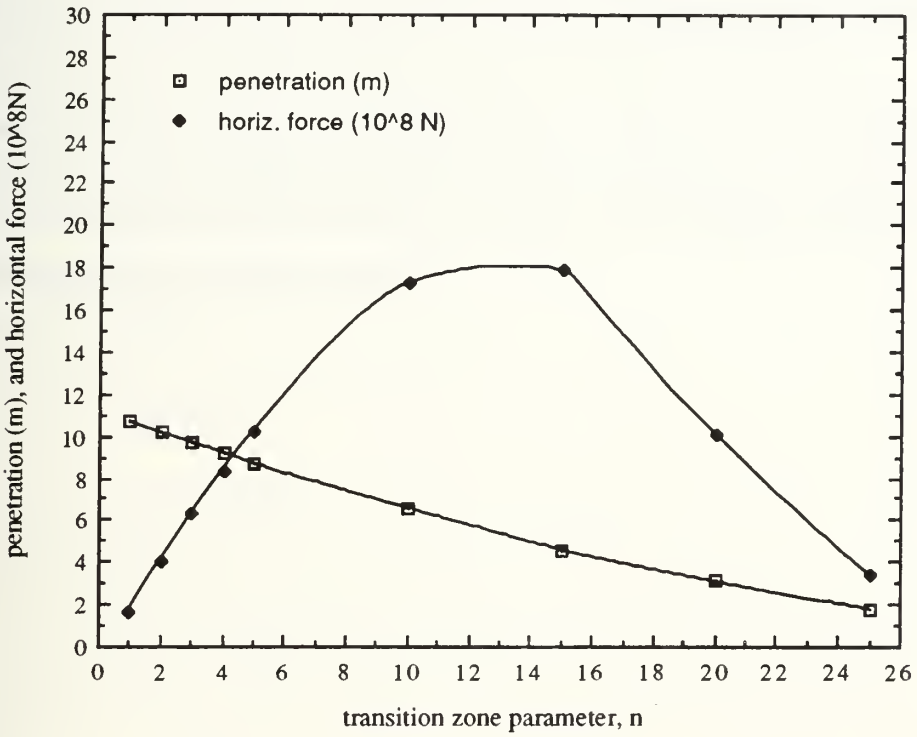

Figure 35: Horizontal resistance (based on penetration vs "n")

Figure 35 illustrates dramatically how the transition zone length affects the penetration depth which in turn affects the horizontal grounding resistance. It may be concluded from Figure 35 that either a very small or a very large transition zone length will reduce the horizontal shear resistance. The combination of a small penetration depth with a large transition zone length may be induced by minor grounding event such as the ship riding over a sand bar. In this situation, the resistance forces associated with shear buckling may be of the same order of magnitude as the forces associated with the damage mechanism's analyzed by Peer[4]. However, further study using both this model and the one developed by Peer to analyze grounding geometries with small penetration depths and large transition zone lengths will be necessary to confirm this.

The fact that the horizontal resistance shown in Figure 35 decreases for shorter transition zone lengths requires additional explanation. This grounding model formulation projects the tangential force on the transition zone surface into the longitudinal direction, however, the vertical component has been ignored. For short transition zones this vertical component will be quite large and, according to Peer, will entirely change the geometry of the transition zone. Therefore the validity of this result should be questioned.

An alternative approach may be considered which assumes all of the shear deformation occurs in the wake of the transition zone where the plate is horizontal. In this approach the horizontal force component will be much larger and the total grounding resistance will not drop as the transition zone length increases.

7. Conclusion

The first part of the thesis focused on developing a set of simple analytical models to describe the in-plane shear load carrying capacity of a flat rectangular plate in both the elastic and plastic regimes. The plastic buckling model was found by experimentation to give a reasonable prediction of both the resistance of the plate and its longitudinal plastic buckling wavelength. This model also predicted the observed shortening in the longitudinal wavelength as plastic buckling progresses. The model for in-plane failure provided an upper envelope for the load observed during the buckling tests.

A grounding resistance model was then developed in the second part of the thesis by incorporating the buckling element model into an assumed ship hull deformation induced by a grounding event. The ship grounding model yielded results from which the following conclusions can be drawn.

(1) The horizontal resistance of the hull to deformation induced by grounding is roughly an order of magnitude greater than the resistance of the energy dissipation mechanisms previously analyzed by Peer[4] which ignore skin effects. This supports the conclusion that the shear buckling mode of failure will be preceded and thus pre-empted other "weaker" failure modes such as fracture. Under these circumstances a majority of the total energy dissipation will be due to these "weaker" failure modes within the VLCC's hull structure.

(2) Larger rock heights result in a more uniform hull resistance along the length of the ship due to grounding. The reduction in the resistance at the ends of the ship is due to lifting of the hull as it attempts to ride over the obstacle. Since the ratio of this lift to the damage penetration is less for large obstacles, less of a reduction in the resistance occurs at the ends of the ship, resulting in a more uniform resistance.

(3) Short damage transition zones result in less lifting of the ship hull which in turn causes the grounding resistance to be nearly constant as the damage progresses down the length of the ship.

(4) The penetration depth required to induce a longitudinal strain in the keel hull plating of 0.1 increases linearly with the transition zone length. Therefore, if the the goal is to build a ship hull to resist membrane rupture due to grounding then some means must be engineered into the bottom hull structure to so that it will

"diffuse" the damage out away from the local point of contact with the obstacle. This will reduce the probability of localized strain concentrations in the portion of the hull being impinged upon by the obstacle by distributing them in a more uniform manner over a larger volume of the structure which will in turn reduce the probability of hull rupture.

(5) The horizontal grounding resistance is independent of transition zone length for small penetration depths (i.e. < 1 meter). Since the transition zone length is unknown, the horizontal grounding force can only be predicted for small penetration depths.

Further study is needed in the area of minor groundings to determine if the resistance associated with hull plate shear buckling is of the same order of magnitude as the resistance associated with other hull failure mechanisms. Specifically, more results are needed from Peer's model for damage penetration depths less than 1 meter in combination with transition zone lengths greater than 10 for comparison with this model. The study of minor groundings should already be of interest when attempting to design a tanker bottom to resist hull plating rupture since it appears impractical to develop a design that is capable of remaining unbreached following impact with a large rock. Finally, the alternative formulation discussed earlier which considers all of the shear deformation to occur in the transition zone wake should also be analyzed and compared with this grounding model.

APPENDIX A

Ship Total Shear Resistance Calculations

Total Horizontal Resistance vs Penetration Depth and "n"

Penetration [m]	Total horizontal resistance for transition zone parameter, n						
Δo	1	3	5	10	15	20	25
1	0.2846	0.465	0.469	0.46934	0.46942	0.46944	0.46946
2	0.3776	0.9404	1.3244	1.8046	1.8768	1.8774	1.8776
3	0.4042	1.116	1.6926	2.776	3.4888	3.9264	4.1528
4	0.4076	1.2016	1.886	3.3026	4.4194	5.3068	6.0062
5	0.403	1.2598	2.0008	3.6294	5.0054	6.1854	7.2084
6	0.3952	1.2902	2.0864	3.8506	5.4052	6.7924	8.0424
7	0.3858	1.306	2.1486	4.0114	5.7016	7.2402	8.6496
8	0.3762	1.3138	2.1866	4.1434	5.9192	7.583	9.1306
9	0.3666	1.3162	2.212	4.2588	6.1004	7.844	9.5
10	0.3572	1.3148	2.2296	4.3422	6.2586	8.063	9.7924

transition zone parameter	Total horizontal resistance for rock height in meters				
n	1	2	3	4	5
1	0.2846	0.3776	0.4042	0.4076	0.403
3	0.465	0.9404	1.116	1.2016	1.2598
5	0.469	1.3244	1.6926	1.886	2.0008
10	0.46934	1.8046	2.776	3.3026	3.6294
15	0.46942	1.8768	3.4888	4.4194	5.0054
20	0.46944	1.8774	3.9264	5.3068	6.1854
25	0.46946	1.8776	4.1528	6.0062	7.2084

transition zone parameter	Total horizontal resistance for rock height in meters				
n	6	7	8	9	10
1	0.3952	0.3858	0.3762	0.3666	0.3572
3	1.2902	1.306	1.3138	1.3162	1.3148
5	2.0864	2.1486	2.1866	2.212	2.2296
10	3.8506	4.0114	4.1434	4.2588	4.3422
15	5.4052	5.7016	5.9192	6.1004	6.2586
20	6.7924	7.2402	7.583	7.844	8.063
25	8.0424	8.6496	9.1306	9.5	9.7924

Rock Penetration and Resistance Calculation Results

Damage penetration for rock height = 3.5 meters				
Distance aft FP x (meters)	Δo (meters) n=5	Δo (meters) n=10	Δo (meters) n=15	Δo (meters) n=20
0	0.00	0.00	0.00	0.00
50	3.76	1.24	0.30	0.05
100	5.15	3.00	1.58	1.00
150	5.60	3.90	2.50	1.65
200	5.20	3.20	1.80	1.17
250	3.95	1.50	0.55	0.15
313	0.00	0.00	0.00	0.00

Damage penetration for rock height = 5 meters				
Distance aft FP x (meters)	Δo (meters) n=5	Δo (meters) n=10	Δo (meters) n=15	Δo (meters) n=20
0	0.00	0.00	0.00	0.00
50	7.00	3.30	1.32	0.60
100	8.35	5.65	3.35	1.95
150	8.70	6.50	4.55	3.10
200	8.35	5.90	3.65	2.30
250	7.20	3.75	1.70	1.00
313	0.00	0.00	0.00	0.00

Horizontal grounding resistance for rock height = 3.5 meters				
Distance aft FP x (meters)	Horiz. Force (Newtons) n=5	Horiz. Force (Newtons) n=10	Horiz. Force (Newtons) n=15	Horiz. Force (Newtons) n=20
0	0	0	0	0
50	1.8504	0.7216	0.0422	0.0012
100	2.0148	2.776	1.1716	0.4694
150	2.0544	3.2608	2.7898	1.2778
200	2.0194	2.9044	1.5204	0.6426
250	1.879	1.0556	0.142	0.0106
313	0	0	0	0

Horizontal grounding resistance for rock height = 5 meters				
Distance aft FP x (meters)	Horiz. Force (Newtons) n=5	Horiz. Force (Newtons) n=10	Horiz. Force (Newtons) n=15	Horiz. Force (Newtons) n=20
0	0	0	0	0
50	2.1486	2.9654	0.8178	0.169
100	2.1966	3.7836	3.8696	1.7846
150	2.2054	3.9352	4.7678	4.0966
200	2.1966	3.832	4.146	2.4826
250	2.1576	3.1928	1.3562	0.4694
313	0	0	0	0

Grounding Resistance Calculation Flow Diagram

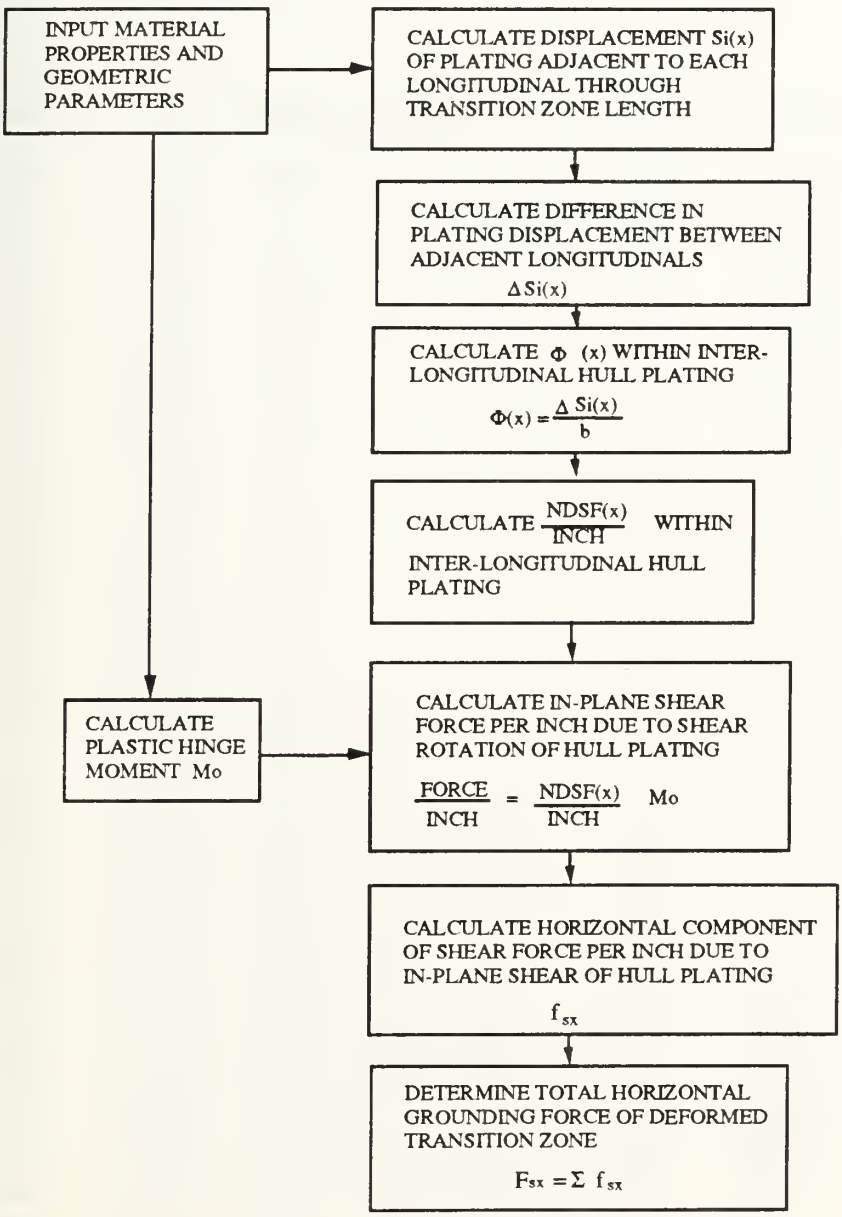

Determination of total horizontal grounding resistance due to in-plane shear of hull plating

Basic Problem Parameters: (* All dimensions in meters)

transverse web frame spacing =	l =	4.88 meters
# transverse webs in transition zone =	n =	5
length of damage transition zone =	η =	24.4 meters
assumed rock height =	Δ r =	5 meters
penetration depth =	Δo =	8.7 meters
distance between longit. bulkhds =	ll =	24.4 meters

Longitudinal	Tabulation of longitudinal elongation as function of x [meters]						
distance x	Longitud. #1	Longitud. #2	Longitud. #3	Longitud. #4	Longitud. #5	Longitud. #6	Longitud. #7
0	0	0	0	0	0	0	0
0.488	6.99613E-05	5.95407E-05	4.99599E-05	4.12189E-05	3.33176E-05	2.62562E-05	2.00348E-05
0.976	0.000697599	0.000593738	0.000498234	0.000411089	0.000332306	0.000261891	0.000199844
1.464	0.002429913	0.002068402	0.001735894	0.001432423	0.00115802	0.000912714	0.000696528
1.952	0.005792872	0.004931887	0.004139715	0.003416502	0.002762381	0.002177475	0.001661891
2.44	0.011281668	0.009606968	0.00806548	0.006657645	0.005383868	0.004244517	0.003239922
2.928	0.01935185	0.016483386	0.013841807	0.011428184	0.009243497	0.007288644	0.00556443
3.416	0.030411537	0.025911248	0.021764635	0.017973926	0.014541174	0.011468258	0.00875687
3.904	0.044814876	0.038195401	0.032092463	0.026510212	0.021452493	0.016922829	0.012924407
4.392	0.062856818	0.053590868	0.04504243	0.037218612	0.03012602	0.023770726	0.018158242
4.88	0.084769261	0.072299377	0.060787271	0.050244312	0.040681109	0.032107444	0.024532225
5.368	0.110718538	0.094467009	0.079453163	0.065694211	0.053206268	0.042004251	0.032101781
5.856	0.140804189	0.120182901	0.101118453	0.08363572	0.067758083	0.053507261	0.040903151
6.344	0.175058943	0.149478984	0.12581323	0.104096259	0.084360692	0.066636939	0.050952951
6.832	0.21344978	0.182330648	0.153519698	0.127063409	0.103005794	0.081388021	0.06224806
7.32	0.25587998	0.218658277	0.184173284	0.152485691	0.123653167	0.097729848	0.074765814
7.808	0.302192021	0.258329539	0.217664419	0.18027391	0.146231672	0.115607077	0.0884645
8.296	0.352171211	0.301162355	0.253840916	0.210303032	0.170640682	0.134940762	0.103284141
8.784	0.405549951	0.346928446	0.292510874	0.242414516	0.196751927	0.155629757	0.119147537
9.272	0.462012516	0.395357375	0.333446047	0.276419063	0.224411686	0.177552434	0.135961556
9.76	0.521200263	0.446141011	0.376385599	0.312099726	0.253443302	0.200568651	0.153618638
10.248	0.5827172	0.498938329	0.421040187	0.349215311	0.283649962	0.224521971	0.171998494
10.736	0.646135823	0.553380504	0.467096328	0.387504055	0.314817714	0.249242072	0.190969973
11.224	0.711003182	0.609076216	0.514220968	0.42668749	0.346718674	0.274547324	0.210393067
11.712	0.776847102	0.665617135	0.562066237	0.466474483	0.379114372	0.300247503	0.230121026
12.2	0.843182532	0.722583518	0.610274318	0.506565391	0.411759229	0.3261466	0.25000256
12.688	0.909517962	0.779549902	0.658482398	0.5466563	0.444404086	0.352045696	0.269884094
13.176	0.975361882	0.83609082	0.706327667	0.586443293	0.476799785	0.377745875	0.289612054
13.664	1.040229241	0.891786533	0.753452308	0.625626728	0.508700744	0.403051127	0.309035148
14.152	1.103647864	0.946228708	0.799508448	0.663915471	0.539868496	0.427771228	0.328006627
14.64	1.165164801	0.999026026	0.844163037	0.701031057	0.570075156	0.451724548	0.346386483
15.128	1.224352548	1.049809661	0.887102588	0.736711719	0.599106772	0.474740765	0.364043564
15.616	1.280815113	1.098238591	0.928037761	0.770716267	0.626766531	0.496663442	0.380857583
16.104	1.334193853	1.144004682	0.96670772	0.802827751	0.652877776	0.517352437	0.39672098
16.592	1.384173043	1.186837498	1.002884216	0.832856873	0.677286786	0.536686122	0.411540621
17.08	1.430485084	1.22650876	1.036375352	0.860645092	0.699865291	0.554563351	0.425239307
17.568	1.472915284	1.262836389	1.067028938	0.886067373	0.720512665	0.570905178	0.43775706
18.056	1.511306121	1.295688053	1.094735406	0.909034524	0.739157766	0.58565626	0.44905217
18.544	1.545560875	1.324984135	1.119430183	0.929495063	0.755760375	0.598785938	0.45910197
19.032	1.575646526	1.350700028	1.141095473	0.947436572	0.77031219	0.610288949	0.467903339
19.52	1.601595803	1.37286766	1.159761365	0.96288647	0.78283735	0.620185755	0.475472896
20.008	1.623508246	1.391576169	1.175506206	0.975912171	0.793392438	0.628522473	0.481846879
20.496	1.641550187	1.406971636	1.188456172	0.986620571	0.802065965	0.63537037	0.487080713
20.984	1.655953526	1.419255789	1.198784	0.995156857	0.808977284	0.640824941	0.491248251
21.472	1.667013214	1.428683651	1.206706828	1.001702599	0.814274961	0.645004555	0.494440691
21.96	1.675083396	1.435560069	1.212483156	1.006473138	0.81813459	0.648048682	0.496765198
22.448	1.680572192	1.44023515	1.21640892	1.009714281	0.820756077	0.650115724	0.498343229
22.936	1.683935151	1.443098635	1.218812741	1.01169836	0.822360438	0.651380485	0.499308592
23.424	1.685667465	1.444573298	1.220050402	1.012719694	0.823186152	0.652031308	0.499805276
23.912	1.686295103	1.445107496	1.220498676	1.013089564	0.823485141	0.652266943	0.499985086
24.4	1.686365064	1.445167037	1.220548635	1.013130783	0.823518458	0.652293199	0.500005121

Longitudinal	Tabulation of longitudinal elongation as function of x [meters]					
distance x	Longitud. #8	Longitud. #9	Longitud. #10	Longitud. #11	Longitud. #12	Longitud. #13
0	0	0	0	0	0	0
0.488	1.46532E-05	1.01116E-05	6.41002E-06	3.5484E-06	1.5268E-06	3.45216E-07
0.976	0.00014617	0.00010087	6.39455E-05	3.53991E-05	1.52317E-05	3.44398E-06
1.464	0.000509487	0.000351609	0.00022291	0.000123403	5.30997E-05	1.20064E-05
1.952	0.001215727	0.000839065	0.000531976	0.000294517	0.000126733	2.86562E-05
2.44	0.002370376	0.001636132	0.001037406	0.000574372	0.000247168	5.58896E-05
2.928	0.004071571	0.002810689	0.001782311	0.00098687	0.000424699	9.60358E-05
3.416	0.006408517	0.004424512	0.002805968	0.0015538	0.000668716	0.00015122
3.904	0.009460068	0.006532293	0.004143192	0.002294498	0.000987559	0.00022333
4.392	0.01329349	0.009180781	0.005823791	0.00322554	0.001388382	0.000313986
4.88	0.01796343	0.012408061	0.007872103	0.004360483	0.001877044	0.000424518
5.368	0.023511098	0.016242969	0.010306617	0.005709653	0.002458017	0.000555939
5.856	0.029963682	0.020704672	0.013139698	0.007279985	0.003134313	0.000708934
6.344	0.037333989	0.025802397	0.016377399	0.009074923	0.00390744	0.000883849
6.832	0.045620321	0.031535324	0.020019389	0.011094362	0.00477738	0.001080682
7.32	0.054806585	0.037892639	0.024058966	0.013334661	0.005742586	0.001299086
7.808	0.064862618	0.04485374	0.028483184	0.015788705	0.006800012	0.001538375
8.296	0.075744734	0.052388595	0.033273067	0.018446016	0.00794516	0.001797533
8.784	0.087396469	0.060458243	0.038403923	0.021292928	0.00917215	0.00207523
9.272	0.099749505	0.069015426	0.043845735	0.024312802	0.010473815	0.002369846
9.76	0.112724775	0.078005351	0.049563645	0.027486288	0.011841814	0.002679492
10.248	0.126233709	0.087366546	0.055518505	0.030791635	0.013266763	0.003002043
10.736	0.140179615	0.097031833	0.061667486	0.03420503	0.014738385	0.003335171
11.224	0.15445917	0.10692936	0.067964749	0.037700972	0.016245667	0.003676381
11.712	0.168964	0.116983719	0.07436216	0.041252673	0.017777038	0.004023051
12.2	0.183582324	0.127117097	0.080810037	0.044832471	0.01932055	0.004372472
12.688	0.198200648	0.137250476	0.087257913	0.048412269	0.020864061	0.004721894
13.176	0.212705478	0.147304834	0.093655325	0.051963969	0.022395432	0.005068564
13.664	0.226985033	0.157202362	0.099952588	0.055459911	0.023902715	0.005409774
14.152	0.240930939	0.166867648	0.106101568	0.058873307	0.025374336	0.005742902
14.64	0.254439873	0.176228844	0.112056428	0.062178654	0.026799285	0.006065453
15.128	0.267415143	0.185218768	0.117774339	0.06535214	0.028167284	0.006375099
15.616	0.279768179	0.193775952	0.123216151	0.068372013	0.029468949	0.006669714
16.104	0.291419913	0.201845599	0.128347006	0.071218925	0.030695939	0.006947412
16.592	0.30230203	0.209380454	0.133136889	0.073876236	0.031841087	0.00720657
17.08	0.312358063	0.216341555	0.137561107	0.07633028	0.032898513	0.007445859
17.568	0.321544327	0.222698871	0.141600685	0.07857058	0.03386372	0.007664263
18.056	0.329830659	0.228431798	0.145242674	0.080590019	0.034733659	0.007861096
18.544	0.337200966	0.233529522	0.148480375	0.082384956	0.035506786	0.008036011
19.032	0.34365355	0.237991225	0.151313456	0.083955289	0.036183082	0.008189006
19.52	0.349201218	0.241826133	0.15374797	0.085304458	0.036764055	0.008320427
20.008	0.353871158	0.245053413	0.155796282	0.086439401	0.037252717	0.008430959
20.496	0.35770458	0.247701902	0.157476882	0.087370443	0.03765354	0.008521615
20.984	0.36075613	0.249809683	0.158814105	0.088111142	0.037972383	0.008593725
21.472	0.363093077	0.251423505	0.159837762	0.088678072	0.0382164	0.008648909
21.96	0.364794272	0.252598062	0.160582668	0.089090569	0.038393931	0.008689055
22.448	0.365948921	0.25339513	0.161088098	0.089370424	0.038514366	0.008716289
22.936	0.366655161	0.253882586	0.161397164	0.089541538	0.038587999	0.008732939
23.424	0.367018478	0.254133325	0.161556128	0.089629542	0.038625867	0.008741501
23.912	0.367149995	0.254224083	0.161613663	0.089661393	0.038639572	0.0087446
24.4	0.367164648	0.254234194	0.161620073	0.089664941	0.038641099	0.008744945

Absolute Value of delta s difference between adjacent longitudinals						
(long. 1 & 2)	(long. 2 & 3)	(long. 3 & 4)	(long. 4 & 5)	(long. 5 & 6)	(long. 6 & 7)	(long. 7 & 8)
0	0	0	0	0	0	0
1.04205E-05	9.58082E-06	8.74105E-06	7.90123E-06	7.06137E-06	6.22148E-06	5.38155E-06
0.00010386	9.55047E-05	8.71453E-05	7.87822E-05	7.04158E-05	6.20464E-05	5.36745E-05
0.000361511	0.000332508	0.000303471	0.000274403	0.000245307	0.000216185	0.000187041
0.000860985	0.000792172	0.000723213	0.00065412	0.000584906	0.000515584	0.000446165
0.001674701	0.001541488	0.001407835	0.001273777	0.001139351	0.001004595	0.000869546
0.002868464	0.002641578	0.002413624	0.002184687	0.001954853	0.001724214	0.001492859
0.00450029	0.004146612	0.003790709	0.003432752	0.003072917	0.002711387	0.002348353
0.006619475	0.006102938	0.005582251	0.005057719	0.004529664	0.003998422	0.003464339
0.009265951	0.008548438	0.007823818	0.007092592	0.006355294	0.005612484	0.004864752
0.012469884	0.011512107	0.010542958	0.009563204	0.008573665	0.007575219	0.006568795
0.016251529	0.015013846	0.013758952	0.012487943	0.011202017	0.009902469	0.008590683
0.020621288	0.019064449	0.017482732	0.015877637	0.014250823	0.01260411	0.010939469
0.025579959	0.023665754	0.021716971	0.019735567	0.017723754	0.015683988	0.013618962
0.031119132	0.028810951	0.026456288	0.024057616	0.021617772	0.019139961	0.016627739
0.037221704	0.034484993	0.031687593	0.028832523	0.025923319	0.022964034	0.019959229
0.043862482	0.040665119	0.037390509	0.034042238	0.030624594	0.027142577	0.023601882
0.051008856	0.047321439	0.043537884	0.03966235	0.03569992	0.03165662	0.027539407
0.058621505	0.054417572	0.050096358	0.045662589	0.04112217	0.03648222	0.031751068
0.06665514	0.061911328	0.057026984	0.052007377	0.046859253	0.041590877	0.036212051
0.075059253	0.069755412	0.064285873	0.058656424	0.052874651	0.046950013	0.040893863
0.083778871	0.077898141	0.071824876	0.06556535	0.05912799	0.052523478	0.045764785
0.09275532	0.086284176	0.079592273	0.072686341	0.065575642	0.058272099	0.050790358
0.101926965	0.094855248	0.087533478	0.079968816	0.07217135	0.064154257	0.055933897
0.111229967	0.103550898	0.095591755	0.08736011	0.07886687	0.070126476	0.061157027
0.120599014	0.112309201	0.103708926	0.094806162	0.08561263	0.076144039	0.066420236
0.12996806	0.121067504	0.111826098	0.102252215	0.09235839	0.082161602	0.071683446
0.139271062	0.129763153	0.119884374	0.109643508	0.09905391	0.088133821	0.076906576
0.148442707	0.138334226	0.12782558	0.116925984	0.105649617	0.094015979	0.082050114
0.157419156	0.14672026	0.135592977	0.124046975	0.112097269	0.099764601	0.087075688
0.166138774	0.15486299	0.143131979	0.130955901	0.118350608	0.105338065	0.09194661
0.174542887	0.162707073	0.150390869	0.137604947	0.124366007	0.110697201	0.096628421
0.182576522	0.170200829	0.157321494	0.143949736	0.130103089	0.115805859	0.101089404
0.190189171	0.177296962	0.163879969	0.149949975	0.135525339	0.120631458	0.105301066
0.197335545	0.183953282	0.170027343	0.155570087	0.140600665	0.125145501	0.10923859
0.203976324	0.190133409	0.175730259	0.160779801	0.14530194	0.129324044	0.112881244
0.210078895	0.195807451	0.180961564	0.165554709	0.149607487	0.133148117	0.116212734
0.215618068	0.200952647	0.185700882	0.169876758	0.153501506	0.136604091	0.119221511
0.220576739	0.205553953	0.18993512	0.173734688	0.156974437	0.139683969	0.121901004
0.224946498	0.209604555	0.193658901	0.177124382	0.160023242	0.142385609	0.12424979
0.228728143	0.213106295	0.196874894	0.180049121	0.162651594	0.144712859	0.126271678
0.231932076	0.216069964	0.199594035	0.182519732	0.164869965	0.146675594	0.127975721
0.234578552	0.218515463	0.201835602	0.184554606	0.166695595	0.148289657	0.129376134
0.236697737	0.220471789	0.203627143	0.186179573	0.168152343	0.149576691	0.13049212
0.238329563	0.221976823	0.205004229	0.187427638	0.169270406	0.150563865	0.131347614
0.239523327	0.223076913	0.206010018	0.188338548	0.170085908	0.151283483	0.131970926
0.240337042	0.223826229	0.206694639	0.188958204	0.170640353	0.151772495	0.132394308
0.240836516	0.224285893	0.207114382	0.189337922	0.170979953	0.152071893	0.132653431
0.241094167	0.224522897	0.207330707	0.189533542	0.171154843	0.152226032	0.132786798
0.241187607	0.224608821	0.207409112	0.189604423	0.171218198	0.152281857	0.132835091
0.241198027	0.224618401	0.207417853	0.189612325	0.171225259	0.152288078	0.132840473

Absolute Value of delta s difference between adjacent longitudinals					
(long. 8 & 9)	(long. 9 & 10)	(long. 10 & 11)	(long. 11 & 12)	(long. 12 & 13)	longitudinal 13 and side shell
0	0	0	0	0	0
4.54159E-06	3.70161E-06	2.86162E-06	2.0216E-06	1.18158E-06	3.45216E-07
4.53002E-05	3.69241E-05	2.85464E-05	2.01674E-05	1.17877E-05	3.44398E-06
0.000157878	0.000128699	9.95064E-05	7.03035E-05	4.10933E-05	1.20064E-05
0.000376662	0.000307089	0.000237459	0.000167784	9.8077E-05	2.86562E-05
0.000734244	0.000598727	0.000463033	0.000327204	0.000191278	5.58896E-05
0.001260882	0.001028378	0.000795442	0.000562171	0.000328663	9.60358E-05
0.001984006	0.001618544	0.001252168	0.000885084	0.000517496	0.00015122
0.002927776	0.002389101	0.001848694	0.001306939	0.000764229	0.00022333
0.004112709	0.003356991	0.002598251	0.001837158	0.001074396	0.000313986
0.005555369	0.004535958	0.00351162	0.002483439	0.001452526	0.000424518
0.007268129	0.005936352	0.004596965	0.003251636	0.001902078	0.000555939
0.00925901	0.007564974	0.005859712	0.004145673	0.002425378	0.000708934
0.011531592	0.009424997	0.007302477	0.005167483	0.003023591	0.000883849
0.014084997	0.011515935	0.008925027	0.006316982	0.003696698	0.001080682
0.016913945	0.013833673	0.010724304	0.007592075	0.0044435	0.001299086
0.020008877	0.016370556	0.012694479	0.008988692	0.005261637	0.001538375
0.023356139	0.019115528	0.014827051	0.010500856	0.006147627	0.001797533
0.026938226	0.02205432	0.017110994	0.012120778	0.00709692	0.00207523
0.030734079	0.025169692	0.019532933	0.013838986	0.008103969	0.002369846
0.034719424	0.028441705	0.022077358	0.015644474	0.009162322	0.002679492
0.038867162	0.031848041	0.02472687	0.017524872	0.01026472	0.003002043
0.043147782	0.035364347	0.027462456	0.019466645	0.011403214	0.003335171
0.04752981	0.038964611	0.030263776	0.021455306	0.012569285	0.003676381
0.051980281	0.042621558	0.033109488	0.023475635	0.013753987	0.004023051
0.056465227	0.046307061	0.035977566	0.025511921	0.014948077	0.004372472
0.060950172	0.049992563	0.038845644	0.027548208	0.016142167	0.004721894
0.065400643	0.05364951	0.041691356	0.029568536	0.017326869	0.005068564
0.069782671	0.057249774	0.044492676	0.031557197	0.018492941	0.005409774
0.074063291	0.06076608	0.047228261	0.033498971	0.019631434	0.005742902
0.078211029	0.064172416	0.049877774	0.035379369	0.020733832	0.006065453
0.082196375	0.067444429	0.052422199	0.037184856	0.021792185	0.006375099
0.085992227	0.070559801	0.054844138	0.038903064	0.022799234	0.006669714
0.089574314	0.073498594	0.057128081	0.040522987	0.023748527	0.006947412
0.092921576	0.076243565	0.059260653	0.04203515	0.024634517	0.00720657
0.096016508	0.078780448	0.061230827	0.043431767	0.025452654	0.007445859
0.098845456	0.081098186	0.063030105	0.04470686	0.026199456	0.007664263
0.101398861	0.083189124	0.064652655	0.04585636	0.026872563	0.007861096
0.103671443	0.085049147	0.066095419	0.04687817	0.027470776	0.008036011
0.105662325	0.086677769	0.067358167	0.047772207	0.027994076	0.008189006
0.107375085	0.088078163	0.068443512	0.048540404	0.028443628	0.008320427
0.108817745	0.089257131	0.069356881	0.049186684	0.028821759	0.008430959
0.110002678	0.09022502	0.070106438	0.049716903	0.029131925	0.008521615
0.110946448	0.090995578	0.070702964	0.050138759	0.029378658	0.008593725
0.111669571	0.091585743	0.07115969	0.050461671	0.029567491	0.008648909
0.112196209	0.092015395	0.071492099	0.050696638	0.029704876	0.008689055
0.112553791	0.092307032	0.071717673	0.050856059	0.029798077	0.008716289
0.112772575	0.092485422	0.071855626	0.050953539	0.029855061	0.008732939
0.112885153	0.092577197	0.071926586	0.051003675	0.029884366	0.008741501
0.112925912	0.09261042	0.07195227	0.051021821	0.029894972	0.0087446
0.112930453	0.092614121	0.071955132	0.051023842	0.029896154	0.008744945

Shear rotation angle (Phi) for hull plate element [radians]						
(long. 1 & 2)	(long. 2 & 3)	(long. 3 & 4)	(long. 4 & 5)	(long. 5 & 6)	(long. 6 & 7)	(long. 7 & 8)
0	0	0	0	0	0	0
1.14511E-05	1.05284E-05	9.60555E-06	8.68267E-06	7.75975E-06	6.83679E-06	5.91379E-06
0.000114132	0.00010495	9.5764E-05	8.65738E-05	7.738E-05	6.81829E-05	5.89829E-05
0.000397265	0.000365393	0.000333485	0.000301542	0.000269568	0.000237566	0.00020554
0.000946137	0.000870519	0.00079474	0.000718814	0.000642754	0.000566575	0.000490291
0.001840328	0.001693941	0.00154707	0.001399754	0.001252033	0.00110395	0.000955545
0.003152148	0.002902825	0.002652328	0.00240075	0.002148187	0.001894738	0.001640503
0.004945333	0.004556685	0.004165591	0.003772237	0.003376819	0.002979538	0.002580602
0.00727402	0.006706425	0.006134265	0.005557876	0.004977612	0.004393842	0.003806948
0.010182012	0.009393611	0.00859739	0.007793899	0.006983726	0.006167487	0.00534583
0.013702312	0.012649992	0.01158515	0.010508628	0.009421331	0.008324224	0.007218331
0.017856925	0.016497235	0.015118575	0.013722153	0.012309288	0.010881405	0.009440031
0.022656878	0.02094688	0.019209431	0.017446182	0.015658965	0.013849785	0.012020815
0.028102445	0.026000463	0.023860274	0.021684037	0.01947419	0.017233445	0.014964775
0.034183528	0.031649813	0.029064657	0.026430784	0.023751326	0.021029824	0.018270208
0.040880183	0.037877472	0.034807467	0.031673495	0.028479461	0.025229848	0.021929703
0.048163254	0.044657235	0.041065373	0.037391617	0.033640704	0.029818167	0.025930321
0.055995091	0.051954784	0.047807373	0.043557432	0.039210574	0.034773472	0.03025385
0.064330348	0.059728401	0.054995432	0.050136617	0.045158475	0.040068894	0.034877135
0.073116832	0.067929747	0.062585174	0.057088863	0.051448243	0.045672477	0.039772479
0.082296401	0.076504689	0.07052665	0.064368561	0.058038756	0.051547715	0.044908098
0.091805898	0.085394176	0.078765145	0.071925547	0.064884605	0.057654141	0.050248639
0.10157811	0.094535148	0.087242022	0.079705878	0.071936799	0.063947963	0.055755733
0.111542744	0.10386146	0.095895599	0.08765265	0.079143517	0.070382734	0.061388589
0.121627409	0.113304824	0.104662041	0.095706828	0.086450873	0.076910057	0.067104617
0.131758599	0.122795754	0.113476258	0.103808099	0.09380371	0.083480303	0.072860068
0.141862657	0.132264503	0.122272803	0.111895718	0.101146389	0.090043332	0.078610688
0.151866724	0.141641979	0.130986757	0.119909352	0.108423579	0.096549228	0.084312371
0.161699649	0.150860641	0.139554592	0.127789904	0.115581034	0.102949013	0.089921807
0.171292869	0.159855358	0.147915009	0.135480316	0.12256635	0.109195348	0.095397121
0.180581243	0.168564231	0.156009736	0.142926335	0.129329693	0.115243209	0.100698477
0.189503835	0.176929369	0.163784283	0.150077244	0.135824488	0.121050529	0.105788668
0.198004659	0.184897621	0.171188665	0.156886553	0.142008072	0.126578801	0.110633658
0.206033367	0.19242126	0.178178057	0.163312629	0.147842296	0.131793637	0.115203088
0.213545895	0.199458613	0.184713414	0.169319293	0.153294074	0.136665273	0.119470731
0.220505068	0.205974653	0.190762036	0.174876346	0.158335883	0.141169026	0.123414894
0.226881161	0.211941532	0.196298071	0.179960045	0.162946196	0.145285681	0.127018766
0.232652411	0.21733907	0.201302968	0.184553513	0.167109845	0.149001814	0.130270695
0.237805494	0.222155177	0.205765859	0.188647078	0.170818327	0.152310053	0.1331644
0.24233594	0.226386226	0.209683874	0.19223854	0.174070014	0.155209249	0.135699117
0.246248478	0.230037332	0.21306237	0.195333344	0.176870291	0.157704572	0.137879656
0.249557303	0.23312255	0.215915062	0.197944667	0.17923159	0.159807518	0.139716386
0.25228622	0.235664949	0.218264045	0.200093384	0.181173332	0.161535816	0.141225134
0.254468659	0.237696562	0.220139681	0.20180792	0.18272174	0.162913244	0.14242699
0.256147505	0.239258156	0.221580337	0.203123963	0.183909553	0.163969329	0.143348029
0.257374733	0.240398836	0.222631967	0.204084036	0.1847756	0.16473895	0.144018944
0.258210805	0.241175435	0.223347505	0.204736919	0.185364248	0.165261827	0.144474585
0.25872382	0.241651689	0.223786087	0.20513691	0.185724734	0.165581915	0.144753422
0.258988401	0.241897202	0.224012088	0.205342949	0.185910362	0.165746692	0.144896927
0.259084344	0.241986204	0.224093993	0.205417601	0.185977602	0.165806367	0.144948889
0.259095044	0.241996128	0.224103124	0.205425922	0.185985097	0.165813018	0.14495468

Shear rotation angle {Phi} for hull plate element {radians}					
(long. 8 & 9)	(long. 9 &10)	(long. 10 &11)	(long. 11 &12)	(long. 12 &13)	longitudinal.13 & side shell
0	0	0	0	0	0
4.99076E-06	4.06771E-06	3.14463E-06	2.22154E-06	1.29844E-06	4.18443E-07
4.97805E-05	4.05759E-05	3.13696E-05	2.2162E-05	1.29535E-05	4.17452E-06
0.000173493	0.000141428	0.000109348	7.72566E-05	4.51575E-05	1.45532E-05
0.000413914	0.000337461	0.000260944	0.000184378	0.000107777	3.47348E-05
0.000806861	0.000657941	0.000508828	0.000359565	0.000210196	6.7745E-05
0.001385584	0.001130085	0.000874112	0.00061777	0.000361168	0.000116407
0.002180222	0.001778618	0.001376008	0.000972619	0.000568677	0.000183297
0.003217325	0.00262538	0.002031529	0.001436196	0.000839812	0.000270703
0.004519429	0.003688984	0.002855213	0.002018853	0.001180654	0.00038059
0.006104725	0.004984528	0.003858904	0.002729047	0.001596182	0.000514567
0.007986785	0.006523371	0.005051567	0.003573211	0.002090193	0.000673865
0.010174385	0.008312967	0.006439155	0.004555653	0.002665245	0.000859314
0.012671401	0.01035677	0.008024527	0.005678491	0.003322615	0.001071331
0.015476783	0.012654198	0.009807408	0.006941627	0.004062283	0.001309916
0.018584613	0.015200668	0.011784404	0.008342747	0.004882928	0.001574648
0.021984235	0.017987682	0.013949072	0.009877363	0.005781955	0.001864695
0.025660453	0.021002986	0.016292021	0.01153889	0.006755532	0.002178824
0.029593804	0.024230773	0.018801075	0.013318749	0.007798655	0.002515426
0.03376088	0.027651952	0.021461466	0.015206505	0.008905225	0.002872533
0.038134717	0.03124445	0.024256075	0.017190036	0.010068146	0.003247858
0.042685224	0.034983569	0.027165701	0.01925572	0.011279434	0.003638824
0.04737966	0.038842374	0.030169366	0.021388656	0.012530348	0.004042609
0.052183142	0.042792115	0.033244644	0.023572892	0.013811523	0.00445619
0.057059184	0.046802674	0.03636801	0.02579168	0.015113121	0.004876387
0.061970249	0.050843024	0.039515207	0.028027737	0.016424981	0.005299917
0.066878323	0.054881715	0.042661621	0.030263513	0.017736785	0.005723445
0.071745484	0.058887343	0.045782662	0.032481469	0.019038214	0.006143637
0.076534469	0.062829037	0.048854147	0.034664347	0.020319116	0.006557208
0.081209236	0.066676925	0.051852666	0.036795441	0.021569658	0.006960981
0.085735498	0.07040259	0.054755952	0.038858856	0.022780489	0.007351932
0.090081234	0.073979499	0.057543215	0.040839759	0.02394288	0.007727239
0.094217175	0.07738341	0.060195472	0.042724605	0.025048863	0.008084326
0.098117237	0.080592742	0.062695834	0.044501355	0.02609136	0.008420906
0.101758927	0.08358891	0.065029774	0.04615966	0.027064288	0.008735014
0.105123686	0.086356611	0.067185352	0.047691027	0.027962659	0.009025039
0.108197186	0.088884071	0.069153405	0.049088949	0.02878266	0.009289749
0.110969563	0.091163233	0.070927695	0.050349015	0.02952171	0.009528313
0.113435596	0.093189896	0.072505009	0.051468976	0.030178501	0.009740311
0.115594812	0.094963797	0.073885223	0.052448784	0.030753022	0.009925742
0.117451526	0.096488632	0.075071306	0.053290599	0.03124656	0.010085024
0.119014808	0.097772017	0.076069287	0.053998755	0.031661678	0.010218988
0.120298377	0.098825387	0.076888167	0.054579698	0.032002175	0.010328863
0.121320424	0.099663841	0.077539789	0.055041884	0.03227303	0.01041626
0.122103351	0.100305913	0.078038656	0.055395653	0.032480322	0.010483142
0.122673449	0.100773301	0.078401709	0.055653063	0.032631134	0.010531799
0.123060494	0.101090527	0.078648068	0.055827706	0.032733444	0.010564805
0.123297286	0.10128456	0.078798726	0.055934493	0.032795996	0.010584985
0.123419125	0.10138438	0.078876221	0.055989415	0.032828165	0.010595362
0.123463236	0.101420514	0.07890427	0.056009293	0.032839808	0.010599118
0.123468151	0.10142454	0.078907396	0.056011508	0.032841105	0.010599536

In-plane [NDSF/in] for hull plate element						
(long. 1 & 2)	(long. 2 & 3)	(long. 3 & 4)	(long. 4 & 5)	(long. 5 & 6)	(long. 6 & 7)	(long. 7 & 8)
0	0	0	0	0	0	0
0.005975408	0.005493889	0.005012342	0.004530769	0.004049172	0.003567554	0.003085918
0.059556018	0.054764823	0.049971324	0.045175722	0.040378218	0.035579013	0.030778308
0.207299566	0.190668555	0.174018025	0.157349651	0.140665115	0.12396611	0.107254337
0.49371068	0.45425168	0.41470891	0.375089415	0.335400316	0.295648813	0.255842171
0.960315184	0.883927938	0.807287904	0.730415815	0.653332785	0.576060281	0.498620086
1.644845655	1.514744508	1.384030678	1.25275293	1.120961337	0.988707182	0.856042845
2.580560629	2.377757563	2.173677515	1.968418622	1.762082622	1.554774605	1.346602731
3	3	3	2.900196057	2.597404343	2.292782902	1.986531343
3	3	3	3	3	3	2.789546894
3	3	3	3	3	3	3
3	3	3	3	3	3	3
3	3	3	3	3	3	3
3	3	3	3	3	3	3
3	3	3	3	3	3	3
3	3	3	3	3	3	3
3	3	3	3	3	3	3
3	3	3	3	3	3	3
3	3	3	3	3	3	3
3	3	3	3	3	3	3
3	3	3	3	3	3	3
3	3	3	3	3	3	3
3	3	3	3	3	3	3
3	3	3	3	3	3	3
3	3	3	3	3	3	3
3	3	3	3	3	3	3
3	3	3	3	3	3	3
3	3	3	3	3	3	3
3	3	3	3	3	3	3
3	3	3	3	3	3	3
3	3	3	3	3	3	3
3	3	3	3	3	3	3
3	3	3	3	3	3	3
3	3	3	3	3	3	3
3	3	3	3	3	3	3
3	3	3	3	3	3	3
3	3	3	3	3	3	3
3	3	3	3	3	3	3
3	3	3	3	3	3	3
3	3	3	3	3	3	3
3	3	3	3	3	3	3
3	3	3	3	3	3	3
3	3	3	3	3	3	3
3	3	3	3	3	3	3
3	3	3	3	3	3	3
3	3	3	3	3	3	3
3	3	3	3	3	3	3
3	3	3	3	3	3	3
3	3	3	3	3	3	3
3	3	3	3	3	3	3
3	3	3	3	3	3	3

In-plane [NDSF/in] for hull plate element					
(long. 8 & 9)	(long. 9 &10)	(long. 10 &11)	(long. 11 &12)	(long. 12 &13)	longitudinal.13 & side shell
0	0	0	0	0	0
0.002604266	0.002122601	0.001640924	0.001159239	0.000677549	0.000218351
0.025976305	0.021173206	0.016369214	0.011564531	0.006759359	0.002178337
0.090531506	0.073799331	0.057059534	0.040313839	0.023563975	0.007594097
0.215987715	0.176092821	0.13616491	0.096211438	0.056239888	0.018125215
0.421034266	0.343325135	0.265515217	0.187627209	0.109683941	0.035350522
0.723021693	0.589697953	0.456126594	0.322363189	0.188463788	0.060743178
1.13767792	0.92811353	0.718025011	0.50752954	0.296745643	0.095647429
1.678855905	1.369968704	1.060086925	0.749431956	0.438228482	0.141257399
2.358316766	1.924975856	1.489899547	1.053472299	0.616085714	0.198598261
3	2.601013472	2.01364287	1.424063995	0.832915269	0.268510076
3	3	2.635995153	1.864563488	1.090698852	0.351634563
3	3	3	2.377218733	1.390771001	0.448404991
3	3	3	2.963135455	1.733798414	0.559039379
3	3	3	3	2.119769848	0.683537077
3	3	3	3	2.547996715	0.821678805
3	3	3	3	3	0.973030139
3	3	3	3	3	1.136948386
3	3	3	3	3	1.312592736
3	3	3	3	3	1.498937544
3	3	3	3	3	1.694788508
3	3	3	3	3	1.898801514
3	3	3	3	3	2.109503825
3	3	3	3	3	2.325317305
3	3	3	3	3	2.544583289
3	3	3	3	3	2.765588725
3	3	3	3	3	2.98659317
3	3	3	3	3	3
3	3	3	3	3	3
3	3	3	3	3	3
3	3	3	3	3	3
3	3	3	3	3	3
3	3	3	3	3	3
3	3	3	3	3	3
3	3	3	3	3	3
3	3	3	3	3	3
3	3	3	3	3	3
3	3	3	3	3	3
3	3	3	3	3	3
3	3	3	3	3	3
3	3	3	3	3	3
3	3	3	3	3	3
3	3	3	3	3	3
3	3	3	3	3	3
3	3	3	3	3	3
3	3	3	3	3	3
3	3	3	3	3	3
3	3	3	3	3	3
3	3	3	3	3	3
3	3	3	3	3	3

In-plane shear resistance [Newtons] for hull plate elements

(long. 1 & 2)	(long. 2 & 3)	(long. 3 & 4)	(long. 4 & 5)	(long. 5 & 6)	(long. 6 & 7)	(long. 7 & 8)
0	0	0	0	0	0	0
4093.32889	3763.474271	3433.600225	3103.708454	2773.80066	2443.878545	2113.943812
40797.60785	37515.49921	34231.81288	30946.68597	27660.25594	24372.66051	21084.0377
142006.2429	130613.5155	119207.4176	107789.0955	96359.70213	84920.39721	73472.34614
338206.2013	311175.6363	284087.6872	256947.1781	229758.9892	202528.0515	175259.3419
657843.8821	605516.3929	553015.7367	500356.1157	447551.9944	394618.0776	341569.2875
1126767.2	1037644.124	948101.3418	858172.259	767891.1779	677293.2281	586414.2921
1767759.222	1628833.213	1489032.434	1348424.111	1207077.939	1065065.907	922462.1073
2055087.413	2055087.413	2055087.413	1986718.803	1779297.657	1570623.094	1360831.852
2055087.413	2055087.413	2055087.413	2055087.413	2055087.413	2055087.413	1910920.903
2055087.413	2055087.413	2055087.413	2055087.413	2055087.413	2055087.413	2055087.413
2055087.413	2055087.413	2055087.413	2055087.413	2055087.413	2055087.413	2055087.413
2055087.413	2055087.413	2055087.413	2055087.413	2055087.413	2055087.413	2055087.413
2055087.413	2055087.413	2055087.413	2055087.413	2055087.413	2055087.413	2055087.413
2055087.413	2055087.413	2055087.413	2055087.413	2055087.413	2055087.413	2055087.413
2055087.413	2055087.413	2055087.413	2055087.413	2055087.413	2055087.413	2055087.413
2055087.413	2055087.413	2055087.413	2055087.413	2055087.413	2055087.413	2055087.413
2055087.413	2055087.413	2055087.413	2055087.413	2055087.413	2055087.413	2055087.413
2055087.413	2055087.413	2055087.413	2055087.413	2055087.413	2055087.413	2055087.413
2055087.413	2055087.413	2055087.413	2055087.413	2055087.413	2055087.413	2055087.413
2055087.413	2055087.413	2055087.413	2055087.413	2055087.413	2055087.413	2055087.413
2055087.413	2055087.413	2055087.413	2055087.413	2055087.413	2055087.413	2055087.413
2055087.413	2055087.413	2055087.413	2055087.413	2055087.413	2055087.413	2055087.413
2055087.413	2055087.413	2055087.413	2055087.413	2055087.413	2055087.413	2055087.413
2055087.413	2055087.413	2055087.413	2055087.413	2055087.413	2055087.413	2055087.413
2055087.413	2055087.413	2055087.413	2055087.413	2055087.413	2055087.413	2055087.413
2055087.413	2055087.413	2055087.413	2055087.413	2055087.413	2055087.413	2055087.413
2055087.413	2055087.413	2055087.413	2055087.413	2055087.413	2055087.413	2055087.413
2055087.413	2055087.413	2055087.413	2055087.413	2055087.413	2055087.413	2055087.413
2055087.413	2055087.413	2055087.413	2055087.413	2055087.413	2055087.413	2055087.413
2055087.413	2055087.413	2055087.413	2055087.413	2055087.413	2055087.413	2055087.413
2055087.413	2055087.413	2055087.413	2055087.413	2055087.413	2055087.413	2055087.413
2055087.413	2055087.413	2055087.413	2055087.413	2055087.413	2055087.413	2055087.413
2055087.413	2055087.413	2055087.413	2055087.413	2055087.413	2055087.413	2055087.413
2055087.413	2055087.413	2055087.413	2055087.413	2055087.413	2055087.413	2055087.413
2055087.413	2055087.413	2055087.413	2055087.413	2055087.413	2055087.413	2055087.413
2055087.413	2055087.413	2055087.413	2055087.413	2055087.413	2055087.413	2055087.413
2055087.413	2055087.413	2055087.413	2055087.413	2055087.413	2055087.413	2055087.413
2055087.413	2055087.413	2055087.413	2055087.413	2055087.413	2055087.413	2055087.413
2055087.413	2055087.413	2055087.413	2055087.413	2055087.413	2055087.413	2055087.413
2055087.413	2055087.413	2055087.413	2055087.413	2055087.413	2055087.413	2055087.413
2055087.413	2055087.413	2055087.413	2055087.413	2055087.413	2055087.413	2055087.413
2055087.413	2055087.413	2055087.413	2055087.413	2055087.413	2055087.413	2055087.413
2055087.413	2055087.413	2055087.413	2055087.413	2055087.413	2055087.413	2055087.413
2055087.413	2055087.413	2055087.413	2055087.413	2055087.413	2055087.413	2055087.413
2055087.413	2055087.413	2055087.413	2055087.413	2055087.413	2055087.413	2055087.413
2055087.413	2055087.413	2055087.413	2055087.413	2055087.413	2055087.413	2055087.413
2055087.413	2055087.413	2055087.413	2055087.413	2055087.413	2055087.413	2055087.413
2055087.413	2055087.413	2055087.413	2055087.413	2055087.413	2055087.413	2055087.413
2055087.413	2055087.413	2055087.413	2055087.413	2055087.413	2055087.413	2055087.413
2055087.413	2055087.413	2055087.413	2055087.413	2055087.413	2055087.413	2055087.413
column total	**column total**	**column total**	**column total**	**column total**	**column total**	**column total**
92446232.43	92123820.6	91799868.77	91406129.29	90872042.85	90335536.62	89652712.03

In-plane shear resistance [Newtons] for hull plate elements

(long. 8 & 9)	(long. 9 &10)	(long. 10 &11)	(long. 11 &12)	(long. 12 &13)	longitudinal.13 & side shell
0	0	0	0	0	0
1783.998164	1454.043305	1124.080936	794.1127638	464.1404902	149.5767592
17794.52575	14504.26311	11213.3884	7922.040368	4630.35789	1492.224267
62016.71948	50554.69224	39087.44323	27616.15433	16142.00979	5202.177901
147957.8782	120628.7134	93276.93075	65907.63808	38525.96229	12416.3006
288420.7403	235187.7214	181885.6604	128530.1052	75136.69565	24216.13758
495290.9266	403960.2803	312460.0072	220828.1775	129103.1858	41610.84689
779342.524	635784.811	491868.0541	347672.523	203279.4121	65521.27571
1150065.212	938468.4797	726190.432	513382.7266	300199.2789	96765.43408
1615515.7	1318664.55	1020624.601	721659.2203	422036.6654	136045.5953
2055087.413	1781770.016	1379404.038	975525.3305	570571.2286	183937.226
2055087.413	2055087.413	1805733.486	1277280.318	747160.494	240879.9212
2055087.413	2055087.413	2055087.413	1628464.099	952718.6591	307170.4844
2055087.413	2055087.413	2055087.413	2029834.125	1187702.432	382958.2638
2055087.413	2055087.413	2055087.413	2055087.413	1452104.111	468242.8141
2055087.413	2055087.413	2055087.413	2055087.413	1745451.992	562873.9229
2055087.413	2055087.413	2055087.413	2055087.413	2055087.413	666553.997
2055087.413	2055087.413	2055087.413	2055087.413	2055087.413	778842.7722
2055087.413	2055087.413	2055087.413	2055087.413	2055087.413	899164.2702
2055087.413	2055087.413	2055087.413	2055087.413	2055087.413	1026815.893
2055087.413	2055087.413	2055087.413	2055087.413	2055087.413	1160979.51
2055087.413	2055087.413	2055087.413	2055087.413	2055087.413	1300734.363
2055087.413	2055087.413	2055087.413	2055087.413	2055087.413	1445071.586
2055087.413	2055087.413	2055087.413	2055087.413	2055087.413	1592910.108
2055087.413	2055087.413	2055087.413	2055087.413	2055087.413	1743113.696
2055087.413	2055087.413	2055087.413	2055087.413	2055087.413	1894508.859
2055087.413	2055087.413	2055087.413	2055087.413	2055087.413	2045903.343
2055087.413	2055087.413	2055087.413	2055087.413	2055087.413	2055087.413
2055087.413	2055087.413	2055087.413	2055087.413	2055087.413	2055087.413
2055087.413	2055087.413	2055087.413	2055087.413	2055087.413	2055087.413
2055087.413	2055087.413	2055087.413	2055087.413	2055087.413	2055087.413
2055087.413	2055087.413	2055087.413	2055087.413	2055087.413	2055087.413
2055087.413	2055087.413	2055087.413	2055087.413	2055087.413	2055087.413
2055087.413	2055087.413	2055087.413	2055087.413	2055087.413	2055087.413
2055087.413	2055087.413	2055087.413	2055087.413	2055087.413	2055087.413
2055087.413	2055087.413	2055087.413	2055087.413	2055087.413	2055087.413
2055087.413	2055087.413	2055087.413	2055087.413	2055087.413	2055087.413
2055087.413	2055087.413	2055087.413	2055087.413	2055087.413	2055087.413
2055087.413	2055087.413	2055087.413	2055087.413	2055087.413	2055087.413
2055087.413	2055087.413	2055087.413	2055087.413	2055087.413	2055087.413
2055087.413	2055087.413	2055087.413	2055087.413	2055087.413	2055087.413
2055087.413	2055087.413	2055087.413	2055087.413	2055087.413	2055087.413
2055087.413	2055087.413	2055087.413	2055087.413	2055087.413	2055087.413
2055087.413	2055087.413	2055087.413	2055087.413	2055087.413	2055087.413
2055087.413	2055087.413	2055087.413	2055087.413	2055087.413	2055087.413
2055087.413	2055087.413	2055087.413	2055087.413	2055087.413	2055087.413
2055087.413	2055087.413	2055087.413	2055087.413	2055087.413	2055087.413
2055087.413	2055087.413	2055087.413	2055087.413	2055087.413	2055087.413
2055087.413	2055087.413	2055087.413	2055087.413	2055087.413	2055087.413
2055087.413	2055087.413	2055087.413	2055087.413	2055087.413	2055087.413
2055087.413	2055087.413	2055087.413	2055087.413	2055087.413	2055087.413
column total	**column total**	**column total**	**column total**	**column total**	**column total**
88816772.14	87704474.07	86211277.22	83983650.84	79773286.07	66406178.5

total In-plane force [Newtons] = **2263063963**

Horizontal shear resistance [Newtons] for hull plate elements						
(long. 1 & 2)	(long. 2 & 3)	(long. 3 & 4)	(long. 4 & 5)	(long. 5 & 6)	(long. 6 & 7)	(long. 7 & 8)
0	0	0	0	0	0	0
4091.162899	3761.790708	3432.321597	3102.764029	2773.126478	2443.417425	2113.645359
40711.79898	37448.76832	34181.10849	30909.21855	27633.49939	24354.35361	21072.18531
141341.2183	130095.9125	118813.8225	107498.0492	96151.7267	84778.02015	73380.12208
335431.1961	309013.3149	282441.6854	255728.8642	228887.6554	201931.0895	174872.4022
649565.1186	599056.2725	548091.71	496707.1539	444939.4463	392826.4615	340407.0136
1106800.962	1022037.928	936187.6388	849331.1134	761553.0923	672941.7788	583588.5518
1726224.66	1596307.475	1464159.161	1329936.186	1193805.012	1055941.486	916530.1403
1993871.024	2002984.828	2011443.802	1952045.406	1754365.104	1553458.802	1349658.943
1980142.805	1991202.772	2001498.183	2010989.371	2019638.768	2027411.289	1891568.23
1965882.554	1978926.364	1991105.357	2002364.81	2012652.472	2021919.184	2030119.481
1951349.954	1966376.005	1980449.102	1993497.252	2005451.14	2016245.053	2025817.79
1936793.457	1953765.132	1969709.42	1984535.303	1998154.412	2010482.313	2021439.818
1922446.047	1941296.43	1959059.278	1975623.341	1990879.703	2004723.488	2017055.649
1908522.291	1929159.001	1948662.018	1966899.25	1983740.31	1999058.699	2012734.118
1895216.561	1917526.419	1938669.423	1958492.62	1976843.833	1993574.342	2008541.772
1882702.242	1906555.573	1929220.375	1950523.373	1970290.876	1988351.957	2004541.939
1871131.709	1896386.155	1920440.037	1943100.791	1964174.047	1983467.284	2000793.92
1860636.884	1887140.663	1912439.451	1936322.869	1958577.199	1978989.508	1997352.303
1851330.177	1878924.757	1905315.477	1930275.951	1953574.897	1974980.653	1994266.381
1843305.648	1871827.873	1899150.95	1925034.581	1949232.056	1971495.127	1991579.681
1836640.248	1865923.949	1894015	1920661.494	1945603.729	1968579.382	1989329.588
1831395.03	1861272.191	1889963.443	1917207.716	1942734.986	1966271.672	1987547.043
1827616.238	1857917.798	1887039.183	1914712.711	1940660.873	1964601.883	1986256.327
1825336.219	1855892.578	1885272.57	1913204.529	1939406.406	1963591.427	1985474.887
1824574.103	1855215.417	1884681.697	1912699.942	1938986.584	1963253.178	1985213.237
1825336.219	1855892.578	1885272.57	1913204.529	1939406.406	1963591.427	1985474.887
1827616.238	1857917.798	1887039.183	1914712.711	1940660.873	1964601.883	1986256.327
1831395.03	1861272.191	1889963.443	1917207.716	1942734.986	1966271.672	1987547.043
1836640.248	1865923.949	1894015	1920661.494	1945603.729	1968579.382	1989329.588
1843305.648	1871827.873	1899150.95	1925034.581	1949232.056	1971495.127	1991579.681
1851330.177	1878924.757	1905315.477	1930275.951	1953574.897	1974980.653	1994266.381
1860636.884	1887140.663	1912439.451	1936322.869	1958577.199	1978989.508	1997352.303
1871131.709	1896386.155	1920440.037	1943100.791	1964174.047	1983467.284	2000793.92
1882702.242	1906555.573	1929220.375	1950523.373	1970290.876	1988351.957	2004541.939
1895216.561	1917526.419	1938669.423	1958492.62	1976843.833	1993574.342	2008541.772
1908522.291	1929159.001	1948662.018	1966899.25	1983740.31	1999058.699	2012734.118
1922446.047	1941296.43	1959059.278	1975623.341	1990879.703	2004723.488	2017055.649
1936793.457	1953765.132	1969709.42	1984535.303	1998154.412	2010482.313	2021439.818
1951349.954	1966376.005	1980449.102	1993497.252	2005451.14	2016245.053	2025817.79
1965882.554	1978926.364	1991105.357	2002364.81	2012652.472	2021919.184	2030119.481
1980142.805	1991202.772	2001498.183	2010989.371	2019638.768	2027411.289	2034274.707
1993871.024	2002984.828	2011443.802	2019220.806	2026290.333	2032628.734	2038214.421
2006801.903	2014049.918	2020758.577	2026910.595	2032489.846	2037481.475	2041872.007
2018671.404	2024178.841	2029263.484	2033915.292	2038124.957	2041883.961	2045184.613
2029224.768	2033162.14	2036789.009	2040100.216	2043091.008	2045757.055	2048094.47
2038225.279	2040806.861	2043180.252	2045343.225	2047293.736	2049029.935	2050550.165
2045463.302	2046943.39	2048301.993	2049538.376	2050651.869	2051641.864	2052507.823
2050764.985	2051431.915	2052043.404	2052599.3	2053099.469	2053543.787	2053932.145
2053999.96	2054168.084	2054322.125	2054462.072	2054587.917	2054699.651	2054797.269
2055087.413	2055087.413	2055087.413	2055087.413	2055087.413	2055087.413	2055087.413
column total	column total	column total	column total	column total	column total	column total
86495617.41	86998922.42	87458641.54	87802027.92	87953043.21	88041168.98	87918620.9

Horizontal shear resistance [Newtons] for hull plate elements					
(long. 8 & 9)	(long. 9 &10)	(long. 10 &11)	(long. 11 &12)	(long. 12 &13)	longitudinal.13 & side shell
0	0	0	0	0	0
1783.818775	1453.946173	1124.036059	794.0969405	464.1373308	149.5766534
17787.39989	14500.40395	11211.60504	7921.411507	4630.232317	1492.220063
61961.24956	50524.64087	39073.55233	27611.25499	16141.03134	5202.145149
147725.0116	120502.495	93218.56541	65887.04669	38521.8492	12416.16291
287720.7579	234808.0879	181710.0274	128468.1193	75124.31116	24215.72294
493587.6534	403035.8522	312032.0864	220677.0876	129072.9903	41609.83579
775763.3995	633840.6986	490967.5285	347354.4109	203215.8164	65519.14588
1143316.579	934799.4203	724489.6637	512781.6011	300079.0614	96761.40724
1603812.625	1312295.632	1017670.005	720614.3217	421827.6178	136038.5916
2037212.183	1771429.712	1374603.065	973826.3929	570231.1904	183925.8314
2034113.575	2041082.907	1798349.134	1274665.479	746636.9141	240862.3723
2030954.3	2038960.946	2045403.937	1624620.991	951948.7959	307144.6751
2027784.766	2036828.804	2044116.775	2024404.497	1186614.261	382921.775
2024654.842	2034720.07	2042842.162	2048948.685	1450617.97	468192.9693
2021613.096	2032667.657	2041600.078	2048322.933	1743482.942	562807.8666
2018706.078	2030703.307	2040409.887	2047722.792	2052562.65	666468.7959
2015977.685	2028857.126	2039290.046	2047157.646	2052368.165	778735.5341
2013468.596	2027157.173	2038257.83	2046636.312	2052188.663	899032.2755
2011215.775	2025629.075	2037329.088	2046166.902	2052026.962	1026656.733
2009252.05	2024295.706	2036518.018	2045756.706	2051885.6	1160791.222
2007605.76	2023176.894	2035836.971	2045412.081	2051766.791	1300515.563
2006300.465	2022289.183	2035296.283	2045138.358	2051672.398	1444821.58
2005354.717	2021645.643	2034904.139	2044939.768	2051603.898	1592628.983
2004781.886	2021255.713	2034666.462	2044819.375	2051562.365	1742802.385
2004590.043	2021125.099	2034586.836	2044779.037	2051548.448	1894169.171
2004781.886	2021255.713	2034666.462	2044819.375	2051562.365	2045537.956
2005354.717	2021645.643	2034904.139	2044939.768	2051603.898	2054724.72
2006300.465	2022289.183	2035296.283	2045138.358	2051672.398	2054731.87
2007605.76	2023176.894	2035836.971	2045412.081	2051766.791	2054741.721
2009252.05	2024295.706	2036518.018	2045756.706	2051885.6	2054754.118
2011215.775	2025629.075	2037329.088	2046166.902	2052026.962	2054768.866
2013468.596	2027157.173	2038257.83	2046636.312	2052188.663	2054785.732
2015977.685	2028857.126	2039290.046	2047157.646	2052368.165	2054804.45
2018706.078	2030703.307	2040409.887	2047722.792	2052562.65	2054824.725
2021613.096	2032667.657	2041600.078	2048322.933	2052769.062	2054846.237
2024654.842	2034720.07	2042842.162	2048948.685	2052984.156	2054868.647
2027784.766	2036828.804	2044116.775	2049590.234	2053204.545	2054891.601
2030954.3	2038960.946	2045403.937	2050237.492	2053426.758	2054914.738
2034113.575	2041082.907	2046683.354	2050880.252	2053647.291	2054937.693
2037212.183	2043160.942	2047934.745	2051508.351	2053862.661	2054960.103
2040200.004	2045161.702	2049138.159	2052111.828	2054069.465	2054981.616
2043028.068	2047052.793	2050274.312	2052681.088	2054264.434	2055001.891
2045649.439	2048803.335	2051324.902	2053207.056	2054444.482	2055020.61
2048020.101	2050384.523	2052272.925	2053681.329	2054606.754	2055037.476
2050099.821	2051770.147	2053102.973	2054096.312	2054748.68	2055052.225
2051852.97	2052937.097	2053801.501	2054445.346	2054868.008	2055064.623
2053249.271	2053865.801	2054357.075	2054722.823	2054962.843	2055074.474
2054264.448	2054540.614	2054760.575	2054924.277	2055031.679	2055081.624
2054880.764	2054950.131	2055005.365	2055046.464	2055073.424	2055085.96
2055087.413	2055087.413	2055087.413	2055087.413	2055087.413	2055087.413
column total	column total	column total	column total	column total	column total
87572372.39	86874570.89	85715722.75	83738669.13	79692484.21	66399463.63

total horizontal force [Newtons] = 2205322651

[GNewtons) = 2.205322651

APPENDIX B

Non-dimensional Shear Force Plots and Calculations

Summary of Analytical Model Results

1. Elastic pre-buckling range of shear deformation

a. elemental shear force:

$$F_e = \left(\frac{G\, t\, \lambda\, b}{2}\right)\Phi$$

$$G = \frac{E}{2(1+\nu)}$$

b. non-dimensional shear per unit length:

$$NDSF_{el}\,/\text{per unit length} = \left[\frac{E}{\sigma_o t\,(1+\nu)}\right]\Phi$$

2. Elastic post-buckling range of deformation

a. elemental shear force:

$$F_{e_B} = \frac{8.98\,\pi^2\, E\, t^3\, \lambda}{12(1-\nu^2)\, b} + \left[\frac{E\, t\, b\, \lambda}{8(1+\nu)}\right]\left[\Phi - \left(\frac{8.98\,\pi^2(1+\nu)\, t^2}{3\,(1-\nu^2)\, b^2}\right)\right]$$

b. non-dimensional shear per unit length:

$$\frac{NDSF_{el_B}}{\text{unit length}} = \frac{8.98\,\pi^2\, E\, t}{3(1-\nu^2)\,\sigma_o\, b^2} + \left[\frac{E}{2\, t\,\sigma_o(1+\nu)}\right]\left[\Phi - \frac{8.98\,\pi^2(1+\nu)\, t^2}{3(1-\nu^2)\, b^2}\right]$$

3. Plastic buckling range of deformation

a. non-dimensional shear force per unit length due to shear strain in aperture:

$$\frac{NDSF_s}{\text{unit length}} = \frac{2\ \cos^2\beta\ \cos^2\Phi}{\sqrt{3}\ t}\sqrt{\left(1 - \frac{\tan\beta}{\lambda}\right)^2 + \frac{1}{\lambda^2}}\ \left[\left(\frac{A_o}{b}\right)\frac{|\dot{\gamma}_{\xi\eta}|}{\dot{\Phi}} + |\gamma_{\xi\eta}|\left(\frac{\dot{A}_o}{\dot{\Phi}\ b}\right)\right]$$

b. non-dimensional shear force per unit length due to membrane strain:

$$\frac{NDSF_m}{\text{unit length}} = \frac{4}{t}\left[\frac{4\left(\frac{w_o}{b}\right)\left(\frac{\dot{w}_o}{\dot{\Phi}\ b}\right)\cos^2\beta\ \cos^2\Phi + \lambda + \frac{\tan\Phi}{\cos^2\beta} + \tan\beta}{\lambda^2 + 2\,\lambda\,\tan\beta + \tan^2\beta + 1}\right]$$

c. non-dimensional shear force per unit length due to plastic hinge bending:

$$\frac{NDSF_b}{\text{unit length}} = \left(\frac{4}{b}\right)\left|\frac{\dot{w}_o}{\dot{\Phi}\ b}\right|\left[\frac{\cos^3\beta\ \cos^2\Phi}{\sqrt{1 - 4\left(\frac{w_o}{b}\right)^2\cos^2\beta}}\right] + \ \ldots$$

$$\left(\frac{2\ \cos^2\Phi\ \cos^2\beta}{b}\right)\sqrt{\left(1 + \frac{\tan\beta}{\lambda}\right)^2 + \frac{1}{\lambda^2}}\ \left|\frac{\dot{w}_o}{\dot{\Phi}\ b}\right|\left[\frac{\frac{\cos\beta\ \sin^{-1}\left(\frac{2w_o}{b}\cos\beta\right)}{\sqrt{1 - 4\left(\frac{w_o}{b}\right)^2\cos^2\beta}} + \frac{\sin^{-1}\left(\frac{2w_o}{\lambda\ b}\right)}{\sqrt{\lambda^2 - 4\left(\frac{w_o}{b}\right)^2}}}{\sqrt{\left[\sin^{-1}\left(\frac{2w_o}{b}\cos\beta\right)\right]^2 + \left[\sin^{-1}\left(\frac{2w_o}{\lambda\ b}\right)\right]^2}}\right]$$

3. Plastic buckling model non-dimensional parameters

a. ratio of maximum aperture opening to plate width:

$$\frac{A_o}{b} = \frac{\tan\Phi}{\cos^2\beta}\sqrt{1 + \left(\lambda\cos^2\beta - \tan\Phi\right)^2}$$

b. ratio of aperture opening velocity to shear translation velocity difference between plate longitudinal edges:

$$\frac{\dot{A}_o}{\dot{\Phi}\, b} = \frac{1}{\cos^2\beta\cos^2\Phi}\left[\frac{2\tan^2\Phi - 3\lambda\tan\Phi\cos^2\beta + \lambda^2\cos^4\beta + 1}{\sqrt{\tan^2\Phi - 2\lambda\tan\Phi\cos^2\beta + \lambda^2\cos^4\beta + 1}}\right]$$

c. shear strain:

$$\gamma_{\xi\eta} = \left[\tan^{-1}\left(\lambda\cos^2\beta - \tan\Phi\right) - \tan^{-1}\left(\lambda - \tan\beta - \frac{\tan\Phi}{\cos^2\beta}\right)\right]$$

d. ratio of aperture shear strain rate to shear rotation rate:

$$\frac{\left|\dot{\gamma}_{\xi\eta}\right|}{\dot{\Phi}} = \sec^2\Phi\left|\frac{1}{\cos^2\beta\left[1 + \left(\lambda - \tan\beta - \frac{\tan\Phi}{\cos^2\beta}\right)^2\right]} - \frac{1}{1 + \left(\lambda\cos^2\beta - \tan\Phi\right)^2}\right|$$

e. ratio of maximum out-of-plane displacement to plate width:

$$\frac{w_o}{b} = \frac{1}{2}\sqrt{\lambda^2 + \left(\frac{\frac{2\lambda\tan\Phi}{\cos^2\beta} - \frac{\tan^2\Phi}{\cos^4\beta} - \lambda^2}{\cos^2\Phi}\right)}$$

3. Plastic buckling model non-dimensional parameters (continued)

f. ratio of plate out-of-plane displacement rate to shear translation velocity difference between plate longitudinal edges:

$$\frac{\dot{w}_o}{\dot{\Phi} b} = \frac{1}{4}\left[\frac{\left(\frac{2\lambda}{\cos^2\beta} - \frac{2\tan\Phi}{\cos^4\beta}\right) + \left(\frac{2\lambda\tan\Phi}{\cos^2\beta} - \frac{\tan^2\Phi}{\cos^4\beta} - \lambda^2\right)\sin(2\Phi)}{\sqrt{\lambda^2\cos^8\Phi + \left(\frac{2\lambda\tan\Phi}{\cos^2\beta} - \frac{\tan^2\Phi}{\cos^4\beta} - \lambda^2\right)\cos^6\Phi}}\right]$$

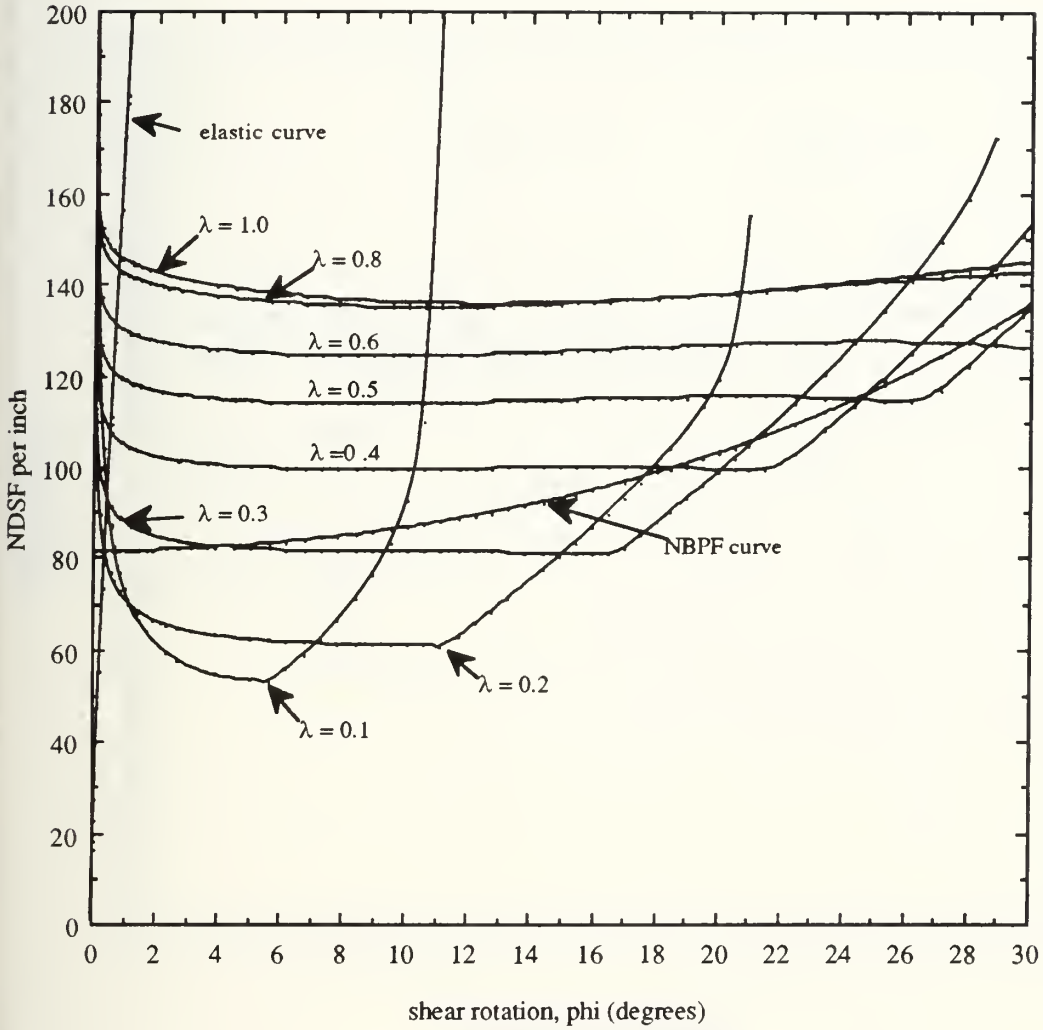

Figure B-1: Analytical results for beta = 0

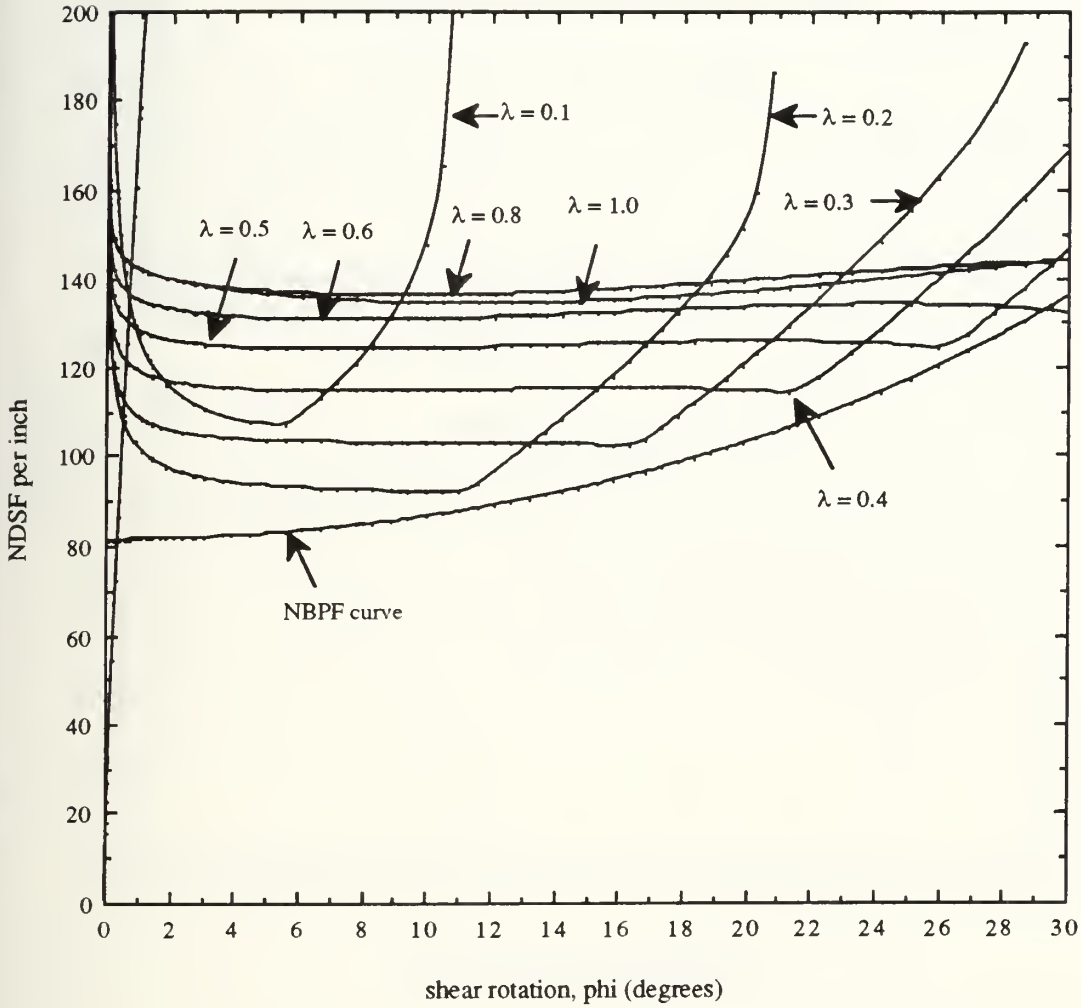

Figure B-2: Analytical results for beta = 0.1

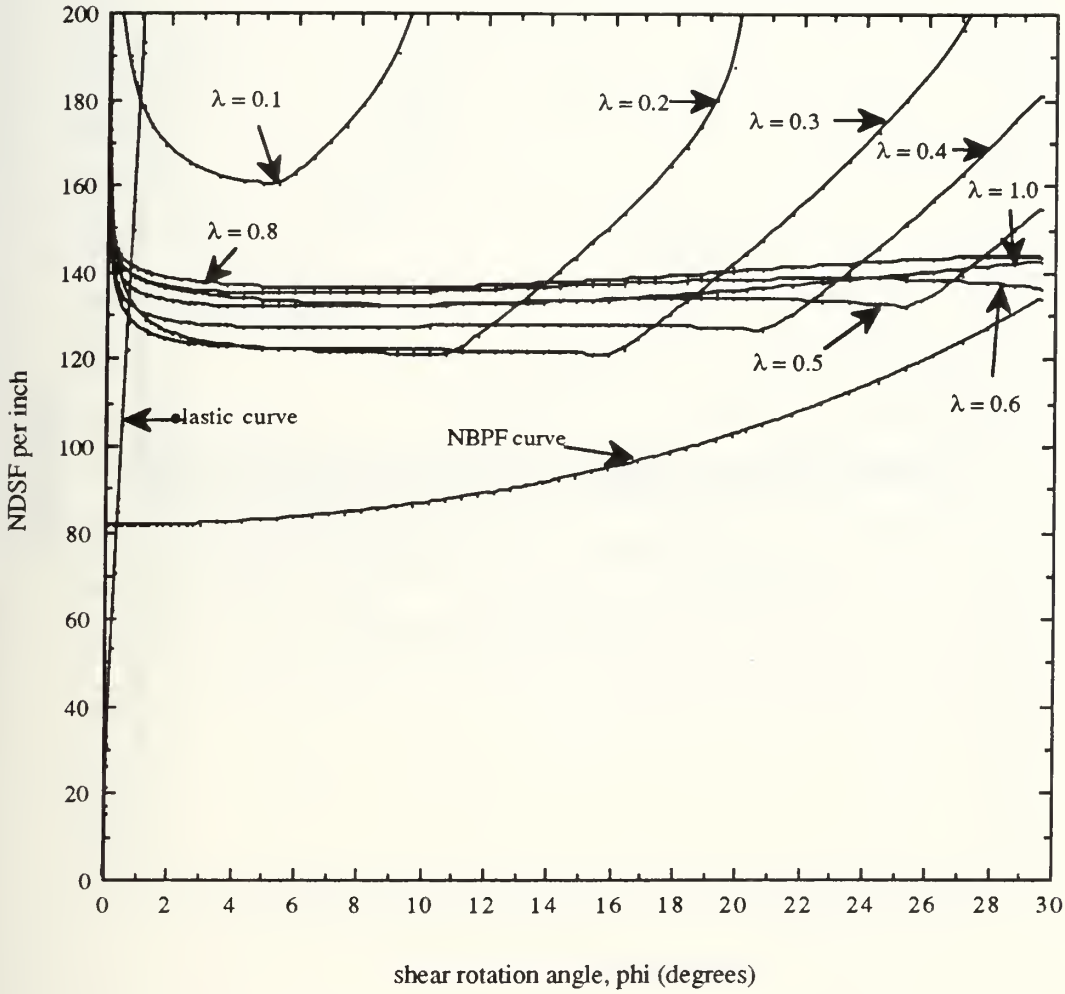

Figure B-3: Analytical results for beta = 0.2

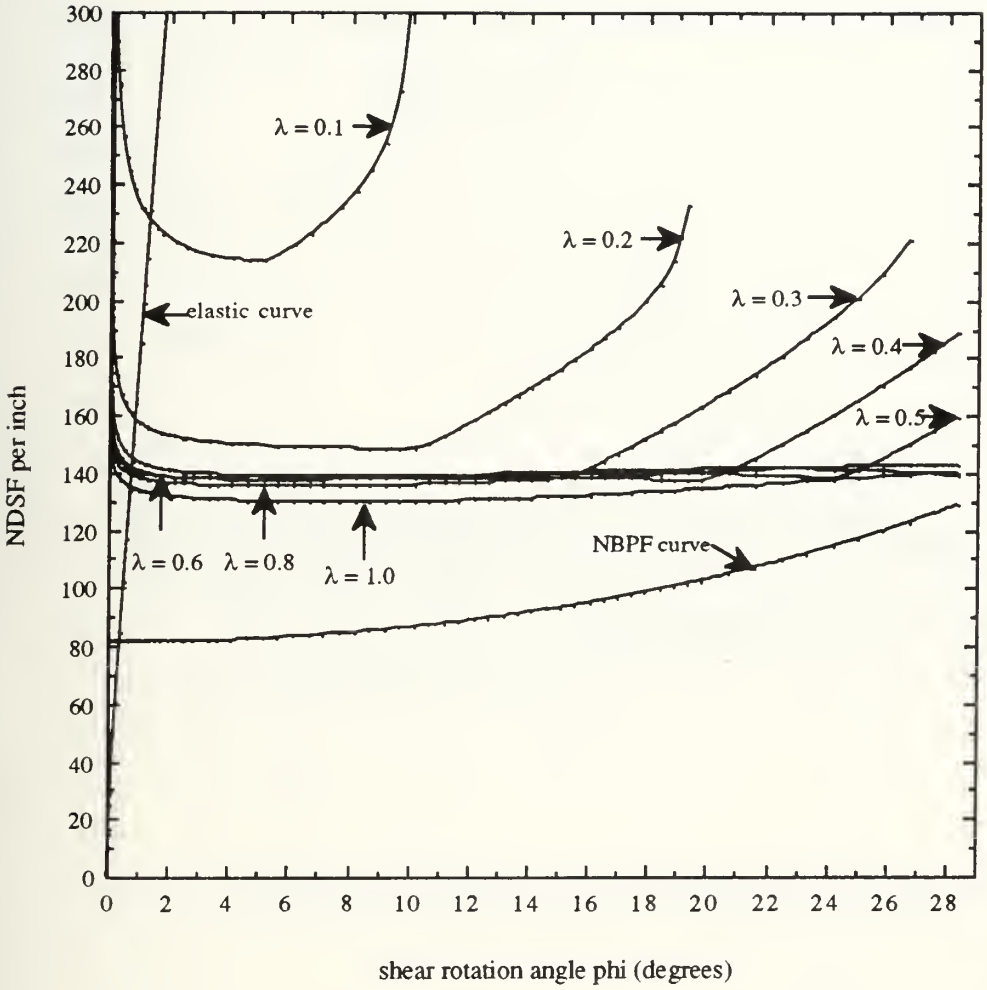

Figure B-4: Analytical results for beta=0.3

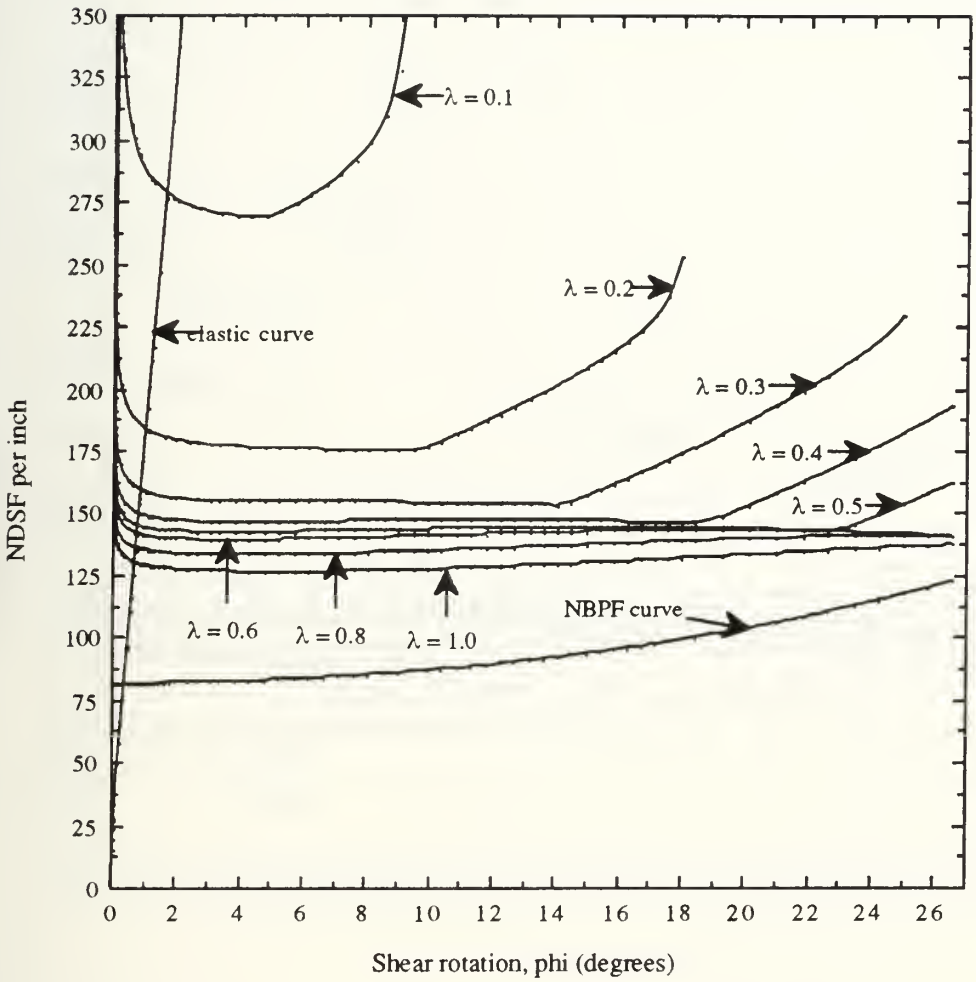

Figure B-5: Analytical results for beta = 0.4

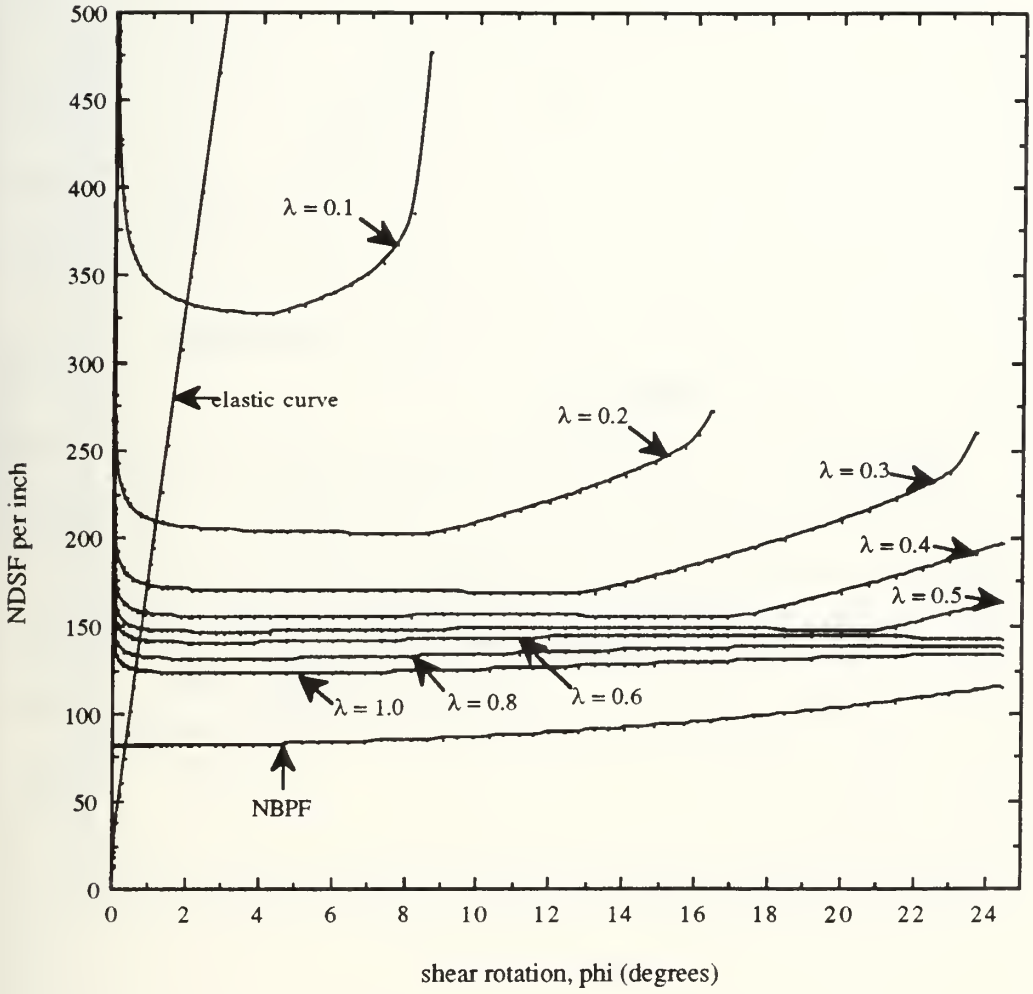

Figure B-6: Analytical results for beta = 0.5

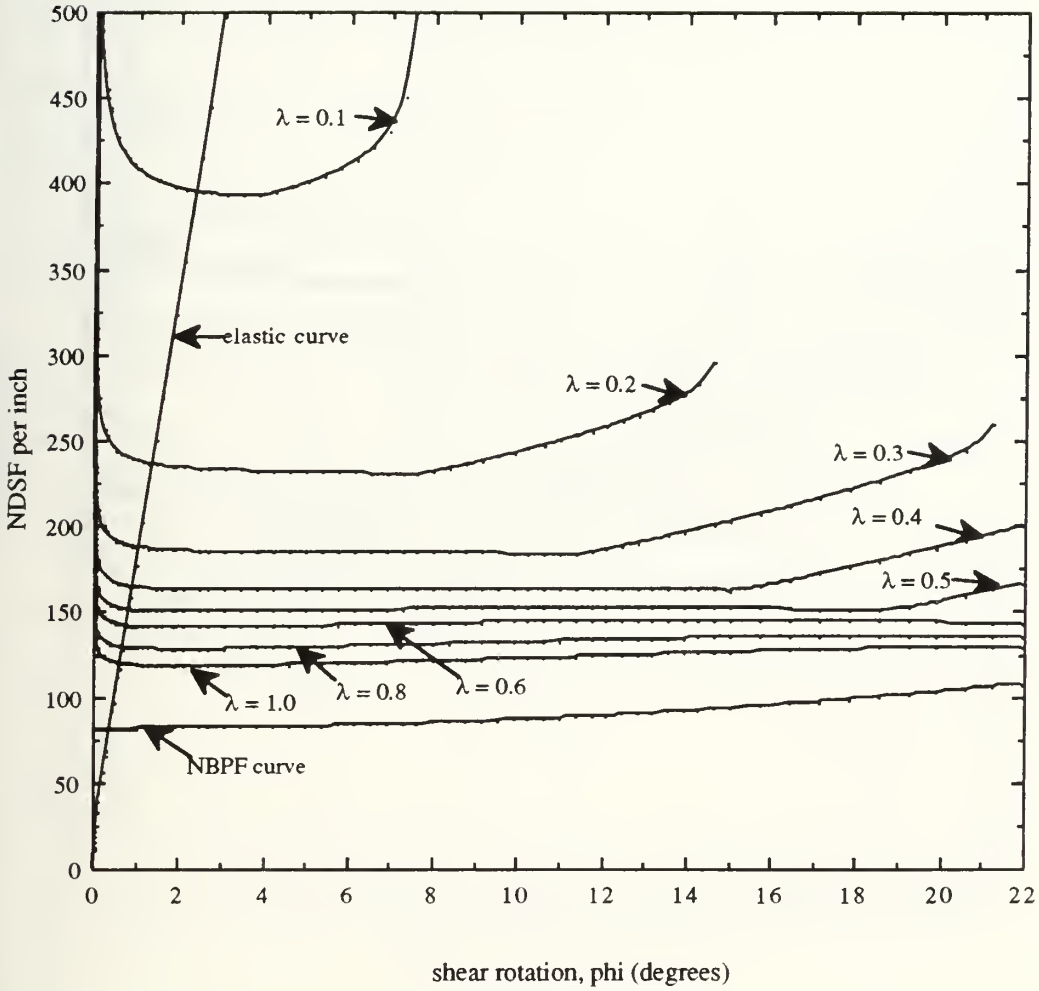

Figure B-7: Analytical results for beta = 0.6

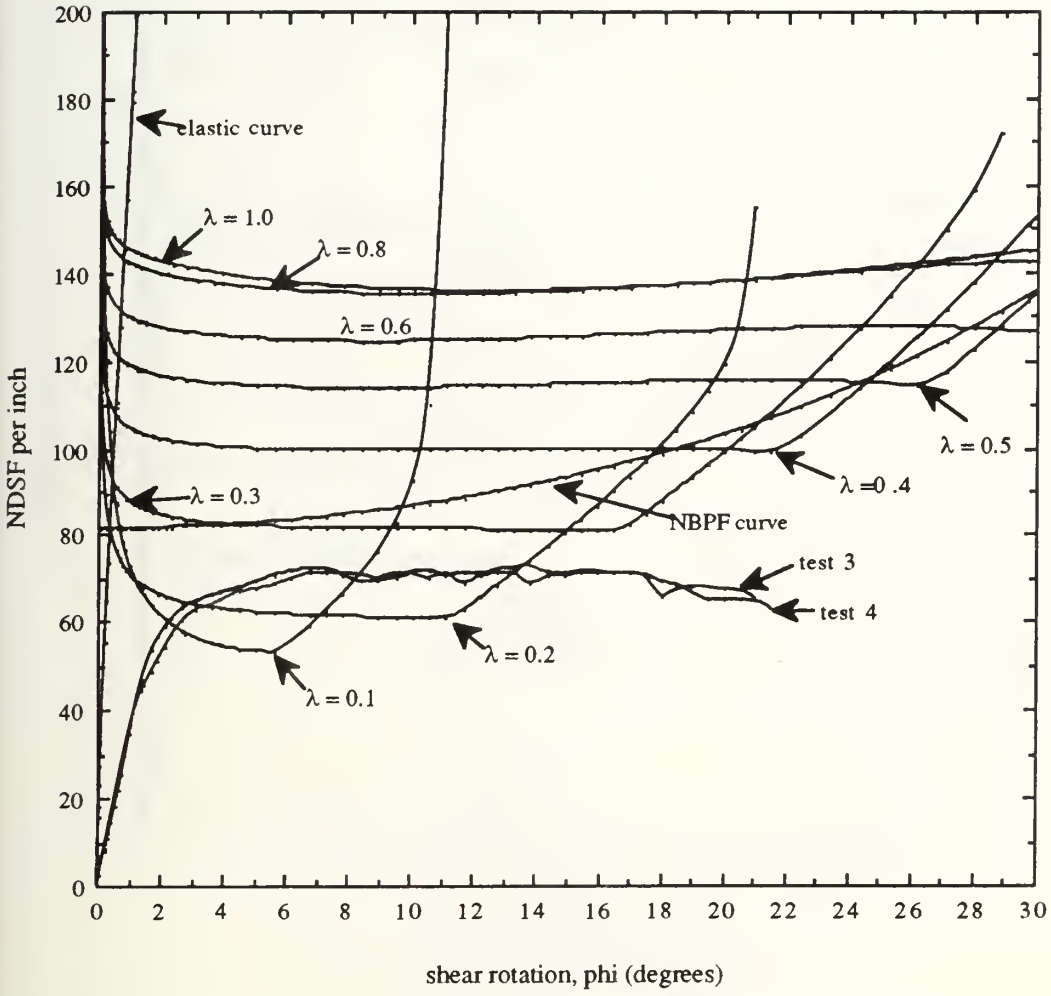

Figure B-8: Comparison of analytical models vs tests 3 and 4 (beta = 0)

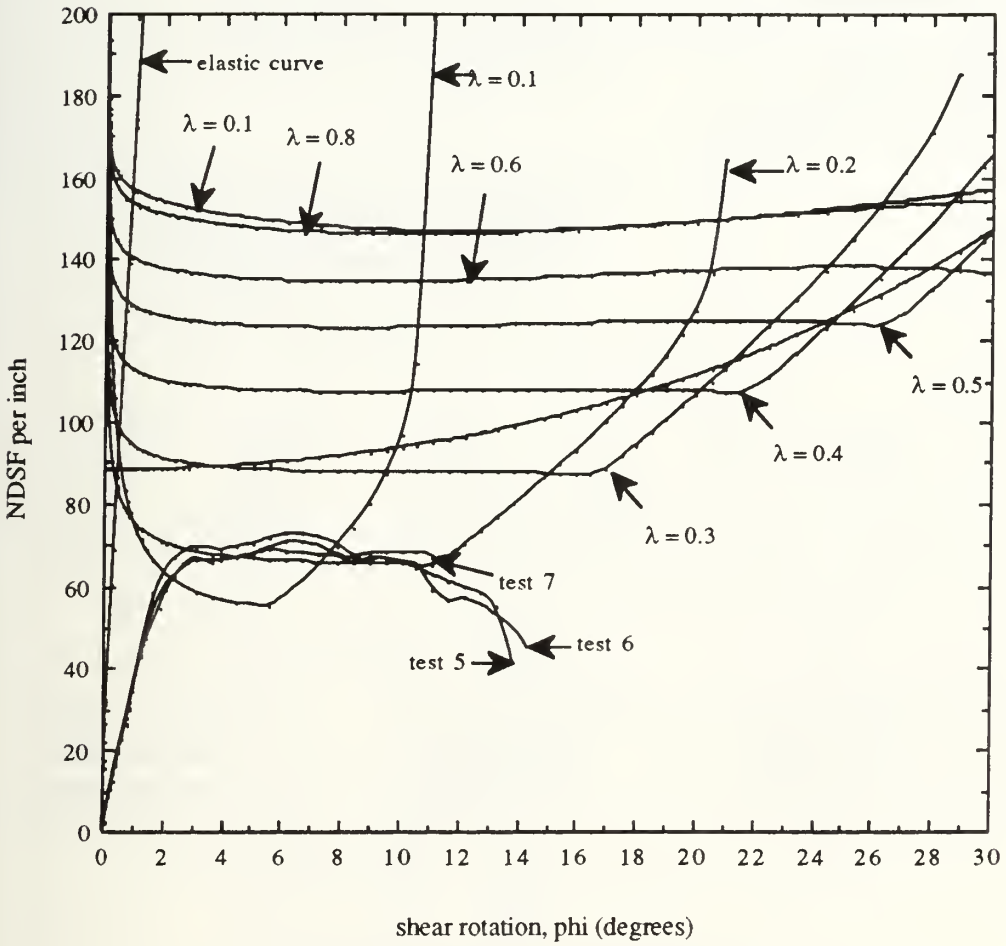

Figure B-9: Comparison of analytical models vs tests 5, 6, and 7 (beta = 0)

Buckling Model Spreadsheet Logic Flow Diagram

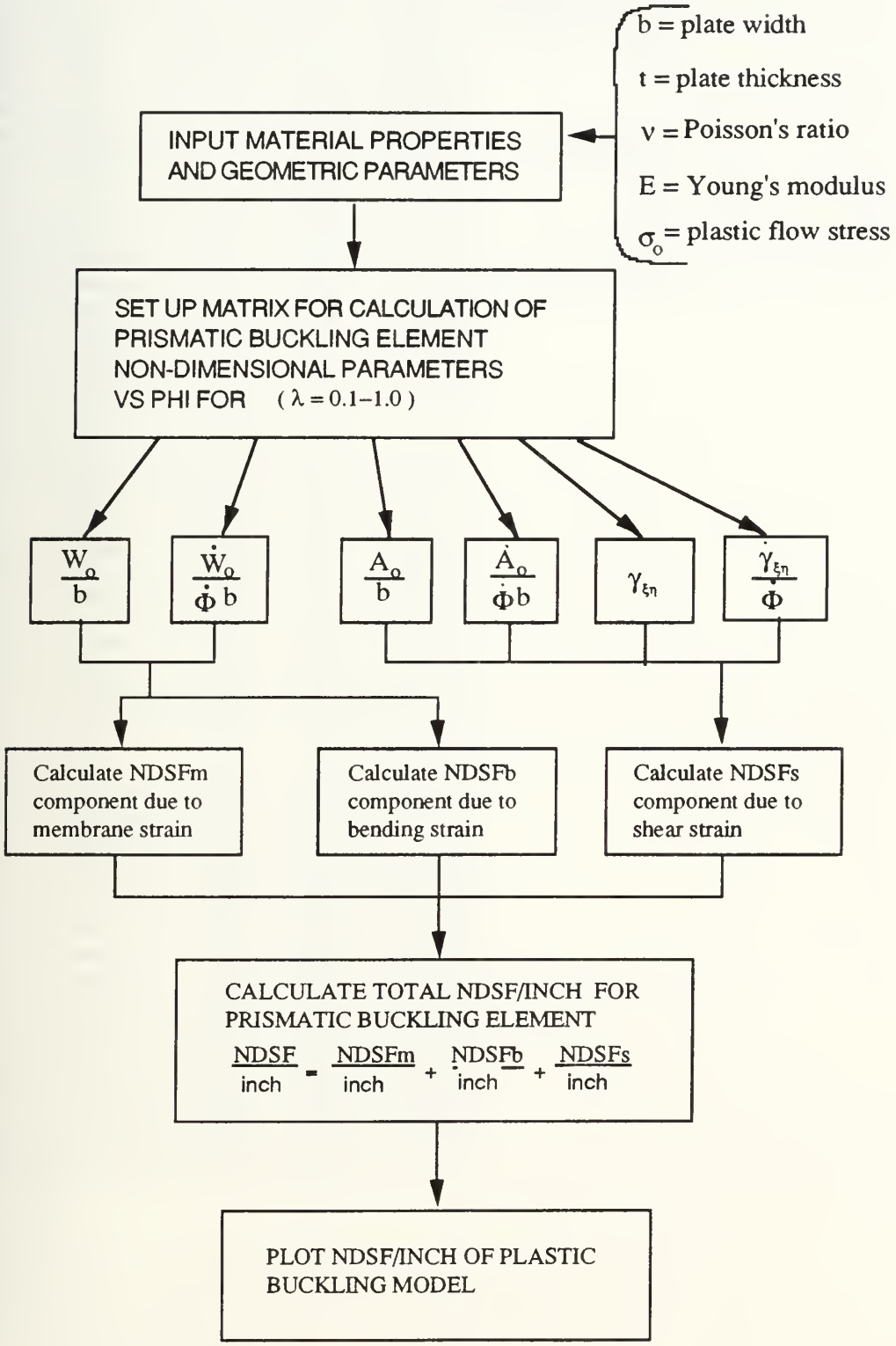

Sample Analytical Calculations (beta=0.1)

	Plate Shear Geometry			
S (mm)	S (inches)	Phi (rads)	Phi (deg)	TAN(Phi)
0.00254	0.0001	2.47508E-05	0.001418118	2.47508E-05
0.0254	0.001	0.000247508	0.014181182	0.000247508
0.0508	0.002	0.000495017	0.028362362	0.000495017
0.0635	0.0025	0.000618771	0.035452951	0.000618771
0.0889	0.0035	0.000866279	0.049634125	0.000866279
0.1	0.003937008	0.000974442	0.055831409	0.000974442
0.127	0.005	0.001237541	0.070905875	0.001237542
0.1524	0.006	0.001485049	0.085087031	0.00148505
0.1778	0.007	0.001732557	0.099268176	0.001732558
0.181166406	0.007132536	0.00176536	0.101147683	0.001765362
0.185816285	0.007315602	0.00181067	0.103743768	0.001810672
0.217564229	0.008565521	0.002120035	0.12146903	0.002120038
0.4	0.015748031	0.003897749	0.223324574	0.003897769
0.5	0.019685039	0.004872173	0.279154922	0.004872211
0.6	0.023622047	0.005846587	0.33498474	0.005846653
0.8	0.031496063	0.00779538	0.446642362	0.007795538
1	0.039370079	0.009744114	0.558296592	0.009744422
1.2	0.047244094	0.011692774	0.669946581	0.011693307
1.4	0.05511811	0.013641345	0.781591482	0.013642191
1.6	0.062992126	0.015589812	0.893230448	0.015591075
1.8	0.070866142	0.017538161	1.004862632	0.01753996
2	0.078740157	0.019486377	1.116487186	0.019488844
2.2	0.086614173	0.021434446	1.228103264	0.021437729
2.4	0.094488189	0.023382351	1.339710021	0.023386613
2.6	0.102362205	0.025330079	1.45130661	0.025335498
3	0.118110236	0.029224943	1.674465905	0.029233266
3.4	0.133858268	0.033118921	1.897574394	0.033131035
4.2	0.165354331	0.040903745	2.34361198	0.040926573
4.8	0.188976378	0.046739162	2.67795671	0.046773226
5	0.196850394	0.048683613	2.789365533	0.048722111
5.5	0.216535433	0.053543096	3.067793428	0.053594322
6.5	0.255905512	0.063254246	3.624201358	0.063338744
7	0.275590551	0.06810546	3.902155428	0.068210955
8	0.31496063	0.077798038	4.457499215	0.077955377
9	0.354330709	0.087475991	5.012005072	0.087699799
10	0.393700787	0.097137543	5.565571274	0.097444221
11	0.433070866	0.106780939	6.118097145	0.107188643
12	0.472440945	0.11640444	6.669483156	0.116933066
13	0.511811024	0.126006332	7.219631036	0.126677488
14	0.551181102	0.135584923	7.768443868	0.13642191
15	0.590551181	0.145138547	8.315826182	0.146166332
16	0.62992126	0.154665564	8.86168405	0.155910754
17	0.669291339	0.164164363	9.405925174	0.165655176
18	0.708661417	0.173633364	9.948458968	0.175399598
19	0.748031496	0.183071017	10.48919664	0.185144021
20	0.787401575	0.192475804	11.02805126	0.194888443
22	0.866141732	0.211180884	12.09977337	0.214377287
24	0.94488189	0.229737161	13.16296975	0.233866131
26	1.023622047	0.248133786	14.21701869	0.253354976
28	1.102362205	0.266360524	15.26133387	0.27284382
30	1.181102362	0.284407782	16.2953656	0.292332664

Test Material and Geometric Parameters		
Parameter	Tests 3 & 4 Average	Tests 5,6,7 Average
b (in) =	4	4
t (inches)=	0.02835	0.0262
b/t=	141.0934744	152.6717557
Poisson's Ratio=	0.3	0.3
Young's Modulus (psi)=	29000000	29000000
Plastic Flow Stress (psi)=	43380	47810
Phi crit =	0.002120035	0.00181067
S crit (in) =	0.008565521	0.007315602
NDSF crit =	38.45519038	32.24586251
Plastic Hinge Mom. (Mo) =	0.008716371	0.008204674
Plate Length =	18	15.5

	Plate Shear Geometry			
S (mm)	S (inches)	Phi (rads)	Phi (deg)	TAN(Phi)
32	1.25984252	0.302266621	17.31860169	0.311821508
34	1.338582677	0.319928768	18.33056816	0.331310353
36	1.417322835	0.337386621	19.33082946	0.350799197
38	1.496062992	0.354633252	20.31898861	0.370288041
40	1.57480315	0.3716624	21.29468693	0.389776885
42	1.653543307	0.388468467	22.25760362	0.40926573
44	1.732283465	0.405046502	23.20745509	0.428754574
46	1.811023622	0.421392191	24.14399409	0.448243418
48	1.88976378	0.437501835	25.0670087	0.467732262
50	1.968503937	0.453372332	25.97632114	0.487221107
52	2.047244094	0.46900115	26.87178647	0.506709951
54	2.125984252	0.484386309	27.75329115	0.526198795
56	2.204724409	0.49952635	28.6207516	0.54568764
58	2.283464567	0.51442031	29.47411263	0.565176484
60	2.362204724	0.529067692	30.31334584	0.584665328

	lamda>	Max. Out-of-Plane Displacemt [wo] divided by plt width [b]						
Phi (deg)	0.1	0.2	0.3	0.4	0.5	0.6	0.8	1
0.001418118	0.001117963	0.001581087	0.001936448	0.002236028	0.002499961	0.002738574	0.003162237	0.00353549
0.014181182	0.003533302	0.004998376	0.006122336	0.00706979	0.007904464	0.008659034	0.009998729	0.011178956
0.028362362	0.004993685	0.007066474	0.008656327	0.009996385	0.011176861	0.012243998	0.014138541	0.015807476
0.035452951	0.005581344	0.007899275	0.009676971	0.011175289	0.012495138	0.013688242	0.015806365	0.017672203
0.049634125	0.006599754	0.009343509	0.011447349	0.01322039	0.014782147	0.016193865	0.018699968	0.020907446
0.055831409	0.00699772	0.00990826	0.012139785	0.014020357	0.015676788	0.017174057	0.01983197	0.022173112
0.070905875	0.007880713	0.011162179	0.013677544	0.015797104	0.017663922	0.019351282	0.022346478	0.024984544
0.085087031	0.008627407	0.012223575	0.014979599	0.017301732	0.019346847	0.021195283	0.024476233	0.027365815
0.099268176	0.00931274	0.01319867	0.016176144	0.018684629	0.020893733	0.022890299	0.026433997	0.029554806
0.101147683	0.009399696	0.013322458	0.016328071	0.018860232	0.021090168	0.02310555	0.026682621	0.029832796
0.103743768	0.009518451	0.013491539	0.016535597	0.019100103	0.021358499	0.023399586	0.027022246	0.030212537
0.12146903	0.010291349	0.014592726	0.017887453	0.020662812	0.023106713	0.025315332	0.029235089	0.032686769
0.223324574	0.013890296	0.019740308	0.024214526	0.0279809	0.031296043	0.034291076	0.03960456	0.044281606
0.279154922	0.015490469	0.022041902	0.02704843	0.031261333	0.034968638	0.038317381	0.044257177	0.04948433
0.33498474	0.016925754	0.024114528	0.029603528	0.0342207	0.038282802	0.041951383	0.048457167	0.054181103
0.446642362	0.019444069	0.027773022	0.034121926	0.039458422	0.044151154	0.048387787	0.055897884	0.062502428
0.558296592	0.021626702	0.030970547	0.038080974	0.044053054	0.049302209	0.054039517	0.062433709	0.069812374
0.669946581	0.023567144	0.033838095	0.041640599	0.048188988	0.05394195	0.059132104	0.068324946	0.076401938
0.781591482	0.02532117	0.036453675	0.044895976	0.051975921	0.058192899	0.063799687	0.073726397	0.082444169
0.893230448	0.026925268	0.038868238	0.047909231	0.055485435	0.062134991	0.068129768	0.078739035	0.08805194
1.004862632	0.028404879	0.04111726	0.050723591	0.058767322	0.06582382	0.072183199	0.083433071	0.093303737
1.116487186	0.029778588	0.043226629	0.053370587	0.061857891	0.069299918	0.076004338	0.087859684	0.098256767
1.228103264	0.031060472	0.045215936	0.055874063	0.06478459	0.072593921	0.079626715	0.092057552	0.102954264
1.339710021	0.032261501	0.047100433	0.058252575	0.067568776	0.075729663	0.083076407	0.096056758	0.107429854
1.45130661	0.033390418	0.048892277	0.060520905	0.070227458	0.078726122	0.086374181	0.099881254	0.111710307
1.674465905	0.035459099	0.052235792	0.064772952	0.075221139	0.084360128	0.092578452	0.107080476	0.119768923
1.897574394	0.037310109	0.055307113	0.068703864	0.07985034	0.089590425	0.098342887	0.113774412	0.127263337
2.34361198	0.04047553	0.060795538	0.075799415	0.088241885	0.099092554	0.108828597	0.125965063	0.140915687
2.67795671	0.042457996	0.064448786	0.080583323	0.093929544	0.105550498	0.115966019	0.134274798	0.150225066
2.789365533	0.043053794	0.065591893	0.082091988	0.095728905	0.107596853	0.118229748	0.13691255	0.153180751
3.067793428	0.044413552	0.068304381	0.085697442	0.100041256	0.112508189	0.123667176	0.143253065	0.160286818
3.624201358	0.046629102	0.073183581	0.092289442	0.107975861	0.121573735	0.133721728	0.154996705	0.1734538
3.902155428	0.047508268	0.075386007	0.095319468	0.111648054	0.12578359	0.13839968	0.160469935	0.179593079
4.457499215	0.048849955	0.079383081	0.100928904	0.118495691	0.13366162	0.147170796	0.170750452	0.191129929
5.012005072	0.04967052	0.082901602	0.106017613	0.124773142	0.14092013	0.155274509	0.180272527	0.20182262
5.565571274	0.049993741	0.08600086	0.110659137	0.130565174	0.147653675	0.162814231	0.189155427	0.211804556
6.118097145	0.049826849	0.088725006	0.114909058	0.135936049	0.153934012	0.16986849	0.197489773	0.221177143
6.669483156	0.049161811	0.091107593	0.118810507	0.140935847	0.159817154	0.176498628	0.205346419	0.230019718
7.219631036	0.047974224	0.093174429	0.122397656	0.145604472	0.165347823	0.182753678	0.212782066	0.238395815
7.768443868	0.0462194	0.094945456	0.125698018	0.149974294	0.170562398	0.18867358	0.21984297	0.246357311
8.315826182	0.043823956	0.096436018	0.128734024	0.154071962	0.175490931	0.194291382	0.226567476	0.253947257
8.86168405	0.040668475	0.09765773	0.131524138	0.157919678	0.180158568	0.199634801	0.23298781	0.26120188
9.405925174	0.036548805	0.098619091	0.134083657	0.161536128	0.184586582	0.20472734	0.239131373	0.26815203
9.948458968	0.031073775	0.0993259	0.136425306	0.164937166	0.188793136	0.209589129	0.245021706	0.274824252
10.48919664	0.023292329	0.099781535	0.138559681	0.168136326	0.192793858	0.214237549	0.250679207	0.281241597
11.02805126	0.008119956	0.099987128	0.140495588	0.171145223	0.196602281	0.21868772	0.256121691	0.287424237
12.09977337		0.099641876	0.143799783	0.176630868	0.203687902	0.227044645	0.266422458	0.299154524
13.16296975		0.098255183	0.146381085	0.181458801	0.210127828	0.234748045	0.276029211	0.310135034
14.21701869		0.095752228	0.148265701	0.185677148	0.215982279	0.2418672	0.285025801	0.320462005
15.26133387		0.092006388	0.149465568	0.189321202	0.221298126	0.248457209	0.293480113	0.330214012
16.2953656		0.086814196	0.149979809	0.192415929	0.226111796	0.254562187	0.301447767	0.339456092
17.31860169		0.079842082	0.149795208	0.194977658	0.230451311	0.260217531	0.308974734	0.348242669
18.33056816		0.070499177	0.148885797	0.197015214	0.234337738	0.265451547	0.316099229	0.356619671
19.33082946		0.057556475	0.147211516	0.198530635	0.237786238	0.270286656	0.322853122	0.364626108
20.31898861		0.037304583	0.144715685	0.199519574	0.240806822	0.274740286	0.329263001	0.372295257
21.29468693			0.141320802	0.19997143	0.243404902	0.278825555	0.33535099	0.379655585
22.25760362			0.136921726	0.199869212	0.245581661	0.282551784	0.341135385	0.38673146
23.20745509			0.131374371	0.199189147	0.247334298	0.285924888	0.346631154	0.393543724
24.14399409			0.124476144	0.197899982	0.248656156	0.288947668	0.351850342	0.400110146
25.0670087			0.115929611	0.195961893	0.249536741	0.291620025	0.356802389	0.406445792
25.97632114			0.105267729	0.193324905	0.249961638	0.29393911	0.36149439	0.412563327
26.87178647			0.091674776	0.189926578	0.249912326	0.295899411	0.365931302	0.418473267
27.75329115			0.073435649	0.185688654	0.249365859	0.297492793	0.370116122	0.424184185
28.6207516			0.045057878	0.180512057	0.248294418	0.298708484	0.374050015	0.429702885
29.47411263				0.174269252	0.24666467	0.29953301	0.377732428	0.435034551
30.31334584				0.166792053	0.244436911	0.29995008	0.381161174	0.440182871

	lamda>	Ratio of absolute vertical apex velocity |wo dot| to shear velocity [Phi dot * b]						
Phi (deg)	0.1	0.2	0.3	0.4	0.5	0.6	0.8	1
0.001418118	22.58150926	31.93801266	39.11706786	45.16912213	50.50099445	55.32131177	63.87981277	71.41987414
0.014181182	7.128724006	10.09082932	12.36233164	14.2767611	15.96310823	17.48748103	20.19363965	22.57740408
0.028362362	5.031195013	7.128334391	8.73554135	10.08972139	11.28235474	12.36029257	14.27361888	15.95871439
0.035452951	4.495753299	6.372663502	7.81064655	9.02207437	10.0888904	11.05304695	12.76428137	14.27126196
0.049634125	3.792358673	5.380621997	6.596707202	7.620910219	8.522690842	9.33758541	10.78367959	12.05694818
0.055831409	3.57270592	5.071047925	6.217972534	7.1838092	8.034133931	8.802485874	10.16589484	11.3662698
0.070905875	3.163811294	4.495147113	5.5135631	6.370925572	7.125606746	7.807439282	9.017125137	10.08196396
0.085087031	2.882605257	4.099469372	5.02974128	5.812678947	6.501726143	7.124177743	8.228341693	9.200126208
0.099268176	2.663634867	3.791649167	4.653460617	5.378576568	6.016622479	6.592925537	7.615069227	8.514511789
0.101147683	2.638096129	3.75576734	4.609606133	5.327987225	5.960092063	6.531018914	7.54360655	8.434619812
0.103743768	2.603958236	3.707810775	4.550996737	5.260378494	5.88454445	6.448287082	7.448104659	8.327853272
0.12146903	2.400665583	3.422411808	4.202272334	4.858146935	5.435104874	5.956123043	6.879989072	7.692731725
0.223324574	1.745769819	2.506203873	3.084005292	3.568960394	3.995017292	4.379397523	5.060221004	5.658409154
0.279154922	1.549281905	2.232867008	2.750984312	3.185360427	3.566711944	3.910578979	4.519272262	5.05371843
0.33498474	1.403134994	2.030327753	2.504513635	2.901613556	3.249992632	3.563962683	4.119393531	4.606738671
0.446642362	1.195718928	1.744462155	2.157244885	2.502146053	2.804301283	3.076325072	3.556958812	3.978092799
0.558296592	1.051977107	1.547889118	1.919027172	2.22843	2.499099876	2.742519289	3.172080934	3.547941676
0.669946581	0.944219067	1.401684192	1.742281041	2.025575917	2.273051054	2.495373492	2.887218069	3.229596807
0.781591482	0.859157006	1.287195379	1.604217715	1.867299563	2.0967865	2.302728092	2.665248305	2.981558145
0.893230448	0.789507599	1.194213531	1.492369476	1.739223957	1.95424421	2.14699572	2.485871822	2.78113209
1.004862632	0.730897076	1.116616499	1.399263141	1.632733342	1.835799765	2.01763868	2.336926518	2.614722593
1.116487186	0.680517252	1.050479128	1.320109506	1.542307463	1.735287367	1.907906557	2.210621894	2.473620774
1.228103264	0.636470354	0.993152625	1.251678141	1.464223567	1.648549404	1.81324784	2.101705498	2.351955093
1.339710021	0.597420765	0.942775576	1.19169991	1.39586725	1.57266642	1.7304667	2.006489573	2.245603198
1.45130661	0.562397002	0.897996125	1.138527585	1.335341043	1.505519794	1.657244111	1.922298307	2.151573989
1.674465905	0.501692784	0.821432695	1.04797616	1.232453293	1.39149006	1.532967173	1.779481743	1.992091126
1.897574394	0.450320561	0.757866223	0.973212211	1.147717706	1.297705877	1.430836135	1.662202537	1.861151325
2.34361198	0.366329679	0.656972528	0.85554265	1.01486149	1.150964114	1.271225446	1.479125765	1.656811673
2.67795671	0.314369227	0.596891544	0.786217337	0.936965033	1.065149044	1.178025686	1.372377337	1.537712216
2.789365533	0.298559921	0.579030876	0.765740215	0.914022286	1.039913126	1.150642892	1.341040902	1.502758558
3.067793428	0.261639341	0.538174095	0.719160591	0.861964951	0.982729789	1.08864376	1.270143687	1.42369467
3.624201358	0.196209459	0.469097544	0.641389095	0.775531492	0.88806974	0.986191756	1.153185765	1.293329205
3.902155428	0.166508887	0.43933697	0.608338788	0.739023691	0.848218304	0.943142992	1.104133635	1.238684987
4.457499215	0.111055405	0.386796891	0.55081407	0.675879825	0.779524351	0.869085348	1.019912591	1.144920152
5.012005072	0.058882104	0.341307315	0.502022901	0.622808275	0.722071066	0.807325566	0.949878122	1.067022577
5.565571274	0.008104835	0.30098563	0.459727127	0.577253045	0.673017003	0.754761268	0.890459343	1.001003819
6.118097145	0.042905364	0.264538644	0.422404681	0.537480342	0.630436911	0.709291709	0.839239741	0.944165447
6.669483156	0.095781101	0.231036469	0.388976254	0.502264663	0.592971802	0.669435097	0.794516015	0.894606007
7.219631036	0.152415983	0.199783263	0.358649597	0.470710109	0.559629821	0.634110885	0.755047138	0.850940597
7.768443868	0.215323338	0.170239035	0.330825876	0.442143015	0.529666639	0.60250902	0.719903681	0.81213249
8.315826182	0.288279183	0.141969976	0.305040778	0.41604448	0.502510331	0.57400784	0.688373216	0.777387429
8.86168405	0.377709888	0.114615464	0.280926032	0.392006366	0.477712392	0.548120559	0.659898667	0.746084747
9.405925174	0.496290456	0.087865155	0.258183451	0.369701666	0.454914783	0.52445926	0.634036847	0.717731037
9.948458968	0.674912241	0.061442292	0.236566919	0.348863995	0.433827129	0.502710002	0.610429788	0.691928125
10.48919664	1.024604691	0.035090856	0.215869553	0.329273051	0.414210569	0.482615182	0.588784445	0.668350396
11.02805126	3.30343861	0.008564998	0.195914363	0.31074408	0.395866073	0.463960793	0.568858027	0.646728408
12.09977337		0.045998833	0.157631859	0.276266073	0.362346791	0.430281238	0.533379941	0.60848536
13.16296975		0.10437125	0.120674432	0.244411621	0.3321956	0.400527955	0.502709578	0.575777457
14.21701869		0.169168141	0.084165452	0.214392771	0.304602487	0.373847933	0.475896978	0.547559238
15.26133387		0.24405238	0.047315238	0.185571393	0.278933329	0.349583215	0.452218831	0.523039255
16.2953656		0.334813002	0.009360173	0.157407035	0.254674153	0.327210674	0.431109544	0.501603181
17.31860169		0.451886922	0.030490451	0.129421197	0.23139423	0.306302429	0.412116113	0.48276352
18.33056816		0.617604129	0.073109487	0.101171215	0.20872061	0.286498902	0.394867596	0.466125619
19.33082946		0.894751001	0.119518737	0.072229669	0.186319849	0.267489886	0.379053853	0.451364063
20.31898861		1.608531797	0.170980926	0.042166628	0.16388431	0.249000815	0.364410376	0.438205862
21.29468693			0.229139122	0.010532714	0.141121387	0.230782514	0.35070718	0.426418212
22.25760362			0.296245349	0.023158745	0.117744536	0.212603267	0.337740522	0.415799406
23.20745509			0.37556457	0.059452313	0.09346534	0.194242484	0.325326562	0.406171966
24.14399409			0.47214984	0.09897609	0.067985975	0.175485417	0.313296444	0.397377354
25.0670087			0.594488201	0.142475622	0.040991569	0.156118563	0.301492369	0.389271843
25.97632114			0.758501942	0.190860988	0.012141918	0.135925466	0.289764407	0.381723236
26.87178647			0.999399701	0.245275127	0.018937996	0.114682679	0.277967843	0.374608224
27.75329115			1.420448806	0.307197152	0.052669394	0.092155682	0.265960906	0.367810221
28.6207516			2.618762185	0.378605576	0.089533926	0.068094565	0.253602782	0.361217564
29.47411263				0.462249123	0.13009203	0.042229253	0.24075181	0.354721992
30.31334584				0.562122791	0.175007325	0.01426403	0.227263801	0.348217335

	lamda>	Max. Aperture Opening [Ao] divided by plate width [b]						
Phi (deg)	0.1	0.2	0.3	0.4	0.5	0.6	0.8	1
0.001418118	2.51222E-05	2.54853E-05	2.60792E-05	2.68887E-05	2.78951E-05	2.90778E-05	3.18911E-05	3.51792E-05
0.014181182	0.000251216	0.000254842	0.000260776	0.000268867	0.000278926	0.00029075	0.000318876	0.000351752
0.028362362	0.00050242	0.000509659	0.000521517	0.000537688	0.000557797	0.000581436	0.000637676	0.000703418
0.035452951	0.000628018	0.000637059	0.000651875	0.000672082	0.000697212	0.000726756	0.000797047	0.000879218
0.049634125	0.000879203	0.000891841	0.000912563	0.000940835	0.000976001	0.001017347	0.001115731	0.001230753
0.055831409	0.00098897	0.001003175	0.001026475	0.001058268	0.001097817	0.001144319	0.001254975	0.001384349
0.070905875	0.00125596	0.001273969	0.00130353	0.00134388	0.001394082	0.001453117	0.001593614	0.001757892
0.085087031	0.001507115	0.001528691	0.00156413	0.001612519	0.001672734	0.001743551	0.001912106	0.002109209
0.099268176	0.001758259	0.00178339	0.001824696	0.001881114	0.001951332	0.002033922	0.002230522	0.002460439
0.101147683	0.001791544	0.001817144	0.001859228	0.001916708	0.001988252	0.002072402	0.002272718	0.002506983
0.103743768	0.001837518	0.001863768	0.001906924	0.001965873	0.002039246	0.00212555	0.002330999	0.00257127
0.12146903	0.002151407	0.002182078	0.002232547	0.002301512	0.002387372	0.002488377	0.002728855	0.003010123
0.223324574	0.003954773	0.004010492	0.004102647	0.004228857	0.004386183	0.004571414	0.005012767	0.005529308
0.279154922	0.004943015	0.005012203	0.005126962	0.005284323	0.005480617	0.005711832	0.006262991	0.006908268
0.33498474	0.005931081	0.006013555	0.006150743	0.006339093	0.006574209	0.006851279	0.007512031	0.008285884
0.446642362	0.007906699	0.008015192	0.008196714	0.008446559	0.00875888	0.009127268	0.010006565	0.011037087
0.558296592	0.00988165	0.010015424	0.01024058	0.010551271	0.010940212	0.011399397	0.012496378	0.013782924
0.669946581	0.011855956	0.012014271	0.012282361	0.01265325	0.013118222	0.013667678	0.014981482	0.016523403
0.781591482	0.013829639	0.014011756	0.014322076	0.014752512	0.015292925	0.015932128	0.017461888	0.019258533
0.893230448	0.015802721	0.016007899	0.016359746	0.016849077	0.017464339	0.01819276	0.019937606	0.021988322
1.004862632	0.017775224	0.018002722	0.018395391	0.018942962	0.019632479	0.020449588	0.022408648	0.024712778
1.116487186	0.019747171	0.019996247	0.020429031	0.021034187	0.021797363	0.022702629	0.024875026	0.027431909
1.228103264	0.021718584	0.021988494	0.022460686	0.023122769	0.023959007	0.024951896	0.027336749	0.030145725
1.339710021	0.023689485	0.023979487	0.024490376	0.025208727	0.026117428	0.027197404	0.029793831	0.032854232
1.45130661	0.025659897	0.025969245	0.026518122	0.02729208	0.028272642	0.029439168	0.032246281	0.035557441
1.674465905	0.02959934	0.029945145	0.030567861	0.031451045	0.032573517	0.033911525	0.037137333	0.040947993
1.897574394	0.033537092	0.033916367	0.034610066	0.035599812	0.036861768	0.038369084	0.042009996	0.04631745
2.34361198	0.04140824	0.041845472	0.042672526	0.043867358	0.04540094	0.047240294	0.051700526	0.056993352
2.67795671	0.047308491	0.047781313	0.048700812	0.050042372	0.051773194	0.05385576	0.058920842	0.064945416
2.789365533	0.049274769	0.04975795	0.050706816	0.052095927	0.053891252	0.056053771	0.061318613	0.067585701
3.067793428	0.054189641	0.054695424	0.055714529	0.057219533	0.059173375	0.061533314	0.067293465	0.07416374
3.624201358	0.064017053	0.064553891	0.065699792	0.067423708	0.069682753	0.072426871	0.079159905	0.087223123
3.902155428	0.068930293	0.069475571	0.070677996	0.072504883	0.074910558	0.077841377	0.08505187	0.093704749
4.457499215	0.078757597	0.079305541	0.080607193	0.082626938	0.085313792	0.088607089	0.09675425	0.106572589
5.012005072	0.088588336	0.089119967	0.090502314	0.092697327	0.095649072	0.099290083	0.108349191	0.119314182
5.565571274	0.098425316	0.098921622	0.100366027	0.102718542	0.105918675	0.109892403	0.119838274	0.131930716
6.118097145	0.108271343	0.108713291	0.110201014	0.112693104	0.116124914	0.120416128	0.131223111	0.144423398
6.669483156	0.118129219	0.118497765	0.12000998	0.122623557	0.126270128	0.130863366	0.142505339	0.156793463
7.219631036	0.128001743	0.128277845	0.129795641	0.132512472	0.136356685	0.141236255	0.153686626	0.169042164
7.768443868	0.137891709	0.138056335	0.139560735	0.14236244	0.146386984	0.151536967	0.164768671	0.181170784
8.315826182	0.147801903	0.147836045	0.149308009	0.152176079	0.156363449	0.161767702	0.175753201	0.193180625
8.86168405	0.157735105	0.157619786	0.159040226	0.161956024	0.166288535	0.171930694	0.186641973	0.205073017
9.405925174	0.167694086	0.167410373	0.168760163	0.171704935	0.176164722	0.182028204	0.197436776	0.216849314
9.948458968	0.177681605	0.177210621	0.178470603	0.18142549	0.185994519	0.192062526	0.208139427	0.228510897
10.48919664	0.187700411	0.187023343	0.188174344	0.191120388	0.195780458	0.202035984	0.218751776	0.24005917
11.02805126	0.19775324	0.196851351	0.197874189	0.200792343	0.205525098	0.21195093	0.229275704	0.251495567
12.09977337	0.217971837	0.216564447	0.217273445	0.220078379	0.22490084	0.231614843	0.250065968	0.274038593
13.16296975	0.238358979	0.236372302	0.236690927	0.239305645	0.244142697	0.251073671	0.270525884	0.296151969
14.21701869	0.25893597	0.256297187	0.256149243	0.258496414	0.263271974	0.270347265	0.29067162	0.317848135
15.26133387	0.279723801	0.27636121	0.275671012	0.277673137	0.282310307	0.289455909	0.310519847	0.339139983
16.2953656	0.300743115	0.296586273	0.29527882	0.296858407	0.301279627	0.308420299	0.330087744	0.36004087
17.31860169	0.32201418	0.316994038	0.314995176	0.31607492	0.320202128	0.32726152	0.349392992	0.380564626
18.33056816	0.343556859	0.337605882	0.334842469	0.33534543	0.339100231	0.346001022	0.368453771	0.400725565
19.33082946	0.365390589	0.358442871	0.354842927	0.354692706	0.35799655	0.364660589	0.387288757	0.420538492
20.31898861	0.387534355	0.379525719	0.375018575	0.374139487	0.376913843	0.383262311	0.405917111	0.440018706
21.29468693	0.410006673	0.40087476	0.395391193	0.393708443	0.395874982	0.401828552	0.424358472	0.459182015
22.25760362	0.432825573	0.422509921	0.415982283	0.413422126	0.414902901	0.420381909	0.442632941	0.478044732
23.20745509	0.456008586	0.444450695	0.436813025	0.433302928	0.434020559	0.438945183	0.460761064	0.496623682
24.14399409	0.479572733	0.466716115	0.457904249	0.45337304	0.45325089	0.457541329	0.47876382	0.514936205
25.0670087	0.503534515	0.489324742	0.4792764	0.473654412	0.472616764	0.476193425	0.496662593	0.533000153
25.97632114	0.527909909	0.51229464	0.50094951	0.494168709	0.492140937	0.494924621	0.514479154	0.550833888
26.87178647	0.552714364	0.535643363	0.522943167	0.514937277	0.511846013	0.513758098	0.53223563	0.568456283
27.75329115	0.577962799	0.559387948	0.545276498	0.535981106	0.531754394	0.532717025	0.549954476	0.585886709
28.6207516	0.603669606	0.583544902	0.567968143	0.557320797	0.551888241	0.55182451	0.567658444	0.603145031
29.47411263	0.629848649	0.608130194	0.591036238	0.578976532	0.572269434	0.571103558	0.585370548	0.620251594
30.31334584	0.656513275	0.633159257	0.614498398	0.600968043	0.592919528	0.59057702	0.603114025	0.637227214

	lamda>	Absolute Aperture Shear Strain [Gamma]						
Phi (deg)	0.1	0.2	0.3	0.4	0.5	0.6	0.8	1
0.001418118	0.099016914	0.096141806	0.091638969	0.08591668	0.079436827	0.072632694	0.059360444	0.04776104
0.014181182	0.099021313	0.096150235	0.091650639	0.085930578	0.07945192	0.072648085	0.059374613	0.047772898
0.028362362	0.099026189	0.09615959	0.091663599	0.085946017	0.079468689	0.072665187	0.059390358	0.047786077
0.035452951	0.099028622	0.096164264	0.091670076	0.085953734	0.079477073	0.072673738	0.059398231	0.047792667
0.049634125	0.099033481	0.096173603	0.091683024	0.085969165	0.079493839	0.072690841	0.059413981	0.047805851
0.055831409	0.0990356	0.096177682	0.09168868	0.085975907	0.079501165	0.072698315	0.059420864	0.047811614
0.070905875	0.099040746	0.096187594	0.091702432	0.085992303	0.079518983	0.072716494	0.05943761	0.047825634
0.085087031	0.099045574	0.096196908	0.091715361	0.086007723	0.079535744	0.072733597	0.059453366	0.047838826
0.099268176	0.09905039	0.096206212	0.091728282	0.086023137	0.079552503	0.0727507	0.059469125	0.047852022
0.101147683	0.099051028	0.096207445	0.091729994	0.08602518	0.079554724	0.072752967	0.059471214	0.047853772
0.103743768	0.099051908	0.096209146	0.091732359	0.086028001	0.079557792	0.072756098	0.059474099	0.047856188
0.12146903	0.099057907	0.096220757	0.091748495	0.08604726	0.079578735	0.072777476	0.059493802	0.047872688
0.223324574	0.099092015	0.096287164	0.091840989	0.086157781	0.079699022	0.072900325	0.059607103	0.047967607
0.279154922	0.099110449	0.096323338	0.091891519	0.086218257	0.07976491	0.072967668	0.059669268	0.04801971
0.33498474	0.099128697	0.096359352	0.091941928	0.086278657	0.079830766	0.073035012	0.059731476	0.048071867
0.446642362	0.099164635	0.096430895	0.092042383	0.086399229	0.079962378	0.073169705	0.059856017	0.048176338
0.558296592	0.099199827	0.096501793	0.092142349	0.086519495	0.080093854	0.073304404	0.059980728	0.048281021
0.669946581	0.099234274	0.096572042	0.092241823	0.08663945	0.080225193	0.073439105	0.060105605	0.048385915
0.781591482	0.099267974	0.09664164	0.092340803	0.086759092	0.08035639	0.073573806	0.060230649	0.048491021
0.893230448	0.099300924	0.096710583	0.092439284	0.086878416	0.080487442	0.073708504	0.060355859	0.048596339
1.004862632	0.099333126	0.09677887	0.092537264	0.086997419	0.080618347	0.073843198	0.060481234	0.048701867
1.116487186	0.099364577	0.096846498	0.092634738	0.087116098	0.0807491	0.073977885	0.060606772	0.048807607
1.228105264	0.099395276	0.096913464	0.092731703	0.087234449	0.0808797	0.074112562	0.060732473	0.048913558
1.339710021	0.099425223	0.096979766	0.092828156	0.087352468	0.081010142	0.074247226	0.060858336	0.04901972
1.45130661	0.099454417	0.097045402	0.092924094	0.087470151	0.081140424	0.074381876	0.060984359	0.049126094
1.674465905	0.099510541	0.097174663	0.093114409	0.087704498	0.081400493	0.074651123	0.061236884	0.049339473
1.897574394	0.099563641	0.09730123	0.093302622	0.08793746	0.081659881	0.07492028	0.061490039	0.049553695
2.34361198	0.099660748	0.097546204	0.093672634	0.088399116	0.082176511	0.075458245	0.061998208	0.049984664
2.67795671	0.099725599	0.097722724	0.093944427	0.088741509	0.082562002	0.075861331	0.062380925	0.050310096
2.789365533	0.099745694	0.097780179	0.094033919	0.088854888	0.082690103	0.075995606	0.062508794	0.050418992
3.067793428	0.099792595	0.097920766	0.094255198	0.089136655	0.083009461	0.076331073	0.062829106	0.050692149
3.624201358	0.099872083	0.098188762	0.094687087	0.089692798	0.083644156	0.077000929	0.063472402	0.051242376
3.902155428	0.099904661	0.09831611	0.094897599	0.089967062	0.083959387	0.077335232	0.063795347	0.05151944
4.457499215	0.099955476	0.098557361	0.095307517	0.090507693	0.084585348	0.078002363	0.064443731	0.05207745
5.012005072	0.099987167	0.09878051	0.095702318	0.091037424	0.085204948	0.078667229	0.065095299	0.05264061
5.565571274	0.099999756	0.098985359	0.096081638	0.091555812	0.085817747	0.079329462	0.065749874	0.053208881
6.118097145	0.099993284	0.099171733	0.096445127	0.092062415	0.086423307	0.079988684	0.06640727	0.053782222
6.669483156	0.099967813	0.099339476	0.096792448	0.092556799	0.087021181	0.08064451	0.067067292	0.054360585
7.219631036	0.099923429	0.099488454	0.097123281	0.093038534	0.087610924	0.081296546	0.067729737	0.054943918
7.768443868	0.099860237	0.099618552	0.097437318	0.093507196	0.088192085	0.081944391	0.06839439	0.055532163
8.315826182	0.099778362	0.099729679	0.097734271	0.09396237	0.088764215	0.082587638	0.06906103	0.056125256
8.86168405	0.099677952	0.099821763	0.098013864	0.094403649	0.089326863	0.083225872	0.069729423	0.056723127
9.405925174	0.099559173	0.099894756	0.098275844	0.094830634	0.089879579	0.083858672	0.070399329	0.0573257
9.948458968	0.099422209	0.099948631	0.098519972	0.095242937	0.090421913	0.084485611	0.071070494	0.057932894
10.48919664	0.099267265	0.099983381	0.098746031	0.095640181	0.090953418	0.085106257	0.071742658	0.058544618
11.02805126	0.099094563	0.099999024	0.09895382	0.096022002	0.09147365	0.085720175	0.07241555	0.059160779
12.09977337	0.098696862	0.099973162	0.099313895	0.096737977	0.092478536	0.086926056	0.073762383	0.060405989
13.16296975	0.098231222	0.099871607	0.099599009	0.097388213	0.093433106	0.088099694	0.075108626	0.061667619
14.21701869	0.097700004	0.099695257	0.099808312	0.097970306	0.094333994	0.089237495	0.076451759	0.062944639
15.26133387	0.097105789	0.099445337	0.099941296	0.098482121	0.09517797	0.090335856	0.07778911	0.064235894
16.2953656	0.096451354	0.099123379	0.099997804	0.098921809	0.095961962	0.091391189	0.079117857	0.065540094
17.31860169	0.095739642	0.098731208	0.099978026	0.099287834	0.096683084	0.092399952	0.080435039	0.066855811
18.33056816	0.094973734	0.098270919	0.099882497	0.099578981	0.097338672	0.093358672	0.081737561	0.068181474
19.33082946	0.094156823	0.097744855	0.099712091	0.099794372	0.097926299	0.094263976	0.083022208	0.069515361
20.31898861	0.093292187	0.09715558	0.099468004	0.099933472	0.098443807	0.09511262	0.084285654	0.0708556
21.29468693	0.092383159	0.096505857	0.099151746	0.099996095	0.098889326	0.095901519	0.08552448	0.072200163
22.25760362	0.091433105	0.095798615	0.098765118	0.099982405	0.099261293	0.096627772	0.086735189	0.073546866
23.20745509	0.090445399	0.095036926	0.098310195	0.099892909	0.099558468	0.097288695	0.087914227	0.074893369
24.14399409	0.0894234	0.094223976	0.097789301	0.099728452	0.099779943	0.097881842	0.089058004	0.076237175
25.0670087	0.088370429	0.093363036	0.097204984	0.099490208	0.099925158	0.098405033	0.090162916	0.077575637
25.97632114	0.087289756	0.092457435	0.096559991	0.099179661	0.099993898	0.098856373	0.091225374	0.078905956
26.87178647	0.086184575	0.09151054	0.095857239	0.098798591	0.099986299	0.099234274	0.092241823	0.080225193
27.75329115	0.085057997	0.090525722	0.095099791	0.098349049	0.09990284	0.099537469	0.09320878	0.081530274
28.6207516	0.083913031	0.089506343	0.094290822	0.097833342	0.099744342	0.099765026	0.094122852	0.082818002
29.47411263	0.082752576	0.088455729	0.093433599	0.097254	0.09951195	0.099916354	0.094980774	0.084085067
30.31334584	0.081579412	0.087377153	0.092531448	0.096613756	0.099207126	0.099991212	0.095779432	0.085328066

	lamda>	Absolute[Gamma dot] divided by Phi dot						
Phi (deg)	0.1	0.2	0.3	0.4	0.5	0.6	0.8	1
0.001418118	0.019768629	0.03785588	0.052404037	0.062401931	0.067761499	0.069095128	0.063599148	0.053227042
0.014181182	0.019725218	0.037818601	0.052376216	0.062384768	0.067754285	0.069095956	0.063609235	0.05323946
0.028362362	0.019676975	0.037777163	0.052345282	0.062365678	0.067746254	0.069096867	0.063620443	0.053253264
0.035452951	0.01965285	0.037756437	0.052329807	0.062356125	0.067742232	0.069097318	0.063626047	0.053260169
0.049634125	0.019604595	0.037714972	0.052298839	0.062337003	0.067734175	0.069098212	0.063637256	0.053273982
0.055831409	0.019583504	0.037696846	0.052285299	0.062328639	0.067730649	0.069098599	0.063642155	0.053280021
0.070905875	0.019532196	0.037652741	0.052252345	0.062308278	0.067722058	0.069099533	0.053654071	0.053294714
0.085087031	0.01948392	0.037611232	0.052221321	0.062289101	0.067713958	0.0691004	0.063665282	0.053308544
0.099268176	0.019435635	0.037569704	0.052190275	0.062269902	0.067705841	0.069101257	0.063676493	0.053322379
0.101147683	0.019429235	0.037564199	0.052186158	0.062267356	0.067704764	0.06910137	0.063677979	0.053324214
0.103743768	0.019420395	0.037556594	0.052180472	0.062263839	0.067703276	0.069101525	0.063680031	0.053326747
0.12146903	0.019360028	0.037504656	0.052141625	0.062239802	0.0676931	0.069102576	0.063694046	0.053344052
0.223324574	0.019012892	0.037205657	0.051917716	0.06210102	0.067634102	0.069108288	0.063774592	0.053443685
0.279154922	0.018822437	0.037041374	0.05179449	0.062024469	0.067601384	0.06911118	0.063818753	0.053498436
0.33498474	0.018631857	0.036876815	0.051670913	0.061947577	0.067568398	0.069113902	0.063862922	0.053553285
0.446642362	0.018250328	0.036546873	0.051422708	0.06179277	0.067501613	0.069118831	0.063951279	0.053663278
0.558296592	0.017868314	0.036215835	0.051173101	0.061636592	0.06743374	0.069123066	0.064039657	0.053773662
0.669946581	0.017485825	0.035883705	0.050922091	0.061479038	0.067364769	0.069126599	0.064128054	0.053884438
0.781591482	0.017102867	0.035550487	0.050669677	0.061320101	0.067294692	0.069129423	0.064216465	0.053995605
0.893230448	0.01671945	0.035216186	0.050415856	0.061159777	0.067223501	0.069131528	0.064304886	0.054107162
1.004862632	0.016335582	0.034880808	0.05016063	0.060998058	0.067151189	0.069132907	0.064393311	0.05421911
1.116487186	0.015951271	0.034544355	0.049903995	0.06083494	0.067077746	0.069133552	0.064481738	0.054331447
1.228103264	0.015566526	0.034206833	0.049645952	0.060670416	0.067003165	0.069133454	0.064570161	0.054444174
1.339710021	0.015181355	0.033868247	0.049386499	0.060504481	0.066927436	0.069132604	0.064658575	0.054557289
1.45130661	0.014795767	0.033528601	0.049125636	0.060337129	0.066850552	0.069130995	0.064746978	0.054670792
1.674465905	0.014023373	0.032846151	0.048599677	0.059998151	0.066693286	0.069125464	0.064923725	0.05489896
1.897574394	0.013249414	0.032159523	0.04806807	0.059653438	0.066531298	0.069116791	0.065100366	0.055128671
2.34361198	0.011697075	0.030773899	0.046987899	0.058946628	0.066192889	0.069089745	0.06545317	0.055592704
2.67795671	0.010529229	0.029724029	0.046162928	0.05840114	0.06592619	0.069060694	0.065717197	0.055944734
2.789365533	0.01013931	0.029372074	0.045885111	0.058216353	0.06583479	0.069049293	0.065805069	0.056062836
3.067793428	0.009163202	0.028487867	0.045184384	0.057747865	0.065600739	0.069016949	0.066024397	0.056359739
3.624201358	0.007205845	0.026701262	0.043756459	0.056782681	0.065108404	0.06893531	0.066461253	0.056960551
3.902155428	0.006224876	0.025799058	0.043029282	0.056285832	0.064849856	0.068885725	0.066678602	0.057264422
4.457499215	0.004259063	0.023977347	0.041548574	0.055263254	0.064307343	0.068768287	0.067110678	0.057878988
5.012005072	0.002289026	0.022133266	0.040032874	0.054201705	0.063730065	0.068625495	0.067538607	0.058502488
5.565571274	0.000315908	0.020267691	0.038482398	0.053100668	0.063116983	0.068456129	0.067961568	0.059134706
6.118097145	0.001659147	0.01838154	0.036897423	0.051959662	0.062467063	0.068258951	0.068378699	0.059775396
6.669483156	0.003634993	0.01647577	0.03527828	0.050778254	0.061779289	0.068032702	0.068789093	0.060424282
7.219631036	0.005610484	0.014551375	0.033625359	0.049556061	0.061052659	0.067776106	0.069191798	0.061081058
7.768443868	0.007584474	0.012609385	0.031939109	0.048292745	0.060286191	0.067487875	0.069585815	0.061745386
8.315826182	0.009555826	0.010650866	0.030220037	0.046988028	0.059478929	0.067166707	0.0699701	0.062416891
8.86168405	0.011523406	0.008676916	0.028468711	0.045641683	0.058629942	0.066811292	0.070343562	0.063095165
9.405925174	0.013486091	0.006688664	0.026685757	0.044253546	0.057738331	0.066420314	0.070705061	0.063779762
9.948458968	0.015442768	0.004687266	0.024871862	0.042823513	0.056803234	0.065992454	0.071053412	0.064470196
10.48919664	0.017392337	0.002673905	0.02302777	0.041351544	0.055823824	0.065526395	0.071387381	0.065165942
11.02805126	0.019333713	0.000649789	0.021154286	0.039837665	0.054799321	0.065020823	0.071705686	0.065866432
12.09977337	0.023187639	0.003425777	0.017322646	0.036684625	0.052612143	0.063885929	0.072289944	0.06727915
13.16296975	0.026996241	0.007529394	0.013384511	0.033366004	0.050236452	0.062577496	0.072795001	0.068702901
14.21701869	0.030751575	0.011650804	0.009348318	0.029884578	0.047667931	0.061085576	0.073208947	0.070131459
15.26133387	0.034446105	0.015779625	0.005223312	0.02624433	0.044903321	0.059400691	0.073519184	0.071557769
16.2953656	0.038072747	0.019905431	0.001019479	0.022450464	0.041940523	0.057513978	0.073712479	0.072973905
17.31860169	0.041624907	0.024017848	0.003252534	0.018509405	0.038778707	0.055417352	0.073775028	0.074371022
18.33056816	0.045096513	0.028106636	0.007581518	0.014428779	0.035418396	0.053103649	0.073692545	0.075739324
19.33082946	0.048482039	0.032161779	0.011955794	0.010217374	0.031861537	0.050566789	0.073450358	0.077068035
20.31898861	0.051776519	0.036173564	0.016363329	0.005885084	0.028111559	0.047801923	0.073033536	0.078345371
21.29468693	0.05497556	0.040132653	0.020791849	0.001442832	0.024173398	0.044805569	0.072427021	0.079558538
22.25760362	0.058075347	0.04403015	0.02522895	0.003097523	0.020053513	0.041575744	0.071615786	0.080693728
23.20745509	0.061072635	0.047857666	0.02966222	0.007723291	0.01575987	0.038112074	0.070585007	0.081736141
24.14399409	0.063964745	0.051607364	0.034079352	0.012421079	0.011301906	0.034415889	0.06932025	0.082670008
25.0670087	0.066749547	0.055272005	0.038468256	0.017176917	0.006690464	0.030490292	0.067807668	0.083478653
25.97632114	0.069425447	0.058844981	0.042817163	0.021976402	0.00193771	0.026340207	0.06603421	0.084144553
26.87178647	0.07199136	0.06232034	0.047114725	0.026804845	0.002942975	0.021972393	0.063987842	0.084649434
27.75329115	0.074446685	0.065692798	0.051350102	0.031647413	0.007937121	0.017395439	0.061657757	0.084974384
28.6207516	0.076791281	0.06895775	0.055513044	0.036489286	0.013029316	0.01261972	0.059034596	0.085099988
29.47411263	0.079025432	0.072111268	0.059593954	0.041315791	0.018203364	0.007657331	0.056110656	0.085006492
30.31334584	0.081149817	0.075150091	0.06358395	0.046112548	0.023442457	0.002521986	0.052880088	0.084673981

	lamda>	Rate of Aperture Opening [Ao dot] divided by shear transltn [Phi dot*b]						
Phi (deg)	0.1	0.2	0.3	0.4	0.5	0.6	0.8	1
0.001418118	1.015000217	1.029667636	1.053662869	1.086368005	1.12702504	1.174808683	1.288470195	1.421314688
0.014181182	1.014956035	1.02958038	1.053534891	1.086202458	1.126825538	1.174578993	1.288190923	1.420998207
0.028362362	1.014907235	1.029483714	1.053392971	1.086018784	1.126604127	1.174324031	1.287880855	1.42064679
0.035452951	1.01488295	1.029435494	1.053322121	1.085927054	1.126493524	1.174196648	1.287725914	1.420471171
0.049634125	1.014834611	1.02933928	1.053180641	1.085743804	1.12627252	1.173942078	1.287416218	1.420120115
0.055831409	1.014813583	1.029297329	1.053118904	1.085663811	1.126176025	1.173830911	1.287280955	1.419966776
0.070905875	1.014762679	1.029195525	1.052968968	1.085469459	1.125941524	1.173560714	1.286952136	1.419593981
0.085087031	1.014715108	1.029100065	1.052828219	1.085286914	1.125721199	1.173306799	1.286643057	1.419243525
0.099268176	1.014667845	1.029004906	1.052687762	1.085104652	1.125501146	1.173053146	1.286334224	1.41889331
0.101147683	1.014661604	1.028992316	1.052669168	1.085080517	1.125472002	1.173019547	1.286293312	1.418846912
0.103743768	1.014652992	1.028974936	1.052643494	1.085047189	1.125431753	1.172973146	1.286236808	1.418782831
0.12146903	1.01459447	1.028856538	1.052468462	1.084819884	1.125157194	1.172656571	1.285851237	1.418345523
0.223324574	1.014267485	1.028185303	1.051471516	1.083522249	1.123587688	1.170845326	1.283643065	1.415839842
0.279154922	1.014094979	1.027823969	1.050931454	1.082817139	1.122733321	1.169858233	1.282438072	1.414471622
0.33498474	1.013927236	1.027467307	1.050395926	1.0821164	1.121883157	1.168875186	1.281236891	1.413107104
0.446642362	1.013606039	1.026767994	1.049338469	1.080728031	1.12019543	1.166921225	1.278845946	1.410389154
0.558296592	1.013303897	1.026087365	1.048299142	1.079357134	1.118524496	1.164983422	1.276470198	1.407685946
0.669946581	1.01302081	1.025425419	1.047277941	1.078003702	1.116870342	1.163061759	1.274109612	1.404997432
0.781591482	1.01275678	1.024782158	1.046274866	1.07666773	1.115232956	1.161156216	1.271764155	1.402323569
0.893230448	1.012511809	1.024157581	1.045289914	1.075349211	1.113612326	1.159266774	1.269433796	1.39966431
1.004862632	1.012285899	1.023551691	1.044323085	1.074048139	1.112008442	1.157393418	1.267118502	1.39701961
1.116487186	1.012079053	1.022964488	1.043374376	1.072764511	1.110421291	1.155536127	1.264818241	1.394389424
1.228103264	1.011891272	1.022395975	1.042443789	1.071498319	1.108850864	1.153694886	1.262532981	1.391773709
1.339710021	1.011722561	1.021846154	1.041531321	1.070249562	1.107297151	1.151869677	1.260262691	1.389172418
1.45130661	1.011572923	1.021315027	1.040636975	1.069018233	1.105760141	1.150060483	1.25800734	1.386585509
1.674465905	1.011330881	1.020308868	1.038902646	1.06660785	1.102736196	1.14649008	1.253541332	1.381454659
1.897574394	1.011165179	1.019377525	1.03724081	1.064267146	1.099778959	1.142983551	1.249134717	1.376380812
2.34361198	1.011062956	1.017739424	1.034134679	1.059794705	1.094064359	1.13616165	1.240498727	1.366402757
2.67795671	1.011187006	1.01670752	1.031995523	1.056623188	1.089953087	1.131212059	1.234175927	1.359066325
2.789365533	1.011266623	1.016401046	1.031318765	1.055600836	1.088615904	1.129593907	1.232097549	1.356648649
3.067793428	1.011549447	1.015716941	1.029706313	1.053121136	1.085345618	1.125617785	1.226965279	1.350664887
3.624201358	1.012474597	1.014700921	1.026822175	1.048488325	1.079116306	1.117961815	1.216972266	1.338954229
3.902155428	1.013117209	1.014369278	1.025550702	1.04633531	1.076157203	1.114281676	1.212110754	1.333226115
4.457499215	1.014763316	1.0140595	1.023349585	1.042356412	1.07055003	1.107216481	1.2026559	1.322021355
5.012005072	1.016891818	1.01422225	1.02160525	1.038814336	1.065357653	1.100544108	1.193556355	1.311148075
5.565571274	1.01950434	1.014859126	1.020319107	1.035710071	1.060580402	1.094264031	1.184809617	1.300601864
6.118097145	1.022602698	1.015971928	1.019492786	1.033044848	1.056218858	1.088375986	1.176413424	1.290378511
6.669483156	1.026188897	1.017562657	1.019128141	1.030820138	1.052273866	1.082879972	1.168365757	1.280474001
7.219631036	1.030265127	1.019633515	1.019227244	1.029037658	1.048746525	1.077776254	1.160664845	1.270884526
7.768443868	1.034833763	1.022186898	1.019792387	1.027699365	1.045638197	1.073065366	1.153309168	1.261606487
8.315826182	1.039897363	1.025225401	1.020826077	1.026807458	1.042950504	1.068748111	1.146297466	1.2526365
8.86168405	1.045458668	1.028751809	1.022331038	1.026364374	1.040685332	1.064825569	1.13962874	1.243971402
9.405925174	1.051520597	1.032769102	1.024310205	1.026372792	1.038844824	1.061299091	1.133302257	1.235608254
9.948458968	1.058086248	1.037280445	1.026766725	1.026835626	1.037431388	1.058170307	1.127317555	1.227544348
10.48919664	1.065158892	1.042289191	1.029703951	1.027756026	1.036447694	1.055441126	1.121674449	1.219777213
11.02805126	1.072741976	1.047798878	1.033125442	1.029137377	1.03589667	1.053113736	1.116373032	1.212304618
12.09977337	1.089454102	1.06033612	1.04143647	1.033297622	1.036105654	1.04967448	1.106797067	1.198235366
13.16296975	1.108253576	1.074924034	1.051732275	1.039348013	1.038086953	1.047875668	1.098596166	1.18532378
14.21701869	1.129173977	1.091597239	1.064048412	1.04732377	1.041873271	1.047744934	1.091781566	1.173561255
15.26133387	1.15225143	1.110393015	1.078423405	1.057263576	1.047501327	1.04931441	1.086369354	1.162943571
16.2953656	1.177524529	1.131351199	1.09489863	1.069209453	1.055011771	1.052620694	1.082380564	1.153471061
17.31860169	1.205034251	1.154514078	1.113518186	1.083206633	1.064449073	1.057704798	1.079841264	1.145148783
18.33056816	1.234823871	1.179926288	1.134328762	1.099303408	1.075861395	1.064612071	1.078782628	1.137986693
19.33082946	1.266938878	1.207634704	1.157379502	1.117550981	1.089300453	1.073392106	1.079240987	1.131999799
20.31898861	1.301426886	1.237688332	1.182721865	1.138003299	1.104821353	1.084098619	1.081257863	1.127208325
21.29468693	1.338337555	1.270138205	1.210409488	1.160716885	1.122482417	1.096789306	1.084879976	1.123637849
22.25760362	1.377722499	1.305037279	1.240498044	1.185750663	1.142344998	1.111525685	1.090159234	1.121319445
23.20745509	1.419635206	1.342440329	1.273045107	1.213165785	1.164473279	1.128372915	1.097152693	1.120289806
24.14399409	1.464130956	1.382403853	1.30811002	1.243025448	1.18893407	1.147399589	1.105922491	1.120591347
25.0670087	1.511266737	1.424985975	1.345753764	1.275394723	1.215796589	1.168677526	1.116535756	1.122272301
25.97632114	1.561101171	1.470246357	1.386038832	1.310340382	1.245132248	1.192281533	1.129064484	1.125386786
26.87178647	1.613694437	1.518246106	1.429029114	1.347930724	1.277014434	1.218289162	1.143585388	1.129994856
27.75329115	1.669108192	1.569047697	1.474789785	1.388235421	1.311518287	1.246780457	1.160179721	1.136162521
28.6207516	1.727405508	1.622714892	1.523387198	1.431325358	1.348720486	1.277837693	1.178933067	1.143961749
29.47411263	1.788650795	1.679312667	1.574888786	1.477272487	1.38869904	1.31154511	1.199935104	1.153470432
30.31334584	1.852909741	1.738907143	1.629362978	1.526149695	1.431533087	1.347988651	1.223279343	1.164772322

	lamda>	Aperture Shear Energy contrib. to NDSF (tests 3,4)						
Phi (deg)	0.1	0.2	0.3	0.4	0.5	0.6	0.8	1
0.001418118	40.52693817	20.0583866	13.23492861	9.82294321	7.775702051	6.410933275	4.705264134	3.682214761
0.014181182	40.52876982	20.06020122	13.23669037	9.824623155	7.777279509	6.412396118	4.706489838	3.683222863
0.028362362	40.53079772	20.06221409	13.23864596	9.826488651	7.779031642	6.414021233	4.707851811	3.684343174
0.035452951	40.53180881	20.0632192	13.239623	9.82742096	7.779907471	6.414833684	4.708532829	3.684903407
0.049634125	40.53382524	20.06522673	13.24157556	9.829284702	7.781658656	6.416458376	4.709894928	3.68602403
0.055831409	40.53470403	20.06610292	13.24242821	9.830098804	7.782423738	6.417168291	4.710490202	3.686513816
0.070905875	40.53683554	20.06823136	13.2445006	9.832078117	7.784284245	6.418894884	4.711938231	3.687705354
0.085087031	40.53883285	20.07022999	13.24644809	9.833938928	7.786033845	6.420518868	4.713300536	3.688826495
0.099268176	40.54082251	20.07222505	13.24839356	9.835798564	7.787782809	6.422142567	4.714662924	3.689947845
0.101147683	40.54108564	20.0724892	13.24865125	9.836044944	7.788014561	6.422357744	4.714843495	3.690096479
0.103743768	40.54144886	20.07285396	13.24900713	9.836385224	7.788334653	6.42265495	4.715092912	3.690301787
0.12146903	40.543922	20.07534121	13.25143515	9.8387075	7.790519569	6.424683928	4.716795933	3.691703756
0.223324574	40.55790183	20.08952579	13.26532585	9.852016425	7.803055521	6.436334474	4.726584571	3.699766265
0.279154922	40.56539712	20.09722261	13.27289519	9.859285585	7.80991283	6.442714195	4.73195182	3.704190148
0.33498474	40.5727737	20.10486389	13.28043277	9.866536252	7.816760052	6.449089329	4.73732026	3.708617217
0.446642362	40.58717054	20.11997946	13.2954123	9.880981778	7.830423969	6.461825636	4.748060618	3.717480881
0.558296592	40.60109205	20.13487183	13.3102637	9.895352348	7.844046737	6.47454299	4.758805453	3.726357191
0.669946581	40.61453799	20.14954032	13.32498626	9.909647308	7.857627823	6.487240988	4.769554576	3.73524608
0.781591482	40.62750812	20.16398427	13.33957925	9.923866005	7.87116669	6.499919222	4.780307791	3.744147481
0.893230448	40.64000223	20.17820304	13.35404197	9.938007787	7.884662802	6.512577284	4.791064905	3.753061323
1.004862632	40.65202016	20.192196	13.3683737	9.952072003	7.898115621	6.525214762	4.80182572	3.761987536
1.116487186	40.66356174	20.20596252	13.38257375	9.966058005	7.911524609	6.537831244	4.812590039	3.77092605
1.228103264	40.67462687	20.219502	13.39664141	9.979965144	7.924889226	6.550426317	4.82335766	3.779876793
1.339710021	40.68521545	20.23281383	13.410576	9.993792773	7.938208932	6.562999564	4.834128383	3.78883969
1.45130661	40.69532742	20.24589743	13.42437682	10.00754025	7.951483186	6.575550567	4.844902003	3.797814669
1.674465905	40.7141214	20.27137769	13.45157446	10.03479216	7.977893172	6.600584164	4.866457111	3.815800567
1.897574394	40.73100887	20.29593835	13.47822896	10.06171575	8.004114842	6.625523733	4.888021322	3.833833873
2.34361198	40.7590667	20.34228422	13.52988751	10.1145576	8.055975819	6.67510715	4.931170258	3.870040172
2.67795671	40.7751124	20.37459981	13.56716708	10.15328941	8.094344801	6.712022395	4.963543068	3.897314528
2.789365533	40.77951021	20.38490378	13.57931135	10.16602533	8.107031213	6.72427329	4.974334939	3.906428315
3.067793428	40.78842776	20.40963622	13.60904884	10.19747712	8.138516201	6.754777838	5.001314516	3.929260804
3.624201358	40.7973813	20.4546775	13.66582172	10.25868518	8.2004669	6.815237613	5.05526095	3.975126757
3.902155428	40.7974313	20.47497568	13.69283931	10.28842251	8.230915495	6.845178892	5.082220425	3.998157278
4.457499215	40.78872068	20.51110444	13.74409439	10.34611723	8.29071642	6.904448984	5.136092914	4.044405711
5.012005072	40.76833188	20.54125254	13.79158948	10.40137805	8.3489988	6.962854909	5.189877334	4.090893191
5.565571274	40.73636244	20.56539893	13.83526502	10.45413406	8.405694697	7.020339029	5.243541359	4.13760609
6.118097145	40.83615555	20.58353138	13.87506644	10.50431665	8.460736648	7.076843113	5.297051543	4.184529996
6.669483156	40.9797835	20.59564648	13.91094435	10.55185975	8.514057826	7.132308442	5.350373327	4.231649698
7.219631036	41.14221341	20.6017496	13.94285472	10.59669999	8.565592205	7.186675905	5.40347104	4.278949167
7.768443868	41.32321882	20.60185496	13.97075904	10.63877691	8.615274726	7.239886107	5.456307917	4.326411531
8.315826182	41.52254006	20.59598547	13.9946244	10.67803317	8.663041468	7.291879486	5.508846108	4.374019061
8.86168405	41.7398852	20.5841727	14.01442369	10.7144147	8.708829819	7.342596428	5.561046697	4.42175315
9.405925174	41.9749311	20.56645678	14.03013562	10.74787094	8.752578647	7.391977391	5.612869724	4.469594294
9.948458968	42.22732467	20.54288617	14.04174485	10.77835492	8.794228478	7.439963037	5.664274209	4.517522077
10.48919664	42.49668402	20.5135176	14.049242	10.8058235	8.833721664	7.486494359	5.715218182	4.565515156
11.02805126	42.78259991	20.47841577	14.05262374	10.83023748	8.871002559	7.531512824	5.765658718	4.613551243
12.09977337	43.40233589	20.67874819	14.04705784	10.86976544	8.938715905	7.616780246	5.864853231	4.709658497
13.16296975	44.08276637	20.96605899	14.02514105	10.8967092	8.996969731	7.695311873	5.961496792	4.805646197
14.21701869	44.8197843	21.28906525	13.98706257	10.91090998	9.045407784	7.766671114	6.055216074	4.901300898
15.26133387	45.60899492	21.64617533	13.93310452	10.91228235	9.083721161	7.830443039	6.145627286	4.996393156
16.2953656	46.44577043	22.03557151	13.86363827	10.90081579	9.111652682	7.886239231	6.232338385	5.090677465
17.31860169	47.32530531	22.45523368	14.03509055	10.8765753	9.129000726	7.933702585	6.314951618	5.183892355
18.33056816	48.24267103	22.90296508	14.30717113	10.83970086	9.135622414	7.97251194	6.393066362	5.275760657
19.33082946	49.19286951	23.37641964	14.60269412	10.79040602	9.131436085	8.002386479	6.466282268	5.365989979
20.31898861	50.17088415	23.87313038	14.92034008	10.72897532	9.116422971	8.023089778	6.534202674	5.454273381
21.29468693	51.17172801	24.39053823	15.25864636	10.65576091	9.090628042	8.034433425	6.596438264	5.540290304
22.25760362	52.19048832	24.92602073	15.61602492	10.80204488	9.054159983	8.036280108	6.652610936	5.623707739
23.20745509	53.22236701	25.47692019	15.99078149	11.07069655	9.007190291	8.028546111	6.702357812	5.704181673
24.14399409	54.26271675	26.04057071	16.38113541	11.35683741	8.949951513	8.011203134	6.745335361	5.781358812
25.0670087	55.30707252	26.61432378	16.78524008	11.65926686	8.882734652	7.984279392	6.781223542	5.854878589
25.97632114	56.35117833	27.19557211	17.20120336	11.97668159	8.805885802	7.947859955	6.809729915	5.924375463
26.87178647	57.39100935	27.78177124	17.62710771	12.3076907	8.928001861	7.902086302	6.830593628	5.989481512
27.75329115	58.42278939	28.37045902	18.06102965	12.65083161	9.199079383	7.847155106	6.843589207	6.049829284
28.6207516	59.44300403	28.9592726	18.50105828	13.00458656	9.4841953	7.78331625	6.848530069	6.105054927
29.47411263	60.44840953	29.54596291	18.94531254	13.36739914	9.782203154	7.710870125	6.845271663	6.154801537
30.31334584	61.4360379	30.12840666	19.39195708	13.73769077	10.09187745	7.630164257	6.833714179	6.198722712

	lamda>	Bending Energy Contribution from 2 longitudinal hinges						
Phi (deg)	0.1	0.2	0.3	0.4	0.5	0.6	0.8	1
0.001418118	22.24481181	31.46188466	38.53401075	44.49596662	49.74850116	54.49712793	62.92843482	70.35654846
0.014181182	7.022588268	9.940838442	12.17887842	14.06524649	15.72699916	17.22925158	19.89643467	22.24621689
0.028362362	4.956409563	7.022723979	8.606545315	9.941220625	11.11685118	12.17957954	14.06632519	15.72850611
0.035452951	4.428980737	6.278402902	7.695592411	8.889725559	9.941507295	10.8922532	12.58015094	14.0671344
0.049634125	3.736123595	5.301294601	6.500014043	7.50985524	8.399222614	9.203109398	10.63022025	11.88743034
0.055831409	3.519764988	4.996391237	6.12702782	7.079428112	7.918169469	8.676276911	10.02209183	11.2076727
0.070905875	3.117008715	4.429198149	5.433345373	6.279011285	7.023674205	7.696706152	8.891437358	9.943897284
0.085087031	2.840030008	4.03952137	4.956925931	5.729380268	6.409505479	7.024172116	8.115248852	9.076375881
0.099268176	2.624355567	3.736383065	4.586427878	5.302017678	5.932010092	6.501335922	7.51188558	8.402056257
0.101147683	2.599201515	3.701047893	4.543249063	5.252216484	5.876370122	6.440415095	7.441585495	8.323491536
0.103743768	2.565577933	3.653822261	4.485543283	5.185662023	5.802013881	6.3590025	7.347640117	8.218502717
0.12146903	2.365350515	3.372781506	4.142211381	4.789727992	5.359697686	5.874734	6.788857849	7.594060515
0.223324574	1.720366822	2.470699072	3.041501357	3.521146868	3.943035193	4.324102733	5.000237253	5.595710449
0.279154922	1.526867245	2.201635606	2.713829477	3.143872931	3.521976932	3.863418046	4.469138423	5.002549782
0.33498474	1.382947842	2.002288432	2.471372329	2.864895556	3.210747787	3.522992411	4.076822321	4.564493838
0.446642362	1.178698602	1.72097346	2.129861151	2.47231607	2.773037647	3.044411461	3.52558203	3.949197396
0.558296592	1.037151799	1.527565014	1.895680831	2.203473077	2.473531482	2.717121243	3.148878098	3.52892164
0.669946581	0.931035466	1.383733225	1.721986496	2.004333554	2.251859082	2.475020101	2.870429569	3.218416128
0.781591482	0.847263446	1.271112838	1.586344332	1.849028019	2.079121539	2.286469023	2.65373056	2.976886386
0.893230448	0.778663426	1.179652692	1.476482555	1.723408916	1.93951706	2.134169831	2.478824895	2.782033981
1.004862632	0.720928619	1.103326022	1.385046497	1.618999532	1.823579258	2.007760821	2.333760433	2.620505214
1.116487186	0.671294076	1.038269262	1.307323601	1.530369718	1.725244941	1.900606071	2.210883787	2.483750042
1.228103264	0.627891409	0.981875482	1.240135624	1.453858183	1.640426625	1.808232468	2.105036733	2.366006454
1.339710021	0.589405814	0.932312915	1.181250439	1.386894186	1.566254762	1.72750008	2.012598936	2.263230725
1.45130661	0.55488105	0.8882514	1.129047943	1.32761232	1.500647442	1.65613107	1.930944429	2.172490064
1.674465905	0.495023142	0.812895762	1.040143598	1.226860571	1.389285596	1.535093494	1.792620289	2.018889348
1.897574394	0.444345104	0.750304044	0.966725742	1.143896504	1.297743292	1.435715133	1.679225937	1.893102203
2.34361198	0.361437628	0.650874056	0.851113332	1.013808728	1.154575056	1.280565441	1.502606354	1.697484025
2.67795671	0.310114007	0.591592412	0.782934446	0.937500875	1.07086368	1.190047153	1.399860741	1.58390759
2.789365533	0.294493933	0.573955544	0.762781802	0.915016115	1.046243981	1.163459858	1.36973363	1.550643078
3.067793428	0.258009095	0.533582228	0.716908882	0.863973179	0.990445435	1.103268858	1.301629506	1.475521837
3.624201358	0.193345311	0.465215568	0.640188931	0.779112027	0.898007669	1.003796587	1.189444043	1.352050341
3.902155428	0.164000725	0.435711824	0.607521194	0.743207364	0.859046554	0.961979981	1.14244775	1.300450553
4.457499215	0.109255922	0.383543129	0.550541285	0.680982784	0.791784029	0.889977404	1.061812419	1.212134604
5.012005072	0.057844563	0.338286566	0.502062581	0.628520972	0.735382008	0.829825363	0.994787961	1.138987469
5.565571274	0.007948305	0.298106408	0.459901297	0.583330081	0.687073888	0.778507662	0.937914064	1.07715794
6.118097145	0.041992379	0.26174581	0.422575525	0.543723017	0.644988661	0.733985993	0.888854685	1.024048246
6.669483156	0.093528692	0.228304835	0.389037073	0.508509745	0.607808231	0.694825551	0.845967301	0.977833589
7.219631036	0.148449781	0.197113673	0.358518805	0.476822258	0.574572578	0.659982241	0.808058156	0.937189235
7.768443868	0.209123237	0.167656054	0.3304429	0.448009489	0.544562812	0.628674986	0.774235465	0.901126856
8.315826182	0.279103335	0.139520709	0.304363203	0.421571336	0.517227801	0.60030564	0.743817361	0.868891941
8.86168405	0.364442786	0.112369219	0.279927603	0.397115664	0.492136373	0.574406823	0.716271973	0.839897027
9.405925174	0.477095387	0.085913814	0.256852693	0.374329393	0.468945182	0.550606874	0.691177172	0.813676864
9.948458968	0.646240622	0.059901318	0.234906203	0.352958499	0.447376512	0.528605637	0.668192774	0.789857457
10.48919664	0.976923739	0.034100943	0.21389453	0.332793866	0.42720257	0.508157338	0.647040886	0.768134192
11.02805126	3.135508825	0.008294387	0.193653669	0.313661048	0.408234137	0.489058222	0.627491723	0.748256044
12.09977337		0.044199529	0.154937676	0.277923075	0.373301806	0.454250295	0.592462966	0.713232235
13.16296975		0.099401762	0.117819966	0.244799027	0.341567941	0.423098726	0.561893811	0.68347539
14.21701869		0.15951649	0.081539392	0.213571077	0.312276803	0.394799152	0.53489002	0.658030618
15.26133387		0.227603192	0.045436657	0.183672231	0.284844265	0.368734431	0.51077088	0.636182293
16.2953656		0.308491764	0.008900308	0.154637318	0.258804789	0.344417147	0.489003281	0.617381013
17.31860169		0.410920668	0.028677892	0.126070177	0.233776728	0.32145213	0.46915873	0.601196048
18.33056816		0.553694048	0.067946644	0.097620512	0.209438826	0.299511239	0.45088438	0.587283413
19.33082946		0.790026192	0.109645818	0.068966521	0.185513787	0.27831593	0.433882964	0.575363822
20.31898861		1.397335367	0.154674503	0.039800849	0.1617564	0.257624913	0.417898543	0.565207115
21.29468693			0.204192965	0.009818095	0.137944666	0.237225217	0.402706162	0.556621007
22.25760362			0.259789376	0.021297493	0.113872885	0.216925613	0.388104207	0.549442815
23.20745509			0.323774861	0.053885505	0.089346006	0.196551654	0.373908651	0.543533257
24.14399409			0.399751449	0.088325583	0.064174704	0.175941872	0.359948693	0.538771721
25.0670087			0.493822725	0.125058472	0.038170786	0.154944791	0.346063407	0.535052589
25.97632114			0.617548863	0.16461503	0.01114255	0.133416496	0.332099184	0.532282322
26.87178647			0.796734086	0.207658286	0.017110282	0.111218568	0.317907799	0.530377085
27.75329115			1.107735594	0.255047198	0.046802466	0.088216243	0.303344998	0.529260752
28.6207516			1.995833253	0.307937823	0.078170521	0.064276623	0.288269544	0.528863163
29.47411263				0.367951986	0.111482102	0.039266828	0.27254267	0.52911851
30.31334584				0.437475309	0.147048512	0.013051917	0.256027935	0.529963752

	lamda>	Bending Energy Contribution from diagonal hinge						
Phi (deg)	0.1	0.2	0.3	0.4	0.5	0.6	0.8	1
0.001418118	1145.946124	420.8299959	241.8748354	168.193388	130.2727281	108.1638254	84.97718887	74.15634844
0.014181182	362.5701341	133.1057044	76.49381879	53.1879415	41.19431666	34.20205006	26.86940771	23.44771179
0.028362362	256.5255121	94.14164753	54.09424428	37.60997068	29.12757702	24.18265437	18.99739054	16.57800704
0.035452951	229.5104577	84.21256736	48.38557935	33.63956896	26.05196005	21.62879859	16.99082192	14.82691348
0.049634125	194.0852882	71.18905779	40.897032	28.43094729	22.01701985	18.27827835	14.3582427	12.52949728
0.055831409	183.043662	67.128668	38.56205094	26.80676378	20.75877075	17.23342992	13.53725892	11.81303087
0.070905875	162.5263005	59.58172691	34.22163817	23.78744971	18.41962966	15.29096059	12.01093371	10.48100934
0.085087031	148.4527419	54.40304449	31.24282434	21.71512723	16.81405937	13.95761412	10.96319589	9.566641442
0.099268176	137.52145	50.37913478	28.92791335	20.10454177	15.56616215	12.92126065	10.14880364	8.855909187
0.101147683	136.2483954	49.9104094	28.65823828	19.916908	15.42077718	12.80051887	10.05391969	8.773102105
0.103743768	134.5473642	49.28407065	28.2978743	19.66617171	15.22649664	12.63916856	9.927123125	8.662444092
0.12146903	124.4352963	45.55972571	26.15486006	18.17500754	14.07104028	11.67953664	9.172980451	8.004283781
0.223324574	92.16380702	33.65703303	19.3023017	13.40537008	10.37446912	8.609049391	6.759655108	5.898038286
0.279154922	82.62861245	30.13178828	17.27097617	11.99078665	9.277783894	7.697913314	6.043364801	5.272856262
0.33498474	75.60866546	27.53219226	15.77214017	10.94667271	8.468139257	7.025157315	5.514398476	4.811154494
0.446642362	65.79394649	23.88865799	13.66956616	9.481270939	7.331457378	6.08046132	4.771453988	4.162649663
0.558296592	59.13465697	21.4075456	12.23600207	8.481451916	6.555577761	5.435440554	4.264031919	3.719695532
0.669946581	54.24884849	19.58016116	11.17879815	7.743603729	5.982738383	4.959075928	3.889173445	3.392438243
0.781591482	50.47596379	18.16321913	10.35796231	7.170313993	5.537456113	4.58867626	3.597611007	3.137880557
0.893230448	47.45534015	17.02381242	9.697000169	6.708347985	5.178476897	4.289976831	3.36241519	2.93252005
1.004862632	44.97123051	16.08239171	9.15011745	6.325832107	4.88109839	4.042459285	3.16745923	2.762282024
1.116487186	42.88565293	15.28805132	8.688002939	6.002362726	4.629506294	3.832987177	3.002417719	2.618154816
1.228103264	41.10572614	14.60650382	8.290909874	5.724192354	4.413044447	3.652708288	2.860332313	2.494065335
1.339710021	39.56634408	14.01369967	7.944984713	5.481675113	4.224235387	3.495410651	2.736319781	2.38575155
1.45130661	38.22034545	13.49220595	7.640183198	5.267816571	4.057656614	3.356589238	2.62683852	2.290122347
1.674465905	35.97644847	12.61429376	7.125794464	4.906465489	3.775985542	3.121742424	2.441538057	2.12824911
1.897574394	34.18003477	11.90092158	6.706327477	4.611290249	3.545661737	2.929580918	2.289817053	1.995690255
2.34361198	31.49076169	10.80484816	6.058173267	4.1539813	3.188268183	2.631108674	2.05392553	1.789547633
2.67795671	30.01309026	10.17845443	5.684924321	3.889727075	2.981338299	2.458078375	1.917006105	1.669865444
2.789365533	29.59616396	9.996773813	5.576143293	3.812550036	2.920830866	2.407445806	1.876911372	1.634813486
3.067793428	28.6879087	9.590032438	5.3315379	3.638686639	2.784377994	2.293188643	1.786377533	1.555657255
3.624201358	27.32773547	8.934688951	4.933340264	3.354453577	2.560782859	2.105697635	1.63761386	1.425559477
3.902155428	26.82689137	8.666991007	4.76868655	3.236362241	2.467645304	2.027478026	1.575460689	1.371193099
4.457499215	26.10626513	8.219982884	4.489952824	3.035435737	2.308753078	1.893825008	1.46910617	1.278146447
5.012005072	25.6997399	7.863569125	4.262783807	2.870424748	2.177751993	1.78338223	1.381041832	1.201086422
5.565571274	25.56700423	7.575438883	4.074136998	2.732201902	2.067546415	1.690244472	1.306617787	1.135954181
6.118097145	25.71127546	7.340688166	3.915238356	2.614617909	1.973352802	1.610429297	1.242697303	1.080011936
6.669483156	26.13072543	7.148989785	3.779944488	2.513359015	1.891812931	1.54113977	1.187076737	1.031336567
7.219631036	26.86024264	6.992991298	3.663813255	2.425298374	1.820490362	1.480345736	1.138156055	0.988531987
7.768443868	27.97538377	6.867359471	3.563547102	2.348107336	1.757568601	1.426532794	1.09474126	0.950556658
8.315826182	29.61507154	6.768186495	3.476644505	2.280011908	1.701661942	1.37854495	1.055920553	0.916615467
8.86168405	32.04273943	6.692609442	3.401173521	2.219634381	1.651692421	1.335482256	1.02098373	0.886089358
9.405925174	35.81081698	6.63856145	3.335619983	2.165887033	1.606807207	1.29663206	0.989368067	0.858488078
9.948458968	42.31822835	6.604608123	3.278782999	2.117898816	1.566321594	1.261421576	0.960620947	0.833417549
10.48919664	56.73804093	6.58984193	3.229701357	2.074963591	1.529678738	1.229384358	0.934373466	0.810556817
11.02805126	163.6169749	6.593818581	3.187600692	2.036502806	1.496420603	1.200136113	0.910321366	0.789641408
12.09977337		6.676070436	3.121957848	1.971170869	1.438597747	1.148777973	0.867829008	0.752800755
13.16296975		6.843163429	3.078161489	1.918944003	1.390477084	1.105342889	0.831551141	0.721515007
14.21701869		7.106233006	3.053872959	1.877723858	1.350342087	1.068373147	0.800323956	0.694778558
15.26133387		7.492888597	3.047762242	1.846001588	1.316922415	1.036779595	0.773272009	0.671838033
16.2953656		8.05442016	3.059327913	1.822690392	1.289260727	1.009730208	0.74972008	0.652115317
17.31860169		8.892114016	3.100946865	1.807019585	1.266626567	0.986577777	0.729135817	0.635157468
18.33056816		10.23513272	3.165965	1.798467161	1.248459144	0.966811542	0.711091231	0.620603082
19.33082946		12.75343463	3.25281087	1.796717902	1.234328535	0.95002405	0.695236139	0.608159089
20.31898861		20.03458246	3.364918137	1.801639701	1.223909072	0.935887978	0.68127943	0.597584364
21.29468693			3.507483331	1.813274218	1.216961076	0.924139693	0.668975593	0.588677911
22.25760362			3.688387741	1.841474709	1.213318532	0.914567467	0.658114862	0.581270188
23.20745509			3.919895505	1.882087414	1.212881215	0.907003019	0.648515924	0.575216621
24.14399409			4.221992715	1.931412533	1.215610338	0.901315469	0.640020478	0.570392693
25.0670087			4.629598063	1.99048525	1.221527207	0.897407121	0.632489148	0.566690148
25.97632114			5.210333459	2.060723311	1.230714714	0.895210655	0.625798443	0.564014033
26.87178647			6.11782074	2.144066298	1.251715337	0.89468747	0.619838511	0.562280325
27.75329115			7.813798462	2.243194646	1.282500845	0.895826991	0.614511547	0.561414012
28.6207516			13.03562996	2.361884738	1.317972453	0.89864686	0.609730739	0.561347478
29.47411263				2.505609	1.358605393	0.903193977	0.605419667	0.562019105
30.31334584				2.682606168	1.405010135	0.909546413	0.601512122	0.563372005

	lamda>	Membrane Energy Contribution (tests 3,4)						
Phi (deg)	0.1	0.2	0.3	0.4	0.5	0.6	0.8	1
0.001418118	40.74016291	64.75303591	85.163388	101.5974246	114.1200982	123.0938282	132.4994918	134.0458593
0.014181182	40.73986622	64.75189894	85.16098098	101.593451	114.1143894	123.0863228	132.4885044	134.0317958
0.028362362	40.73954127	64.75064466	85.15831925	101.5890516	114.1080644	123.0780034	132.4763178	134.016192
0.035452951	40.73938065	64.75002107	85.15699339	101.5868581	114.104909	123.0738515	132.4702331	134.0083988
0.049634125	40.7390631	64.74878097	85.15435169	101.5824835	114.0986125	123.0655632	132.4580809	133.9928301
0.055831409	40.73892586	64.74824201	85.15320143	101.580577	114.0958668	123.0619478	132.4527775	133.9860338
0.070905875	40.73859594	64.74693851	85.15041412	101.5759526	114.0892034	123.05317	132.4398954	133.969521
0.085087031	40.73829059	64.74572195	85.14780571	101.5716193	114.0829543	123.0449338	132.4278003	133.9540108
0.099268176	40.73799008	64.74451476	85.14521057	101.5673024	114.0767242	123.0367183	132.4157281	133.938524
0.101147683	40.73795061	64.74435546	85.14486761	101.5667315	114.0758999	123.035631	132.4141298	133.9364732
0.103743768	40.73789623	64.74413571	85.14439429	101.5659435	114.0747619	123.0341298	132.4119228	133.9336412
0.12146903	40.73752926	64.74264364	85.14117443	101.5605773	114.0670089	123.0238986	132.3968745	133.9143261
0.223324574	40.73556356	64.73435015	85.1230708	101.5302374	114.023028	122.9657325	132.3110907	133.8040405
0.279154922	40.73458721	64.73000479	85.11343385	101.5139634	113.9993315	122.9343009	132.2645662	133.7440986
0.33498474	40.73368054	64.72579964	85.10399792	101.4979403	113.9759247	122.9031875	132.2183926	133.6845166
0.446642362	40.73207015	64.71780416	85.08572368	101.4666415	113.9299752	122.8419114	132.1270943	133.5664299
0.558296592	40.7307202	64.7103521	85.06823717	101.4363308	113.8851703	122.7818956	132.0371887	133.4497747
0.669946581	40.72961853	64.70343185	85.05152747	101.4069981	113.8415006	122.7231318	131.9486688	133.3345453
0.781591482	40.72875296	64.6970318	85.03558368	101.3786333	113.7989569	122.6656114	131.8615277	133.2207361
0.893230448	40.72811133	64.69114034	85.02039488	101.3512263	113.7575298	122.6093259	131.7757582	133.1083411
1.004862632	40.72768147	64.68574584	85.00595017	101.3247669	113.71721	122.5542669	131.6913536	132.9973548
1.116487186	40.72745121	64.68083671	84.99223863	101.299245	113.6779882	122.5004257	131.6083067	132.8877714
1.228103264	40.72740837	64.67640133	84.97924936	101.2746506	113.6398552	122.4477941	131.5266106	132.7795851
1.339710021	40.72754078	64.67242809	84.96697144	101.2509734	113.6028016	122.3963633	131.4462582	132.6727903
1.45130661	40.72783628	64.66890538	84.95539397	101.2282034	113.566818	122.346125	131.3672426	132.5673812
1.674465905	40.72886785	64.6631651	84.93429671	101.1853443	113.4980241	122.2491918	131.2131939	132.3606973
1.897574394	40.73040571	64.65908759	84.91587031	101.1459922	113.4333989	122.1569265	131.0644084	132.1594875
2.34361198	40.73461085	64.65554932	84.88668093	101.0774855	113.3163571	121.9861277	130.7824033	131.7733072
2.67795671	40.73836958	64.65656951	84.87115071	101.0347092	113.2389651	121.8697765	130.5842996	131.4977009
2.789365533	40.73967279	64.65754743	84.86712756	101.0220353	113.2150971	121.8331852	130.5207801	131.4084738
3.067793428	40.7429255	64.6612775	84.85948973	100.9937212	113.1595591	121.7464222	130.3674168	131.1911304
3.624201358	40.74876155	64.67362899	84.8540061	100.9510014	113.0656979	121.5926535	130.0836139	130.7806721
3.902155428	40.75096456	64.68188756	84.85581935	100.9362794	113.0270839	121.5253825	129.9529557	130.5873783
4.457499215	40.75298972	64.70166318	84.86770362	100.91932	112.9657621	121.4094035	129.7135797	130.2242141
5.012005072	40.75057267	64.72457393	84.88946175	100.9179521	112.9246793	121.3172906	129.5027292	129.8916846
5.565571274	40.74219208	64.74916835	84.91972995	100.9309104	112.9026723	121.247982	129.3195303	129.589074
6.118097145	42.99708596	64.77399499	84.95714443	100.9569292	112.8985779	121.2004161	129.163109	129.3156666
6.669483156	45.69221987	64.79760243	85.00034138	100.9947429	112.9112331	121.1735313	129.0325914	129.0707466
7.219631036	48.39788124	64.81853921	85.04795702	101.043086	112.9394747	121.1662659	128.9271036	128.8535982
7.768443868	51.11559138	64.83535389	85.09862756	101.1006929	112.9821394	121.1775583	128.8457716	128.6635056
8.315826182	53.84687159	64.84659503	85.1509892	101.1662982	113.0380641	121.2063467	128.7877215	128.4997532
8.86168405	56.59324318	64.85081118	85.20367816	101.2386362	113.1060857	121.2515696	128.7520792	128.3616251
9.405925174	59.35622746	64.84655091	85.25533063	101.3164414	113.185041	121.3121652	128.737971	128.2484056
9.948458968	62.13734575	64.83236276	85.30458282	101.3984482	113.2737668	121.387072	128.7445228	128.1593789
10.48919664	64.93811934	64.80679529	85.35007095	101.4833911	113.3711001	121.4752282	128.7708606	128.0938293
11.02805126	67.76006955	64.76839707	85.39043121	101.5700045	113.4758775	121.5755722	128.8161107	128.0510409
12.09977337		69.13904442	85.45031299	101.7431808	113.7031125	121.8085771	128.9598514	128.030885
13.16296975		74.42414302	85.47331781	101.9078525	113.9461664	122.0775934	129.1687533	128.0931851
14.21701869		79.78959354	85.44853533	102.0538953	114.195734	122.3741278	129.4358249	128.232215
15.26133387		85.2470075	85.36505521	102.1711847	114.4425101	122.689687	129.7540747	128.4422487
16.2953656		90.80799647	85.21196711	102.2495964	114.6771892	123.0157779	130.1165111	128.7175601
17.31860169		96.48417198	88.9875032	102.2790058	114.8904662	123.3439072	130.5161426	129.052423
18.33056816		102.2871456	94.10010628	102.2492886	115.0730358	123.6655815	130.9459775	129.4411113
19.33082946		108.2285288	99.31504836	102.1503203	115.2155927	123.9723078	131.3990244	129.877899
20.31898861		114.3199333	104.6432398	101.9719766	115.3088317	124.2555927	131.8682917	130.3570599
21.29468693			110.0955909	101.7041329	115.3434473	124.506943	132.3467878	130.8728678
22.25760362			115.6830121	104.8801044	115.3101344	124.7178655	132.8275213	131.4195968
23.20745509			121.4164136	109.8000202	115.1995877	124.8798668	133.3035004	131.9915206
24.14399409			127.3067059	114.8398092	115.0025018	124.9844538	133.7677338	132.5829133
25.0670087			133.3647992	120.0095958	114.7095716	125.0231332	134.2132298	133.1880486
25.97632114			139.601604	125.3195044	114.3114917	124.9874117	134.632997	133.8012004
26.87178647			146.0280304	130.7796595	116.8924604	124.8687962	135.0200436	134.4166427
27.75329115			152.654989	136.4001855	121.6120062	124.6587932	135.3673783	135.0286493
28.6207516			159.49339	142.1912067	126.4646174	124.3489097	135.6680093	135.6314941
29.47411263				148.1628477	131.4595994	123.9306524	135.9149453	136.2194511
30.31334584				154.3252328	136.6062575	123.395528	136.1011946	136.786794

	lamda>	Total Analytical NDSF (tests 3,4)						
Phi (deg)	0.1	0.2	0.3	0.4	0.5	0.6	0.8	1
0.001418118	1249.458037	537.103303	378.8071627	324.1097224	301.9170295	292.1657148	285.1103797	282.240971
0.014181182	450.8613584	227.858643	187.0703686	178.6712621	178.8129847	180.9300206	183.9608366	183.4089474
0.028362362	342.7522606	185.9772303	161.0977548	158.9667315	162.1315242	165.8542585	170.2478854	170.0070483
0.035452951	315.2106279	175.3042105	154.4777882	153.9435736	157.8782838	162.0097369	166.7497388	166.5873501
0.049634125	279.0943001	161.3043601	145.7929733	147.3525708	152.2965136	156.9634094	162.1564388	162.0957818
0.055831409	267.8370569	156.9394042	143.0847084	145.2968677	150.5552308	155.3888229	160.7226184	160.6932512
0.070905875	246.9187407	148.8260949	138.0498983	141.4744917	147.3167915	152.4597316	158.0542047	158.082133
0.085087031	232.5698954	143.2585178	134.5940041	138.8500657	145.092553	150.4472389	156.2195456	156.2858546
0.099268176	221.4246182	138.9322577	131.9079454	136.8096605	143.3626793	148.8814575	154.7910802	154.8864373
0.101147683	220.1266331	138.428302	131.5950062	136.571901	143.1610618	148.6989227	154.6244784	154.7231634
0.103743768	218.3922872	137.7548826	131.176819	136.2541624	142.8916071	148.4549558	154.4017789	154.5048898
0.12146903	208.082098	133.7504921	128.689681	134.3640204	141.2882664	147.0028531	153.0755087	153.2043741
0.223324574	175.1776392	120.951608	120.7321997	128.3087708	136.1435878	142.3352191	148.7975676	148.9975555
0.279154922	165.455464	117.1606513	118.3711347	126.5079086	134.6090052	140.9383464	147.5090213	147.7236947
0.33498474	158.2980675	114.3651442	116.6279432	125.1760448	133.4715718	139.9004265	146.5469337	146.7687821
0.446642362	148.2918858	110.4474151	114.1805633	123.3012102	131.8648942	138.4286098	145.1721909	145.3957578
0.558296592	141.503621	107.7803346	112.5101838	122.0166081	130.7583263	137.4090004	144.2089042	144.4247491
0.669946581	136.5240405	105.8168666	111.2772984	121.0645827	129.9337259	136.6444688	143.4778264	143.6806458
0.781591482	132.6794883	104.295348	110.3194696	120.3218413	129.2867012	136.0406759	142.893177	143.0796505
0.893230448	129.6021171	103.0728085	109.5479196	119.7209909	128.7601865	135.5460499	142.4080632	142.5759565
1.004862632	127.0718608	102.0636596	108.9094878	119.2216705	128.3200032	135.1297017	141.994399	142.1421296
1.116487186	124.94796	101.2131198	108.3701389	118.7980355	127.9442641	134.7718502	141.6341982	141.7606023
1.228103264	123.1356528	100.4842826	107.9069363	118.4326663	127.6182155	134.4591611	141.3153373	141.4195337
1.339710021	121.5685061	99.85125451	107.5037826	118.1133355	127.3315006	134.1822736	141.0293053	141.1106123
1.45130661	120.1983902	99.29526017	107.1490019	117.8311725	127.0766053	133.9343959	140.7699276	140.8278083
1.674465905	117.9144609	98.36173231	106.5518092	117.3534625	126.6411884	133.5066119	140.3138093	140.3236363
1.897574394	116.0857945	97.60625157	106.0671525	116.9628947	126.2809188	133.1477463	139.9214727	139.8821138
2.34361198	113.3458769	96.45355575	105.325855	116.3598332	125.7151762	132.572909	139.2701055	139.130379
2.67795671	111.8366862	95.80121616	104.9061766	116.0152266	125.3855119	132.2299244	138.8647095	138.6487885
2.789365533	111.4098409	95.61318057	104.785364	115.9156268	125.2892031	132.1283641	138.74176	138.5003587
3.067793428	110.4772711	95.19452838	104.5169853	115.6938581	125.0728987	131.8976575	138.4567384	138.1515703
3.624201358	109.0672236	94.52821101	104.093357	115.3432522	124.7249553	131.5173854	137.9659327	137.5334087
3.902155428	108.539288	94.25956607	103.9248664	115.2042715	124.5846912	131.3600194	137.7530845	137.2571792
4.457499215	107.7572314	93.81629364	103.6522921	114.9818557	124.3570156	131.0976549	137.3805912	136.7589009
5.012005072	107.276489	93.46768215	103.4458976	114.8182759	124.1868121	130.8933531	137.0684363	136.3226517
5.565571274	107.0535071	93.18811257	103.2890333	114.7005764	124.0629873	130.7370732	136.8076035	135.9397922
6.118097145	109.5865093	92.95996036	103.1700247	114.6195867	123.9776561	130.6216745	136.5917125	135.6042568
6.669483156	112.8962575	92.77054353	103.0802673	114.5684714	123.9249121	130.5418051	136.4160088	135.3115664
7.219631036	116.5487871	92.61039379	103.0131438	114.5419066	123.9001298	130.4932698	136.2767889	135.0582685
7.768443868	120.6233172	92.47222437	102.9633766	114.5355867	123.8995455	130.4726521	136.1710563	134.8416007
8.315826182	125.2635865	92.3502877	102.9266213	114.5459146	123.9199953	130.4770768	136.0963055	134.6592797
8.86168405	130.7403106	92.23996255	102.899203	114.5698009	123.9587443	130.5040551	136.0503816	134.5093647
9.405925174	137.6190709	92.13748295	102.8779389	114.6045287	124.013372	130.5513815	136.031386	134.3901648
9.948458968	147.3291394	92.03975837	102.8600169	114.6476604	124.0816934	130.6170622	136.0376107	134.300176
10.48919664	165.149768	91.94425577	102.8429088	114.6969721	124.161703	130.6992642	136.0674932	134.2380354
11.02805126	277.2951532	91.8489258	102.8243093	114.7504059	124.2515348	130.7962794	136.1195825	134.2024896
12.09977337		96.53806257	102.7742664	114.8620402	124.4537279	131.0283856	136.2849966	134.2065765
13.16296975		102.3327672	102.6944403	114.9683047	124.6751812	131.3013469	136.523695	134.3038217
14.21701869		108.3444083	102.5710102	115.0561002	124.9037607	131.6039712	136.826255	134.4863251
15.26133387		114.6136746	102.3913586	115.1131409	125.1279979	131.9256441	137.1837449	134.7466622
16.2953656		121.2064799	102.1438336	115.1277399	125.3369074	132.2561645	137.5875729	135.0777339
17.31860169		128.2424404	106.1522185	115.0886708	125.5198703	132.5856396	138.0293887	135.4726689
18.33056816		135.9789374	111.641189	114.9850771	125.6665562	132.9044163	138.5010195	135.9247585
19.33082946		145.1484093	117.2801992	114.8064108	125.7668711	133.2030343	138.9944258	136.4274119
20.31898861		159.6249815	123.0831725	114.5423924	125.8109201	133.4721954	139.5016723	136.9741247
21.29468693			129.0659136	114.1829861	125.7889811	133.7027414	140.0149079	137.5584571
22.25760362			135.2472141	117.5449214	125.6914858	133.8856387	140.5263513	138.1740175
23.20745509			141.6508655	122.8066897	125.5090052	134.0119676	141.0282828	138.8144522
24.14399409			148.3095855	128.2163847	125.2322384	134.0729143	141.5130384	139.4734365
25.0670087			155.2734601	133.7844064	124.8520042	134.0597645	141.9730059	140.1446699
25.97632114			162.6306896	139.5215244	124.3592348	133.9638988	142.4006245	140.8218722
26.87178647			170.569693	145.4390748	127.0892879	133.7767885	142.7883835	141.4987816
27.75329115			179.6375527	151.5492589	132.1403889	133.4899916	143.128824	142.1691533
28.6207516			193.0259115	157.8656158	137.3449557	133.0951495	143.4145397	142.8267597
29.47411263				164.4038078	142.71189	132.5839833	143.6381793	143.4653902
30.31334584				171.1830051	148.2501936	131.9482906	143.7924489	144.0788525

Tabulation of Elastic and NBPF non-dimensional shear					
	NBPF for	NBPF for		Elastic Model NDSF	
Phi (deg)	Tests 3,4	Tests 5,6,7	Phi (deg)	Test 3,4	Test 5,6,7
0.001418118	81.46035554	88.14507937	0.001418118	0.448953995	0.440782574
0.014181182	81.46036542	88.14509007	0.014181182	4.489539863	4.407825651
0.028362362	81.46039536	88.14512246	0.028362362	8.979079176	8.815650763
0.035452951	81.46041782	88.14514676	0.035452951	11.22384845	11.01956295
0.049634125	81.4604777	88.14521156	0.049634125	15.71338591	15.42738624
0.055831409	81.46051014	88.14524666	0.055831409	17.67534856	17.35363916
0.070905875	81.46060496	88.14534926	0.070905875	22.44768831	22.03911746
0.085087031	81.46071474	88.14546805	0.085087031	26.93721993	26.44693501
0.099268176	81.46084449	88.14560845	0.099268176	31.42674824	30.85474932
0.101147683	81.46086318	88.14562867	0.101147683	32.0217706	31.43894167
0.103743768	81.46088958	88.14565724	0.103743768	32.8436505	32.24586251
0.12146903	81.4610877	88.14587161	0.12146903	38.45519038	35.00056457
0.223324574	81.46283063	88.14775757	0.223324574	54.57812448	50.83004479
0.279154922	81.46422292	88.14926412	0.279154922	63.41563093	59.5066996
0.33498474	81.46592462	88.15110545	0.33498474	72.25305346	68.18327201
0.446642362	81.4702562	88.15579249	0.446642362	89.92757967	85.53610379
0.558296592	81.47582538	88.16181868	0.558296592	107.6015689	102.8884083
0.669946581	81.48263215	88.16918402	0.669946581	125.2748869	120.2400539
0.781591482	81.49067651	88.17788852	0.781591482	142.9473995	137.5909087
0.893230448	81.49995847	88.18793217	0.893230448	160.6189726	154.9408412
1.004862632	81.51047803	88.19931497	1.004862632	178.2894721	172.2897195
1.116487186	81.52223518	88.21203692	1.116487186	195.9587639	189.6374122
1.228103264	81.53522992	88.22609803	1.228103264	213.6267141	206.9837876
1.339710021	81.54946226	88.24149829	1.339710021	231.2931887	224.3287144
1.45130661	81.5649322	88.2582377	1.45130661	248.9580539	241.6720609
1.674465905	81.59958485	88.29573399	1.674465905	284.2824208	276.3534883
1.897574394	81.63918788	88.33858689	1.897574394	319.5987456	311.0270199
2.34361198	81.73324509	88.44036253	2.34361198	390.2029988	380.3462036
2.67795671	81.81678273	88.53075536	2.67795671	443.1271484	432.3070796
2.789365533	81.8471038	88.56356461	2.789365533	460.7622917	449.6212453
3.067793428	81.92832096	88.65144654	3.067793428	504.8352447	492.8920255
3.624201358	82.11396018	88.8523195	3.624201358	592.9102581	579.3639837
3.902155428	82.21838223	88.96531055	3.902155428	636.9082083	622.5611262
4.457499215	82.45043125	89.21640175	4.457499215	724.8147762	708.8677048
5.012005072	82.71342014	89.50097179	5.012005072	812.5887062	795.0440596
5.565571274	83.00734889	89.81902065	5.565571274	900.2138964	881.0743818
6.118097145	83.33221752	90.17054835	6.118097145	987.6744101	966.9430248
6.669483156	83.68802601	90.55555487	6.669483156	1074.954493	1052.634521
7.219631036	84.07477438	90.97404021	7.219631036	1162.03859	1138.133598
7.768443868	84.49246261	91.42600439	7.768443868	1248.911358	1223.425194
8.315826182	84.94109071	91.91144739	8.315826182	1335.557687	1308.494471
8.86168405	85.42065868	92.43036922	8.86168405	1421.962709	1393.326833
9.405925174	85.93116652	92.98276988	9.405925174	1508.111812	1477.907934
9.948458968	86.47261423	93.56864937	9.948458968	1593.990658	1562.223698
10.48919664	87.04500181	94.18800768	10.48919664	1679.585192	1646.260324
11.02805126	87.64832925	94.84084482	11.02805126	1764.881654	1730.004303
12.09977337	88.94780375	96.24695559	12.09977337	1934.526862	1896.561795
13.16296975	90.37103773	97.78698166	13.16296975	2102.822515	2061.794295
14.21701869	91.91803118	99.46092305	14.21701869	2269.670199	2225.605181
15.26133387	93.58878411	101.2687798	15.26133387	2434.977106	2387.903333
16.2953656	95.38329652	103.2105518	16.2953656	2598.656221	2548.603321
17.31860169	97.3015684	105.2862391	17.31860169	2760.626473	2707.625549
18.33056816	99.34359976	107.4958417	18.33056816	2920.812831	2864.896352
19.33082946	101.5093906	109.8393597	19.33082946	3079.146354	3020.348043
20.31898861	103.7989409	112.3167929	20.31898861	3235.564201	3173.918925
21.29468693	106.2122507	114.9281415	21.29468693	3390.009596	3325.553256
22.25760362	108.7493199	117.6734054	22.25760362	3542.431759	3475.20118
23.20745509	111.4101487	120.5525846	23.20745509	3692.7858	3622.818624
24.14399409	114.1947369	123.5656791	24.14399409	3841.032581	3768.367163
25.0670087	117.1030846	126.7126889	25.0670087	3987.138559	3911.813862
25.97632114	120.1351918	129.993614	25.97632114	4131.07559	4053.131092
26.87178647	123.2910584	133.4084544	26.87178647	4272.82073	4192.296326
27.75329115	126.5706845	136.9572102	27.75329115	4412.356011	4329.291922
28.6207516	129.9740701	140.6398812	28.6207516	4549.6682	4464.104889
29.47411263	133.5012152	144.4564676	29.47411263	4684.748562	4596.72665
30.31334584	137.1521197	148.4069693	30.31334584	4817.592599	4727.15279

Experimental Results (KN)					
Phi (deg)	Test 3	Test 4	Test 5	Test 6	Test 7
0.001418118	0	0	0	0	0
0.014181182					
0.028362362					
0.035452951					
0.049634125					
0.055831409	3.4	3.3	2.3	1.9	3.1
0.070905875					
0.085087031					
0.099268176					
0.101147683					
0.103743768					
0.12146903					
0.223324574	11.7	10.8	10.4	9.7	11.8
0.279154922	14.4	13.7	13	12.1	13.3
0.33498474	16.9	15.4	16	14.2	15.9
0.446642362	23.1	20	20.4	18.4	19.2
0.558296592	29	24.9	23.6	22	22.8
0.669946581	34.1	30	27.2	25.6	26
0.781591482	39.5	35	31.3	30.3	29.3
0.893230448	44.8	41.2	35.9	34.5	33.9
1.004862632	50.1	48	40.3	38.9	39
1.116487186	54.8	54.5	44.35	44	44
1.228103264	58.7	60	49.5	48.7	49.6
1.339710021	61.3	65	54.2	52.2	55
1.45130661	63.5	68.8	57.6	53.8	59.3
1.674465905	67	74	62.35	58.8	66
1.897574394	70.6	78.1	65.75	61.4	70.6
2.34361198	79.3	84.4	70.75	70.8	75.35
2.67795671	83.5	87.4	73.4	74.1	77.51
2.789365533	84.7	88.2	74	74.8	78.08
3.067793428	86.6	89.4	75.25	75.85	78.75
3.624201358	88.6	91.5	74.7	74.49	78.58
3.902155428	90	92.3	74.9	74.95	77.8
4.457499215	92.4	93.8	75.6	75.31	78.57
5.012005072	93.3	95.7	76.75	76.56	79.5
5.565571274	94.8	97.8	78.4	77.72	80.98
6.118097145	96.5	99.2	79.8	77.5	82.05
6.669483156	98.35	100	80	77.35	82.4
7.219631036	98.8	100.2	79	76.6	81.35
7.768443868	97.9	98.4	77	76.5	79.65
8.315826182	95.5	98.35	75.4	74.35	76.4
8.86168405	95.9	97	75.3	75.08	76.7
9.405925174	96.5	98.1	75.75	75.4	77.12
9.948458968	98.1	98.75	75	75.22	77.31
10.48919664	97	99.25	73	74.2	77.2
11.02805126	98.1	97.7	71	67	76.23
12.09977337	97.4	98.25	67.8	64.35	
13.16296975	98.8	100.2	62.2	60	
14.21701869	97.2	98.9		51.3	
15.26133387	98.03	98.85			
16.2953656	98.5	98.65			
17.31860169	98.1	98.1			
18.33056816	93	94.9			
19.33082946	94.1	90			
20.31898861	93.2	90.05			
21.29468693		87.6			

Experimental NDSF					
Phi (deg)	Test 3	Test 4	Test 5	Test 6	Test 7
0.001418118	0	0	0	0	0
0.014181182					
0.028362362					
0.035452951					
0.049634125					
0.055831409	2.435871181	2.364227911	2.032911118	1.679361358	2.740010637
0.070905875					
0.085087031					
0.099268176					
0.101147683					
0.103743768					
0.12146903					
0.223324574	8.382262595	7.737473164	9.192293751	8.573581672	10.42971791
0.279154922	10.31663089	9.815127995	11.49036719	10.69488023	11.75552951
0.33498474	12.10771264	11.03306359	14.14199039	12.55101647	14.05360295
0.446642362	16.54959538	14.32865401	18.03103774	16.26328894	16.97038846
0.558296592	20.77654831	17.83917424	20.85943582	19.44523678	20.1523363
0.669946581	24.43035508	21.49298101	24.04138366	22.62718462	22.98073438
0.781591482	28.29909167	25.07514451	27.66526869	26.78139429	25.89751989
0.893230448	32.09618498	29.51702726	31.73109093	30.49366677	29.96334213
1.004862632	35.89327829	34.38876962	35.62013829	34.38271413	34.47110157
1.116487186	39.26051198	39.04558217	39.1998296	38.89047356	38.89047356
1.228103264	42.05459951	42.98596202	43.75178276	43.04468324	43.8401702
1.339710021	43.91732453	46.56812553	47.90599243	46.13824364	48.61309195
1.45130661	45.49347647	49.29056979	50.91116539	47.55244267	52.41375187
1.674465905	48.00099093	53.01601983	55.10956879	51.97181467	58.33571034
1.897574394	50.58014865	55.9533939	58.11474174	54.26988811	62.40153258
2.34361198	56.81311314	60.46691991	62.53411374	62.57830746	66.59993598
2.67795671	59.82213048	62.61621801	64.8763809	65.49509298	68.50910468
2.789365533	60.68184972	63.18936417	65.40670554	66.11380506	69.01291309
3.067793428	62.04307185	64.04908341	66.51154854	67.04187318	69.60510893
3.624201358	63.47593725	65.55359209	66.02541762	65.83980399	69.45485028
3.902155428	64.47894304	66.12673825	66.2021925	66.24638622	68.76542825
4.457499215	66.19838152	67.2013873	66.82090458	66.564581	69.44601154
5.012005072	66.84317095	68.56260943	67.83736013	67.669424	70.26801473
5.565571274	67.91782	70.0671181	69.29575289	68.6947183	71.57614884
6.118097145	69.13575559	71.07012388	70.53317705	68.50026593	72.52189445
6.669483156	70.46115608	71.64327004	70.70995193	68.36768477	72.83125049
7.219631036	70.7835508	71.78655658	69.82607753	67.70477897	71.90318237
7.768443868	70.13876137	70.49697772	68.05832873	67.61639153	70.40059589
8.315826182	68.41932289	70.46115608	66.6441297	65.71606158	67.52800409
8.86168405	68.70589597	69.49397194	66.55574226	66.36128989	67.79316641
9.405925174	69.13575559	70.28204791	66.95348574	66.6441297	68.16439366
9.948458968	70.28204791	70.74772916	66.29057994	66.4850323	68.3323298
10.48919664	69.49397194	71.10594551	64.52283114	65.58348042	68.23510361
11.02805126	70.28204791	69.99547483	62.75508234	59.21958474	67.37774545
12.09977337	69.78054502	70.38951281	59.92668426	56.87731758	
13.16296975	70.7835508	71.78655658	54.97698763	53.03246395	
14.21701869	69.63725848	70.85519407			
15.26133387	70.23189762	70.81937243			
16.2953656	70.56862099	70.67608589			
17.31860169	70.28204791	70.28204791			
18.33056816	66.62824114	67.98946327			
19.33082946	67.41631711	64.47894304			
20.31898861	66.77152768	64.51476467			
21.29468693		62.75950455			

APPENDIX C

Experimental Data

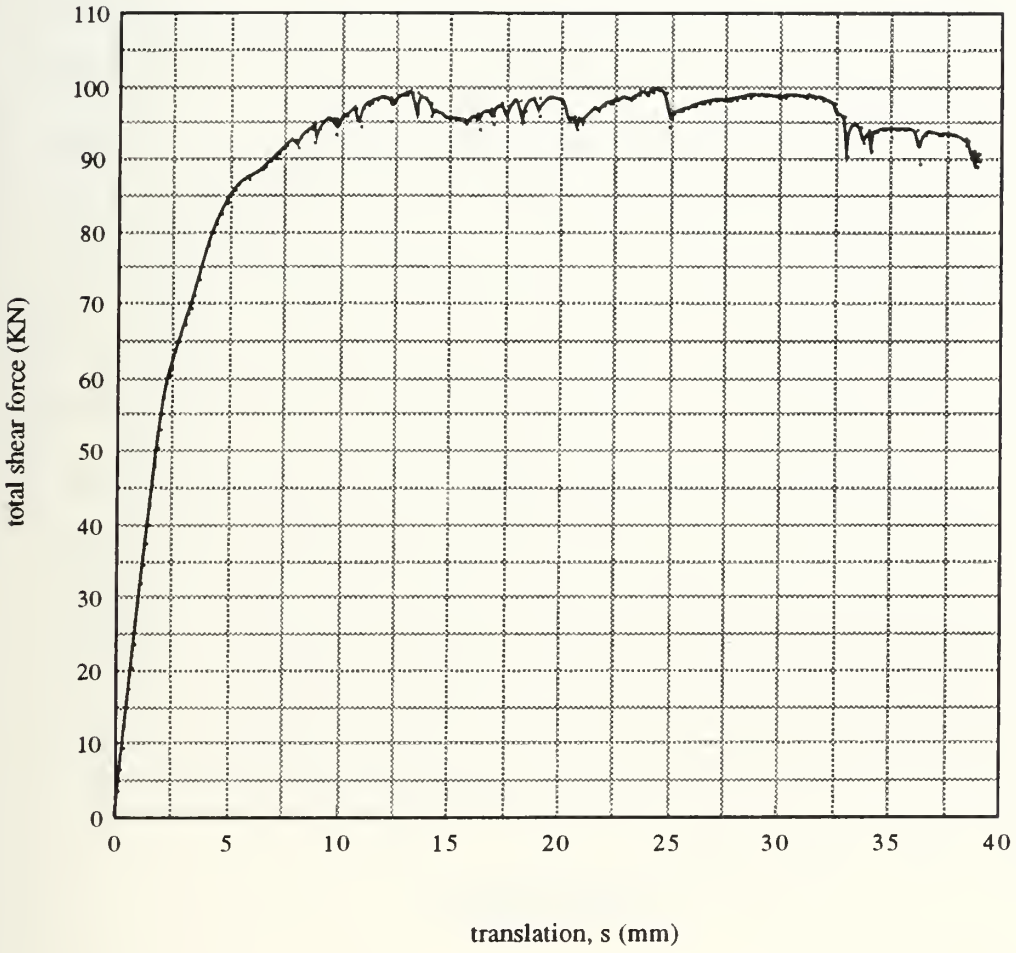

Figure C-1: Shear buckling load test 3 data

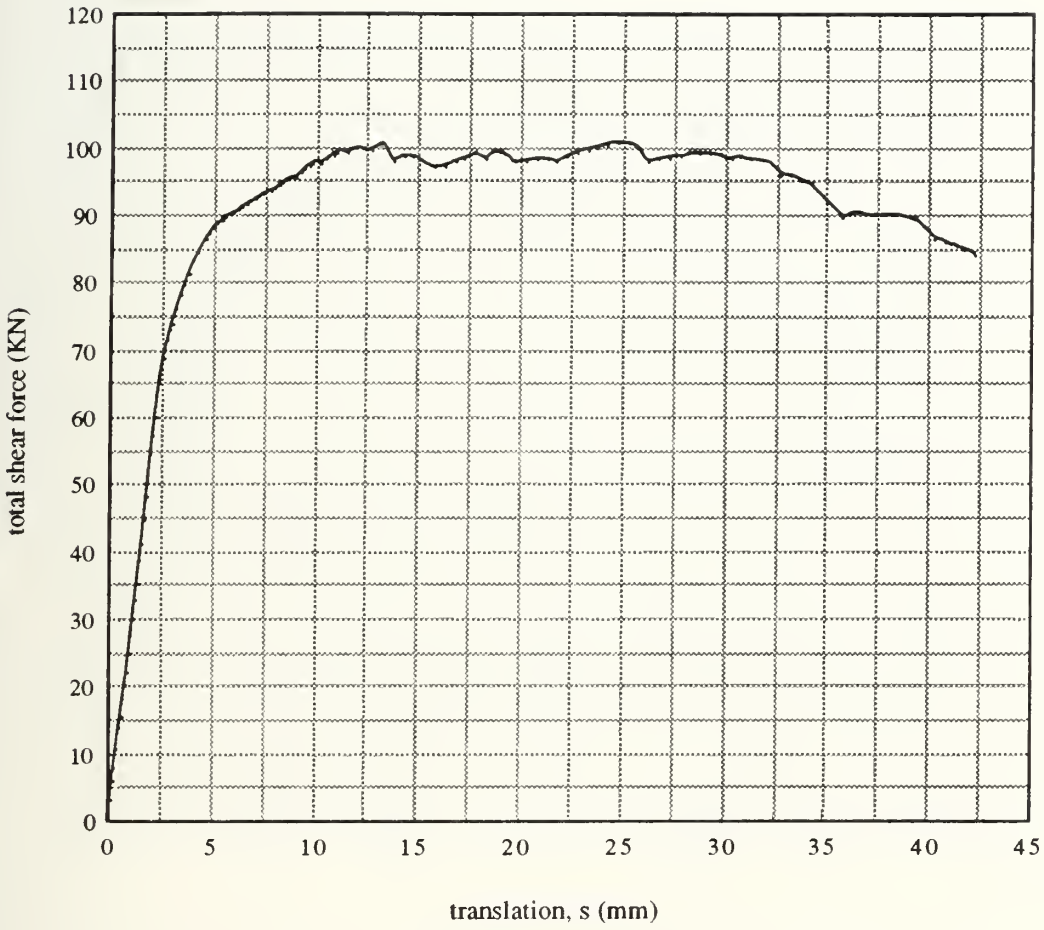

Figure C-2: Shear buckling load test 4 data

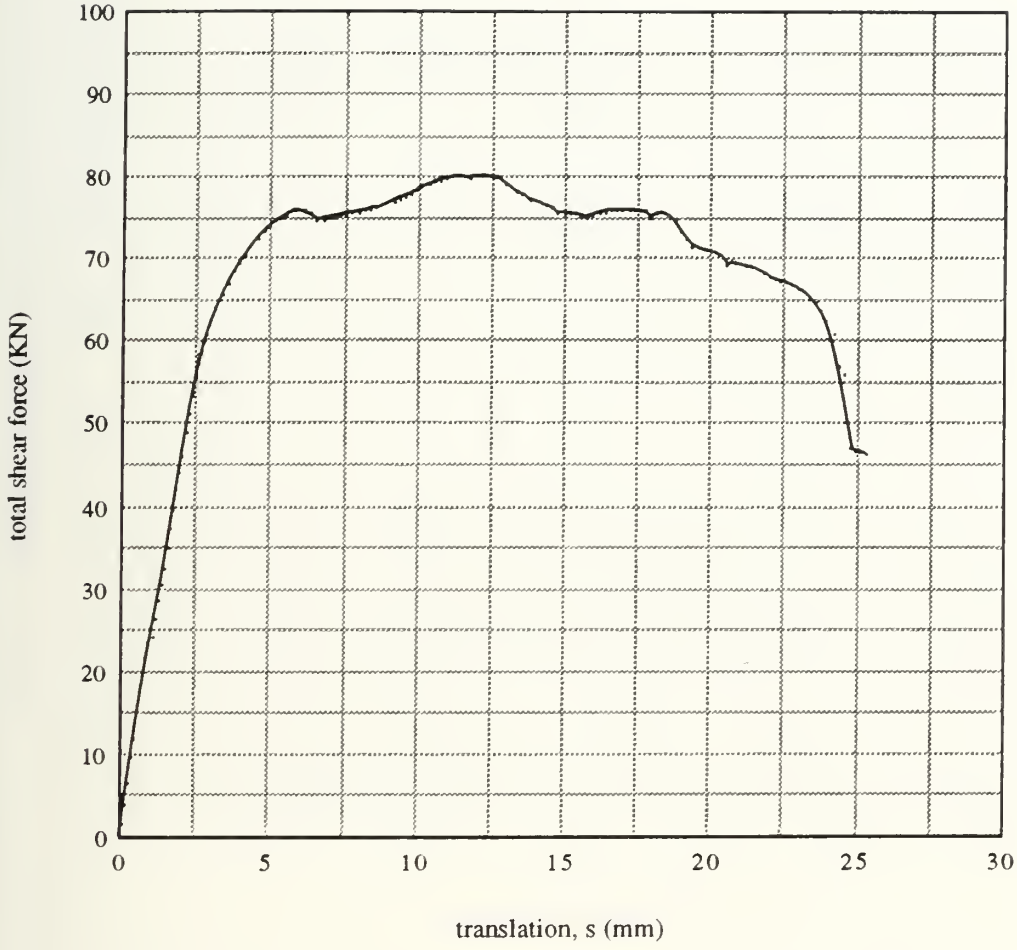

Figure C-3: Shear buckling load test 5 data

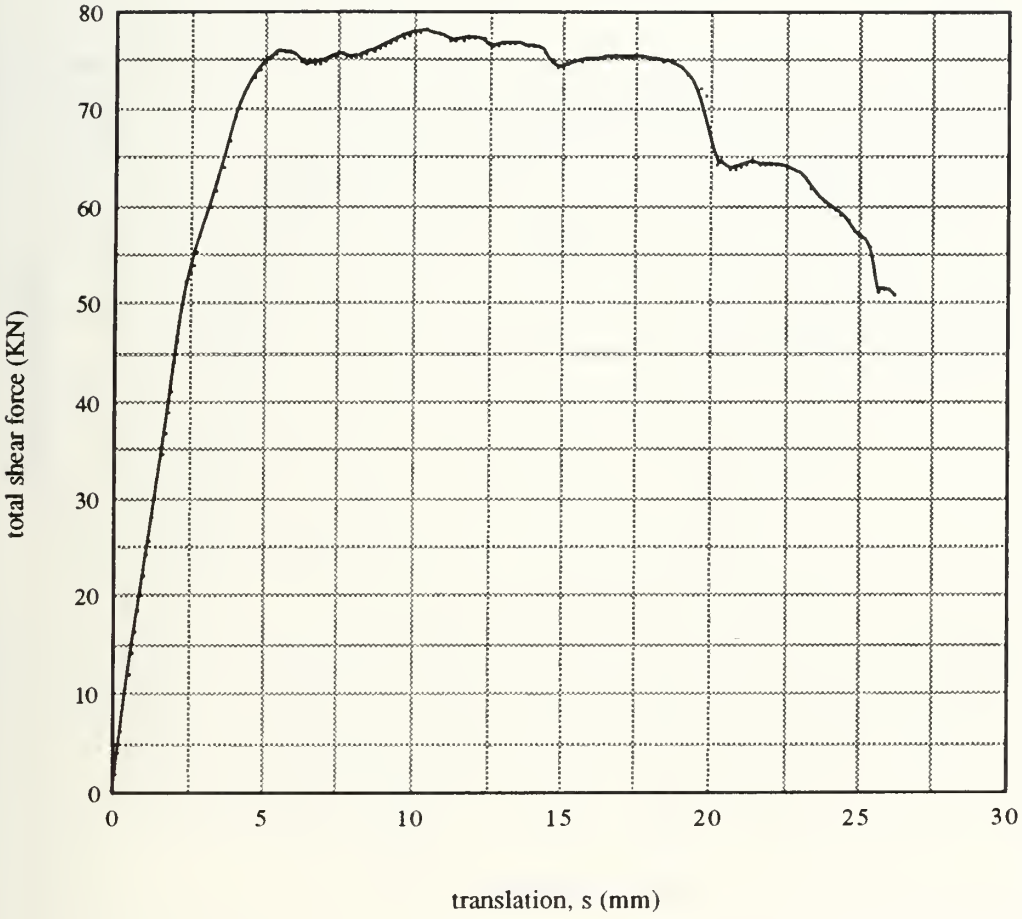

Figure C-4: Shear buckling load test 6 data

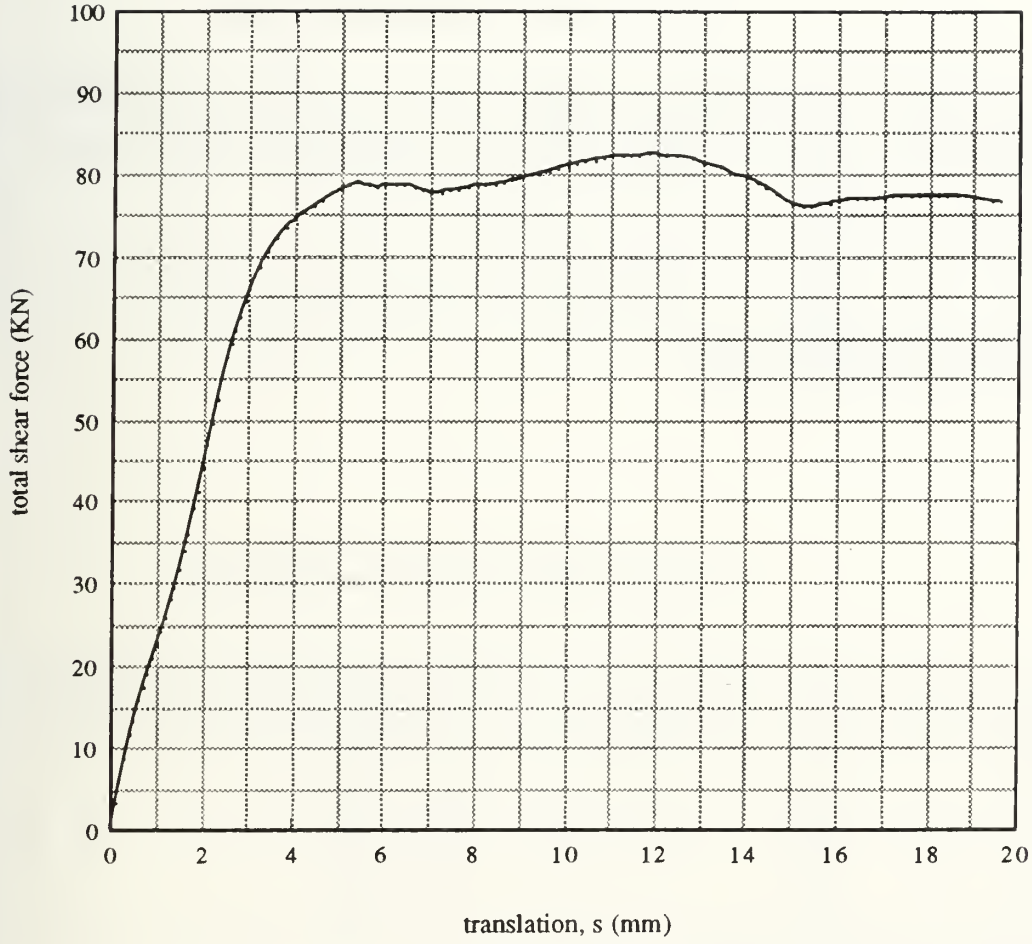

Figure C-5: Shear buckling load test 7 data

Specimen Tensile Test Data for Buckling Tests 3, 4

Specimen	Orientation to cold roll axis	Rockwell Superficial Hardness	Knoop Hardness	Approximate Yield Strength (ksi) = UTS *.65	Specimen thickness t (in)	Specimen width w (in)	Specimen X-Sectional Area (sq-in)	Specimen Yield Pt. (KN)	Specimen Yield Stress (ksi)	Specimen Avg. Flow Force (KN)	Specimen Plastic Flow Stress (ksi)
1	90	57.16	122	38.3286208	0.0282	0.444	0.0125208	2.07	37.16836766	2.361	42.39348602
2	0	59.68	129	40.52780396	0.028	0.444	0.012432	2.14	38.69973519	2.457	44.43235952
3	90	56.63	120	37.70028275	0.0281	0.441	0.0123921	2.09	37.91722958	2.372	43.03333424
4	0	57.6	124	38.95695884	0.0272	0.453	0.0123216	2.09	38.13417906	2.394	43.68096874
5	90	56.07	119	37.38611373	0.0283	0.44	0.012452	2.05	37.0126321	2.343	42.30273025
6	0	57.35	123	38.64278982	0.0281	0.457	0.0128417	2.2	38.515486	2.536	44.39785113
7	90	54.76	116	36.44360666	0.0282	0.442	0.0124644	2.09	37.69728994	2.366	42.67549665
8	0	58.04	123	38.64278982	0.0279	0.442	0.0123318	2.11	38.46725568	2.419	44.10061208
								Average =	37.9515219	Average =	43.37710483

Specimen Tensile Test Data for Buckling Tests 5, 6, 7

Specimen	Orientation to cold roll axis	Rockwell Superficial Hardness	Knoop Hardness	Approximate Yield Strength (ksi) = UTS *.65	Specimen thickness t (in)	Specimen width w (in)	Specimen X-Sectional Area (sq-in)	Specimen Yield Pt. (KN)	Specimen Yield Stress (ksi)	Specimen Avg. Flow Force (KN)	Specimen Plastic Flow Stress (ksi)
1	0	71.3	89.7	34.68426013	0.0284	0.489	0.0138876	2.03	32.86276189	2.153	34.85395387
2	0	72.8	94.3	36.46294014	0.0283	0.485	0.0137255	2.02	33.08707811	2.14	35.05264711
3	0	72.8	94.3	36.46294014	0.0282	0.485	0.013677	2.01	33.04002992	2.127	34.96325554
4	90	72.2	92.7	35.84426883	0.0281	0.484	0.0136004	1.9	31.40777281	2.093	34.59814132
5	90	78.1	110.7	42.80432103	0.0261	0.489	0.0127629	2.95	51.96463378	2.783	49.02290705
6	90	78.5	112	43.30699147	0.0258	0.483	0.0124614	2.74	49.43322534	2.583	46.60073761
7	45	73	95	36.73360884	0.0281	0.482	0.0135442	2.05	34.02794517	2.167	35.97002789
8	45	73	95	36.73360884	0.0282	0.483	0.0136206	2.06	34.00213621	2.187	36.09838441
9	45	72.9	94.7	36.61760797	0.0283	0.478	0.0135274	2.03	33.73781304	2.18	36.23075489
								Average =	41.93271743	Average =	41.60356581
								Average flow stress for tests 5 & 6 =			47.81182233

Thesis
P9423
c.1

Price
Plastic shear buckling of ship hull plating induced by grounding.